Subversion of the Host Cell by Enteropathogenic *Escherichia coli* through Effector Interplay

Alexander Ray Chong Wong

Imperial College London

Division of Cell and Molecular Biology

This thesis is presented for the degree of Doctor of Philosophy of Imperial College London and Diploma of Imperial College London 2012.

The copyright of this thesis rests with the author and no quotation from it or information derived from it may be published without the prior written consent of the author.

Candidate's Declaration

I, Alexander Wong, hereby confirm that this thesis represents my own work, and that any external contributions to the research are duly acknowledged.

Alexander Wong

Abstract

Enteropathogenic *Escherichia coli* (EPEC) strains are diarrheagenic pathogens that colonize the gut mucosa via attaching-and-effacing (A/E) lesion formation. EPEC utilize a type III secretion system (T3SS) to translocate effector proteins, including Tir and EspH that subvert host cell signalling to sustain colonization and multiplication. *In vitro*, EPEC induces the formation of an actin-rich 'pseudopod'-like structure, termed pedestals. My research focussed on EspH, which is implicated in the elongation of actin pedestals, and inactivation of Rho GTPase signalling.

In the first study, I showed that EspH promotes Tir-dependent actin assembly at the bacterial attachment sites independently of the Tir tyrosine residues Y454 and Y474, which are implicated in actin pedestal formation. Moreover, EspH promotes the recruitment of N-WASP and the Arp2/3 complex to the bacterial attachment sites. EspH-mediated N-WASP recruitment is dependent on the N-WASP binding protein WIP. Expression of WIP and EspH during EPEC infection induces extensive actin cytoskeletal rearrangements at the bacterial attachment site, forming a protrusive actin patch that is associated with EPEC microcolonies, termed "macro-pedestals". This study implicates the critical role of WIP in EPEC-mediated actin polymerization, and represents the first instance whereby N-WASP is efficiently activated at the EPEC attachment sites independently of the canonical Tir:Nck and Tir:IRTKS/IRSp53 pathways.

In my second study, I investigated the interplay of EspH, a eukaryotic RhoGEF inhibitor, and T3SS bacterial RhoGEFs during EPEC infection. EspH does not inhibit

the *E. coli* RhoGEFs Map, EspT, and EspM, as well as the *Salmonella* RhoGEF SopE. Expression of EspH induces cell rounding, detachment, caspase-3 activation and death. Importantly, EPEC EspT and EspM2, and *Salmonella* SopE are able to block EspH-induced cell detachment and caspase-3 activation. In addition, the bacterial RhoGEFs blocked staurosporine-induced caspase-3 activation, and can functionally compensate for the anti-apoptotic T3SS effector NleH. Therefore, this study expands the role of bacterial RhoGEFs to include cell adhesion and survival, and demonstrates that A/E pathogens silence eukaryotic DH-PH RhoGEFs while translocating their own RhoGEFs to hijack Rho GTPase signalling for the exclusive benefit of the pathogen.

Highlighted in the two studies is also the concept of effector interplay, where T3SS effectors function in concert with other effectors during the subversion of host cell signaling pathways. Understanding the functional interactions between effectors enables us to gain further insight into the sophisticated nature of their biological relevance beyond that of their biochemical functions.

Acknowledgements

I dedicate this thesis to my parents, who have been unyielding in their love and support for my academic aspirations, for which I can proudly say “I am a Doctor”.

I’d like to thank Prof. Gad Frankel for giving me the wonderful opportunity to embark on this PhD – Gadi, I’ve come a long way since the time I first sat in your office, and hope that I passed your “training”. I also express my heartfelt gratitude to Drs. Valerie Crepin and Benoit Raymond for their patience and advice in all aspects of the project, but above all, for sharing with me the extraordinary joys and sacrifices of parenthood. A big thank you to all lab members and alumni for your camaraderie, especially Gunnar Schroeder, Aurelie Mousnier, Mariella Lomma, James Collins, Richard Bulgin, and Eric Martinez – I leave with many unforgettable evenings of dinner parties and alcohol-fuelled fun (carwash anyone?). My fellow PhD peers, Scott, Cordula, Nick, Clare and Joanna – the “Starbucks” sessions have always been a welcome distraction, but it is the companionship that makes the cafe latte that extra bit warming. And to everyone on CMMI-1 I did not mention, thank you very much.

Credit goes to Drs. Rey Carabeo, Alan Hall, Michael Way, John Leong, Scott Snapper and Roberto La Regione for kindly providing reagents. Also, thanks to Drs. Valerie Crepin, James Collins, Artemis Kosta, Michael Bright, Abigail Clements, and Ms. Leah Ensell for technical assistance during my research.

Finally, to my girlfriend Meiting whom, despite the spatiotemporal restrictions, has endowed me with her love, care and encouragement. Even in the drieriest of times, you have been the shining hope of bliss, the bedrock of my happiness.

The Choice

The intellect of man is forced to choose
Perfection of the life, or of the work,
And if it take the second must refuse
A heavenly mansion, raging in the dark.
When all that story's finished, what's the news?
In luck or out the toil has left its mark:
That old perplexity an empty purse,
Or the day's vanity, the night's remorse.

- William Butler Yeats

"Fate rarely calls upon us at the moment of our choosing."

- Optimus Prime

Table of Contents

Candidate's Declaration 2

Abstract 3

Acknowledgements 5

Table of Contents 7

Index of Tables 12

Index of Figures 13

Abbreviations 15

Chapter 1 – Introduction 18

1.1 The actin cytoskeleton 18

1.1.1 Actin polymerization 18

1.1.2 Arp2/3 complex machinery 21

1.1.3 Nucleation promoting factors (NPFs) 21

1.1.4 Formins 25

1.1.5 WH2 domain-containing actin nucleators 26

1.2 Apoptosis 27

1.2.1 Morphology of apoptosis 28

1.2.2 Intrinsic (mitochondria) pathway 29

1.2.3 Extrinsic (death-receptor) pathway 31

1.2.4 Execution pathway 32

1.3 Rho GTPases 33

1.3.1 Classical Rho GTPases 33

1.3.2 Rho guanine nucleotide exchange factors (GEFs) 34

1.3.3 Rho GTPase-activating proteins (GAPs) 35

1.3.4 Rho GDP dissociation inhibitors (GDIs) 36

1.3.5 Regulation of actin dynamics by Rho GTPases 37

1.3.6 Regulation of focal adhesions by Rho GTPases 39

1.3.7 Regulation of apoptosis by Rho GTPases 40

1.4 Gram-negative bacterial secretion systems....42
1.4.1 General secretory (Sec) and two-arginine (Tat) pathways....43
1.4.2 Type I secretion....44
1.4.3 Type II secretion....44
1.4.4 Type III secretion....45
1.4.5 Type IV secretion....46
1.4.6 Type V secretion....47
1.4.7 Type VI secretion....47
1.5 Pathogenic *Escherichia coli*....48
1.5.1 Enterotoxigenic *E. coli* (ETEC)....50
1.5.2 Enteroaggregative *E. coli* (EAEC)....50
1.5.3 Enteroinvasive *E. coli* (EIEC)....51
1.5.4 Diffusely adherent *E. coli* (DAEC)....51
1.5.5 Enteropathogenic *E. coli* (EPEC)....52
1.5.6 Enterohaemorrhagic *E. coli* (EHEC)....52
1.6 Subversion of actin dynamics by bacterial pathogens....53
1.6.1 Bacterial actin nucleation factors....54
1.6.2 Bacterial NPF mimics....55
1.6.3 Bacterial NPF activators....56
1.6.4 Subversion of Rho GTPase signaling by bacterial pathogens....57
1.7 Attaching and effacing (A/E) pathogens....60
1.7.1 Locus of Enterocyte Effacement (LEE) Pathogenicity Island....61
1.7.2 Intimate attachment by the bacterial adhesin intimin....62
1.7.3 LEE and non-LEE encoded T3SS effectors....63
1.7.4 Tir-mediated actin polymerization and A/E lesion formation....68
1.7.5 Subversion of Rho GTPases by A/E pathogens....71
1.7.6 Regulation of cell survival and death....72
1.7.7 EspH, an actin cytoskeletal modulator....74
1.8 Aims of the study....75
Chapter 2 – Materials and Methods....77

2.1 Strains, Primers and Plasmids....77
2.1.1 Strains....77
2.1.2 Plasmids....78
2.1.3 Primers....79
2.2 Molecular Biology Techniques....80
2.2.1 Polymerase Chain Reaction (PCR)....80
2.2.2 Restriction Digest and DNA Ligation....81
2.2.3 Bacterial Transformation....82
2.2.4 Plasmid Extraction....83
2.2.5 Agarose gel electrophoresis....83
2.2.6 Protein BCA assay....84
2.2.7 SDS-PAGE....84
2.2.8 Coomassie staining....85
2.2.9 Western blot....85
2.3 Construction of EPEC *tir* chromosomal mutants....86
2.4 Construction of GFP-N-WASP and HA-TirNM deletion variants....87
2.5 Cell culture....88
2.6 Transfection....88
2.7 siRNA knockdown....89
2.8 EPEC Infection....89
2.9 Secretion assay....90
2.10 Translocation assay....91
2.11 Cell detachment assay....91
2.12 Pharmacology....92
2.13 Cytotoxicity assay....92
2.14 Immunofluorescence microscopy....93
2.15 Antibodies....93
2.16 Oral infection of mice....94
2.17 Indirect immunofluorescence assay of mice colon sections....95
2.18 Indirect immunofluorescence assay of cryosections....96

2.19 Scanning electron microscopy 96
2.20 Transmission electron microscopy 97
2.21 Bioinformatics analysis....97
2.22 Statistical analysis....97
Chapter 3 – Tir and EspH in EPEC actin pedestal dynamics 99
3.1 EspH is a secreted and translocated T3SS effector....99
3.2 EspH promotes actin pedestal formation and elongation 102
3.3 Inhibition of Cdc42 restores actin pedestal length in *espH* mutant 104
3.4 Characterization of EPEC *tir* chromosomal mutants....106
3.5 EspH promotes Tir-dependent actin polymerization independently of tyrosine residues 454 and 474....108
3.6 N-WASP and Arp2 are recruited during EspH-mediated actin polymerization....110
3.7 IRSp53 and WAVE2 are not recruited during EspH-mediated actin polymerization 112
3.7 Nck and Rho GTPases are not required for EspH-mediated actin polymerization 114
3.8 EspH-mediated N-WASP recruitment is dependent on the C-terminus of Tir....116
3.9 Expression of GFP-N-WASP deletion variants....118
3.10 EspH-mediated actin polymerization requires WH1 domain of N-WASP 120
3.11 Dominant-negative of WIP abolishes EspH-mediated actin polymerization 124
3.12 EspH recruits WIP independently of Tir-mediated actin polymerization pathways 126
3.13 N-WASP is required for WIP recruitment to bacterial attachment site....128
3.14 Tir, EspH, WIP, N-WASP and cortactin are recruited to macro-pedestals 129
3.15 Tir:Nck, Tir:IRTKS/IRSp53 and EspH-mediated actin polymerization pathways are dispensable for colonization or A/E lesion formation *in vivo*....131
3.16 Discussion 133
Chapter 4 – Bacterial RhoGEFs and EspH in modulating actin dynamics, adhesion, and cell death 138
4.1 EspH induces detachment, cytotoxicity and FA disassembly 138
4.2 EspH mediates FA disassembly in a caspase-independent manner....141
4.3 FAK is involved in EspH-induced cell rounding, detachment and caspase-3 activation 144
4.4 Bacterial RhoGEFs are active in the presence of EspH....146

4.5 EspT, EspM2 and SopE block EspH-induced detachment and FA disassembly 150
4.6 EspT, EspM2 and SopE inhibit EspH-induced caspase-3 activation 152
4.7 EspT, EspM2 and SopE inhibit staurosporine-induced caspase-3 activation.....154
4.8 EspT and EspM2 can compensate for NleH in inhibiting caspase-3 activation, detachment and cytotoxicity 156
4.9 Screening for additional T3SS effectors that block EspH-induced cell detachment.....158
4.10 Discussion.....160
Chapter 5 – General discussion.....164
5.1 EspH as a modulator of actin pedestal dynamics.....164
5.2 EspH as a modulator of host cell adhesion and survival 168
5.3 Coordination of Rho GTPase subversion by bacterial pathogens 171
5.4 Effector interplay: an emerging theme 173
5.5 Concluding remarks.....176
References.....177
Appendices.....202

Index of Tables

Table 1. Translocome of A/E pathogens. 65

Table 2. List of strains used in this study 77

Table 3. List of plasmids used in this study.....78

Table 4. List of primers used in this study.....79

Table 5. List of antibodies used in this study 93

Index of Figures

Figure 1. Overview of actin polymerization in mammalian cells. 19

Figure 2. Overview of mammalian actin nucleators and nucleation promoting factors (NPFs). 22

Figure 3. Overview of intrinsic and extrinsic apoptotic pathways. 30

Figure 4. Overview of Rho GTPase regulation in mammalian cells. 33

Figure 5. Overview of gram-negative bacterial secretion systems. 42

Figure 6. Overview of the different intestinal Escherichia coli pathotypes. 49

Figure 7. Subversion of the Arp2/3 complex by bacterial pathogens. 56

Figure 8. Subversion of Rho GTPase signaling by bacterial pathogens. 58

Figure 9. A/E lesion histopathology and the locus of enterocyte effacement (LEE). 61

Figure 10. Subversion of actin signaling pathways by EPEC/EHEC. 69

Figure 11. EspH is a secreted and translocated T3SS effector. 100

Figure 12. EspH promotes filopodia withdrawal, pedestal formation and pedestal elongation. 103

Figure 13. Inhibition of Cdc42 restores pedestal elongation in espH mutant. 105

Figure 14. Construction and characterization of EPEC tir chromosomal point mutants. 107

Figure 15. EspH promotes Tir-mediated actin polymerization independently of Tir Y454 and Y474. 109

Figure 16. N-WASP and Arp2 are recruited during EspH-mediated actin polymerization. 111

Figure 17. IRSp53 and WAVE2 are not recruited during EspH-mediated actin polymerization. 113

Figure 18. Nck and Rho GTPases are not required for EspH-mediated actin polymerization. 115

Figure 19. EspH-mediated N-WASP recruitment is dependent on the C-terminus of Tir. 117

Figure 20. Construction and expression of GFP-N-WASP deletion variants. 119

Figure 21. EspH-mediated actin polymerization requires WH1 domain of N-WASP. 121

Figure 22. EspH-mediated actin polymerization requires WH1 domain of N-WASP. 122

Figure 23. Disruption of WIP/N-WASP binding abolishes EspH-mediated actin polymerization. 125

Figure 24. Tir-mediated actin polymerization pathways and EspH recruit WIP to bacterial attachment sites. 127

Figure 25. N-WASP is required for WIP recruitment to bacterial attachment site. 128

Figure 26. Tir, EspH, WIP, N-WASP and cortactin, but not Nck, are recruited to macro-pedestals. 130

Figure 27. Tir:Nck, Tir:IRTKS/IRSp53 and EspH-mediated actin polymerization pathways are not required for colonization or A/E lesion formation in vivo. 132

Figure 28. EspH induces cell detachment, cytotoxicity and FA disassembly. 139
Figure 29. EspH mediates FA disassembly in a caspase-independent manner. 143
Figure 30. FAK is involved in EspH-induced cell rounding, detachment and caspase-3 activation. ...145
Figure 31. Ectopic expression of EspH does not inhibit WxxxE effectors during EPEC infection. 147
Figure 32. Bacterial RhoGEFs are active when co-expressed with EspH. 149
Figure 33. EspT, EspM2 and SopE block EspH-induced detachment and FA disassembly. 151
Figure 34. EspT, EspM2 and SopE inhibit EspH-induced caspase-3 activation. 153
Figure 35. EspT, EspM2 and SopE inhibit staurosporine-induced caspase-3 activation. 155
Figure 36. EspT and EspM2 can compensate for NleH inhibiting caspase-3 activation, detachment and cytotoxicity. 157
Figure 37. Screening for T3SS effectors that block EspH-induced cell detachment. 159
Figure 38. A model for EPEC actin polymerization pathways. 166
Figure 39. EspH and WxxxE bacterial RhoGEFs mediate diverse cellular processes. 170

Abbreviations

Amp	Ampicillin
ATCC	American type culture collection
BSA	Bovine serum albumin
Cm	Chloramphenicol
CRIB	Cdc42/Rac interactive binding domain
DH-PH	Tandem Dbl-homology-pleckstrin homology
DMEM	Dulbecco's modified Eagle's medium
DNA	Deoxyribonucleic acid
Esp	*E. coli* secreted protein
FCS	Fetal calf serum
g	Grams
GAP	GTPase activating protein
GDI	GDP-dissociation inhibitor
GDP	Guanine diphosphate
GEF	Guanine nucleotide exchange factor
GTP	Guanine triphosphate
h	Hours
HA	Haemmagglutinin (influenza epitope)
HBSS	Hanks' balanced salt solution
HC	Hemorrhagic colitis
HRP	Horseradish peroxidase
HUS	Hemolytic uremic syndrome
IPTG	Iso-propanyl-β-D- thiogalactopyranoside

Kn	Kanamycin
l	Litres
LB	Luria Bertani
LEE	Locus of enterocyte effacement
min	Minutes
NPY	Asn-Pro-Tyr motif
OD_{600}	Optical density measured at 600 nm
PAI	Pathogenicity island
PBS	Phosphate buffered saline
PCR	Polymerase chain reaction
PFA	Paraformaldehyde
PRD	Proline-rich domain
RFP	Red fluorescent protein
rpm	Revolutions per minute
SDS-PAGE	Sodium dodecyl sulphate-polyacrylamide gel electrophoresis
T3SS	Type III secretion system
Tet	Tetracycline
U	Unit of enzymes
V	Volts
WBD	WASP binding domain
WCA	WH2-central-acidic region
WH1/2	WASP-homology 1/2 domain
WT	Wild-type
WxxxE	Trp-xxx-Glu motif

Chapter 1 - Introduction

Chapter 1 – Introduction

1.1 The actin cytoskeleton

1.1.1 Actin polymerization

The actin cytoskeleton is one of the major filamentous networks that the eukaryotic cell relies on to coordinate cellular morphological changes. While often thought of as a mechanical system of defined structural filaments with a set of motor proteins to drive cell shape changes and motility (movement), the actin network also functions as a scaffold to recruit many regulatory factors. It is the result of this dynamic system that the actin cytoskeleton also affects other cellular functions including adhesion, endocytosis, vesicle trafficking, cell cycle progression, and cell death (Welch, 2002, Campellone *et al.*, 2010). The recent discovery that actin-like networks exist in prokaryotes suggests that the evolution of the actin cytoskeleton could even predate the divergence of prokaryotes and eukaryotes (Thanbichler *et al.*, 2008).

The major component of the microfilament cytoskeleton is actin. Actin is the most abundant protein in a mammalian cell, and is an ATP-binding protein that exists as a 42kDa monomer (G-actin or globular-actin), or in filaments (F-actin or filamentous-actin). Actin filaments are assembled by the reversible linking of actin monomers by ATP hydrolysis, and release of inorganic phosphate (P_i) in a process known as actin polymerization (Pollard *et al.*, 2003). Actin filaments are polar in nature. The fast-growing end, also known as barbed or plus (+) end, is where polymerization primarily occurs, while the slower-growing end, also known as pointed or minus (-) end, does not appear to elongate at a rate that is biologically relevant (Zigmond, 2004a).

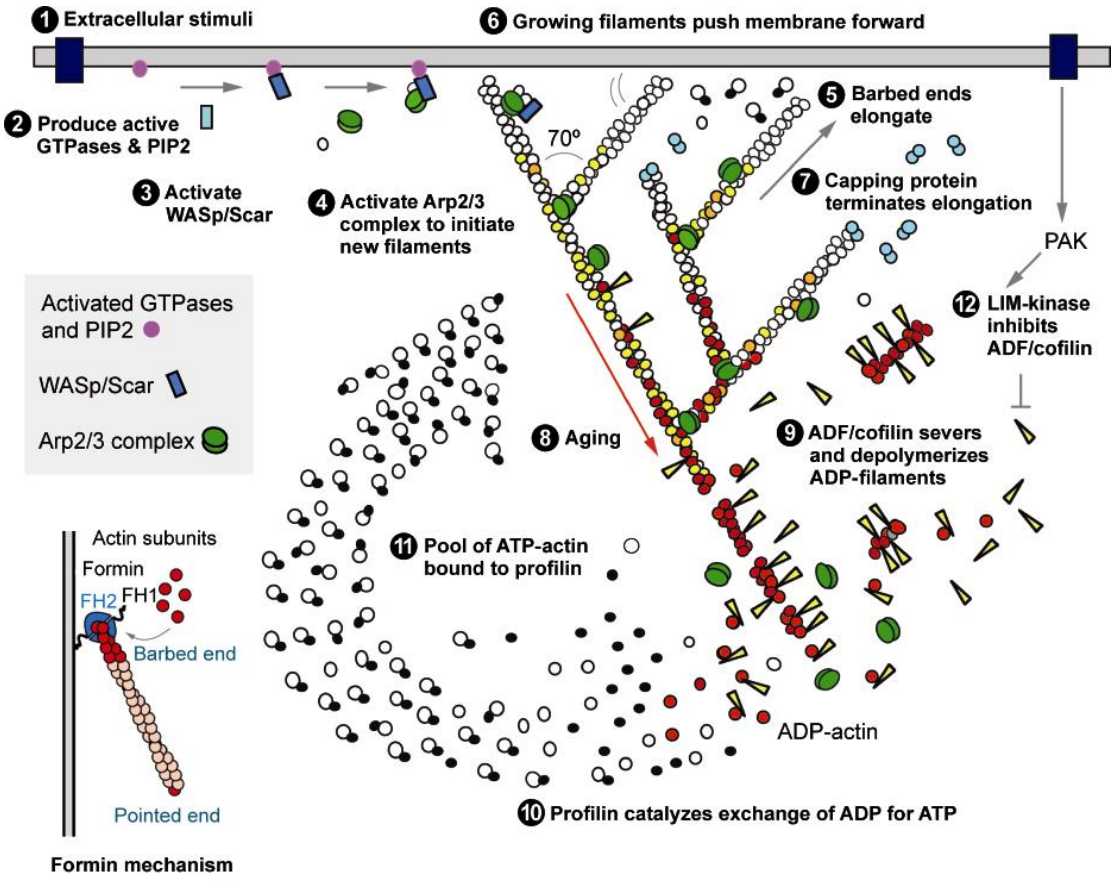


Figure 1. Overview of actin polymerization in mammalian cells.

Schematic representation of actin polymerization in response to stimuli. Detailed mechanisms of actin polymerization are found in section 1.1. Details of regulation by Rho GTPases are found in section 1.3. Image taken from (Pollard, 2007).

Elongation of actin filaments is regulated by the availability of barbed ends to bind additional actin monomers, as well as the concentration of readily polymerizing G-actin monomers. Profilins, which are G-actin-binding proteins that catalyze the exchange of actin-bound ADP to ATP, maintain a readily polymerizing ATP-actin monomer pool (Zigmond, 2004a) (Figure 1). Free barbed ends are kept in low concentrations by barbed end binding proteins such as capping protein (CapZ in muscles), or gelsolin that prevent the promiscuous elongation of actin filaments and depletion of available ATP-actin monomer pool (Condeelis, 2001). The process of

initiating actin polymerization can be classified into three non-exclusive categories that probably work in tandem during cellular processes.

(i) Uncapping of pre-existing filaments

The uncapping of barbed ends is initiated by the binding of capping protein or gelsolin to polyphosphoinositides, e.g. phosphatidylinositol 4,5-bisphosphate [PI(4,5)P_2] that disrupts its capping functions, thus allowing for the incorporation of monomeric actin into existing filaments (Hartwig *et al.*, 1995).

(ii) Severing of existing filaments to create free barbed ends

The severing of existing filaments by the actin depolymerizing factors (ADF)/cofilin and gelsolin/villin family of proteins are thought to play a dual role in promoting depolymerization of actin filaments, but also create more ends for the initiation of new actin filaments (Condeelis, 2001). ADF/cofilin are ADP-binding proteins that bind to both monomeric and filamentous actin, and sever filamentous actin by enhancing the rate of actin dissociation mainly from the pointed ends (Bamburg, 1999). This leads to the generation of an ADP-actin monomeric pool that can then be recycled into ATP-actin by profilin (Figure 1).

(iii) *De novo* filament nucleation

Nucleation has been defined as "the initiation of actin polymerization from free actin monomers" (Welch, 2002). Compared to the affinity of an actin monomer to bind to the barbed end of an existing filament, the affinity to spontaneously form an actin dimer is seven orders of magnitude higher (Pollard, 1986). As such, actin nucleation

factors, which help overcome this large kinetic barrier, represent one of the most critical steps in controlling the initiation of actin polymerization in cells.

1.1.2 Arp2/3 complex machinery

Three groups of actin nucleation factors have been identified and characterized thus far; the Arp2/3 complex represents the best studied to date. It is a 220kDa complex consisting of actin-related protein (Arp) subunits Arp2 and Arp3, as well as a five addition subunits ARPC1–5 (Machesky *et al.*, 1994). The Arp2/3 complex binds to existing actin filaments to initiate a new actin filament branch that is extended at a ~70° branch angle (Blanchoin *et al.*, 2000). By itself, the Arp2/3 complex is an inefficient nucleator as the Arp2 and Arp3 subunits are too spaced apart to mimic an actin dimer (Robinson *et al.*, 2001, Nolen *et al.*, 2004). To activate the Arp2/3 complex, the ARPC subunits first bind to existing actin filaments, which reorients Arp2 and Arp3 subunits into a dimer that acts as the first two subunits of the new filament (Rouiller *et al.*, 2008). Efficient nucleation also requires the phosphorylation of the Arp2 subunit (LeClaire *et al.*, 2008). Finally, the Arp2/3 complex also requires the recruitment of co-factors known as nucleation promoting factors (NPFs).

1.1.3 Nucleation promoting factors (NPFs)

Nucleation promoting factors (NPFs) are an integral component of Arp2/3-mediated actin nucleation cascade. The majority belong to a class I group of NPFs that utilize a C-terminal WCA/VCA domain comprising one or more WASP-homology 2 (WH2) domain or verprolin-homology (V) sequence, followed by a central (C) region, and an acidic (A) region (Takenawa *et al.*, 2007). The CA region binds to the Arp2/3 complex and actin at various binding sites, inducing a global conformational change

in the complex that results in the stabilization of the Arp2 and Arp3 subunits in close proximity (Goley *et al.*, 2004). The WH2 domain binds and delivers G-actin to the primed complex (Hertzog *et al.*, 2004). Class I NPFs are sub-classified according to their modular N-terminal domains that regulate their localization and activity within the cell. Two of the best-characterized are the Wiskott-Aldrich syndrome protein (WASP) and WASP-family verprolin homologue (WAVE/SCAR) family of NPFs (Figure 2).

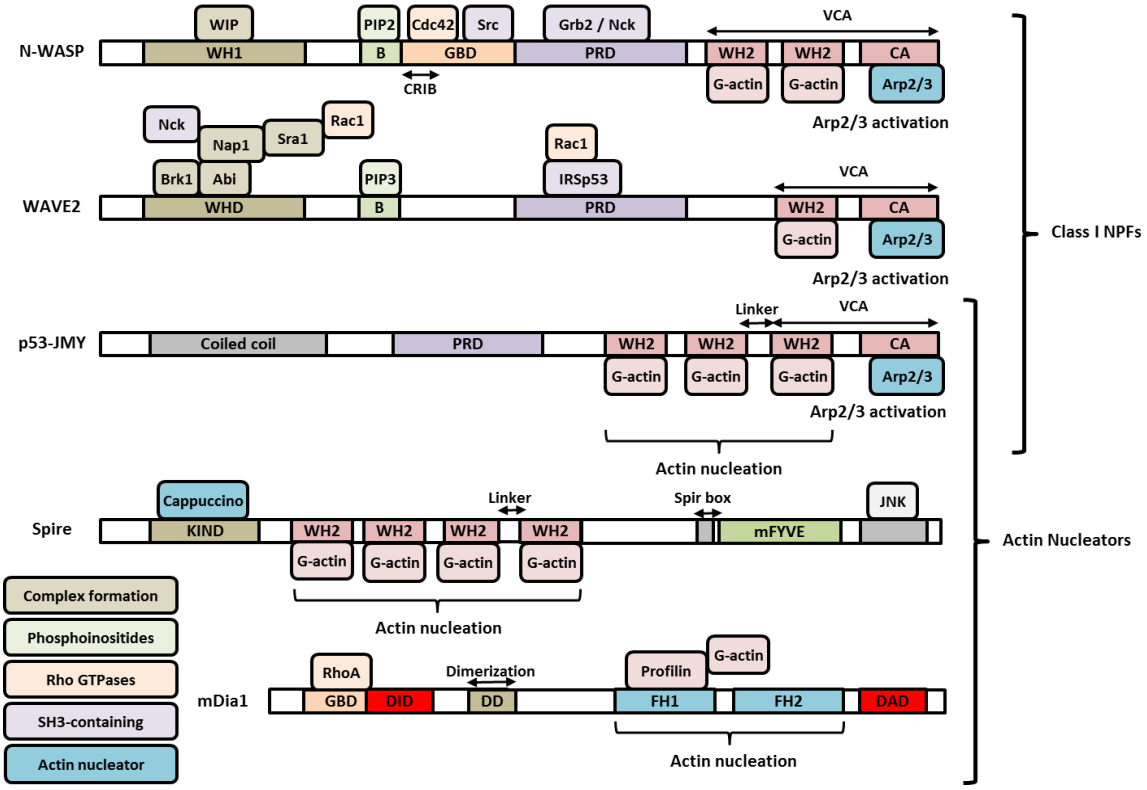


Figure 2. Overview of mammalian actin nucleators and nucleation promoting factors (NPFs).

Schematic representation of class I NPFs N-WASP, WAVE2 and p53-JMY, as well as actin nucleators mDia1 and Spire, with their interacting partners. Mechanism of activation or autoinhibition relief is found in sections 1.12 to 1.15. WH1/2 – WASP homology 1/2, B – basic region, GBD – GTPase-binding domain, PRD – proline-rich domain, VCA – verprolin-central acidic region, WHD – WAVE homology domain, KIND - kinase non-catalytic C-lobe domain, FYVE – modified FYVE domain, DID - Diaphanous inhibitory domain, DD – dimerization domain, FH1/2 – formin homology, DAD - Diaphanous autoregulatory domain.

(i) WAVE/SCAR-family NPFs

The WAVE and *Dictyostelium* homologue suppressor of cyclic-AMP receptor (SCAR) family of NPFs are characterized by an N-terminal region that consists of a WAVE-homology domain (WHD), a basic region which binds to phosphatidylinositol 3,4,5-trisphosphate [PI(3,4,5)P_3], followed by a proline-rich domain. The WHD of WAVE proteins is required for the formation of a pentameric heterocomplex consisting of WAVE, Abelson-interacting protein-1 (Abi1), Nck-associated protein-1 (Nap1), specifically Rac1-associated protein-1 (Sra1) (also known as PIR121/CYFIP1) and BRICK/Brk1 (also known as HSPC300), known as the WAVE regulatory complex (WRC) (Gautreau *et al.*, 2004) (Figure 2). WHD binds both Abi1 and Brk1, while Nap1 interacts with Abi1 and Sra1 (Gautreau *et al.*, 2004). WAVE proteins are trans-inhibited when part of the WRC (Derivery *et al.*, 2009). Most of the signaling cascades leading to Arp2/3 complex activation are achieved through indirect interactions with the WRC. Nap1 binds Nck (Eden *et al.*, 2002), while Sra1 binds activated Rac (Innocenti *et al.*, 2004). Regulation by Rac can also be mediated by indirect binding of insulin receptor substrate p53 (IRSp53) to Rac via its IRSp53/MIM-homology domain (IMD), and binding of IRSp53 to the PRD domain of WAVE2 via its SH3 domain (Suetsugu *et al.*, 2006) (Figure 2).

(ii) WASP-family NPFs

WASP was initially identified as the causative gene of Wiskott-Aldrich syndrome. Expression of WASP is restricted to hematopoietic cells, while its homologue neural (N-) WASP is ubiquitously found (Takenawa *et al.*, 2007). The N-terminal region of WASPs differs from WAVEs, and consists of a WASP homology 1 (WH1) domain (also known as Ena-VASP-homology-1 (EVH1) domain), followed by basic (B)

region, a GTPase-binding domain (GBD) that encompasses a Cdc42/Rac-interactive binding (CRIB) region, and a proline-rich domain (PRD) (Figure 2). Under resting conditions, WASP/N-WASP is inactive, owing to an intramolecular interaction between the VCA and the CRIB and its surrounding regions (Kim *et al.*, 2000). N-WASP activation occurs when the autoinhibition is released by competitive binding of other molecules that lead to Arp2/3 complex activation. WASP/N-WASP exist mainly in hetero-complexes with the WASP-interacting family (WIP) family of proteins which comprise WIP (Ramesh *et al.*, 1997), CR16 (Ho *et al.*, 2001) and WICH/WIRE (Aspenstrom, 2002). WIP proteins bind to the WH1 domain of WASP/N-WASP via its WASP-binding domain (WBD) (Volkman *et al.*, 2002, Zettl *et al.*, 2002, Peterson *et al.*, 2007). The function of WIP is still unclear. Interaction with WIP suppresses N-WASP activity by stabilizing the autoinhibited state (Volkman *et al.*, 2002), but other roles have been described. WIP acts as a chaperone for WASP but not N-WASP (de la Fuente *et al.*, 2007). WIP is required for Cdc42-dependent N-WASP activation, but also inhibits it *in vitro* (Martinez-Quiles *et al.*, 2001). WIP also acts as scaffold for adaptor proteins, and possesses G-actin binding sites and a proline-rich region that binds SH3-containing adaptors such as CrkL and Nck, and the class II NPF cortactin, all of which can subsequently participate in N-WASP or Arp2/3 complex activation (Anton *et al.*, 1998, Anton *et al.*, 2007).

The basic (B) region links WASP-family NPFs to the membrane via its ability to bind $PI(4,5)P_2$ (Papayannopoulos *et al.*, 2005). Importantly, the basic region has been shown to stabilize N-WASP autoinhibition (Rohatgi *et al.*, 2000), but also synergize with Cdc42-induced N-WASP activation, which is mediated by binding of Cdc42 to the CRIB region located beside the basic region (Rohatgi *et al.*, 2000). Within the

GBD is also a phosphorylation site of N-WASP at Tyr-256. Phosphorylation by Src kinases enhances Cdc42-mediated N-WASP activation, but also targets N-WASP for proteasomal degradation, suggesting that it may exert fine-tuning effects of N-WASP activity (Suetsugu *et al.*, 2002). The PRD domain binds to Src-homology 3 (SH3) domain-containing proteins including those of Nck and Grb2, as well as SH3 domain-containing proteins from different family groups that integrate multiple upstream signals to then bind and activate N-WASP (Carlier *et al.*, 2000, Rohatgi *et al.*, 2001). For example, transducer of Cdc42 activation-1 (Toca-1) binds both Cdc42 and the PRD domain of N-WASP, and is required for Cdc42-mediated N-WASP activation (Ho *et al.*, 2004). Another example is the Rho guanine nucleotide exchange factor (RhoGEF) intersectin (ITSN) that activates Cdc42 but also binds to the PRD domain of N-WASP, thus triggering Cdc42 and N-WASP activation in a positive feedback loop (Hussain *et al.*, 2001). Rho GEFs are further discussed in section 1.3.2.

1.1.4 Formins

Formins represent a group of actin nucleators that produce unbranched filaments, and are defined by the presence of conserved formin homology (FH) domains FH1 and FH2 (Figure 2). In contrast to the Arp2/3 complex, FH2 domains are sufficient to trigger actin nucleation *in vitro* (Zigmond, 2004b). Contemporary studies suggest a "processive capping" model for formin-mediated nucleation, where FH2 domains homodimerize to form a donut-shaped ring which displaces the capping protein by binding to two terminal actin subunits at the pointed end (Otomo *et al.*, 2005). Actin nucleation occurs when the ring steps up in an open conformation, allowing the incorporation of new actin subunits, although the sequence of events during this "stepping" process is not known (Otomo *et al.*, 2005). The FH1 domain accelerates

filament elongation by recruiting profilin:actin complexes to promote the delivery of actin at the growing end (Romero *et al.*, 2004).

While all formins possess FH1 and FH2 domains, these modules are slightly divergent in the different subclasses of formins, and are often coupled to a diverse array of other regulatory motifs (Campellone *et al.*, 2010). The best-characterized formins belong to the subclass of Diaphanous-related formins (DRFs), more commonly known as mDia1–3. DRFs are divided into three functional regions. The N-terminus contains regulatory sequences such as a GTPase-binding domain (GBD) and a Diaphanous inhibitory domain (DID) (Figure 2). The central region contains a central coiled-coil and dimerization domain (DD) that is required for formation of the donut-shaped dimer, while the C-terminus contains the FH1-FH2 domain, as well as a Diaphanous autoregulatory domain (DAD) that binds to the DID in an autoinhibited state (Li *et al.*, 2005). Rho-family GTPases like RhoA (discussed below) activate formins by binding to the GBD domain, thereby disrupting the autoinhibited state (Otomo *et al.*, 2005).

1.1.5 WH2 domain-containing actin nucleators

The most recently discovered group of actin nucleators are classified based on the possession of tandem clusters of G-actin binding WASP-homology 2 (WH2) domain-containing motifs, including Spire, cordon-bleu (Cobl), and leiomodin (Lmod) family of proteins (Qualmann *et al.*, 2009). Little is known about the mechanism of these actin nucleators, although the ability of WH2 domains to bind G-actin suggests they overcome the kinetic barrier of actin nucleation by tethering monomeric actin to form multimer-actin nuclei. Despite possessing the same WH2 domains that bind actin,

most class I NPFs do not nucleate actin *in vitro*. Recent progress on our understanding of WH2-mediated actin nucleation arose from studies of Spire and the chimeric NPF p53-cofactor JMY (Figure 2). Although Spire possesses four tandem WH2 domains that provide maximal activity, the third and fourth WH2 domains linked by a novel 15 aa actin-binding motif are sufficient to drive actin nucleation (Quinlan *et al.*, 2005, Bosch *et al.*, 2007). This novel linker motif is also conserved in JMY, an NPF that possesses three tandem WH2 domains followed by a CA domain (Zuchero *et al.*, 2009). JMY thus activates Arp2/3-mediated actin nucleation, but also possesses Spire-like Arp2/3-independent nucleation activity. Intriguingly, swapping of this linker motif between the WH2 domains of N-WASP is sufficient to trigger Arp2/3-independent nucleation activity *in vitro* (Zuchero *et al.*, 2009). Importantly, Spire also contains an N-terminal kinase non-catalytic C-lobe domain (KIND) that interacts with the FH2 domain of the *Drosophila* formin cappuccino, and that a Spire:cappuccino complex enhances actin nucleation by Spire (Quinlan *et al.*, 2005, Bosch *et al.*, 2007).

1.2 Apoptosis

Apoptosis is a term first used by Kerr and co-workers (1972) to describe a distinct form of programmed cell death (Kerr *et al.*, 1972). Physiologically, apoptosis occurs during development and ageing and as a "homeostatic mechanism to maintain cell populations in tissues" (Elmore, 2007). Apoptosis also occurs during immune reactions or infection, or triggered by the absence of stimuli. For example, "anoikis", or detachment-induced apoptosis, is a variant of apoptosis that is triggered by the misregulation or absence of integrin-dependent survival signals during adherence to the extracellular matrix (ECM) (Gilmore, 2005). Depending on the stimulus,

apoptosis occurs via two distinct, classical pathways – the extrinsic or death receptor pathway and the intrinsic or mitochondrial pathway (Figure 3). A third pathway also exists for cytotoxic T-cell lymphocytes (CTL) that trigger perforin/granzyme-mediated apoptosis but is not discussed further (Elmore, 2007). All apoptotic pathways eventually converge on an execution pathway that is initiated by cleavage/activation of cysteine-dependent aspartate-directed proteases (caspases).

Caspases are a family of cysteine proteases necessary for the apoptotic and inflammatory responses. Caspases are synthesized as inactive procaspases, which are activated upon proteolytic processing (Budihardjo *et al.*, 1999). Once active, caspases have strict specificity for their intracellular substrates, and cleave proteins at aspartic acid residues. Caspases are subdivided into initiator caspases (caspase-2, -8, -9, and -10) and executioner caspases (caspase-3, -6, and -7), as well as inflammatory caspases (caspase-1, -4, and -5) (Budihardjo *et al.*, 1999). The main substrates of initiator caspases are the executioner caspases, which then process other cellular proteins during apoptosis. Initiator caspases are activated upon signals transduced by the intrinsic or extrinsic pathways. The process of apoptosis is generally considered irreversible upon activation of caspase-3 (Elmore, 2007).

1.2.1 Morphology of apoptosis

Several stages of apoptosis have been identified based on morphological changes that occur as the cell dies. The early stage of apoptosis is characterized by cell contraction, dynamic membrane blebbing, and condensation of nuclear chromatin (pyknosis) (Kerr *et al.*, 1972). The apoptotic cell appears rounded with a dense cytoplasm, tightly packed organelles and a uniformly dense nucleus. This is followed closely by

dynamic membrane blebbing, a feature that occurs when the hydrodynamic forces within the cell exceed the tethering force given by cytoskeletal structures (Elmore, 2007). The next stage of apoptosis is characterized by the breakdown of cytoskeletal structures, and the "budding" of membrane blebs into smaller vesicles known as apoptotic bodies (Elmore, 2007). The final stage of apoptosis involves the engulfment and degradation of apoptotic bodies within phagolysosomes by macrophages (Elmore, 2007). Beyond morphological features, apoptosis is also characterized by the fragmentation of nuclear DNA, (Enari *et al.*, 1998, Sakahira *et al.*, 1998) and restricted caspase-mediated proteolysis of hundreds of proteins (Elmore, 2007). While cell lysis does not occur during apoptosis, the plasma membrane is permeabilized, allowing the release of small cytoplasmic proteins such as lactate dehydrogenase (LDH). LDH is routinely used as a marker for dead cells.

1.2.2 Intrinsic (mitochondria) pathway

The intrinsic pathway is mediated by intracellular signals that can be triggered by absence of signals (e.g. lack of growth factors or cytokines that lead to the relief of apoptotic suppression pathways), or positive stimuli that activate the intrinsic pathway, (e.g. toxins or infections). The summation of these signals induces changes to mitochondrial membrane potential (Elmore, 2007) (Figure 3). Mitochondrial outer membrane permeabilization (MOMP) leads to the release of pro-apoptotic proteins from the mitochondrial intermembraneal space (IMS) (Green *et al.*, 2004). A group of pro-apoptotic proteins are released which participates in the induction of the intrinsic pathway. This includes cytochrome *c,* second mitochondria-derived activator of caspase (Smac)/DIABLO, and the serine protease HtrA2/Omi (Cai *et al.*, 1998, Du *et al.*, 2000, van Loo *et al.*, 2002). Cytochrome *c* binds and activates the apoptotic

protease-activating factor 1 (Apaf-1) to form the "apoptosome". The apoptosome then activates procaspase-9 to trigger the caspase cascade. Smac/DIABLO and HltrA2/Omi have both been shown to block X-linked inhibitor of apoptosis proteins (IAPs), which inhibits caspase activity (Du *et al.*, 2000, van Loo *et al.*, 2002). A second group of pro-apoptotic proteins are also released which function after the cell commits to die. These include AIF (Joza *et al.*, 2001), endonuclease G (Li *et al.*, 2001), and caspase-activated DNAse (CAD) (Enari *et al.*, 1998, Sakahira *et al.*, 1998) which induce chromatin condensation and oligonucleosomal DNA fragmentation.

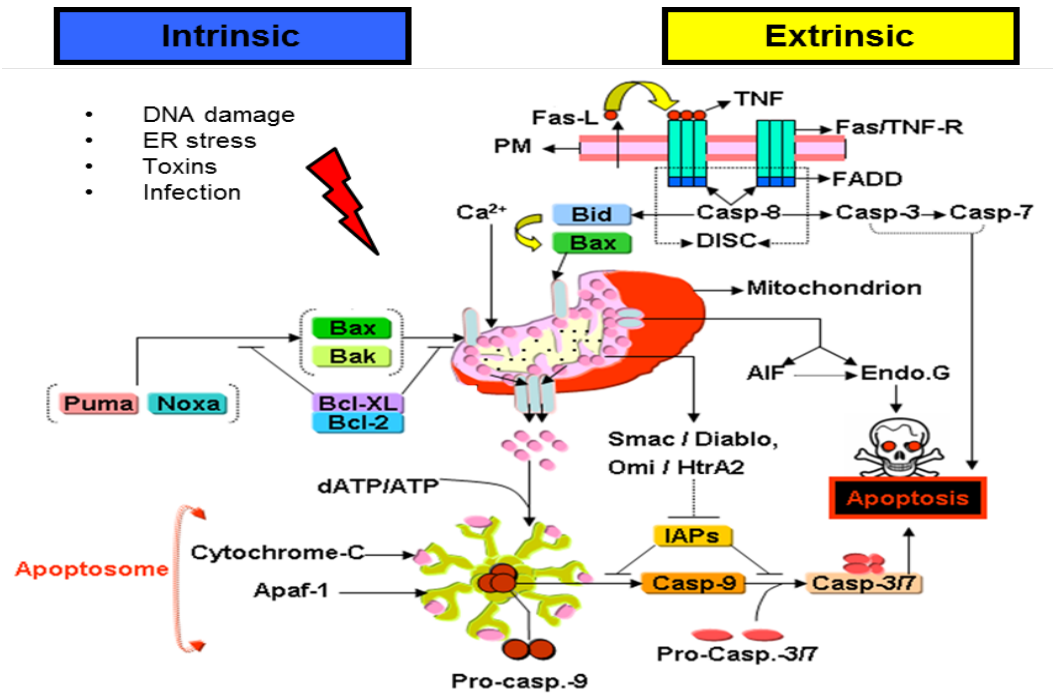


Figure 3. Overview of intrinsic and extrinsic apoptotic pathways.

Schematic representation of the intrinsic and extrinsic apoptotic pathways leading to the execution pathway. Details are found in sections 1.2.2 to 1.2.4. Image adapted from (Elmore, 2007).

MOMP is tightly regulated by the B cell lymphoma-2 (Bcl-2) family of proteins, which are classified based on their Bcl-2 homology (BH) domain organization (Youle *et al.*, 2008). Pro-apoptotic proteins, such as Bax and Bak, are essential for the

activation of MOMP. Bax translocates into the mitochondria during apoptosis, while Bak is normally bound to Bcl-XL at the mitochondria. Anti-apoptotic proteins, such as Bcl-2 and Bcl-XL, bind and inhibit Bax and Bak (Youle *et al.*, 2008). A third group consists of Bcl-2 homology 3 (BH3)-only proteins such as Bid, Noxa, Bad, and PUMA. Their pro-apoptotic mechanism remains controversial; opposing studies have shown that BH3-only proteins either binds and sequesters anti-apoptotic Bcl-2 members to de-repress Bax and Bak (Yang *et al.*, 1995, Willis *et al.*, 2007), or bind directly to Bax and Bak to activate them (Kuwana *et al.*, 2005). Bad has also been shown to be serine-phosphorylated and this leads to its association with 14-3-3 which sequesters it in the cytosol (Zha *et al.*, 1996).

1.2.3 Extrinsic (death-receptor) pathway

The extrinsic pathway is mediated by transmembrane receptors at the cell surface, including death receptors that are members of the tumor necrosis factor (TNF) receptor superfamily (Elmore, 2007) (Figure 3). Members of death receptors share a cytoplasmic domain known as the "death domain" which transmit extrinsic death signals from the cell surface to intracellular signaling pathways (Ashkenazi *et al.*, 1998). The best-characterized are the fatty acid synthetase receptor (FasR)/CD95 and TNF-receptor (TNFR). The extrinsic pathway initiates upon binding of CD95/Fas ligand (FasL) and TNF-α to their respective receptors, which induces the recruitment of cytoplasmic adaptor proteins Fas-associated death domain (FADD) or TNF receptor-associated death domain (TRADD) with the recruitment of FADD and receptor-interacting serine/threonine-protein kinase 1 (RIP1/RIPK1) (Hsu *et al.*, 1995, Grimm *et al.*, 1996). FADD in turn dimerizes and binds procaspase-8, resulting in the formation of a death-inducing signaling complex (DISC) that triggers activation of

procaspase-8 and subsequent activation of caspase-3 and -7 (Kischkel *et al.*, 1995). However, the ability of active caspase-8 to trigger MOMP-independent apoptosis is limited to a subgroup of cells (termed type I) (Scaffidi *et al.*, 1998). A second subgroup of cells (termed type II) requires MOMP, which occurs through caspase-8-mediated cleavage of the BH3-interacting domain death agonist (Bid) (Luo *et al.*, 1998) (Figure 3). This step is crucial as MOMP-induced xIAP antagonism is required for induction of apoptosis in type II cells.

1.2.4 Execution pathway

Both extrinsic and intrinsic pathways end in the execution phase, and this occurs upon activation of the executioner caspases. Hundreds of substrates are cleaved by caspase-3, including cytoskeletal constituents such as actin, myosin, gelsolin and Rho GTPases (Riedl *et al.*, 2004). One prominent substrate is Rho-associated protein kinase 1 (ROCK1), where cleavage by caspase-3 leads to its constitutive activity (Sebbagh *et al.*, 2001). ROCK1 stimulates acto-myosin contractibility to generate the mechanical force required for cell shrinkage (Coleman *et al.*, 2001). Intermediate filaments and microtubule-associated proteins are also degraded, contributing to cytoskeletal collapse (Taylor *et al.*, 2008). Caspases also dismantle cell-matrix adhesion sites by degrading focal adhesion proteins, including focal adhesion kinase (Levkau *et al.*, 1998) and p130cas (Kook *et al.*, 2000), leading to the extrusion of dying cells.

In addition to activating endonucleases, caspases trigger the disintegration of nuclear lamins (Rao *et al.*, 1996) to promote nuclear fragmentation (Croft *et al.*, 2005). The culmination of the execution pathway is formation of apoptotic bodies. ROCK1-

mediated actin:myosin contractions generate membrane blebs which pinch off into independent vesicles (Cotter *et al.*, 1992). Microtubules are implicated in relocating fragmented chromatin into peripheral blebs (Moss *et al.*, 2006), although our overall understanding of apoptotic body formation is patently lacking.

1.3 Rho GTPases

1.3.1 Classical Rho GTPases

Rho GTPases are a subgroup of the Ras superfamily of GTPases that are ubiquitously expressed in yeast, plants and mammals. Mammalian Rho GTPases comprise a family of 20 intracellular signaling molecules that regulate various cellular processes including actin polymerization, microtubule dynamics, cell polarity, vesicle trafficking and cytokinesis (Heasman *et al.*, 2008). They are however best known as key regulators of actin dynamics, of which Rho, Rac and Cdc42 are the three best-characterized members of the family (Hall, 1998).

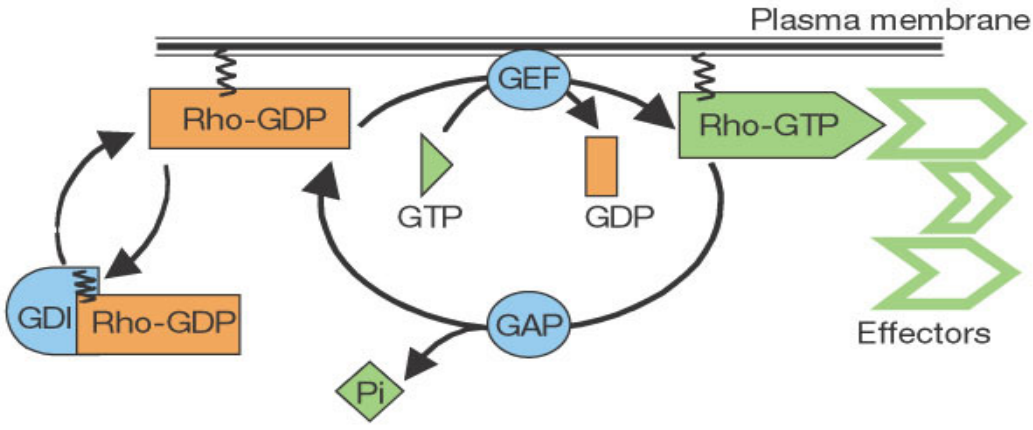


Figure 4. Overview of Rho GTPase regulation in mammalian cells.

Schematic representation of the role of GEFs, GAPs and GDIs in the regulation of Rho GTPases. Details are found in section 1.3. Image taken from (Etienne-Manneville *et al.*, 2002)

Classical Rho GTPases switch between active GTP-bound and inactive GDP-bound forms, and the cycling between these two states is regulated by three sets of proteins – guanine exchange factors (GEFs), GTPase-activating proteins (GAPs) and guanine nucleotide-dissociation inhibitors (GDI) (Figure 4) (Jaffe *et al.*, 2005). It is in the active GTP-bound state that Rho GTPases perform their regulatory function through interactions with target effector proteins to initiate downstream signaling. The association of Rho GTPases in subcellular compartments is dictated by post-translational modification at their C-terminal CAAX motif, in which the cysteine residue is prenylated by addition of farnesyl or geranylgeranyl isoprenoid lipids (Jaffe *et al.*, 2005). Over 60 effectors have been identified so far for Rho, Rac, and Cdc42 that include serine/threonine kinases, tyrosine kinases, lipid kinases and scaffold proteins (Jaffe *et al.*, 2005). Exceptions of classical Rho GTPases are Rnd1, Rnd2, Rnd3 (RhoE), and RhoH which exhibit no or low GTPase activity because they lack essential amino acids required to catalyze this reaction (Ridley, 2006).

1.3.2 Rho guanine nucleotide exchange factors (GEFs)

Rho GTPases possess two loops called switch I and II that bind guanine nucleotides on either side, a phosphate (P) loop that binds to phosphates of the bound nucleotide, and an Mg^{2+} binding pocket which binds a Mg^{2+} co-factor and is required for high-affinity binding of nucleotides at the switch region (Rossman *et al.*, 2005). RhoGEFs catalyze the exchange of GDP to GTP within the switch region by promoting the release of Mg^{2+} and guanine nucleotides. Replacement of guanine nucleotides favour GTP-binding as there is an order higher concentration of GTP than GDP in the cytoplasm (Rossman *et al.*, 2005). Two major classes of RhoGEFs have emerged –

the diffuse B-cell-lymphoma (Dbl) family of RhoGEFs, and the dedicator of cytokinesis (DOCK) family of RhoGEFs.

Dbl RhoGEFs are characterized by the presence of Dbl homology-peckstrin homology (DH-PH) tandem domains that function cooperatively to catalyze GDP/GTP exchange. The DH domain forms the catalytic core, while the PH domain mediates phospholipid binding and/or participates in DH-mediated GEF activity. DOCK RhoGEFs are grouped based on the presence of two conserved domains, DOCK homology regions 1 and 2 (DHR1/2). DHR1 mediates phosphoinositide binding, while DHR2 acts as the catalytic site for nucleotide exchange (Meller *et al.*, 2005, Cote *et al.*, 2007). Activation of GEFs by DH and DHR2 domains occur by different molecular mechanisms. The DHR2 domain interacts mainly with switch I region without altering the switch II regions (Yang *et al.*, 2009), while the DH domain binds both switch I and II regions (Liu *et al.*, 1998, Worthylake *et al.*, 2000). Either mechanism leads to disruption of bound-GDP, and exposes the nucleotide-binding site for subsequent binding of GTP. In addition, most RhoGEFs possess additional catalytic, protein-protein and protein-lipid interacting domains, including Ser/Thr kinase, PDZ, SH3, FYVE and BAR domains (Rossman *et al.*, 2005). These domains serve as scaffolds that mediate localization and activity of RhoGEF, or integrate different upstream signals that converge on its GEF function.

1.3.3 Rho GTPase-activating proteins (GAPs)

Despite being GTPases, the intrinsic GTP hydrolysis activity of Rho GTPase is low – RhoGAPs accelerate the GTP hydrolysis process by many orders. RhoGAPs are classified based on the presence of a conserved RhoGAP domain, and also contain

additional domains that mediate its localization and function (Peck *et al.*, 2002). Structural studies of GAPs in complex with small G proteins have revealed general similarities in their activation (Barrett *et al.*, 1997, Scheffzek *et al.*, 1997). A loop containing a primary arginine residue (also called "arginine finger") contacts the β-phosphate of GTP and the switch region (Rittinger *et al.*, 1997a, Rittinger *et al.*, 1997b). The result is a better-ordered transition-state complex that presents a water molecule in an optimal position for hydrolysis.

1.3.4 Rho GDP dissociation inhibitors (GDIs)

The RhoGDI family consists of three members, namely the ubiquitous RhoGDIα, the haemotopoeitic RhoGDIβ, and the selectively expressed RhoGDIγ (Dovas *et al.*, 2005). RhoGDIα specifically binds Rho GTPases in its prenylated form (Hoffman *et al.*, 2000, Grizot *et al.*, 2001). The N-terminal domain of RhoGDIα interacts with nucleotide-bound Rho GTPases at the switch region, and has been shown to inhibit both GDP association and GTPase functions, effectively neutralizing GEF/GAP-mediated regulation (Keep *et al.*, 1997). The C-terminal domain interacts with the isoprenyl group of at the CAAX motif, and in doing so directs the N-terminal inhibitory domain to sequester active Rho GTPases at the membrane into the cytosol (Gosser *et al.*, 1997). The function of RhoGDI is not solely inhibitory; RhoGDIs maintain a pool for cytosolic Rho GTPases, which are quickly degraded if not bound in a Rho-RhoGDI complex (Dovas *et al.*, 2005). Dissociation of Rho-RhoGDI complexes occur via phosphorylation of RhoGDIα by protein kinase C or PAK (Price *et al.*, 2003, DerMardirossian *et al.*, 2004), binding of RhoGDI to the ezrin/radixin/moesin (ERM) family of proteins (Hirao *et al.*, 1996), and binding of $PI(4,5)P_2$ (Chuang *et al.*, 1993). As such, phospholipids can coordinate the

dissociation of Rho-RhoGDI complexes with the recruitment and activation of Rho GTPases by RhoGEFs.

1.3.5 Regulation of actin dynamics by Rho GTPases

As described in sections 1.1.3 and 1.1.4, Cdc42 and Rac play a pivotal role in Arp2/3-mediated actin polymerization through the binding and activation of WASP and WAVE family NPFs, while RhoA activates formins to trigger the formation of unbranched actin filaments. The result of this is the generation of distinct higher-order actin structures that are associated with their respective Rho GTPases – filopodia (Cdc42), lamellipodia (Cdc42/Rac1) and stress fibers (RhoA) (Hall, 1998). Filopodia are finger-like projections that extend beyond the leading edge of migrating cells and contain straight cross-linked actin bundles. Initial studies using dominant-positive and dominant-negative Cdc42 showed that the GEF/Cdc42/N-WASP pathway triggers filopodia formation (Nobes *et al.*, 1995). However, N-WASP-deficient and Arp2/3-deficient cells are still able to form filopodia, indicating that this is not the only pathway (Snapper *et al.*, 2001, Steffen *et al.*, 2006). Furthermore, it is not known how N-WASP is able to trigger the formation of bundled actin filaments from Arp2/3-mediated actin polymerization that generates branched filaments; indeed recent studies have implicated formins in filopodium formation (Schirenbeck *et al.*, 2005). While the overall picture is still unclear, the current evidence suggests that there may be different types of filopodia that exist within the cell.

Lamellipodia are a meshwork of actin filaments that extend at the leading edge of a migrating cell (Nobes *et al.*, 1995). As actin filaments from lamellipodia are branched at 70°, it is most likely Arp2/3-mediated. Furthermore, WAVE2 has been shown to be

essential for lamellipodia formation downstream of Rac, as WAVE2-deficient fibroblasts are unable to form lamellipodia (Steffen *et al.*, 2006). Embedded within the lamellipodia are also ribs of actin filaments that become filopodia when they extend beyond the lamellipodium. It is thought that Cdc42/N-WASP cooperates by initiating actin nucleation, which then serves as branching points during Rac/WAVE activation (Ridley, 2006).

Stress fibers are composed of actin bundles held together by the actin-crosslinking protein α-actinin (Pellegrin *et al.*, 2007). α-actinin is located periodically along stress fibers, and alternates with bands of actin that are rich in myosin II (Lazarides *et al.*, 1975). Myosin motors are proposed to slide between alternating polar arrays of actin filaments to cause shortening, although the actin filaments do not always orientate with alternating polarity (Pellegrin *et al.*, 2007). Stress fibers are divided into three classes: ventral stress fibers that lie across the base of the cell and are attached to integrin-rich focal adhesion at each end, dorsal stress fibers that have one end attached to focal adhesions at the base of the cell and the other terminating at the dorsal surface, and transverse arcs that form beneath the dorsal surface, just behind the protrusive lamella (Cramer *et al.*, 1997). In addition to mDia1, ROCK1/2 are implicated in the formation of thick parallel stress fibers upon RhoA activation (Leung *et al.*, 1995, Watanabe *et al.*, 1997). ROCK partially localizes to stress fibers and phosphorylates myosin light chain 2 (MLC2), leading to increased stress fiber contractibility (Katoh *et al.*, 2001). In addition, ROCK also phosphorylates the myosin binding subunit (MBS) of myosin phosphatase to inhibit its phosphatase activity, leading to increased stress fiber formation (Kimura *et al.*, 1996).

Rho GTPases are also known to affect actin polymerization by regulating cofilin. Phosphorylation of cofilin leads to its inactivation, and this occurs primarily through the activity of LIM kinases (LIMK) (Jaffe *et al.*, 2005). The p21-activating kinase (PAK) family are somewhat promiscuous targets for Rho GTPases as most of the closest relatives of Rac1 and Cdc42 have been reported to activate at least one of these kinases (Figure 8), implying that they should all act via LIMK to inactivate cofilin (Ridley, 2006). In addition, LIMK can also be induced by Rho acting through ROCK, and it has been suggested that this may be important for the stability of actin:myosin filaments (Ohashi *et al.*, 2000).

1.3.6 Regulation of focal adhesions by Rho GTPases

The regulation of focal adhesions by Rho GTPases is inextricably linked to cell migration, a process that involves dynamic phases of cell protrusion and contraction. As filopodia extend out at the front of the cell to form initial contact with the substrate, a lamellipodium then protrudes in the direction of the filopodium, and attaches to the substrate (Nobes *et al.*, 1999). Lamellipodial protrusions then coincide with contractile forces generated by stress fibers, leading to the retraction of the tail (Nobes *et al.*, 1999). Cell adhesion provides the necessary traction for the pulling force, and this is achieved by the formation of nascent focal complexes at lamellipodial protrusions that mature into focal adhesions (FA) (Owen *et al.*, 2007). Lamellipodia that fail to establish stable adhesions become detached from the substrate, generating waves of densely packed actin filaments known as “membrane ruffles” that emerge at the cell edge and move centripetally, finally disappearing at the cell body (Abercrombie *et al.*, 1970a, Abercrombie *et al.*, 1970b). In addition, the formation of focal adhesions at the leading edge of the cell must also be coordinated

with the disassembly of mature focal adhesions at the trailing edge to allow cell retraction. This dynamic process of focal adhesion assembly and disassembly is known as "FA turnover" (Webb *et al.*, 2002). Interestingly, a stationary cell possesses increased stress fibers and focal adhesions compared to a migrating cell, indicating that stress fibers are not only required for efficient cell migration but also for anchorage onto the substrate (Webb *et al.*, 2002).

An important mediator of focal adhesion dynamics is focal adhesion kinase (FAK) (Mitra *et al.*, 2005). FAK is a protein tyrosine kinase that is implicated in the formation of nascent focal complexes at lamellipodial protrusions (Nobes *et al.*, 1995, Zaidel-Bar *et al.*, 2003), as well as disassembly of mature focal adhesions (Ren *et al.*, 2000). The major phosphorylation site of FAK is Y397 (Kornberg *et al.*, 1991, Kornberg *et al.*, 1992), which recruits c-Src to form a FAK-Src signaling complex (Schaller *et al.*, 1994) that then activates multiple signaling pathways (Mitra *et al.*, 2005). Intriguingly, FAK-null fibroblasts show reduced migration, and severe FA turnover defects but are strongly adherent, exhibiting high Rho activity and increased focal adhesion numbers (Ilic *et al.*, 1995). Recent studies have shown that FAK regulates the localization and activity of Rho GTPases by recruiting RhoGEFs (Chikumi *et al.*, 2002, Zhai *et al.*, 2003, Lim *et al.*, 2008) and RhoGAPs (Tomar *et al.*, 2009a) at focal adhesion sites to facilitate FA turnover and cell migration.

1.3.7 Regulation of apoptosis by Rho GTPases

As Rho GTPases are upstream regulators of diverse cellular processes, it is difficult to assess the contributions of individual downstream signaling pathways. Nevertheless, studies using *Clostridial* C3 toxin and TcdA/B that inactivate Rho GTPases have

conclusively demonstrated the cytotoxic effects of Rho inactivation in different cell types (Fiorentini *et al.*, 1998, Hippenstiel *et al.*, 2002, Qa'Dan *et al.*, 2002, Gerhard *et al.*, 2008). These observations include cell contraction, nuclear condensation, mitochondrial dysfunction, and caspase-3 activation, all of them features of apoptosis. However, constitutive expression of Rho GTPases is not necessarily anti-apoptotic – several studies have implicated the role of Cdc42/Rac1 in promoting survival through PAK-mediated phosphorylation of Bad and activation of NF-κB (Schurmann *et al.*, 2000, Karin *et al.*, 2002), but the induction of inflammatory cytokines has also been shown to trigger Fas/TNF extrinsic pathways (Brenner *et al.*, 1997).

While RhoA triggers ROCK phosphorylation and stress fiber formation which promotes cell survival, ROCK is implicated in MLC phosphorylation and cell contraction during the early stage of apoptosis independently of RhoA (Coleman *et al.*, 2001). As the apoptotic program progresses, caspase-mediated cleavage of Cdc42/Rac1 results in the termination of their downstream signaling function, thus relieving PAK-mediated inhibition of Bad to facilitate commitment to apoptosis (Schurmann *et al.*, 2000). However, caspase-mediated cleavage of PAK2 releases constitutively active kinase fragments that promote actin-myosin destabilization through phosphorylation and inhibition of MLCK, thus antagonizing ROCK activity (Rudel *et al.*, 1997). The events that occur during apoptosis thus appear to be decoupled from that of regular Rho signaling, and that the contribution of these contradictory signals during the apoptotic process would ultimately depend on their signal intensities over time (Coleman *et al.*, 2002).

1.4 Gram-negative bacterial secretion systems

Protein secretion plays a critical role in modulating the interactions between the bacterium and other organisms. In Gram-negative bacteria, proteins have to be translocated across inner (IM) and outer (OM) membranes. There are now six general classes of protein secretion systems that mediate the export of proteins out of the bacterial cell wall. This includes specialized secretion systems that translocate protein across both membranes in a single step (e.g. type I, III IV, VI secretion systems), as well as secretion systems that first export proteins into the periplasm via general secretory pathways (e.g. Sec, Tat), then translocated across the OM via other secretion systems (e.g. type II, V secretion systems) in two-steps (Figure 5). A specialized type VII secretion secretion system has been described in Gram-positive *Mycobacterium*, but is not discussed further.

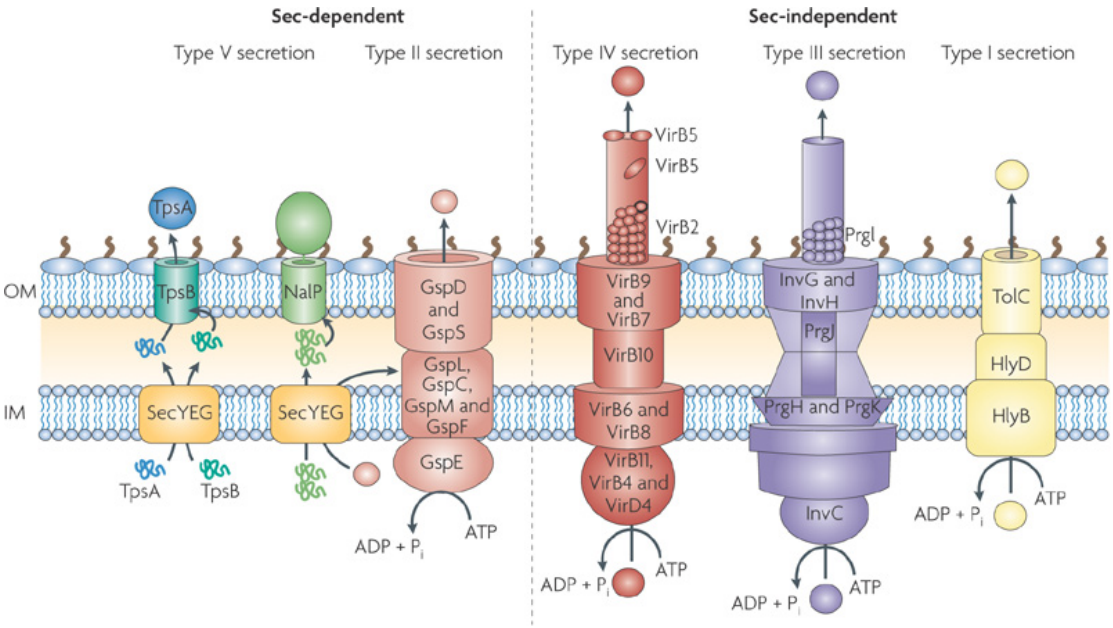


Figure 5. Overview of Gram-negative bacterial secretion systems.

Schematic representation of the different Sec-dependent (type II and V) and Sec-independent (type I, III, IV) secretion systems. Details are found in section 1.4. Image taken from (Fronzes *et al.*, 2009).

1.4.1 General secretory (Sec) and two-arginine (Tat) pathways

The general secretory (Sec) and two-arginine (Tat) pathways are utilized by Archaea and Gram-positive bacteria to secrete proteins across a single plasma membrane; in Gram-negative bacteria, they are responsible for the secretion of proteins into the periplasm (Papanikou *et al.*, 2007). The Sec translocase consists of a SecY/SecE/SecG heterotrimer that is inserted into the inner membrane, as well as a cytoplasmic SecA ATPase that binds SecY to provide the energy required for translocation (Papanikou *et al.*, 2007). Proteins targeted for export are recognized in two ways. A hydrophobic N-terminal leader sequence in proteins targets it, together with its bound ribosome, to the translocase (Papanikou *et al.*, 2007). Other secreted proteins are first translated, then recognized by the SecB chaperone and targeted to SecA at the translocase in a bound complex.

The Tat secretion translocase consists of membrane proteins TatA, TatB and TatC. TatA has been proposed to be major pore-forming subunit of the translocase, while TatC is involved in substrate recognition (Muller, 2005). Several studies have implicated a proton-motive force as the source of energy for protein export, although no distinct mechanism has been identified for Tat-dependent export (Muller, 2005). The Tat secretion signal is given by a distinct twin-arginine motif with the consensus motif S-R-R-x-F-L-K that is present at the N-terminal region of proteins. One major difference between the two secretion pathways is that the Tat pathway transports proteins across the transmembrane in a fully-folded state (Muller, 2005).

1.4.2 Type I secretion

Type I secretion systems (T1SS) are capable of exporting a diverse range of macromolecules including small peptides, complex carbohydrates and large proteins. A typical T1SS consists of 3 major components: an ATP-binding cassette (ABC) transporter, outer membrane factors (OMFs), and membrane fusion proteins (MFP) (Holland *et al.*, 2005). OMFs provide a channel that spans the periplasm through to the OM while the ABC transporter contains 2 cytoplasmic domains for ATP hydrolysis, and 2 integral transmembrane domains that embed it within the IM. The MFP connects the OMF and ABC transporter in the periplasmic space. One of the best-studied T1SS is the TolC-HlyD-HlyB complex of uropathogenic *Escherichia coli* that exports the haemolytic toxin HlyA (Koronakis *et al.*, 2004). TolC (OMF) forms a trimer comprising an α-helical trans-periplasmic tunnel and a β-barrel embedded in the OM, HlyB (ABC) is located within the IM and periplasm, while HlyD (MFP) binds and connects both proteins in the periplasm.

1.4.3 Type II secretion

The type II secretion system (T2SS) bears evolutionary similarities to the type IV pilus apparatus (Filloux, 2004). A set of 12 – 16 core components are found in all functional T2SS, including the outer membrane secretin (GspD), a cytoplasmic ATPase (GspE), an inner transmembrane protein (GspF), pseudopilins that span the periplasm (GspG – K), and connectors that facilitate the attachment of ATPase to the inner membrane (GspL, GspM) (Filloux, 2004). GspD forms a homomultimeric channel at the outer membrane with a large central opening in the periplasm, while GspL/M anchors the cytoplasmic ATPase GspE and GspF to form the inner membrane platform (Filloux, 2004). Pseudopilins are incorporated into a pseudopilus

structure that extends from the inner membrane platform within the periplasm. The pseudopilus either mechanically pushes out proteins destined for export, or retracts to allow access to the central opening (Filloux, 2004). Access to the opening of GspD is also governed by GspC, which interacts with the periplasmic domain of GspD. The ADP-ribosylating toxins of ETEC (heat-labile toxin) and *V. cholerae* (cholera toxin) are secreted by the T2SS (Filloux, 2004).

1.4.4 Type III secretion

The type III secretion system (T3SS) is found in Gram-negative bacteria that interact with eukaryotic hosts, either as pathogens or mutualists, and bear evolutionary similarities to the flagellum (Grant *et al.*, 2006, Cornelis, 2006). The principal function of the T3SS apparatus is to directly translocate effector proteins across both bacterial and host membranes into the cytosol of host cells to modulate host cell functions. The central component is a supramolecular structure known as the needle complex, which is composed of two pairs of rings that span the inner and outer membrane, joined together by a periplasmic rod (Cornelis, 2006). Visualization of different T3SS needle complexes using transmission electron microscopy (TEM) reveal a generally similar structure and shape (Cornelis, 2006). Assembly of the T3SS is sequential, first involving the export of membrane-bound components by the Sec pathway to form a basal structure. Cytosolic components are then added to the existing basal structure to energize and promote protein secretion.

In enteropathogenic *Eschierichia coli* (EPEC) and enterohaemorrhagic *E. coli* (EHEC), the OM ring structure is composed of EscC (InvG in *Salmonella*), a member of the secretin family of proteins. EscV (PrgH in *Salmonella*), together with EscR–U

form the membrane-bound components of IM ring structures (Gauthier *et al.*, 2003). EscJ has been proposed to fulfill the functions of both PrgJ and PrgK of *Salmonella*, by spanning the periplasm to bridge the inner and outer membrane protein rings (Crepin *et al.*, 2005a). EscF (PrgI in *Salmonella*) is the needle that forms an outward projection channel required for secretion of translocator and effector proteins (Wilson *et al.*, 2001). The F_0F_1-related ATPase EscN (InvC in *Salmonella*) is then added to the basal structure, and provides the energy to promote the export machinery and protein secretion (Akeda *et al.*, 2004). The unique feature of the EPEC/EHEC T3SS is a filamentous extension to the EscF needle, called the EspA filament (Daniell *et al.*, 2003). The EspA filament is a hollow helical tube composed of EspA monomers that polymerize at the distal end of the growing filament, a process similar to flagellar elongation (Crepin *et al.*, 2005b). Effector proteins are then delivered into the host cell cytoplasm using this filamentous extension, through a translocation pore formed by translocator proteins EspB and EspD (Daniell *et al.*, 2001, Kresse *et al.*, 1999).

1.4.5 Type IV secretion

The type IV secretion system (T4SS) is perhaps the most versatile of all secretion systems. Three groups of T4SS have been defined according to function (Fronzes *et al.*, 2009). The first mediates DNA conjugation into both prokaryotic and eukaryotic cells, the second mediates DNA transformation with extracellular milieu through uptake and release of DNA, while the third mediates effector protein delivery into eukaryotic cells. Despite the diverse functions, all T4SS share several core components that probably possess similar functions. The best studied is the VirB/D T4SS of *Agrobacterium tumefaciens* which comprises VirB1 – B11/VirD4, and is capable of exporting DNA-protein complexes into plant cells (Christie *et al.*, 2005).

In a contemporary model, the core complex consisting of VirB7/VirB9/VirB10 is first assembled before the inner-membrane pore proteins VirB6/VirB8, and ATPase complex consisting VirB4/VirB11/VirD4, dock onto the core complex to establish the secretion channel (Fronzes *et al.*, 2009). VirB2/VirB5 are then recruited to form the extracellular pilus of the secretion channel (T-pilus), completing T4SS assembly.

1.4.6 Type V secretion

The type V secretion system (T5SS) is divided into three subclasses, namely the autotransporter system (T5aSS), the two-partner system (T5bSS), and an oligomeric autotransporter system (T5cSS) (Dautin *et al.*, 2007). Proteins secreted via the T5aSS consists of an N-terminal signal peptide that directs their export into the periplasm via the Sec system, a passenger domain that confers effector function, and a C-terminal helper domain that adopts a β-barrel tertiary structure within the outer membrane to facilitate translocation of the passenger domain through the outer membrane (Dautin *et al.*, 2007). An example of this is the autotransporter NalP of *Neisseria meningitis*. In contrast, the T5bSS system consists of protein pairs where one is the passenger domain (TpsA), while the other carries the helper domain (TpsB) (Dautin *et al.*, 2007). T5cSS proteins oligomerize to form a single β-barrel structure that then facilitates the transport of multiple passenger domains (Dautin *et al.*, 2007). The energy dependence of the T5SS is unresolved (Dautin *et al.*, 2007).

1.4.7 Type VI secretion

The core complex of the recently identified type VI secretion (T6SS) is still not well-characterized, although several components appear to resemble the tail spike complex of the T4 bacteriophage (Filloux *et al.*, 2008). This includes Hcp1, which

spontaneously form hexameric ring tubes that constitutes the phage tail tube (Mougous *et al.*, 2006), and VgrG that appear to be a fusion of proteins that constitute the puncturing device of the tail spike complex (Pukatzki *et al.*, 2007). Other components include IcmF-like and DotU-like proteins of the *L. pneumophila* T4SS are located in the inner membrane (Filloux *et al.*, 2008). Recent studies have also identified the ATPase ClpV as the energizing force for T6SS (Filloux *et al.*, 2008). Recent work on the characterization of T6SS effectors has uncovered intriguing insights to the function of the T6SS. Russell and co-workers (2011) showed that the HSI-I/T6SS of *P. aeruginosa* is capable of delivering Tse1 and Tse3 into the periplasm where it promotes lysis of other bacteria by targeting the peptidoglycan cell wall while protecting itself from the toxins by also synthesizing Tsi1 and Tsi3 immunity proteins (Russell *et al.*, 2011). A similar HSI-I/T6SS-mediated Tse2/Tsi2 toxin-antitoxin strategy has also been reported (Hood *et al.*, 2010).

1.5 Pathogenic *Escherichia coli*

Escherichia coli is a Gram-negative bacterium that constitutes one of the predominant strains of bacteria in the human gastrointestinal tract, where they naturally colonize the mucous layer of the mammalian colon. While this commensal relationship between host and microbe is seldom breached, several highly adapted *E. coli* clones have acquired the ability to cause enteric diseases, referred to as pathogenic strains. Pathogenic strains possess novel genomic islands and small gene clusters that are associated with virulence, conferring the bacteria a superior level of adaptation that facilitates efficient colonization of new ecological niches as well as dissemination to new hosts (Kaper *et al.*, 2004). Among the intestinal *E. coli* pathogens are six well-

described categories: enteropathogenic *E. coli* (EPEC), enterohaemorrhagic *E. coli* (EHEC), enterotoxigenic *E. coli* (ETEC), enteroaggregative *E. coli* (EAEC), enteroinvasive *E. coli* (EIEC) and diffusely adherent *E. coli* (DAEC) (Kaper *et al.*, 2004) (Figure 6). Together, these pathotypes are implicated in over 2 million deaths each year. Pathotypes are classified by shared O (lipopolysaccharide, LPS) and H (flagellar) antigens that define its serotype (Nataro *et al.*, 1998), as only a few clonal subtypes of *E. coli* are associated with each pathotype (Deborah Chen *et al.*, 2005).

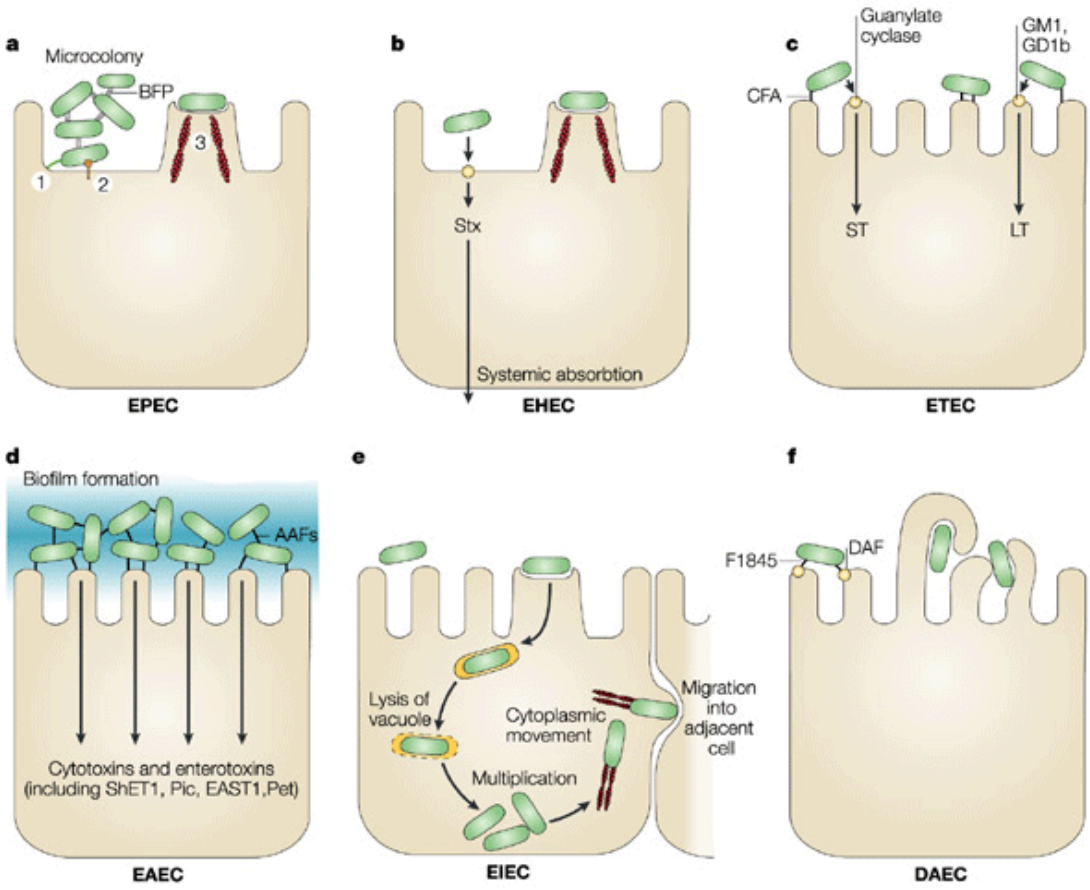


Figure 6. Overview of the different intestinal *Escherichia coli* pathotypes.

Schematic representation of the infection strategies of the six categories of intestinal *E. coli* pathogens - enteropathogenic *E. coli* (EPEC), enterohaemorrhagic *E. coli* (EHEC), enterotoxigenic *E. coli* (ETEC), enteroaggregative *E. coli* (EAEC), enteroinvasive *E. coli* (EIEC) and diffusely adherent *E. coli* (DAEC). Details are found in section 1.5 and 1.7. Image taken from (Kaper *et al.*, 2004).

1.5.1 Enterotoxigenic *E. coli* (ETEC)

ETEC is defined as *E. coli* that secretes at least one of two groups of enterotoxins – heat-labile toxins (LT) or heat-stable toxins (ST) (Nataro *et al.*, 1998). ETEC is a major cause of travellers' diarrhea, as well as childhood diarrhea in developing countries. Symptoms of ETEC vary from self-limiting watery diarrhea to severe purging (Nataro *et al.*, 1998). Colonization is mediated by fimbrial or fibrillar colonization adhesins (CFAs) (Wolf, 1997). The induction of watery diarrhea is mediated by secretion of LT and/or ST. LT constitutively activates adenylate cyclase activity by ADP-ribosylating the stimulatory G protein that regulates adenylate cyclase activity. This results in increased levels of intracellular cyclic AMP (cAMP), activation of the major chloride ion channel cystic fibrosis transmembrane conducatance regulator (CFTR), and chloride ion secretion that passively draws water out (Spangler, 1992). STs are small peptide toxins that include STa and STb. STa appears to mimic the endogenous ligand guanylin and activate the guanylate cyclase receptor, leading to increased cGMP levels and ultimately fluid secretion (Currie *et al.*, 1992). STb was shown to increase intracellular calcium levels and release of prostaglandin E2, both of which lead to increased ion secretion (Nataro *et al.*, 1998).

1.5.2 Enteroaggregative *E. coli* (EAEC)

EAEC is defined as *E. coli* that do not secrete LT or ST and adhere to HEp-2 cells in a "stacked-brick", or auto-aggregative manner (Nataro *et al.*, 1998). EAEC are known to cause large diarrheal outbreaks in children and adults worldwide, most notably being the May 2011 outbreak in Germany (Rasko *et al.*, 2011). Its infection cycle begins with colonization of the intestinal mucosa, followed by secretion of enterotoxins and cytotoxins. Adherence to the intestinal mucosa is primarily mediated

by fimbrial structures known as aggregative adherence fimbriae (AAFs) (Nataro *et al.*, 1992). Another protein, dispersin, forms a loose layer of EAEC strains and appears to counteract AAF adhesion to facilitate spreading across the mucosal surface or penetration of the mucous layer (Sheikh *et al.*, 2002). Several toxins are secreted which contribute to EAEC-induced diarrhea, including *Shigella* enterotoxin 1 (ShET1) and enteroaggregative *E. coli* ST 1 (EAST1) (Noriega *et al.*, 1995, Savarino *et al.*, 1993). In the Germany outbreak, the EAEC strain laterally acquired a prophage containing the *Shiga* toxin 2 (Stx2) that resulted in a large proportion of patients developing hemolytic uremic syndrome (HUS) (Rasko *et al.*, 2011).

1.5.3 Enteroinvasive *E. coli* (EIEC)

EIEC has been shown to be closely related to *Shigella* species in terms of pathogenesis (Nataro *et al.*, 1998). Most genes involved in *Shigella* pathogenesis, such as the *mxi* and *spa* loci, are also found in EIEC. Infection with EIEC initiates with penetration of the epithelial cell layer, followed by lysis of the endocytic vacuole, intracellular replication, cytoplasmic motility and dissemination in to adjacent epithelial cells (Kaper *et al.*, 2004). The Mxi/Spa encodes a T3SS that translocates multiple effectors to mediate cell signaling events including uptake, lysis of the endocytic vacuole and inflammatory pathways (Kaper *et al.*, 2004). Movement within the cytoplasm is mediated by IcsA (Chapter 1.6.3).

1.5.4 Diffusely adherent *E. coli* (DAEC)

In contrast to EAEC, DAEC is defined as *E. coli* which show a diffuse pattern of adherence to HEp-2 monolayers (Nataro *et al.*, 1998). DAEC is an important cause of diarrhea in children more than 12 months of age (Nataro *et al.*, 1998). Little is known

about DAEC pathogenesis, although studies on their adherence show that DAEC induces finger-like projections that extend and "wrap" around the bacteria without complete internalization (Yamamoto *et al.*, 1994, Cookson *et al.*, 1996). This phenotype is dependent on a fimbrial adhesin known as F1845. F1845 binds to the decay accelerating factor (DAF), a cell surface protein that protects the cells from its complement system (Bernet-Camard *et al.*, 1996, Peiffer *et al.*, 1998). A DAF-independent phenotype has also been described where brush-border hydrolases are impaired (Peiffer *et al.*, 2001).

1.5.5 Enteropathogenic *E. coli* (EPEC)

EPEC is the first pathotype to be implicated in human disease (Levine *et al.*, 1978). It remains an important agent of infantile diarrhea in the developing world (Nataro *et al.*, 1998, Deborah Chen *et al.*, 2005). EPEC is distinguished between typical EPEC (harbouring the EPEC adherence factor (EAF) plasmid) and atypical EPEC (missing the EAF plasmid) (Kaper, 1996). The World Health Organisation has assigned typical EPEC to serogroups O26, O55, O111, O114, O119, O125, O127, O128, O142 and O158 (Deborah Chen *et al.*, 2005). EPEC is further divided into 4 EPEC lineages based on its H antigen and intimin subtype (Kaper, 1996, Whale *et al.*, 2007). EPEC-1 (H6 and intimin-α) is represented by the prototypical O127:H6 strain E2348/69, EPEC-2 (H2/H- and intimin-β) is represented by O111:H- strain B171 while EPEC-3 (H34 and intimin-κ) and EPEC-4 (H6 and intimin- β2) are more recent additions.

1.5.6 Enterohaemorrhagic *E. coli* (EHEC)

EHEC represents a different epidemiological scenario from EPEC, largely affecting industrialised and developed countries (Karch *et al.*, 2005). The principal reservoir of

EHEC is the bovine intestinal tract, and EHEC only incidentally cause disease in humans (Vega *et al.*, 2007). Outbreaks are typically associated with the consumption of undercooked meat, and notably the consumption of a wide range of contaminated food items ranging from lettuce to radish sprouts (Kaper *et al.*, 2004). EHEC is known to cause haemorrhagic colitis (HC) and haemolytic uremic syndrome (HUS). Expression of Shiga toxin (Stx) is a major discriminator of EHEC from EPEC, and the severe clinical symptoms are generally attributed to its cytotoxic activity (Karch *et al.*, 2005). EHEC is divided into 2 lineages. The EHEC-1 O157:H7 serotype (expressing intimin-γ) remains the most important EHEC pathogens in North America, the United Kingdom and Japan, although EHEC-2 O26 and O111 serogroups (expressing intimin-β) are also prominent in many countries (Kaper *et al.*, 2004). EHEC is represented by the O157:H7 strain EDL933 (Perna *et al.*, 2001). EPEC and EHEC are classified under a subgroup of intestinal pathogens that have evolved the use of attaching-and-effacing (A/E) lesion formation as their infection strategy (further discussed in section 1.7).

1.6 Subversion of actin dynamics by bacterial pathogens

Several bacterial pathogens are known to subvert the actin cytoskeleton during pathogenesis to facilitate attachment, intracellular entry, motility, fitness and dissemination (Cossart *et al.*, 2004, Stevens *et al.*, 2006). While the molecular mechanisms utilized by bacterial pathogens are varied, their cellular targets are often similar, suggesting that pathogens have co-evolved independently to target or mimic the same host cell proteins.

1.6.1 Bacterial actin nucleation factors

Bacterial effector proteins have been shown to directly nucleate actin filaments via the use of multiple WH2 domains in a formin-like dimerization manner reminiscent of Spire:cappuccino complex formation (Qualmann *et al.*, 2009). Thus far, four effectors, namely *Vibrio* outer protein (Vop)F from *V. cholerae*, VopL from *V. parahaemolyticus*, the translocated actin-recruiting phosphoprotein (TARP) of *Chlamydia trichomatis*, and the surface cell antigen 2 (Sca2) of *Rickettsia* have been identified and characterized (Jewett *et al.*, 2006, Tripathi *et al.*, 2010, Liverman *et al.*, 2007, Haglund *et al.*, 2010). VopL induces formation of stress fibers and is recruited along their lengths, while VopF induces aberrant actin-rich protrusions and is recruited to the tips of these protrusions (Tam *et al.*, 2010). Both consist of one or two proline-rich motifs, followed by three tandem WH2 domains, and a unique VopL C-terminal domain (VCD). The VCD dimerizes to form a U-shaped dimeric structure that enhances actin nucleation by stabilizing the lateral contacts of actin monomers bound to the third WH2 domain (Yu *et al.*, 2011). Remarkably, Sca2 of *Rickettsia* also share similar attributes – it possesses an N-terminal domain that is similar to the FH2 domain of formins, and three tandem WH2 domains and one proline-rich motif (Haglund *et al.*, 2010). Sca2 may thus mechanistically operate in the same manner as VopF/VopL. Interestingly, some *Rickettsia* species also possesses RickA, an NPF mimic that activates the Arp2/3 complex. In contrast, TARP only possesses a single WH2 domain, and requires oligomerization mediated by an N-terminal proline-rich motif for nucleation activity *in vitro* (Jewett *et al.*, 2006). The relevance of actin nucleation activity in TARP to invasion is not clear, as TARP also binds Rac GEFs to activate WAVE2-mediated Arp2/3 actin polymerization (Backert *et al.*, 2005).

1.6.2 Bacterial NPF mimics

Bacterial pathogens have also developed strategies to target Arp2/3-mediated actin polymerization. These can generally be grouped into two groups – bacterial effectors that mimic NPFs and bacterial effectors that activate NPFs (Figure 7). *Listeria monocytogenes*, a facultative intracellular pathogen, is able to invade non-phagocytic cells and utilize actin-based motility, characterized by the formation of actin-rich "comet tails", to spread from cell to cell (Lambrechts *et al.*, 2008). The outer protein both necessary and sufficient for actin-based motility is ActA, which activates the Arp2/3 complex by mimicking the NPF activity of N-WASP (Welch *et al.*, 1998). The N-terminal region of the protein contains a WCA-like domain and is sufficient to activate the Arp2/3 complex *in vitro* (Welch *et al.*, 1998). The *R. coronii* effector RickA is also capable of activating the Arp2/3 complex *in vitro* in a manner similar to ActA (Gouin *et al.*, 2004). However, expression of a dominant-negative VCA segment only abrogates actin tails formed by *R. coronii*, but not other *Rickettsia* species (Harlander *et al.*, 2003, Serio *et al.*, 2010). Indeed, unlike ActA which forms branched actin filament tails, *Rickettsia rickettsii* tails comprise long parallel actin filaments, suggesting that *Rickettsia* species may have co-opted two different strategies to mediate actin-based motility (Van Kirk *et al.*, 2000). Alternatively, RickA and Sca2 could cooperate in a manner where RickA initiates actin polymerization while Sca2 or other host cell factors mediate actin tail elongation.

A third member belonging to the group of NPF mimics is BimA, a T5SS effector that is found in *Burkholderia* species (Stevens *et al.*, 2005). BimA of *B. thaliendensis* possesses a unique CA domain in addition to N-terminal WH2 domains that is indicative of NPFs (Sitthidet *et al.*, 2010). However, other species like *B. mallei*, and

B. pseudomallei, possess BimA homologues that are capable of weakly stimulating actin polymerization in an Arp2/3-independent manner, suggesting that BimA could also operate in a manner similar to WH2-containing actin nucleators (Stevens *et al.*, 2005). This is supported by the observation that expression of a VCA segment does not abrogate *B. pseudomallei*-induced actin tails (Breitbach *et al.*, 2003).

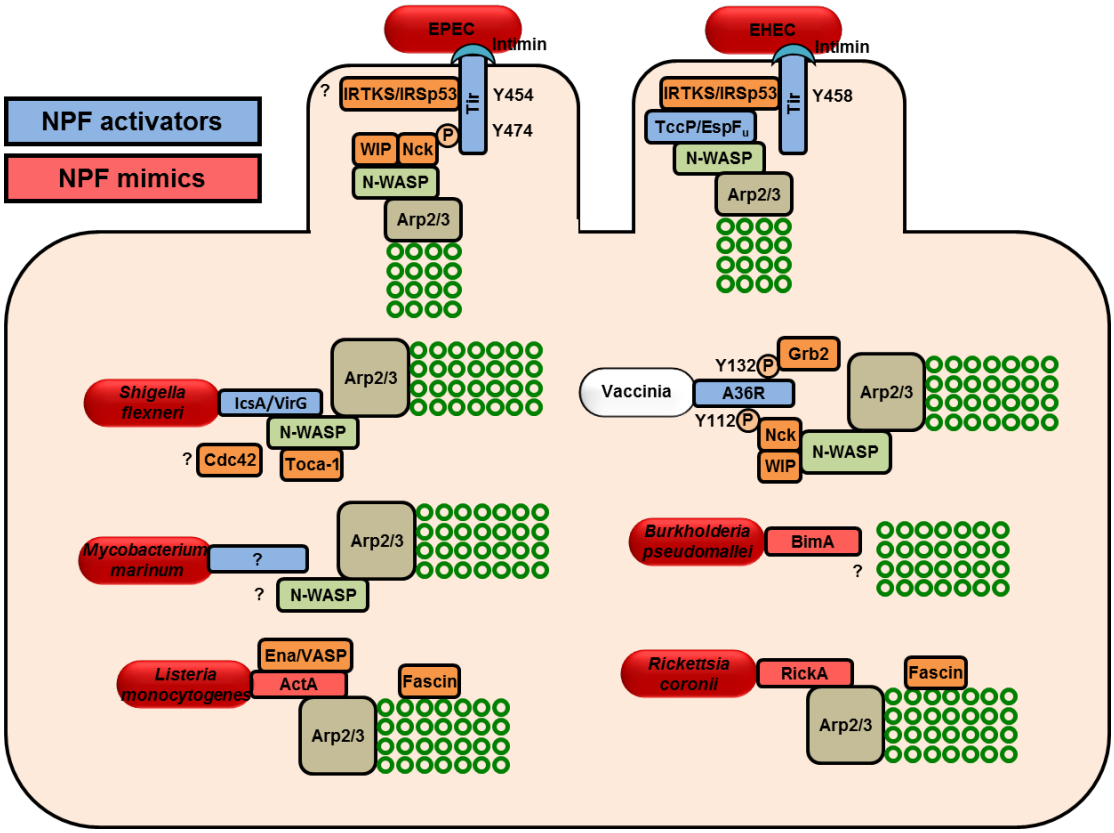


Figure 7. Subversion of the Arp2/3 complex by bacterial pathogens.

Schematic representation of the different strategies utilized by bacterial pathogens to subvert Arp2/3-mediated actin polymerization during infection. Note that *Vaccinia* (white) is not a bacterium, but shares many characteristics of Arp2/3 activation with EPEC. Details are found in section 1.6.2, 1.6.3, and 1.8.2.

1.6.3 Bacterial NPF activators

Several pathogens have also opted to hijack cellular NPFs during infection. *Shigella* is a facultative intracellular pathogen that uses actin-based motility to facilitate cell-to-cell spreading (Cossart *et al.*, 2004). In contrast to *L. monocytogenes*, *Shigella*

encodes the T5SS outer membrane protein IcsA/VirG that recruits and activates N-WASP (Figure 7). There are however alternative reports describing the molecular mechanism of N-WASP activation. It has been proposed that IcsA utilizes Cdc42 for N-WASP activation (Suzuki *et al.*, 2000). However, other reports have shown that Ccdc42 (Moreau *et al.*, 2000), and the CRIB domain of N-WASP is dispensable for tail formation (Lommel *et al.*, 2001). The role of Cdc42 during actin-based motility is also unclear. Although inactivation of Cdc42 by *Clostridium* toxin B does not affect actin tail formation (Mounier *et al.*, 1999), the inactivation of the upstream regulator Toca-1 abolishes *Shigella* actin tail formation (Leung *et al.*, 2008). Recently, the Gram-positive bacterium *Mycobacterium marinum* has also been reported to utilize N-WASP to mediate Arp2/3-dependent actin tail formation (Stamm *et al.*, 2005), although the mechanism is not known.

1.6.4 Subversion of Rho GTPase signaling by bacterial pathogens

As Rho GTPases are master regulators of the actin cytoskeleton, bacterial pathogens have also evolved several elaborate strategies to subvert Rho GTPase signaling in mammalian cells. These can be generally classified into three types of mechanisms, namely covalent modification, molecular mimicry and competitive inhibition (summarized in Figure 8). Most of the covalent modifications occur at or near the switch regions of Rho GTPases. ADP-ribosylation by *Clostridium botulinum* c3 toxin at Asn41 (Rubin *et al.*, 1988, Sekine *et al.*, 1989), AMPylation by *Vibrio parahaemolyticus* VopS (Yarbrough *et al.*, 2009) as well as glucosylation by *Clostridium difficile* toxin B (TcdB) at Thr37 (Just *et al.*, 1995), all occur along the switch I region of Rho GTPases, while deamidation by uropathogenic *E. coli* cytotoxic necrotizing factor 1 (CNF1) (Schmidt *et al.*, 1997, Flatau *et al.*, 1997) as

well as ADP-ribosylation by *Photorhabdus luminescens* toxin complex C5 (TcC5) at Gln63 (Lang *et al.*, 2010) occur along the switch II region. Covalent modifications at the switch I region all appear to inhibit Rho GTPase activity by preventing GEF association; in addition, ADP-ribosylated Rho GTPases also appear to bind more tightly to RhoGDIs (Genth *et al.*, 2003). On the other hand, the same modification at the switch II region by TcC5 has been shown to inhibit its GTP hydrolysis activity, leading to constitutive activation (Lang *et al.*, 2010). Intriguingly, deamidation of Rho GTPases by CNF1 leads its constitutive activation, but also increases its susceptibility to ubiquitination and consequent degradation (Doye *et al.*, 2002). In addition, covalent modification of Rho GTPases is not solely confined at the switch region. The *Yersinia* T3SS effector YopT has been shown to be target the CAAX motif of Rho GTPases, and acts as a cysteine protease that cleaves the CAAX motif, thus abolishing membrane localization of Rho GTPases leading to its loss of function (Shao *et al.*, 2002, Shao *et al.*, 2003).

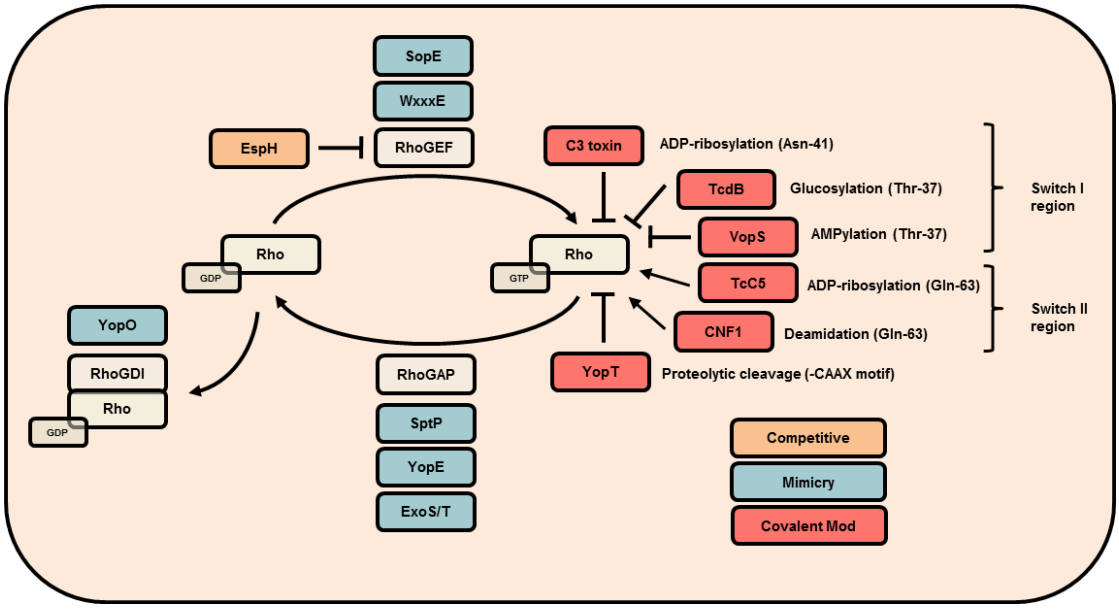


Figure 8. Subversion of Rho GTPase signaling by bacterial pathogens.

Schematic representation of the different strategies utilized by bacterial pathogens to subvert Rho GTPase signaling during infection. Details are found in section 1.6.4.

Covalent modification of Rho GTPases is more often than not irreversible. Molecular mimicry is a mechanism where bacterial pathogens utilize bacterial effectors that mimic the cellular functions of RhoGEFs, RhoGAPs or RhoGDIs to exercise spatiotemporal control over Rho GTPase signaling. For example, *Salmonella* Typhimurium temporally regulates Cdc42/Rac1 by delivering SopE (Hardt *et al.*, 1998) and SptP (Fu *et al.*, 1998). SopE is a bacterial RhoGEF that activates Cdc42/Rac1 which induces the "trigger mechanism" of bacterial invasion (Wood *et al.*, 1996, Hardt *et al.*, 1998), but is quickly degraded (Kubori *et al.*, 2003). SptP exhibits GAP activity (Stebbins *et al.*, 2000) but slower degradation kinetics, thus allowing recovery from SopE-induced membrane ruffling (Kubori *et al.*, 2003).

Recently, a group of T3SS effectors were, based on an invariant Trp-xxx-Glu motif, grouped together as the WxxxE-family of effectors. Members include EspM, EspT and Map of EPEC/EHEC (discussed in Chapter 1.7.5), as well as SifA and SifB of *Salmonella*, and IpgB1 and IpgB2 of *Shigella* (Alto *et al.*, 2006, Bulgin *et al.*, 2010). With the exception of SifA and SifB, all members have been shown to activate Rho GTPases, with structural studies of Map, EspM2 and IpgB2 showing that they possess a SopE-like fold and hence mimic the activity of mammalian RhoGEFs (Huang *et al.*, 2009, Arbeloa *et al.*, 2010, Klink *et al.*, 2010). Examples of mimicry are also evident in RhoGAPs, including ExoS and ExoT of *Pseudomonas aeruginosa* (Barbieri *et al.*, 2004), and YopE of *Yersinia* (Andor *et al.*, 2001, Aili *et al.*, 2006). In addition, the *Yersinia* effector YpkA/YopO has also been shown to possess a GDI-like domain, and is able to bind and sequester both Rac1 and RhoA (Prehna *et al.*, 2006). Another mechanism is that of competitive inhibition. Thus far, only the EPEC/EHEC effector

EspH has been shown to bind promiscuously to DH-PH domains of RhoGEFs and inhibit Rho GTPase signaling (Dong *et al.*, 2010) (EspH is further discussed in 1.7.7).

1.7 Attaching and effacing (A/E) pathogens

Enteropathogenic *E.coli* (EPEC) and Enterohaemorrhagic *E. coli* (EHEC) are a subgroup of intestinal pathogens that have evolved the use of attaching-and-effacing (A/E) lesion formation (Figure 9) as a major mechanism for tissue colonization and histopathology. The A/E histopathology is characterized by the effacement of microvilli, and intimate adherence between bacterium and epithelial cell membrane over an elevated 'pedestal-like' structure (Figure 9) (Knutton *et al.*, 1987). This is concomitant with the induction of rapid watery diarrhea, inhibition of nutrient/water transporter function, mitochondrial dysfunction, weak inflammatory response and tight junction disruption (Deborah Chen *et al.*, 2005, Dean *et al.*, 2009). In the bovine host, EHEC O157:H7 colonizes the terminal rectum to produce A/E lesions, although they are generally not associated with clinical disease (Naylor *et al.*, 2003). The initial site of EHEC colonization in humans is at present unknown, although it was shown *ex vivo* that binding and A/E lesion formation of EHEC O157:H7 was restricted to the follicle-associated epithelium of ileal Peyer's patches (Phillips *et al.*, 2000b, Phillips *et al.*, 2000a). Significantly, the murine-specific pathogen *Citrobacter rodentium* is also able to induce the A/E histopathology and colonic hyperplasia in mice, and serves as an *in vivo* model for the study of A/E pathogenesis (Mundy *et al.*, 2005).

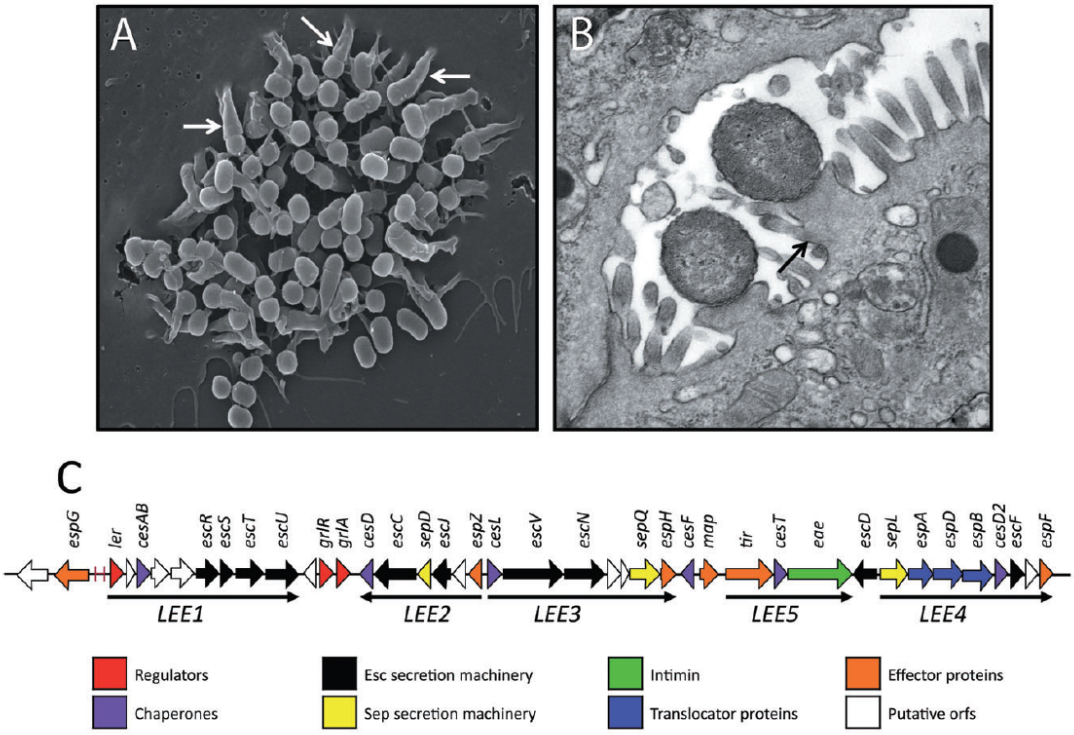


Figure 9. A/E lesion histopathology and the locus of enterocyte effacement (LEE).

(A) Scanning electron micrograph of actin pedestal induced by adherent bacteria. (B) Transmission electron micrograph showing intestinal A/E lesions. (C) Genetic organization of the locus of enterocyte effacement (LEE) region from EPEC. Image taken from (Wong *et al.*, 2011).

1.7.1 Locus of Enterocyte Effacement (LEE) Pathogenicity Island

The ability to induce A/E histopathology is encoded by genes on a pathogenicity island (PAI) called the locus of enterocyte effacement (LEE) (McDaniel *et al.*, 1995). The complete sequence of the LEE of the EPEC strain E2348/69 shows 41 open reading frames arranged in five polycistronic operons LEE1 to LEE5 (Figure 9C) (Elliott *et al.*, 1998). These open reading frames encode LEE gene regulators, the adhesin intimin, a T3SS apparatus, effector proteins and their associated chaperones. Seven LEE-encoded effectors are known to date – EspB, EspZ, Map, EspH, EspG, EspF and Tir (Figure 2). Regulation of LEE is complex and not well understood. In addition to environmental conditions and quorum sensing, several regulators, notably the EAF plasmid-encoded regulator (Per), LEE-encoded regulator (Ler), global

regulator of LEE activator (GrlA) and global regulator of LEE repressor (GrlR) are implicated in the regulation of LEE gene expression (Kaper *et al.*, 2004). Regulation of the secretion machinery is also achieved post-translation by the activity of SepD and SepL. A *sepD* and *sepL* mutant secretes markedly lower quantities of translocator proteins EspA, EspB and EspD, and also excessively secretes effector proteins (Deng *et al.*, 2004, O'Connell *et al.*, 2004). This suggests that they could serve as a molecular "switch" from secretion of translocator to effector proteins.

1.7.2 Intimate attachment by the bacterial adhesin intimin

The gene *eae* encodes the 94kDa outer membrane adhesin intimin. Intimin possesses two functional regions. The N-terminal region is highly conserved between different EPEC and EHEC strain and is inserted into the bacterial outer membrane, forming a β-barrel-like structure (Touze *et al.*, 2004). A 280 amino acid sequence at the C-terminal (Int280) is however variable, and defines several intimin subtypes that contribute to tissue tropism; EPEC-1 expresses intimin-α, EPEC-2 and *C. rodentium* express intimin-β that colonize the small intestine, while EHEC O157:H7 expresses intimin-γ and colonizes the colon and Peyer's patches in the gut (Frankel *et al.*, 2001, Phillips *et al.*, 2000a). Int280 is made up of two immunoglobulin-like domains and a C-type lectin-like domain, which together with the last immunoglobulin-like domain contains the receptor-binding site (Batchelor *et al.*, 2000, Luo *et al.*, 2000).

Intimin binds to the translocated intimin receptor (Tir) (Kenny *et al.*, 1997). Upon translocation, Tir spontaneously inserts into the plasma membrane of the eukaryotic cell (Kenny *et al.*, 1997). Tir contains two transmembrane domain, and forms a hairpin-like topology such that both its N- and C- termini are located within the host

cell, and the region between the two transmembrane domains forming an extracellular loop that interacts with intimin (de Grado *et al.*, 1999, Hartland *et al.*, 1999). The conformation of the intimin-Tir complex is such that each of the two Tir-binding domains of the intimin dimer interacts with Tir molecules of different Tir dimers, thus generating a reticular array-like conformation that clusters Tir under adherent bacteria (Touze *et al.*, 2004). This directly links and anchors the bacterium to the host cell membrane, allowing it to remain on the extracellular surface while subverting host cell functions through several other effector proteins. The ability to translocate its own unique receptor is however difficult to reconcile with the concept of intimin-mediated tissue tropism (Deborah Chen *et al.*, 2005). Indeed intimin has been shown to be able to bind to β1-integrins (Frankel *et al.*, 1996) and nucleolin (Sinclair *et al.*, 2004), and that nucleolin is colocalized under adherent bacteria. This suggests that host cell receptors could still potentially play a role in bacterial-host interaction.

1.7.3 LEE and non-LEE encoded T3SS effectors

In addition to the LEE-encoded effectors that are conserved in both EPEC and EHEC, it is now evident that a number of effector proteins that are found in many A/E pathogens are carried on prophages (PP) or other integrative elements (IE), and are translocated into the host cell via the LEE-encoded T3SS (Deng *et al.*, 2004, Tobe *et al.*, 2006). The completion of the E2348/69 genomic sequence (Iguchi *et al.*, 2009) has now confirmed the presence of 21 putative LEE and non-LEE encoded effector genes, compared to 28 in EPEC B171-8, 40 in rabbit EPEC E22, and over 50 effector genes in EHEC O157:H7 (Tobe *et al.*, 2006). Our current knowledge of the A/E translocome is summarized in Table 1. Indeed, non-LEE encoded effectors have been shown to play important roles– examples include TccP that is encoded in prophage

CP-933U (Garmendia *et al.*, 2004, Campellone *et al.*, 2004a), as well as the WxxxE effectors EspT and EspM that modulate actin dynamics through the activation of Rho GTPases (Arbeloa *et al.*, 2008, Bulgin *et al.*, 2009b). The simplicity of the E2348/69 translocome may however represent a core set of effectors for A/E pathogenesis.

Table 1. Translocome of A/E pathogens.
Taken from (Wong et al., 2011).

T3SS effector	Presence[a]			Subcellular localization	Host binding partners	Homologs [BLASTp]	Cellular function	References
	EPEC	EHEC	CR[b]					
LEE encoded effectors								
EspB	1	1	1	Cytosol PM[c]	α_1-antitrypsin, α-catenin, Myosin-1c	YopD	Translocation pore component, AJ disruption, binds myosins to inhibit phagocytosis	(Iizumi *et al.*, 2007, Knappstein *et al.*, 2004, Kodama *et al.*, 2002, Hamaguchi *et al.*, 2008)
Tir	1	1	1	PM	14-3-3tau, α-actinin, cortactin, CK18, IQGAP1, IRTKS, IRSp53, Nck, PI3K, Talin, Vinculin	None known	Receptor for the adhesion intimin, actin pedestal formation, down-regulates Map-dependent filopodia formation, SGLT-1 inactivation	(Patel *et al.*, 2006, Goosney *et al.*, 2000, Freeman *et al.*, 2000, Cantarelli *et al.*, 2007, Nieto-Pelegrin *et al.*, 2009, Batchelor *et al.*, 2004, Brown *et al.*, 2008, Vingadassalom *et al.*, 2009, Weiss *et al.*, 2009, Gruenheid S, 2001, Kenny *et al.*, 2002, Berger *et al.*, 2009, Dean *et al.*, 2006)
EspF	1	1	1	Mitochondria Cytosol Nucleus TJ[d] Apical membrane Lateral membrane	14-3-3zeta, ABCF2, actin, Arp2, CK18, N-WASP, Profilin, SNX9, ZO-1/ZO-2	TccP/EspFu	Mitochondrial disruption, NHE3 inactivation, SGLT-1 inactivation, TJ disruption, disrupts nucleolus, disrupts intermediate filaments, activates SNX9 to induce membrane remodelling, binds and activates N-WASP, inhibits PI3K-dependent phagocytosis	(Viswanathan *et al.*, 2004, Nougayrede *et al.*, 2007, Peralta-Ramirez *et al.*, 2008, Marches *et al.*, 2006, Alto *et al.*, 2007, Hodges *et al.*, 2008, Dean *et al.*, 2006, Thanabalasuriar *et al.*, 2010, Dean *et al.*, 2004, Muza-Moons *et al.*, 2004, McNamara *et al.*, 2001, Guttman *et al.*, 2006, Dean *et al.*, 2010, Quitard *et al.*, 2006)
Map	1	1	1	Mitochondria	EBP50 (NHERF1), NHERF2, Cdc42	IpgB, SopE	Cdc42 GEF that induces transient filopodia formation, mitochondrial disruption, SGLT-1 inactivation, TJ disruption	(Alto *et al.*, 2006, Simpson *et al.*, 2006, Huang *et al.*, 2009, Martinez *et al.*, 2010, Papatheodorou *et al.*, 2006, Dean *et al.*, 2006, Ma *et al.*, 2006, Dean *et al.*, 2004, Thanabalasuriar *et al.*, 2010)
EspG	2	1	1	Cytosol Golgi	Tubulin, Arf1/6, PAK1/2/3	VirA	Disrupts microtubules, blocks ARF GTPase signaling and stimulates PAKs to inhibit endomembrane trafficking	(Matsuzawa *et al.*, 2004, Selyunin *et al.*, 2011, Tomson *et al.*, 2005, Hardwidge *et al.*, 2005, Shaw *et al.*, 2005b)
EspH	1	1	1	PM	DH-PH RhoGEFs	None known	Blocks Rho GTPase signaling and	(Tu *et al.*, 2003, Dong *et al.*, 2010)

EspZ	1	1	1	PM	CD98	None known	Enhances β1-integrin and FAK signaling to inhibit apoptosis and cellular cytotoxicity	(Shames *et al.*, 2010)
Non-LEE encoded effectors								
EspI/ NleA	1	1	1	Golgi PM	Syntrophin, Sec23/24, MALS3, PDZK11, SNX27, TCOF1, NHERF1/2, MAGI-3, SAP97, SAP102, PSD-95	None known	Inhibits COPII-dependent protein export from ER, TJ disruption	(Gruenheid *et al.*, 2004, Lee *et al.*, 2008, Kim *et al.*, 2007, Thanabalasuriar *et al.*, 2010)
EspJ	1	1	1	Cytosol Mitochondria	Unknown	HopF	Inhibits FCγR-mediated and CR3-mediated trans-phagocytosis	(Marches *et al.*, 2008) (Kurushima *et al.*, 2010)
EspK	0	1	1	Unknown	Unknown	GogB	Unknown	
EspL	3 (2)	4 (1)	1	Pedestal	Annexin 2	OspD	Enhances F-actin bundling activity of Annexin 2	(Miyahara *et al.*, 2009)
EspM	0	2	3 (1)	Cytosol	RhoA	IpgB, SopE	RhoA GEF that induces stress fibre formation	(Arbeloa *et al.*, 2010, Arbeloa *et al.*, 2008)
EspN	0	1	3 (2)	Unknown	Unknown	SARI_01330 SARI_01464 SeAg_B1500 CNF1	Unknown	
EspO	1 (1)	2	1	Unknown	Integrin-linked kinase (ILK)	OspE, SopO	Stabilizes focal adhesions	(Kim *et al.*, 2009)
EspR	0	4 (1)	0	Unknown	Unknown	SF1757	Unknown	
EspS	0	0	1	Unknown	Unknown	OspB	Unknown	
EspT	0	0	1	Mitochondria	Unknown	IpgB, SopE	Activates Cdc42 and Rac1 that induces membrane ruffles and lammelipodia, promotes intracellular bacterial uptake via trigger mechanism	(Bulgin *et al.*, 2009b, Bulgin *et al.*, 2009a)
EspV	0	1(1)	1	Cytosol	Unknown	AvrA1	Modulates cytoskeleton	(Arbeloa *et al.*, 2011)
EspW	0	1	0	Unknown	Unknown	HopPmaA, HopW1	Unknown	
EspX	0	7 (1)	1	Unknown	Unknown	Sd1012_0237 SSON_0027	Unknown	
EspY	0	5 (1)	0	Unknown	Unknown	SopD	Unknown	
NleB	3 (1)	3 (1)	2 (1)	Cytosol	Unknown	SseK	Inhibits TNF-induced NF-κB activation	(Newton *et al.*, 2010, Nadler *et al.*, 2010)

NleC	1	1	1	Cytosol Nucleus	p65 (RelA), p50, c-Rel, IκB	AIP56	Metalloprotease that cleaves p65 (RelA), c-Rel, p50 and IκB to inhibit NF-κB activation	(Yen *et al.*, 2010, Baruch *et al.*, 2011, Muehlen *et al.*, 2010, Pearson *et al.*, 2011)
NleD	1	1	2	Cytosol	JNK	HopAP1, HopH1	Metalloprotease that cleaves JNK to inhibit AP-1 activation	(Baruch *et al.*, 2011)
NleE	2	1	1	Cytosol	Unknown	OspZ	Blocks IκB degradation to inhibit NF-κB activation	(Newton *et al.*, 2010, Nadler *et al.*, 2010, Vossenkamper *et al.*, 2010)
NleF	1	1	1	Unknown	Unknown	None known	Unknown	
NleG/ NleI	1	14 (5)	5 (2)	Cytosol	UBE2D2	STY1076	U-box E3 ubiquitin ligase	(Wu *et al.*, 2010)
NleH	3 (1)	2	1	ER[e] PM Cytosol	Bax-inhibitor 1, NHERF2, RPS3	OspG	Binds Bax-inhibitor 1 to block apoptosis, sequesters RPS3 to inhibit NF-κB signalling	(Hemrajani *et al.*, 2010, Gao *et al.*, 2009, Martinez *et al.*, 2010);(Royan *et al.*, 2010)
NleK	0	0	1	Unknown	Unknown	STY1628	Unknown	
Cif	1 (1)	0	0	Nucleus	NEDD8, Ubiquitin	CHBP, Plu2515, Ypk19711, Pha4011	Inhibits CRL activity via NEDD8 deamidation to induce p21 and p27 accumulation and G(2) / G(1) cell cycle arrest	(Cui *et al.*, 2010, Morikawa *et al.*, 2010, Jubelin *et al.*, 2010)
Ibe	0	0	0	Cytosol	IQGAP1	OspB	Enhances pedestal formation	(Buss *et al.*, 2009)
TccP/ EspFu	0	2 (1)	0	Cytosol	N-WASP, IRTKS, IRSp53, Cortactin	EspF	Relieves N-WASP autoinhibition to trigger actin pedestal formation	(Garmendia *et al.*, 2004, Garmendia *et al.*, 2006, Campellone *et al.*, 2004a, Campellone *et al.*, 2008, Cheng *et al.*, 2008, Sallee *et al.*, 2008, Vingadassalom *et al.*, 2009, Weiss *et al.*, 2009, Morita-Ishihara *et al.*, 2009)
Total	**27 (6)**	**62 (12)**	**35 (6)**					

[a] number of effector genes present in EPEC O127:H6 strain E2348/69, EHEC O157:H7 strain Sakai and *C. rodentium* strain ICC168, () indicates pseudogene
[b] *Citrobacter rodentium*
[c]PM, plasma membrane
[d]TJ, tight junction,
[e]ER, endoplasmic reticulum

1.7.4 Tir-mediated actin polymerization and A/E lesion formation

Tir is the principal effector protein that is required for A/E lesion formation *in vivo*, and the formation of actin pedestals in cultured cells (Kenny *et al.*, 1997, Rosenshine *et al.*, 1996). Intracellularly, the N- and C- termini of Tir interact with a number of focal adhesion and cytoskeletal proteins, linking the extracellular bacterium to the host cell cytoskeleton. The N-terminus domain of EPEC Tir has been shown to bind several host focal adhesion proteins including α-actinin, talin and vinculin (Goosney *et al.*, 2000, Cantarelli *et al.*, 2001, Freeman *et al.*, 2000), as well as cortactin (Cantarelli *et al.*, 2002, Cantarelli *et al.*, 2007). Actin polymerization in cell culture has thus far been attributed to the C-terminus of Tir (Campellone *et al.*, 2006, Campellone *et al.*, 2004b). Two tyrosine residues of EPEC Tir, Y_{454} (Y_{458} in EHEC) and Y_{474}, are involved in triggering actin polymerization to form pedestals.

(i) Tir:Nck actin polymerization pathway

In EPEC, phosphorylation of Tir tyrosine residue 474 (Y_{474}) by redundant host cell tyrosine kinases c-Fyn (Phillips *et al.*, 2004), Abl, Arg and Etk (Swimm *et al.*, 2004, Bommarius *et al.*, 2007) generates a consensus docking site (YpDEP/D/V) for the adaptor proteins Nck1/2 via its Src homology 2 (SH2) domain (Figure 10). Importantly, it was shown that a 12-amino acid phosphopeptide of EPEC $Tir_{470-481}$ was sufficient to recruit Nck and induce actin polymerization (Campellone *et al.*, 2002, Campellone *et al.*, 2004b). Although it was believed that Nck then activates the N-WASP to stimulate Arp2/3-mediated actin polymerization (Kenny, 1999, Gruenheid *et al.*, 2001) by binding to the PRD domain of N-WASP through its SH3 domains (Rohatgi *et al.*, 2001), the PRD is dispensable for pedestal formation (Lommel *et al.*, 2001). Instead, the WH1 domain of N-WASP is essential for EPEC

pedestal formation *in vitro* (Lommel *et al.*, 2001). WIP, which binds Nck and the WH1 domain of N-WASP (Anton *et al.*, 1998) has been proposed as the linker between Nck and N-WASP. However, dominant-negative WIP constructs do not abrogate pedestal formation (Lommel *et al.*, 2004). This suggests the involvement of other host cell adaptors or T3SS effectors, or the ability of Tir to recruit N-WASP via WIP/WH1 and Nck/PRD interactions to trigger actin assembly.

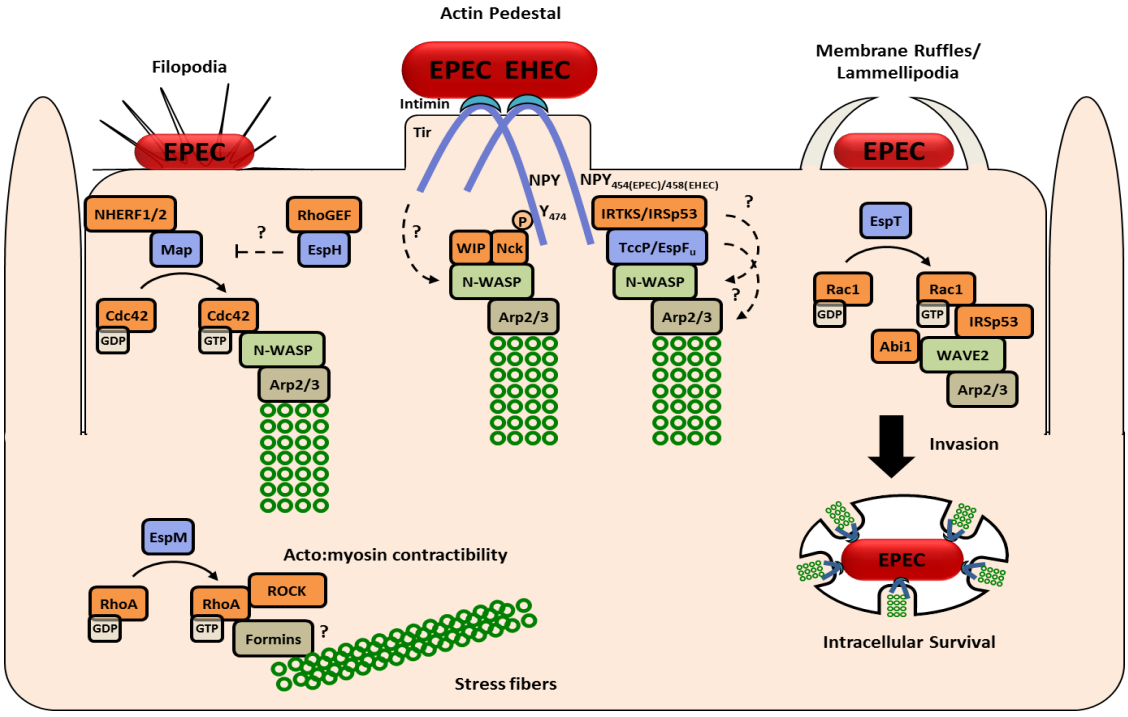


Figure 10. Subversion of actin signaling pathways by EPEC/EHEC.

EPEC/EHEC utilizes Tir:Nck and Tir:IRTKS/IRSp53:TccP/EspF$_u$ pathways to trigger actin pedestal formation. The WxxxE effectors Map, EspT and EspM2 are RhoGEF mimics that activate Cdc42, Rac1 and RhoA to induce the formation of transient localized filopodia, membrane ruffling resulting in bacterial invasion and formation of stress fibers respectively. Details are found in section 1.7.6 and 1.7.7. Image adapted from (Wong *et al.*, 2011).

(ii) Tir:IRTKS/IRSp53:TccP/EspF$_u$ actin polymerization pathway

EHEC Tir lacks Y_{474}, and instead utilizes a conserved Asn-Pro-Tyr (NPY_{458}) motif, which is also found in EPEC Tir as NPY_{454}, to recruit the IRSp53/MIM proteins, IRTKS (Vingadassalom *et al.*, 2009) and IRSp53 (Weiss *et al.*, 2009, Campellone *et*

al., 2005, Brady *et al.*, 2007). The Tir:IRTKS/IRSp53 complex induces inefficient Nck-independent pedestal formation in EPEC (Campellone and Leong, 2005). This pathway is amplified in EHEC by the non-LEE effector TccP/EspF$_U$, which contains an N-terminal secretion signal followed by six almost identical 47 amino acid proline-rich repeats that bind IRTKS/IRSp53 (Vingadassalom *et al.*, 2009) and the GBD domain of N-WASP (Garmendia *et al.*, 2004, Campellone *et al.*, 2004a) (Figure 10). Rather than mimicking Cdc42 activation, each TccP/EspF$_U$ repeat mimics an auto-inhibitory element within the GBD, thus competitively binding to the GBD to relieve N-WASP auto-inhibition, triggering actin polymerization (Cheng *et al.*, 2008, Sallee *et al.*, 2008). While a minimum of 2 proline-rich repeat is required for pedestal formation, additional repeats act synergistically to enhance N-WASP activation and actin polymerization (Campellone *et al.*, 2008; Garmendia *et al.*, 2006). Interestingly, the Tir:IRTKS/IRSp53:TccP/EspF$_u$ pathway is also able to trigger Arp2/3-mediated actin polymerization independently of N-WASP (Vingadassalom *et al.*, 2010), implying that additional host cell factors must also play a role in actin polymerization.

(iii) A/E lesion formation *in vivo*

The Tir:Nck and Tir:IRTKS/IRSp53:TccP/EspF$_u$ pathways are conserved in EPEC belonging to lineage 1 and EHEC O157, respectively (Whale *et al.*, 2007, Ogura *et al.*, 2007). Somewhat unexpectedly, both pathways are active in most non-O157 EHEC strains and in EPEC strains belonging to lineage 2 as well as EPEC O119:H6 (Whale *et al.*, 2007, Ogura *et al.*, 2007), implying functional redundancy. Importantly, although Tir is essential for A/E lesion formation on mucosal surfaces and the pathways responsible for actin polymerization in cell lines *in vitro* appear to be under intense selective pressure, neither the Tir:Nck nor Tir:IRTKS/IRSp53:TccP/EspF$_u$

signalling complexes are necessary for A/E lesion formation or N-WASP recruitment during *C. rodentium* infection of mice (Crepin *et al.*, 2009), or EPEC infection of human intestinal *in vitro* organ cultures (IVOC) (Schuller *et al.*, 2007). In addition, TccP/$EspF_u$ contributes to colonization efficiency of EHEC in rabbits and gnotobiotic piglets, but is not essential for the development of A/E lesions (Ritchie *et al.*, 2008). Overall these studies highlight the fact that our understanding of Tir-mediated actin signaling pathways *in vivo* is far from complete.

1.7.5 Subversion of Rho GTPases by A/E pathogens

The recent characterization of the WxxxE-family *E. coli* bacterial RhoGEFs – Map, EspM and EspT, has deepened our understanding of actin cytoskeletal manipulation by EPEC/EHEC beyond pedestal formation (Alto *et al.*, 2006, Bulgin *et al.*, 2010) (Figure 10). While carriage of *map* is completely conserved among EPEC and EHEC strains, a screen of ~1000 clinical and environmental isolates showed that *espM* is found in 50% of EPEC and EHEC strains while *espT* is found in less than 2% of EPEC and none of the EHEC strains tested (Arbeloa *et al.*, 2009). Map and EspM exhibit GEF activity towards Cdc42 (Huang *et al.*, 2009) and RhoA (Arbeloa *et al.*, 2010) respectively, triggering formation of filopodia (Map) and stress fibers (EspM) (Arbeloa *et al.*, 2008, Alto *et al.*, 2006, Bulgin *et al.*, 2009a). EspT activates both Cdc42/Rac1 to trigger membrane ruffles and lammellipodia (Arbeloa *et al.*, 2008, Alto *et al.*, 2006, Bulgin *et al.*, 2009a).

Map induces transient filopodia formation at bacterial attachment sites during the early stages of EPEC infection (Kenny *et al.*, 2002, Berger *et al.*, 2009). Filopodia retraction is dependent on Tir, either via a putative GTPase-activating protein (GAP)-

like arginine finger motif (GLXR) present in the C-terminus, and/or by activation of Tir actin polymerization cascades (Kenny *et al.*, 2002, Berger *et al.*, 2009). Indeed, RhoA also appears to be required for stabilization of filopodia (Berger *et al.*, 2009). The relevance of Map-mediated filopodia formation during *in vivo* infection is not yet known. EspT was shown to utilize the "trigger" mechanism to promote EPEC invasion into non-phagocytic cells via Rac1-dependent membrane ruffle formation (Bulgin *et al.*, 2009a). Intriguingly, internalized EPEC mobilizes Tir to the vacuolar membrane, forming intracellular actin rich-pedestals that contribute to intracellular bacterial survival (Bulgin *et al.*, 2009a) (Figure 10). EspT also induces the production of pro-inflammatory cytokines that is dependent on Rac1, ERK, JNK, and NF-κB (Raymond *et al.*, 2011).

1.7.6 Regulation of cell survival and death

During infection of intestinal epithelial cells, surface properties of EPEC/EHEC induce extrinsic apoptotic pathways (Abul-Milh *et al.*, 2001), while T3SS effectors such as EspF, Map and Cycle inhibitory factor (Cif) trigger intrinsic apoptotic pathways. EspF induces mitochondrial lysis, opens tight junctions and promotes degradation of anti-apoptotic proteins (Nougayrede *et al.*, 2007, Nougayrede *et al.*, 2004, McNamara *et al.*, 2001). Map disrupts tight junctions, triggers mitochondrial dysfunction, and inactivates the sodium-dependent glucose co-transporter SGLT-1, affecting enterocyte fluid uptake (Kenny *et al.*, 2000, Dean *et al.*, 2004, Dean *et al.*, 2006, Ma *et al.*, 2006). Cif arrests the host cell cycle at G1/S and G2/M, inhibits protein ubiquitination, and stabilizes cell cycle inhibitory proteins $p21^{waf1}$ and $p27^{kip1}$, thereby inducing a delayed form of apoptosis (Marches *et al.*, 2003, Taieb *et al.*, 2006, Samba-Louaka *et al.*, 2008, Samba-Louaka *et al.*, 2009). Interestingly, although

EPEC/EHEC-mediated cell death exhibits early-stage apoptosis (membrane blebbing, cell shrinkage, nuclear condensation), late-stage apoptotic features (exposure of phosphatidylserine on the cell surface and DNA cleavage) are not evident (Crane *et al.*, 2001, Crane *et al.*, 1999, Hemrajani *et al.*, 2010).

The antagonism of pro-apoptotic effects by EPEC/EHEC is mediated by the translocation of anti-apoptotic effectors such as NleH and NleD. EPEC/EHEC harbour two NleH effectors, NleH1 and NleH2, which share a high degree of similarity, including a conserved kinase active site and a PDZ-binding motif (PBD) that interacts with the PDZ domain of NHERF2 (Iguchi *et al.*, 2009, Perna *et al.*, 2001, Petty *et al.*, 2010, Hemrajani *et al.*, 2008, Martinez *et al.*, 2010, Gao *et al.*, 2009). Over-expression of NHERF2 appears to sequester NleH and hinder its anti-apoptotic capacity. Indeed, NHERF2 also binds the PDZ motifs of EspI and Map, suggesting that it acts as a cellular hub at the plasma membrane for effector distribution (Martinez *et al.*, 2010). NleH blocks multiple intrinsic apoptotic pathways, including cell death induced by the global kinase inhibitor staurosporine and *Clostridium difficile* toxin B (Hemrajani *et al.*, 2010, Robinson *et al.*, 2010). This ability appears to be largely due to the interaction of NleH1 and NleH2 with the anti-apoptotic protein, Bax inhibitor-1 (BI-1) (Hemrajani *et al.*, 2010). Recently, NleD was described as a zinc metalloprotease that cleaves JNK, thereby compromising activity of the transcriptional regulator, AP-1, which regulates cell death, differentiation and proliferation (Baruch *et al.*, 2011). EspZ is an additional effector that promotes cell survival and maintenance of the epithelium. Infection of cell monolayers with an *espZ* mutant results in strong cytotoxicity. EspZ interacts with the host cell protein CD98, which enhances β1-integrin and focal adhesion kinase (FAK)

signaling (Shames *et al.*, 2010). *In vivo*, *C. rodentium* Δ*espZ* mutants are severely attenuated exhibiting markedly reduced colonization (Deng *et al.*, 2004). Therefore, the role of EspZ may be to stabilize the epithelium during bacterial colonization, thereby reducing the cytotoxic effect of bacterial infection (Shames *et al.*, 2010). Interestingly, the *Shigella flexneri* effector OspE, which shares homology with EspO, has also been shown to promote host cell adherence by interacting with integrin-linked kinase (ILK) to stabilize focal adhesions (Kim *et al.*, 2009).

1.7.7 EspH, an actin cytoskeletal modulator

EspH is a LEE-encoded effector that is implicated in modulating filopodia:pedestal dynamics. Deletion of *espH* results in prolonged filopodia formation concomitant with delayed pedestal formation, while over-expression of EspH results in pedestal elongation (Tu *et al.*, 2003). Recently, Dong *et al.* reported that EspH inactivates endogenous Dbl-homology and pleckstrin-homology (DH-PH) RhoGEFs by competitively binding to tandem DH-PH domains to inhibit Rho activation (Dong *et al.*, 2010). The expression of EspH in *S. cerevisiae* also seems to activate specific yeast MAP kinase pathways, namely Slt2/Mpk1 (Rodriguez-Escudero *et al.*, 2005). *In vivo* studies of EspH have been somewhat inconsistent; separate studies on EspH using murine or leporine models showed that *espH* mutants are attenuated or not in colonization respectively (Mundy *et al.*, 2004, Ritchie *et al.*, 2005). Nevertheless, it has been shown to be important for attachment to mucosal surfaces, as human intestinal mucosa infected with an *espH* mutant resulted in the formation of bacterial "footprints" that are characteristic of bacterial detachment (Shaw *et al.*, 2005a).

1.8 Aims of the study

EspH is hitherto only known to be an actin cytoskeletal modulator that represses filopodia formation, and promotes the formation of actin pedestals (Tu *et al.*, 2003). In light of the recent study that EspH is a global mammalian RhoGEF inhibitor (Dong *et al.*, 2010), the aims of the project are therefore to:

1. Characterize the role that EspH plays in modulating filopodia:pedestal *in vitro*

2. Investigate the interplay between EspH and Tir in mediating actin pedestal formation

3. Characterize the disruption of Rho GTPase signaling by EspH during infection and transfection

4. Investigate the interplay between EspH and bacterial RhoGEFs in modulating actin dynamics

5. Investigate additional phenotypes in relation to the interplay between EspH and bacterial RhoGEFs

Chapter 2 – Materials and Methods

Chapter 2 – Materials and Methods

2.1 Strains, Primers and Plasmids

2.1.1 Strains

Bacterial strains used in this study are listed in Table 2. Strains were grown in Luria-Bertani (LB) broth at 200 rpm or agar plates containing appropriate antibiotics at 37°C overnight unless otherwise stated. Antibiotics were used at the following concentration: Ampicillin (Amp) (100 μg ml^{-1}) [diluted in water], Kanamycin (Kn) (50 μg ml^{-1}) [diluted in water], Chloramphenicol (Cm) (37 μg ml^{-1}) [diluted in ethanol], Nalidixic acid (Nal) (50 μg ml^{-1}) [diluted in water] and Tetracycline (Tet) (5 μg ml^{-1}) [diluted in DMSO].

Table 2. List of strains used in this study

Strains	Description	Source
TOP10	Cloning strain	Invitrogen
EPEC WT	Prototypical E2348/69 O127:H6 strain	(Levine *et al.*, 1978)
EPEC Δ*escN*	EPEC *escN* deletion mutant (T3SS-deficient)	(Garmendia *et al.*, 2004)
EPEC Δ*espH*	EPEC *espH* deletion mutant	(Marches *et al.*, 2008)
EPEC Δ*map*	EPEC *map* deletion mutant	(Simpson *et al.*, 2006)
EPEC Δ*nleH1nleH2*	EPEC *nleH1*and *nleH2* double deletion mutant	(Hemrajani *et al.*, 2010)
EPECtir_{WT}	EPEC strain with addition of *aphT* cassette at the *tir-cesT* intergenic region	This study
EPECtir_{Y474A}	EPEC strain with *tir* mutated at Tyr 474 to Ala	This study
EPECtir_{Y454A}	EPEC strain with *tir* mutated at Tyr 454 to Ala	This study
EPEC$tir_{Y454A/Y474A}$	EPEC strain with *tir* mutated at Tyr 454/474 to Ala	This study
EPEC Δ*espH*/$tir_{Y454A/Y474A}$	EPEC Δ*espH* with *tir* mutated at Tyr 454/474 to Ala	This study
ICC169	Nal-resistant *C. rodentium* wild-type	(Wiles *et al.*, 2004)
CR Δ*espH*/$tir_{Y454A/Y474A}$	*C. rodentium* Δ*espH* with *tir* mutated at Tyr 451/471 to Ala	V. Crepin

2.1.2 Plasmids

Plasmids used in this study are listed in Table 3.

Table 3. List of plasmids used in this study

Plasmid Name	Antibiotic	Description	Source
pCX340	Tet	Inducible vector encoding β-lactamase TEM-1	(Charpentier *et al.*, 2004)
pCX340-EspH	Tet	pCX340 expressing EspH fused to TEM-1	This study
pCX340-(8)EspH	Tet	pCX340 expressing (+8)EspH fused to TEM-1	This study
pCX340-NleD	Tet	pCX340 expressing NleD fused to TEM-1	This study
pGEMT	Amp	Cloning vector	Promega
pKD46	Amp	Coding the lambda-red recombinase	(Datsenko *et al.*, 2000)
pSB315	Kn	Coding the kanamycin resistance *aphT* cassette	(Galan *et al.*, 1992)
PSB315-CM	Cm	pSB315 with chloramphenicol resistance *cat* cassette replacing the *aphT* cassette	This study
pACYC184-TccP	Cm	Low-copy plasmid constitutively expressing $TccP_{EHEC}$	(Girard *et al.*, 2009)
pSA10	Amp	pKK177-3 containing *lacI* gene	(Schlosser-Silverman *et al.*, 2000)
pSA10-EspH	Amp	pSA10 derivative encoding EPEC EspH	This study
pSA10-(8)EspH-HA	Amp	pSA10 derivative encoding haemagglutinin (HA)-tagged EspH with additional 8 amino acids	This study
pSA10-EspH-HA	Amp	pSA10 derivative encoding haemagglutinin (HA)-tagged EspH	This study
pSA10-Tir	Amp	pSA10 derivative encoding EPEC Tir	(Berger *et al.*, 2009)
pSA10-Map	Amp	pSA10 encoding EPEC Map	(Simpson *et al.*, 2006)
pSA10-EspT	Amp	pSA10 encoding E11 EspT	(Bulgin *et al.*, 2009a)
pSA10-$EspT_{W63A}$	Amp	pSA10 encoding E11 EspT with point mutation at Trp 63 to Ala	(Bulgin *et al.*, 2009a)
pSA10-EspM2	Amp	pSA10 encoding EHEC EspM2	(Arbeloa *et al.*, 2008)
pSA10-$EspM2_{W70A}$	Amp	pSA10 encoding EHEC EspM2 with point mutation at Trp 63 to Ala	(Arbeloa *et al.*, 2008)
pGEMT-Ct-Kn-Nc	Amp	pGEMT vector containing 3'end of tir_{EPEC} (bp 1072-1653), *aphT*, *tir-cesT* intergenic region and 5'end of *cesT* (bp 1-369)	This study
pGEMT-Ct_{Y454A}-Kn-Nc	Amp	pGEMT-Ct-Kn-Nc with tir_{Y454A} mutation	This study
pGEMT-Ct_{Y474A}-Kn-Nc	Amp	pGEMT-Ct-Kn-Nc with tir_{Y474A} mutation	This study
pGEMT-$Ct_{Y454A/Y474A}$-Kn-Nc	Amp	pGEMT-Ct-Kn-Nc with $tir_{Y454A/Y474A}$ mutation	This study
pEGFP-C1	Kn	Mammalian expression vector encoding GFPmut1	Invitrogen
pEGFP-N-WASP	Kn	pEGFP-C1 derivative encoding N-WASP	E. Caron
pEGFP-ΔWH1	Kn	pEGFP-N-WASP with aa 1-156 deletion	This study
pEGFP-ΔB	Kn	pEGFP-N-WASP with aa 156-200 deletion	This study
pEGFP-ΔCRIB	Kn	pEGFP-N-WASP with aa 200-226 deletion	This study
pEGFP-ΔGBD	Kn	pEGFP-N-WASP with aa 200-274 deletion	This study
pEGFP-ΔPRD	Kn	pEGFP-N-WASP with aa 274-385 deletion	This study
pEGFP-WH1-VCA	Kn	pEGFP-N-WASP with aa 156-385 deletion	This study
pCB6-WIP	Amp	GFP fused to WIP transfection vector	(Moreau *et al.*, 2000)
pCB6-WBD	Amp	Encodes GFP fused to WASP-binding domain of WIP transfection vector	(Moreau *et al.*, 2000)
pRK5myc-IRSp53	Amp	Myc-tagged IRSp53 construct	L. Machesky

pRK5myc-WAVE2	Amp	Myc-tagged WAVE2 construct	L. Machesky
pCDNA3-TirMC	Amp	HA-tagged Tir derivative	(Campellone *et al.*, 2004b)
pCDNA3-TirMC$_{Y474F}$	Amp	HA-tagged Tir derivative with with *tir*$_{Y474F}$ mutation	(Campellone *et al.*, 2004b)
pCDNA3-TirNMC	Amp	pCDNA3-TirMC with Tir (aa 1-233) insertion before the Newcastle virus TM domain	This study
pCDNA3-TirNM	Amp	pCDNA-TirNMC with aa 388-547 deletion	This study
pGEMT-UpH-cat-DnH	Amp	pGEMT vector containing 325 bp upstream region of *espH*$_{EPEC}$, *cat*, and 499 bp downstream region of *espH*$_{EPEC}$	This study
pCMV-RFP	Amp	Mammalian expression vector encoding RFP	M. Seabra
pCMV-RFP-EspH	Amp	Encoding RFP-EspH fusion protein	This study
pRK5myc	Amp	Mammalian expression vector	Invitrogen
pRK5myc-GFP	Amp	Encoding Myc-tagged GFP	(Clements *et al.*, 2011)
pRK5myc-EspH	Amp	Encoding Myc-tagged EPEC EspH	This study
pRK5myc-p115RhoGEF	Amp	Encoding Myc-tagged p115RhoGEF	A. Hall
pRK5myc-Map	Amp	Encoding Myc-tagged EPEC Map	(Martinez *et al.*, 2010)
pRK5myc-EspT	Amp	Encoding Myc-tagged E11 EspT	(Bulgin *et al.*, 2009b)
pRK5myc-EspM2	Amp	Encoding Myc-tagged EHEC EspM2	(Arbeloa *et al.*, 2008)
pRK5myc-SopE$_{78-240}$	Amp	Encoding Myc-tagged SopE (78-240 residue)	(Bulgin *et al.*, 2010)
pRK5myc-Cdc42(L61)	Amp	Encoding Myc-tagged dominant-positive Cdc42	E. Caron
pRK5myc-Rac1(L61)	Amp	Encoding Myc-tagged dominant-positive Rac1	(Nobes *et al.*, 1999)
pRK5myc-RhoA(L63)	Amp	Encoding Myc-tagged dominant-positive RhoA	E. Caron
pRK5myc-NleH1	Amp	Encoding Myc-tagged EPEC NleH1	(Martinez *et al.*, 2010)
pRK5myc-NleH2	Amp	Encoding Myc-tagged EPEC NleH2	This study

2.1.3 Primers

Primers used in this study to generate mutants or plasmids are listed in Table 4.

Table 4. List of primers used in this study

Primer Name	Sequence (5' – 3') [Restriction sites underlined]	Usage
EcoRI-EspH-E69-Fw	CGGGAATTCATGTCGTCATCATTATCAGGTATAAC	pSA10-EspH pSA10-EspH-HA
EcoRI-(8)EspH-E69-Fw	CGGGAATTCATGCGTTATATAGGGAGGTGTATG	pSA10-(8)EspH-HA
PstI-EspH-E69-Rv	AAAACTGCAGTTAAACTGTCACACCTGATAAAG	pSA10-EspH pCMVRFP-EspH
PstI-EspH-E69-HA-Rv	AAAACTGCAGTTATGCGTAATCTGGTACATCGTATGGGTATGCTCCAACTGTCACACCTGATAAAGAGTTTAATG	pSA10-EspH-HA pSA10-(8)EspH-HA
NdeI-(8)EspH-E69-Fw	CCCGAGCATATGCGTTATATAGGGAGGTGTATG	pCX340-(8)EspH
NdeI-EspH-E69-Fw	CCCGAGCATATGTCGTCATCATTATCAGG	pCX340-EspH
EcoRI-EspH-E69-Rv(NoSTOP)	CGGAATTCCCAACTGTCACACCTGATAAAGAG	pCX340-(8)EspH pCX340-EspH

BamHI-EspH-E69-Fw	CGCGGATCCTCGTCATCATTATCAGGTATAAC	pRK5myc-EspH
HindIII-EspH-E69-Fw	CCCAAGCTTTCGTCATCATTATCAGGTATAAC	pCMVRFP-EspH
EcoRI-EspH-E69-Rv	CGGAATTCTTAAACTGTCACACCTGATAAAG	pRK5myc-EspH
EPEC *tir* mutagenesis		
TirC-E69-Fw	TACAGCTTTCATCGGGTATTGG	PCR (tirC)
EcoRI-TirC-E69-Rv	CGGGAATTCTTAAACGAAACGTACTGGTCCC	PCR (tirC)
EcoRI-NcesT-E69-Fw	CGGGAATTCATATATCTGTGAGTATTTAGTTGAG	PCR (NcesT)
NcesT-E69-Rv	CGTTAAGTCGATGGAAAATCTG	PCR (NcesT)
TirC-E69-Y454A-Rv	GGCAGGATTAACCACTTCGCTAGA	Inverse PCR (Y454A)
TirC-E69-Y454A-Fw	GCTGAAGTTGGGGGGGCTC	Inverse PCR (Y454A)
TirC-E69-Y474A-Rv	GGCTATATGCTCTTCTGGCTGATG	Inverse PCR (Y474A)
TirC-E69-Y474A-Fw	GATGAGGTCGCTGCAGATCCT	Inverse PCR (Y474A)
EPEC *espH* mutagenesis		
Up-EspH-E69-Fw	GGCAACCGTAAAGCTGAGC	PCR (Up-espH)
BamHI-Up-EspH-E69-Rv	CGCGGATCCCATACACCTCCCTATATAACG	PCR (Up-espH)
BamHI-Dn-EspH-E69-Fw	CGCGGATCCCTCTTTATCAGGTGTGACAG	PCR (Dn-EspH)
Dn-EspH-E69-Rv	GTCATGAGTGGATACTTGAG	PCR (Dn-EspH)
GFP-N-WASP variants		
NWASP-WH1del-Rv	CATGGTGTCGCCGGACTTG	Inverse PCR (ΔWH1)
NWASP-WH1del-Fw	GCTACAGTTGACATAAAAAATCC	Inverse PCR (ΔWH1)
NWASP-Bdel-Rv	CATGGGTAGATTGGGACCATT	Inverse PCR (ΔB)
NWASP-Bdel-Fw	GGAACACCAAGTAATTTCCAGC	Inverse PCR (ΔB)
NWASP-CRIBdel-Rv	AATATCTGCCTTGGTTAATCTCTTC	Inverse PCR (ΔCRIB)
NWASP-CRIBdel-Fw	CCAGAATTAAAGAATCTTTTTGATATG	Inverse PCR (ΔCRIB)
NWASP-GBDdel-Fw	CCACCACCTCCACCCTCGAG	Inverse PCR (ΔGBD)
NWASP-PRDdel-Rv	TGGTGCTTGTCTTCGGAGTTC	Inverse PCR (ΔPRD)
NWASP-PRDdel-Fw	CATCAAGTTCCAGCTCCTTCAG	Inverse PCR (ΔPRD)
HA-TirNM		
HindIII-TirN(1-233)-E69-Fw	CCCAAGCTTCAATGCCTATTGGTAACCTTGGTAAT	PCR (Tir1-233)
HindIII-TirN(1-233)-E69-Rv	CCCAAGCTTGTTTAGGATCTGAGCGAACGCTG	PCR (Tir1-233)
pCDNA3-TirNM(EPEC)-Rv	TCTATGGAGCGCAGTCGTTAC	Inverse PCR (TirNM)
pCDNA3-TirNM(EPEC)-Fw	CGTTTCGTTTAAATATATCCGCG	Inverse PCR (TirNM)

2.2 Molecular Biology Techniques

2.2.1 Polymerase Chain Reaction (PCR)

DNA products were amplified by PCR with the appropriate forward and reverse primers (100 pmol/µl, Thermohybaid) in a mix of 50 ng of DNA template, 0.5 µl of each primers, 1.5 µl of $MgCl_2$ (100 mM, NEB UK), 1 µl of dNTP (25mM, NEB UK), 5 µl of Thermo polymerase buffer (10X, NEB UK), and 0.5 µl of DeepVent DNA polymerase (2 U/µl, NEB UK) all resuspended in 40 µl of sterile dH_2O.

For colony PCR screening, the RedTaq Polymerase Mix (2X, Sigma) was used in a mix of 0.3 µl forward primer, 0.3 µl reverse primer and 14.4 µl RedTaq mix, and resuspended in 15 µl sterile dH_2O. Bacteria colonies were picked and patched on fresh agar plates, before being resuspended in individual reaction mixes.

For inverse PCR, the KOD Hot Start DNA polymerase kit (Novagen) was used in a mix of 1.5 µl forward and reverse primers, 0.3 – 1 µl of plasmid DNA, 3 µl of $MgSO_4$ (25 mM, Novagen), 5 µl of dNTP (2 mM, Novagen), 5 µl KOD polymerase buffer (1U/µl, Novagen) all resuspended in sterile dH_2O to give 50 µl reaction volume.

A typical PCR run consists of an initial denaturation step of 93°C for 3 min, followed by 30 cycles of 93°C for 20 s, 60°C for 30 s, and 74°C for 1 min/kb (70°C, 15 s/kb for KOD), before a further 5 min at 74°C (70°C for KOD) to finish any incomplete reactions. All PCR products were run on agarose gels (described in section 2.2.5), and then gel-purified using QIAPrep Gel Extraction kit (Qiagen).

2.2.2 Restriction Digest and DNA Ligation

DNA restriction digest was performed overnight at 37°C in a final volume of 100 µl using 1 µg of DNA template, 10 U for each restriction enzyme (NEB UK) with the appropriate restriction buffer (NEB UK) and 1 mM BSA (NEB UK). Digested DNA products were extracted by gel-purification using Qiagen Gel Extraction kit. Ligation was performed overnight at 14°C in a final volume of 20 µl with a vector to insert ratio of 1:3, 2 µl of T4 ligation buffer (10X, NEB UK) and 400 U of T4 DNA ligase (NEB UK).

2.2.3 Bacterial Transformation

Transformation of ligated products was achieved using heat-shock. *E. coli* TOP10 (Invitrogen) cells were first made chemically competent by inoculating 1:100 of overnight TOP10 cultures in fresh LB broth and grown to mid-log phase (OD_{600} 0.4 – 0.5) before harvest by centrifugation at 4000 x g, 4°C for 7 min. Cells were re-suspended in 0.4X volume of ice-cold TFBI buffer (30 mM potassium acetate, 10 mM $CaCl_2$, 50 mM $MnCl_2$, 15% (v/v) glycerol, pH 5.8) and then incubated on ice for 5 minutes before pelleted by centrifugation as before. Cells were re-suspended in ice-cold TFBII buffer (10 mM MOPS, 75 mM $CaCl_2$, 10 mM $RbCl_2$, 15% (v/v) glycerol, pH 6.5) and then stored at -80°C for long-term use. 50 µl of chemically competent cells were incubated at 4°C with 5–10 µl of ligated products for at least 30 min before heat-shocking for 90 seconds in a 42°C water bath. The cells were then transferred immediately to 4°C to allow recovery for 5 minutes before 800 µl of LB broth without antibiotics was added. The transformation mix was incubated at 37°C shaking for 90 min before 300 µl of the mix was plated onto LB plates containing the appropriate antibiotics and incubated at 37°C overnight.

Purified recombinant plasmid DNA was transformed into *E. coli* strains by electroporation. Bacteria were made electrocompetent by first being grown in LB broth to mid-log phase as described previously. Bacterial cultures were then cooled to 4°C for 30 min, and then pelleted down by centrifugation before re-suspension in 20 ml 15% (v/v) glycerol at 4°C. This step was repeated twice before a final 80 µl of 15% (v/v) glycerol was added. Aliquots were then mixed with recombinant plasmid in an electroporation cuvette of 0.2 cm width (Bio-Rad). Electroporation was performed using the GenePulser™ electroporation system (Bio-Rad) using the following

parameters: resistance (200 Ω for *E. coli*; 300 Ω for *C. rodentium*), voltage (2.5 kV) and capacity (25 μF). 800 μl of LB broth without antibiotics was then added immediately. The transformation mix was incubated at 37°C shaking for 90 min before 300 μl of the mix was plated onto LB plates containing the appropriate antibiotics and incubated at 37°C overnight.

2.2.4 Plasmid Extraction

Plasmid extraction was carried out from 5 ml bacterial overnight cultures with QIAPrep Spin Miniprep kits (Qiagen) or 150 ml cultures with QIAPrep Spin Midiprep kits (Qiagen) according to manufacturer's instructions. Plasmids were eluted with sterile dH_2O. Plasmid DNA concentration was assessed using a NanoDrop ND-1000 reader (Thermo Scientific). Plasmids were filtered through a 0.2 μm sterile filter (BD) prior to cell transfection.

2.2.5 Agarose gel electrophoresis

Following PCR, DNA was resolved by agarose gel electrophoresis. Gels were cast using 0.5 – 1.5 % agarose with 1:10,000 dilution of SYBRSafe™ DNA gel stain (Invitrogen) for visualization. DNA samples were mixed with 6X loading buffer (NEB UK) and run in 1X TAE buffer (40 mM Tris-acetate, 1 mM EDTA) at 80 – 180 V. DNA band sizes were estimated using a 2-log DNA loader (NEB UK). DNA bands were visualized using a SafeImager™ blue light trans-illuminator (Invitrogen). Images were acquired and processed using BioImaging Syngene software (Syngene).

2.2.6 Protein BCA assay

Cells in tissue culture flasks (BD Biosciences) or 24-well plates (BD Biosciences) were lysed with cold RIPA buffer (25 mM Tris-HCl pH 7.6, 150 mM NaCl, 1% (v/v) NP-40, 1% (v/v) sodium deoxycholate, 0.1% SDS) supplemented with protease inhibitor cocktail (Roche) for 45 min. Lysates were harvested using cell scrapers and centrifuged at 14,000 rpm at 4°C for 20 min to remove insoluble debris. Protein concentration of cleared lysates was quantified using Pierce bicinchoninic acid (BCA) Protein Assay kit (Thermo Scientific). Samples were incubated in duplicates with reconstituted BCA reagent in a 1:10 to 1:20 ratio, and incubated for 30 min at 37°C. Samples were read at 562 nm using a 96-well plate reader. Protein concentration of samples was determined using a 0.1 – 1.0 mg BSA standard ladder.

2.2.7 SDS-PAGE

Resolving gels were cast using 8 – 12 % acrylamide in Tris-SDS buffer (0.375 M Tris-HCl pH 8.8, 0.1 % SDS), while stacking gels were cast using 4% acrylamide in Tris-SDS buffer (0.125 M Tris-HCl pH 6.8, 0.1 % SDS). 0.1 % (w/v) ammonium persulfate and 0.1 % (v/v) TEMED were added to induce acrylamide polymerization. Protein samples were boiled in 5X Laemmli buffer (60 mM Tris-HCl pH 6.8, 2% SDS, 10% (v/v) glycerol, 5% (v/v) β-mercaptoethanol, 0.01% (w/v) bromophenol blue) for 8 – 10 min. Samples were separated on the polyacrylamide gel between 90 – 200 V in 1X Tris-Glycine-SDS buffer (Bio-Rad). Molecular weight of protein samples was estimated using a prestained broad range protein marker (NEB UK).

2.2.8 Coomassie staining

Following SDS-PAGE separation, gels were immersed in Coomassie stain solution (45% (v/v) ethanol, 10% (v/v) acetic acid, 0.25% (w/v), coomassie R250) and incubated rocking at RT for 1 – 2 h. Gels were de-stained by successive washes in de-stain solution (45% (v/v) ethanol, 10% (v/v) acetic acid, 0.25% (w/v)) until protein bands are clearly visualized.

2.2.9 Western blot

Resolved protein gels and nitrocellulose membranes (Bio-Rad) were immersed separately in transfer buffer (1X Tris-Glycine-SDS buffer (Bio-Rad), 20 % (v/v) methanol) for at least 15 min. A gel/membrane transfer sandwich is then assembled by saturating 3 layers of filter paper in transfer buffer and laying it at the bottom, followed by the equilibrated membrane, then the equilibrated gel, and finally covered with another 3 layers of wet filter paper. Proteins were transferred onto the membrane blot using a TransBlot® semi-dry electrophoretic transfer machine (Bio-Rad) at 0.2 – 0.4 A (depending on number of sandwiches) for 30 – 60 min depending on molecular weight of target protein. Membrane blots were then washed with TBS-T buffer (50 mM Tris-HCl, 150 mM NaCl, 0.1% Tween-20) and blocked with TBS-T/5% BSA for 1 h at RT. Blots were probed with antibodies of specified dilution in TBS-T/5% BSA overnight at 4°C rocking. Antibodies are listed in Table 5. After 3 successive washes of 5 min with TBS-T, blots were probed with horseradish peroxidase-linked secondary antibodies (1:10,000 dilution) for 1 h. Blots were washed another 5 times, and immunoreactive bands were visualized using and ECL reagent (GE Healthcare). Chemiluminescence was detected using a LAS-3000 Fuji Imager.

2.3 Construction of EPEC *tir* chromosomal mutants

EPEC strains expressing mutated Tir were generated using a lambda red-based mutagenesis system (Datsenko *et al.*, 2000), via the introduction of site-directed *tir* mutagenesis into the endogenous chromosomal *tir* gene together with a kanamycin cassette in the *tir-cesT* intergenic region. To mutate the C-terminus tyrosine residues of *tir,* the 3' end of *tir*, followed by a non-polar *aphT* cassette (Galan *et al.*, 1992), and then the *tir-cesT* intergenic region and 5' end of *cesT* were first cloned into pGEMT vector. The 3' end of *tir* was amplified using primer pair Up-TirC-E69-Fw and Dn-EcoRI-TirC-E69-Rv, while the intergenic region and 5' end of *cesT* was amplified using primer pair Dn-EcoRI-TirC-E69-Fw and Dn-TirC-E69-Rv. Both fragments were then digested with *EcoR*I, ligated together, and then cloned into pGEMT. The non-polar *aphT* cassette was then inserted into the *EcoR*I site between the two fragments and the orientation of the kanamycin cassette ascertained by PCR. This plasmid, pGEMT-TirYY, was used to generate the control mutant.

EPEC*tir* mutagenesis was then carried out by inverse-PCR using pGEMT-TirYY. The primer pairs TirC-E69-Y454A-Fw/TirC-E69-Y454A-Rv and TirC-E69-Y474A-Fw/TirC-E69-Y474A-Rv were used to mutate the tyrosine residues Y454 and Y474 into alanines (Tir_{Y454A} and Tir_{Y474A}) generating pGEMT-TirAY and pGEMT-TirYA respectively. The double tyrosine mutant ($Tir_{Y454A/Y474A}$) was generated by superimposing Y474A on the Y454A mutant, generating pGEMT-TirAA. All pGEMT derivatives were checked by DNA sequencing.

To introduce *tir*$_{ctrl}$, *tir*$_{Y454A}$, *tir*$_{Y474A}$ and *tir*$_{Y454A/Y474A}$ site-directed mutants into bacterial chromosome, the inserts in all pGEMT derivatives were amplified using the primer pair Up-TirC-E69-Fw and Dn-TirC-E69-Rv. The PCR products were electroporated into E2348/69 or JPN15 containing pKD46 encoding the lambda Red recombinase following induction with 1mM arabinose (Datsenko *et al.*, 2000). Strains containing pKD46 were incubated at 30°C as the plasmid is heat-sensitive. Transformants were selected on kanamycin plates and the insertion of site-directed *tir* mutants confirmed by PCR and DNA sequencing. Confirmed *tir* mutants were then cured of pKD46 by growing them in LB broth at 42°C shaking overnight.

2.4 Construction of GFP-N-WASP and HA-TirNM deletion variants

Construction of the different GFP-N-WASP expression variants was carried out by inverse PCR, using pEGFP-N-WASP expression vector (kindly provided by Dr. Emmanuelle Caron) as template. The primer pairs NWASP-WH1del-Rv / NWASP-WH1del-Fw, NWASP-Bdel-Rv / NWASP-Bdel-Fw, NWASP-CRIBdel-Rv / NWASP-CRIBdel-Fw, NWASP-CRIBdel-Rv / NWASP-GBDdel-Fw, NWASP-PRDdel-Rv / NWASP-PRDdel-Fw and NWASP-WH1del-Rv / NWASP-PRDdel-Fw were used to delete the WH1 (1-156), B (156-200), CRIB (200-226), GBD (226-274), PRD (274-392) and all domains except WH1 (156-392), generating GFP-ΔWH1, GFP-ΔB, GFP-ΔCRIB, GFP-ΔGBD, GFP-ΔPRD and GFP-WH1-VCA respectively. All pEGFP-N-WASP expression variants were sequenced and assessed with western blot analysis to ensure stable expression.

Construction of HA-TirNM was carried out first by re-inserting the N-terminus of Tir (aa 1-233) into the HindIII restriction site of pCDNA3-TirMC to generate pICC626. Using pICC626 as template, the primer pairs pCDNA3-TirNM(EPEC)-Rv / pCDNA3-TirNM(EPEC)-Fw was used to delete the C-terminus of Tir (aa 388-547), generating pCDN3-TirNM. All pCDNA3-Tir expression variants were sequenced and assessed for membrane localization by transfection.

2.5 Cell culture

HeLa (ATCC), FAK-/- (ATCC) and FAK+/+ (ATCC) cells were grown at 37°C in a humidified atmosphere containing 5% CO_2 in Dulbecco's modified Eagles' medium (DMEM) low glucose (1000 mg L^{-1}) (Sigma) supplemented with 10% (v/v) heat-inactivated fetal bovine serum (Gibco) and 2 mM glutamax (Sigma). Swiss 3T3, N-WASP-/- (S. Snapper) and Nck-/- fibroblasts were grown at 37°C in a humidified atmosphere containing 5% CO_2 in DMEM high glucose (4500 mg L^{-1}) (Sigma) supplemented with 10% (v/v) heat-inactivated fetal bovine serum (Gibco) and 2 mM glutamax (Sigma). Cell culture lines were routinely passaged (typically 3 – 4 days) by trypsinization (PBS, 1 mM EDTA, 2 mM trypsin) and resuspending cells in 1:10 dilution of DMEM media. Cells were seeded onto glass coverslips in 24-well cell culture plates at approximately 5×10^4 density of cells per well and grown to 80–100% confluence (typically 2 – 3 days).

2.6 Transfection

Plasmids were isolated using Qiagen Midi Prep kit as per manufacturer's instructions. HeLa cells were transfected with pRK5myc, pEGFP, pCDNA3 or pRFP mammalian

expression vectors using Fugene 6 (Roche) according to the manufacturer's instructions. Briefly, plasmid DNA and Fugene 6 were combined in a 1:3 ng/µl ratio in 20 µl Opti-MEM® reagent (Invitrogen) per 24-well for 30 min to allow complex formation before adding to each well. Swiss 3T3, N-WASP-/-, Nck-/-, FAK-/- or FAK+/+ cells were transfected in a similar manner, but using Lipofectamine 2000 (Invitrogen). Transfected cells were incubated at 37°C in a humidified incubator with 5% CO_2 for 24 hours unless otherwise stated.

2.7 siRNA knockdown

For siRNA knockdown of Cdc42, Rac1, and RhoA, siRNA pool sequences were selected from a proprietary Rho GTPase siRNA library (Dharmacon). siRNA knockdown was performed on Swiss 3T3 fibroblasts using HiPerfect (Qiagen) according to manufacturer's instructions. Briefly, 0.75 ng of siRNA (20 µM stock concentration is equivalent to 0.25 µg/µl) was combined with 3 µl of HiPerfect transfection reagent in 100 µl Opti-MEM® reagent (Invitrogen) per 24-well for 10 min to allow complex formation, and added to 500 µl of newly-seeded cells (10 nM siRNA final concentration). siRNA knockdown was allowed to proceed at 37°C in a humidified incubator with 5% CO_2 for 48 h before EPEC infection. Effectiveness of RNAi-mediated gene silencing of Rho GTPases was assessed by western blot using the appropriate antibodies (listed in Table 5).

2.8 EPEC Infection

EPEC strains were primed for infection by dilution of 1:50 or 1:100 of overnight bacterial culture with pre-warmed 1000 mg L^{-1} glucose or 4500 mg L^{-1} glucose

serum-free DMEM (Sigma), depending on cell culture type. Bacteria are incubated as static cultures at 37°C in 5% CO_2 for 2 hours and 30 minutes. Static cultures were induced with 1 mM IPTG for expression of pSA10-encoded effector proteins as appropriate, and then incubated for a further half hour. Cell layers were washed thrice in PBS before infection with 0.5 ml of primed bacterial culture at 37°C. Infection was allowed to proceed for the appropriate period of time. Monolayers were washed thrice with PBS and fixed in 3% paraformaldehyde in PBS for 15 minutes. They were then washed thrice again with PBS.

2.9 Secretion assay

15 ml of Dulbecco's modified eagle medium (DMEM) was inoculated with a 1:50 dilution of overnight LB cultures of EPEC WT or Δ*escN* strains transformed with pSA10 vector containing the appropriate HA-tagged effectors. Cultures were grown for 3½ hours at 37°C and 100 rpm before induction with 1mM IPTG and grown for a further 3 hours. OD_{600} levels were measured before the samples were centrifuged at 4000 rpm for 10 minutes. The pellet was resuspended in Laemmli buffer (normalized to OD_{600} measurements) to form the whole cell lysate fraction. The supernatant (normalized to OD_{600} measurements) was passed through 0.2 μm filters (BD) into Amicon-ultra-15 centrifugal devices (MWCO 3000, Millipore) and centrifuged until the sample was concentrated to 900 μL. Protein was precipitated with addition of 10% final concentration tricarboxylic acid at 4°C overnight. Samples were then centrifuged at 14,000 rpm for 20 minutes, washed with ice-cold acetone and centrifuged as before. Protein pellet was finally resuspended in 35 μl of SDS loading buffer with 30 mM Tris-HCl pH 8.8. Samples were then processed for western blotting.

2.10 Translocation assay

Effector translocation was detected as previously described (Charpentier *et al.*, 2004) with some modifications. HeLa cells were grown with 1000 mg L^{-1} glucose DMEM (Sigma) supplemented with 10% fetal bovine serum in black 96-well, clear bottom cell culture plates to 80-90% confluency. EPEC WT or Δ*escN* strains were primed for infection by static culture with pre-warmed serum-free DMEM media in 5% CO_2 for 2 hours and 30 minutes. Monolayers were then infected by replacing the DMEM media with 200 μl of primed culture. Cells were incubated for 30 minutes before induction of fusion protein expression with 1 mM IPTG, and then incubated for a further one hour. Cell monolayers were then washed thrice with Hanks' balanced salt solution (HBSS), and covered with 100 μl HBSS, 20mM HEPES, 6% probenecid plus 20 μl of 6x CCF2/AM solution (Invitrogen) freshly prepared as per manufacturer's instructions. The cell culture plate was then incubated at RT in the dark for 1 hour and 30 minutes. Cell monolayers were then washed thrice with HBSS, 20mM HEPES, 6% probenecid. Fluorescence was quantified on a Fluostar Optima reader with excitation at 410 nm (10-nm band-pass), and emission was detected via 447-nm (blue fluorescence) and 520-nm (green fluorescence) filters.

2.11 Cell detachment assay

HeLa cells grown in 24-well plates were infected with 500 μl primed EPEC strains for 1 h (MOI 1:100), washed once in PBS, then treated with 200 μg ml^{-1} gentamicin (Sigma) in DMEM media for a further 3 hours to inhibit bacterial replication. Cells were washed 5 times with PBS and then trypsinized; trypsin was inactivated with culture media. Cells were counted using a Neubauer haemocytometer. Counts were

expressed as a percentage of cells left adhering compared to uninfected cells. Percentage cell detachment was expressed as the difference in cell adherence compared to uninfected cells.

2.12 Pharmacology

Staurosporine (STS) (Calbiochem) was used at a final concentration of 1 μM in DMEM medium and added to HeLa cells for 5 hours to induce apoptosis. To show caspase-dependent cell detachment, the pan-caspase inhibitor zVAD-fmk (Promega) was used at a final concentration of 66 μM (together with bacteria or with STS in DMEM media).

2.13 Cytotoxicity assay

HeLa cells grown in 96-well plates were infected with 1 ml of primed EPEC culture (MOI 1:200) in phenol red-free DMEM media and centrifuged for 4 min at 200 g to synchronize infection. Cells were incubated for 30 min, washed once with PBS and then incubated with 200 μg ml^{-1} gentamicin (Sigma) in phenol red-free DMEM media for a further 4 hours. LDH release during EPEC infection was assayed using a CytoTox96® cytotoxicity assay kit (Promega) according to manufacturer's instructions. Briefly, the supernatant containing LDH of lysed cells was collected and combined with 1:1 ratio of the substrate mixture for 30 min in the dark. Total LDH is assessed by addition of 1% Tween-20 to an uninfected well to trigger cell permeabilization. Cytotoxicity was assayed using a 96-well plate reader at 492 nm, and calculated as a percentage of (experimental LDH activity – basal LDH activity) / (total LDH activity – basal LDH activity).

2.14 Immunofluorescence microscopy

Following fixation of cells with paraformaldehyde (PFA), coverslips were treated with 50mM NH_4Cl PBS for 10 minutes to neutralize residual PFA. Monolayers were permeabilized with 0.2% Triton-X100 in PBS for 4 minutes, and then blocked with PBS containing 1% BSA. Coverslips were incubated with primary antibodies diluted in PBS-BSA for 1 hour. After washing thrice with PBS, coverslips were then incubated with secondary antibodies diluted in PBS-BSA for a further 45 minutes. Coverslips were washed thrice again in PBS, and once in water before being mounted in Gold Pro-Long Anti-fade medium (Invitrogen), and examined by conventional epifluoresecence microscopy using a Zeiss Axio LSM-510 microscope. Images were deconvoluted and processed using AxioVision 4.7 LE software (Zeiss) and Photoshop CS4 (Adobe) and Illustrator CS4 (Adobe).

2.15 Antibodies

Antibodies used in the study are listed in Table 5.

Table 5. List of antibodies used in this study

Antibody/Conjugate	Concentration (IF)	Concentration (WB)	Source
Primary Antibodies			
Haemagglutinin (HA)	500	1000	Covance
Myc	500	1000	BD Biosciences
O127 (EPEC)	500	NA	R. La Ragione
Tir	200	NA	R. La Ragione
Intimin	500	NA	(Frankel *et al.*, 1996)
N-WASP	100	1000	Sigma
Arp2	200	NA	L. Machesky
GFP	1000	1000	Abcam
Nck	200	NA	BD Biosciences
Cortactin	200	NA	BD Biosciences
Cdc42	NA	1000	BD Biosciences
Rac1	NA	1000	Cell signaling
RhoA	NA	500	Santa Cruz
B-actin	NA	1000	Sigma

Vinculin	750	NA	Abcam
Caspase-3 (cleaved)	50	NA	Cell Signaling
EVH1 (N-WASP)	200	NA	(Crepin *et al.*, 2009)
O152 (*Citrobacter*)	300	NA	(Crepin *et al.*, 2009)
Secondary Antibodies			
Anti-mouse Cy2	200	NA	Jackson ImmunoResearch
Anti-mouse RRX	200	NA	Jackson ImmunoResearch
Anti-mouse Cy5	200	NA	Jackson ImmunoResearch
Anti-rabbit Cy2	200	NA	Jackson ImmunoResearch
Anti-rabbit RRX	200	NA	Jackson ImmunoResearch
Anti-rabbit Cy5	200	NA	Jackson ImmunoResearch
Anti-chicken Cy5	200	NA	Jackson ImmunoResearch
Chemicals			
Oregon Green Phalloidin	100	NA	Invitrogen
TRITC Phalloidin	500	NA	Sigma
Alexa647 Phalloidin	100	NA	Invitrogen
DAPI	1000	NA	Sigma

2.16 Oral infection of mice

All *in vivo* mice experiments were performed by Dr. Valerie Crepin of the Frankel group. Female C57BL/6 mice (18-20 grams) were purchased from Charles River, Inc. All animals were housed in individually HEPA-filtered cages with sterile bedding and free access to sterilized food and water. All animal experiments were performed in accordance with the Animals Scientific Procedures (Act 1986) and were approved by the local Ethical Review Committee. Independent single infection experiments were performed twice using 5 mice per group. Mice inoculated with wild-type strain and uninfected mice were included in parallel with mutant strains. 2 uninfected mice were also included in every experiment as negative controls. Mice were inoculated by oral gavage with ~ 5 x 10^9 of *C. rodentium* suspension in PBS. The inoculum was determined by retrospective plating onto LB agar containing appropriate antibiotics. Stool samples were then collected at regular intervals post inoculation and viable bacterial count per gram of stool was determined after homogenisation in PBS and plating on LB agar containing the appropriate antibiotics. At day 8 post inoculum, the

mice were culled and colonic tissues were collected for histopathological or microscopic studies.

2.17 Indirect immunofluorescence assay of mice colon sections

All tissue harvesting was performed by Dr. Valerie Crepin of the Frankel group. Sectioning of colon samples for microscopy was performed by Ms. Lorraine Lawrence. Segments of the terminal colon of each mouse were collected post mortem at day 8 post inoculation, and fixed in 10% buffered formalin for microscopic examination. Formalin-fixed tissues were then paraffin-embedded, sectioned at 5 μm, and processed for indirect immunofluorescence assay as previously described (Girard *et al.*, 2005, Girard *et al.*, 2007). Formalin-fixed, paraffin-embedded (FFPE) sections were de-paraffinised in Histoclear solution, rehydrated in a graded series of 100%, 95%, 85%, 75%, and 50% ethanol, and treated with a blocking solution containing 10% normal donkey serum (Jackson ImmunoResearch) in PBS containing 1% Tween 20 (PBS-T). After several washes in PBS-T, sections were incubated with an appropriate dilution in PBS-T of rabbit anti-O152 antibody, followed by an additional incubation step with donkey anti-rabbit RRX-conjugated secondary antibody (Jackson ImmunoResearch). DNA of epithelial cells and bacteria was counterstained with DAPI (Sigma). Samples were mounted in Gold Anti-fade medium (Invitrogen), and examined by conventional epifluoresecence microscopy using a Zeiss Axio image microscope. Images were acquired and processed using AxioVision 4.7 LE software (Zeiss).

2.18 Indirect immunofluorescence assay of cryosections

Additional colonic segments were embedded in optimal cutting temperature medium (Raymond A Lamb Limited, UK), then snap-frozen in liquid nitrogen for further cryosectioning. After defrosting to RT, Cryosections were fixed in 3% PFA/PBS as previously described (Girard *et al.*, 2005, Girard *et al.*, 2007). Cryosections were then processed for indirect immunofluorescence assay by blocking with 0.5% BSA and 2% normal donkey serum (Jackson ImmunoResearch) in PBS. After several washes in PBS-T, sections were incubated with an appropriate dilution in PBS-T of anti-EVH1 antiserum to visualize N-WASP, followed by incubation with donkey anti-rabbit Cy2-conjugated secondary antibody (Jackson ImmunoResearch). DNA of epithelial cells and bacteria was counterstained with DAPI (Sigma). Samples were mounted in Gold Anti-fade medium (Invitrogen), and examined by conventional epifluoresecence microscopy using a Zeiss Axio image microscope. Images were acquired and processed using AxioVision 4.7 LE software (Zeiss).

2.19 Scanning electron microscopy

Coverslips were infected as previously described, and fixed in 2.5% glutaraldehyde PBS overnight at 4°C post infection. They were then washed thrice in PBS for 1 1/2 hours with regular changes. Tissues were further postfixed in aqueous 1% osmium tetroxide (OsO_4), rinsed in water, and then dehydrated in a graded series of 50%, 75%, 85%, 95% and 100% ethanol. Samples for scanning electron microscopy (S EM) were then critical-point dried, mounted on aluminium stubs, sputter-coated with gold–palladium for 90 seconds and examined using a JEOL JSM-6390 scanning electron microscope.

2.20 Transmission electron microscopy

All transmission electron microscopy processing and image acquisitions were performed by Dr. Artemis Kosta of the Frankel Group. Colonic segments were fixed in 2.5% glutaraldehyde PBS overnight at 4°C. Samples were washed once in phosphate buffer pH 7.2 and post-fixed in 1% Osmium Tetroxide (TAAB O018) for 1 h at 4°C. Samples were washed thrice (30 min each) in distilled water and treated with 1% uranyl acetate (EMS 22400) for 1 h at 4°C in the dark. Samples were washed again with distilled water, dehydrated in a graded series of acetone (50%, 70%, 90%, 100%), embedded in resin (TAAB 812) and polymerized at 60°C for 48 h. Ultrathin sections (60–90 nm) were cut with an ultramicrotome (Leica Ultracut *UCT),* stained with 2% uranyl acetate (10 min) and lead citrate (3 min) and examined using a Tecnai12 (FEI) electron microscope. Images were taken with a CCD camera (TVIPS, Gauting, Germany).

2.21 Bioinformatics analysis

DNA nucleotide and primary protein sequences were aligned using ClustalW v2.0 software. Images were processed using BioEdit sequence editor v7.0 (BioEdit) and Photoshop CS4 (Adobe).

2.22 Statistical analysis

Results were expressed as mean ± standard deviation. Statistical significance was determined by a two-tailed student's t-test. A p-value of < 0.05 (1-asterisk), <0.01 (2-asterisks), or <0.001 (3-asterisks) was considered to be significant.

Chapter 3 – Tir and EspH in EPEC actin pedestal dynamics

Chapter 3 – Tir and EspH in EPEC actin pedestal dynamics

3.1 EspH is a secreted and translocated T3SS effector

The EPEC *espH* had been reported to encode a 176 aa effector that is translocated into host cells (Tu *et al.*, 2003, Mundy *et al.*, 2004, Rodriguez-Escudero *et al.*, 2005). However, the recently published genomic sequence of EPEC E2348/69 has annotated the gene as a 168 aa effector that lacks 8 aa at the N-terminus. To investigate this inconsistency, nucleotide and protein sequence alignments were generated, from ClustalW2, using EspH from EPEC, EHEC and *C. rodentium*. This revealed two putative START codons separated by 7 aa that is encoded at the beginning of EPEC and *C. rodentium* EspH, but not that of EHEC (Figure 11A). The absence of the first methionine sequence in EHEC can be attributed to a single nucleotide substitution in EHEC, thus deferring the *espH* START codon to the next methionine that is conserved among all EspH effectors (Figure 11A). In addition, nucleotide alignment of *espH* sequences also revealed a conserved strong ribosome binding site located 6 bp upstream of the distal ATG sequence (Figure 11A). This suggests that translation of EspH is initiated by the conserved distal ATG sequence.

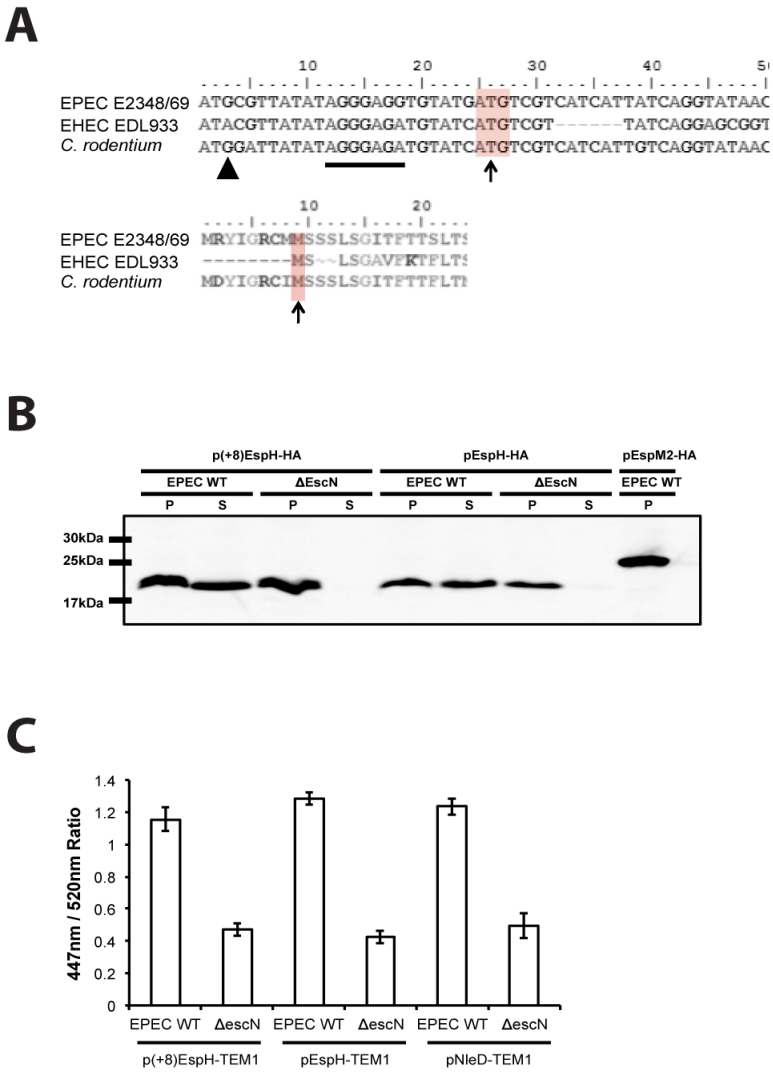


Figure 11. EspH is a secreted and translocated T3SS effector.

(A) Sequence alignment of genomic and protein sequences of EspH from EPEC E2348/69, EHEC EDL933 and *C. rodentium*. Point mutation in EHEC *espH* leading to loss of methionine sequence is denoted by (▲). Strong ribosome binding site is underlined. The suggested start of the coding sequence for EspH is indicated by the black arrow.

(B) Secretion profile of EspH. HA-tagged EspH of the 2 variants (denoted as (+8) for the longer variant) was visualized in pellet (P) and supernatant (S) extracts of EPEC/p(+8)EspH-HA, EPECΔ*escN*/p(+8)EspH-HA, EPEC/pEspH-HA and EPECΔ*escN*/pEspH-HA. EspH was secreted independently of the first 8 amino acids in a T3SS-dependent manner as the *escN* mutant was unable to secrete the effector. EPEC/pEspM2-HA was used as a positive control for HA detection.

(C) Translocation of EPEC/p(+8)EspH-TEM1, EPECΔ*escN*/p(+8)EspH-TEM-1, EPEC/pEspH-TEM-1 and EPECΔ*escN*/pEspH-TEM-1 were quantified as a ratio of cleaved CCF2/AM substrate (447nm) by the TEM-1 β-lactamase fusion proteins to total uncleaved substrate (520nm). NleD-TEM1 was used with wild-type and T3SS-deficient strains as a positive control. Results are presented as a mean ± SD of three independent experiments.

As the first 20 aa have been reported to act as secretion signals for the T3SS apparatus, a secretion profile was performed to determine if the difference in *espH* START codons affected EspH secretion. A C-terminus haemagglutinin (HA) tag was fused to the two variant sequences of EPEC EspH within a pSA10 vector (termed pEspH-HA or p(+8)EspH-HA with the additional 8 aa), and transformed into EPEC wild-type (EPEC WT) or the T3SS-deficient *escN* mutant. EspH expression was induced by IPTG and secretion was allowed to proceed for 3 hours. Bacteria were then pelleted, and the supernatant collected for analysis by western blot. An EPEC WT expressing EspM2-HA was used as a positive control. Both (+8)EspH-HA and EspH-HA were secreted in a T3SS-dependent manner, as no HA-tagged EspH was found in the supernatant of Δ*escN* strains expressing the 2 EspH variants (Figure 11B).

A translocation assay using the fluorescence-based CCF2/AM substrate (Charpentier *et al.*, 2004) was also performed to determine if the the difference in *espH* START codons play a role in the translocation of EspH. To achieve this, EPEC EspH with or without the first eight amino acids were fused to the TEM-1 reporter encoding β-lactamase within a pCX340 vector (termed pEspH-TEM1 or p(+8)EspH-TEM1) and transformed into EPEC WT and the *escN* mutant. The effector NleD was used as a positive control (Marches *et al.*, 2005). Translocation was measured as a ratio between cleaved CCF2/AM substrate that fluoresces at 447nm versus the total amount of uncleaved substrate measured at 520nm. No significant difference was found in the translocation efficiencies of both EspH constructs, indicating that the first 8 aa do not affect effector translocation (Figure 11C). Taken together, these results show that EspH is a T3SS-dependent secreted and translocated effector, and that the first 8 aa

are not required for EspH secretion or translocation. For the purpose of consistency, the EspH sequence used hence forth would be the one that is 168 aa in length.

3.2 EspH promotes actin pedestal formation and elongation

Tu *et al.* (2003) had previously reported that EspH modulates the kinetics of filopodia withdrawal and actin pedestal formation. Specifically, overexpression of EspH inhibited filopodia formation and enhanced pedestal length, while filopodia withdrawal was delayed in an *espH* mutant, and the mutant formed short pedestals. To elucidate the influence of EspH on filopodia and pedestal formation, a kinetics assay was performed using Swiss 3T3 cell lines that show more robust actin cytoskeletal changes compared to HeLa cells.

Swiss 3T3 fibroblasts were infected with EPEC WT and Δ*espH*, or Δ*espH* complemented with plasmid-encoded EspH (Δ*espH*/pEspH). As seen from Figure 12A, the presence of EspH did not inhibit the formation of filopodia during the first 10 minutes of infection in any of the strains. Filopodia formed was however not as prominent in the Δ*espH*/pEspH strain (Figure 12B). Conversely, Δ*espH* formed more prominent filopodia, but showed delayed filopodia withdrawal, as more than 50% of microcolonies observed microscopically had associated filopodia at the site of bacterial attachment after 30 minutes, compared with approximately 10% in all the other strains. The inability to retract filopodia in the *espH* mutant is concomitant with the delay in pedestal formation, as only approximately 70% of microcolonies formed pedestals after 45 minutes (Figure 12A). Complementation of the Δ*espH* with EspH restored efficient filopodia withdrawal, and also led to the sharp increase in pedestal formation at 30 minutes post infection (Figure 12A). The result reaffirms previous

reports that EspH is an effector that promotes filopodia withdrawal and pedestal formation.

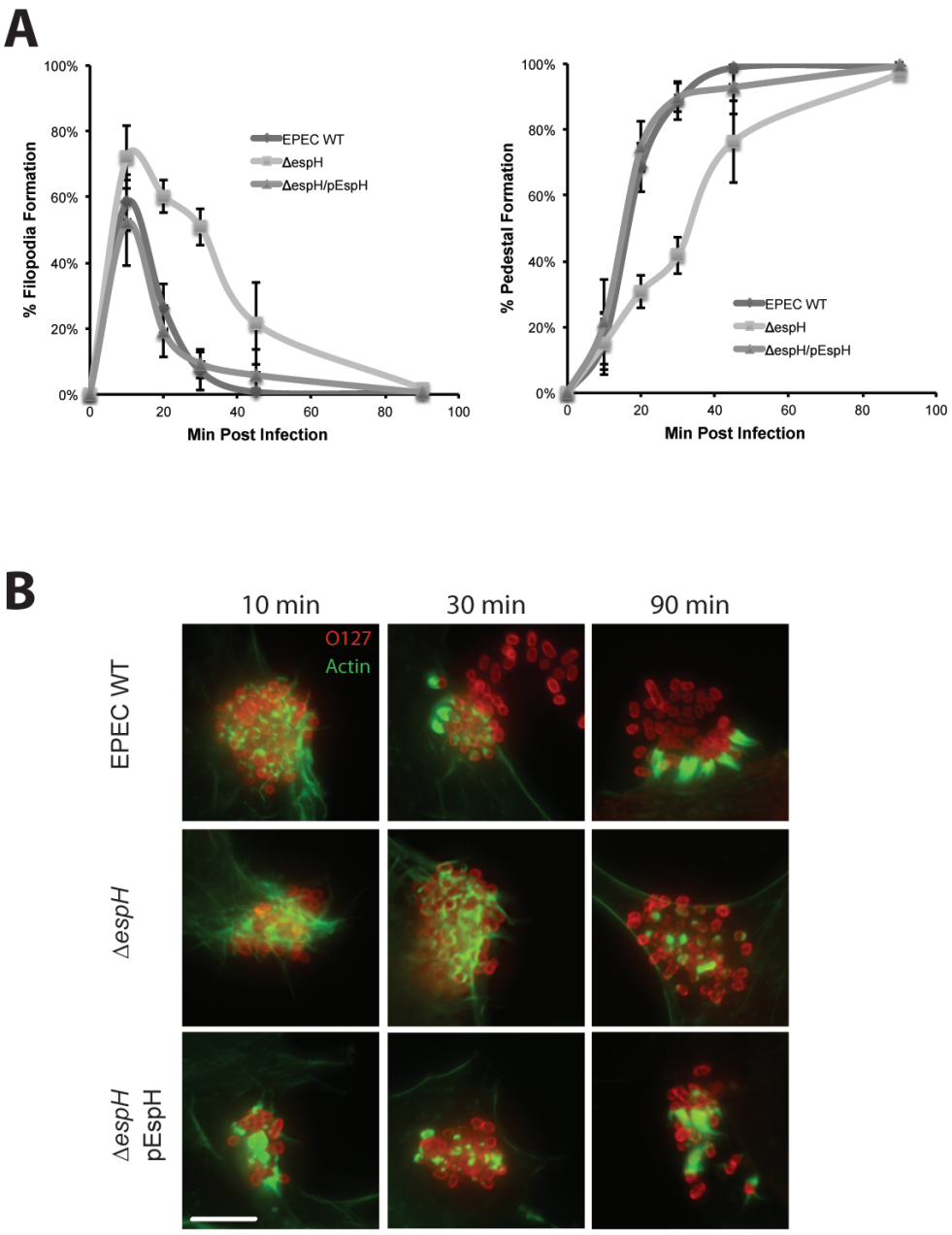


Figure 12. EspH promotes filopodia withdrawal, pedestal formation and pedestal elongation.

(A) Kinetics of microcolony-associated filopodia or actin pedestal formation in Swiss 3T3 fibroblasts infected with EPEC WT, Δ*espH*, or Δ*espH* complemented with EspH (Δ*espH*/pEspH) for 10, 20, 30, 45 and 90 min post infection. 100 microcolonies were counted in triplicates for filopodia or pedestal formation at 10, 20, 30, 45, and 90 min post infection. Only 41.7 ± 5.5 % of Δ*espH* microcolonies formed actin pedestals at 30 min post infection, compared to over 85% in

the wild type and the complemented mutant strains. Results are presented as a mean ± SD of three independent experiments.

(B) Immunofluorescence microscopy of Swiss 3T3 fibroblasts infected with EPEC WT, Δ*espH*, or Δ*espH* complemented with EspH (Δ*espH*/pEspH). Respresentative images were taken at 10, 30 and 90 min post infection. Actin was stained with Oregon green phalloidin (green) and EPEC were detected with anti-O127 antibody (red). Deletion of *espH* resulted in formation of short pedestals at 90 min. Bar = 5µm.

Furthermore, whilst pedestals were eventually formed in all EPEC strains after 90 minutes post infection, the elongated pedestal phenotype that was commonly observed in EPEC WT was notably absent in the *espH* mutant (Figure 12B). Complementation of Δ*espH* with plasmid-encoded EspH restored pedestal length to that of wild-type levels (Figure 12B). Therefore, EspH also modulates pedestal elongation in EPEC.

3.3 Inhibition of Cdc42 restores actin pedestal length in *espH* mutant

Inactivation of Rho GTPases has also reported to play a role in inducing actin pedestal elongation in EPEC. To investigate the involvement of Rho GTPases in the modulation of actin pedestal length by EspH, Cdc42, Rac1 or RhoA was inactivated using siRNA knockdown for 48 h in Swiss 3T3 fibroblasts, and then infected with EPEC WT, Δ*espH* or Δ*espH*/pEspH for 2 h. Immunoblotting of siRNA-inactivated cells showed that the knockdown was specific for their respective target (Figure 13A). Coverslips were then processed for immunofluorescence, and actin pedestal length of individual bacteria was measured using AxioVision 4.7 LE software (Zeiss). When assessed for the ability of EPEC WT to induce elongated actin pedestals, knockdown of Cdc42 and RhoA induced a modest elongation of actin pedestals compared to EPEC WT. In contrast, knockdown of Cdc42, but not Rac1 or RhoA, was able to restore actin pedestal length in Δ*espH* (Figure 13B). This suggests that Cdc42 may

play an important role in EspH-mediated modulation of actin pedestal formation and elongation.

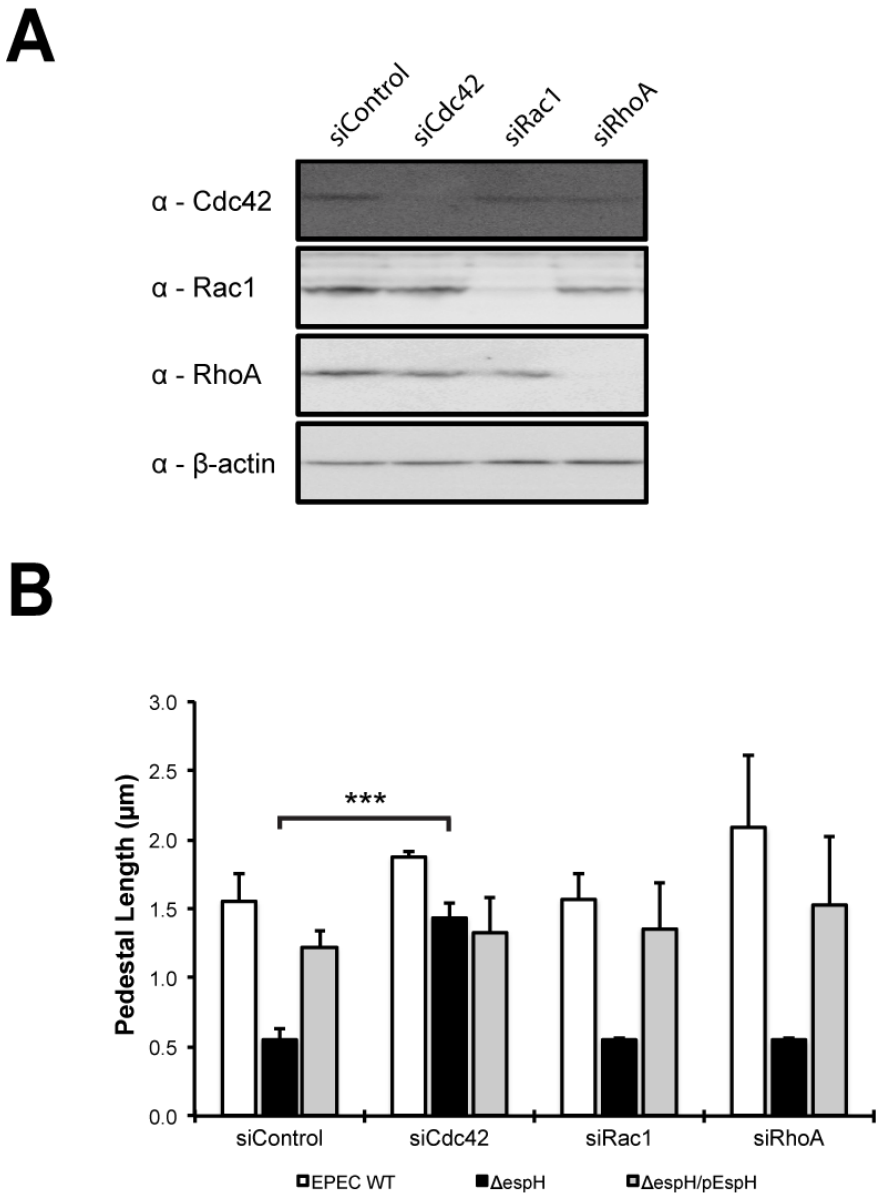


Figure 13. Inhibition of Cdc42 restores pedestal elongation by an EPEC *espH* mutant.

(A) Lysates of Swiss 3T3 fibroblasts transfected with siRNA of scrambled (control), Cdc42, Rac1, RhoA were immunoblotted and probed with anti-Cdc42, anti-Rac1 or anti-RhoA antibodies. B-actin was used as a loading control. Rho GTPases were detected as ~ 20kDa proteins. siRNA knockdown was specific for their respective silencing targets.

(B) Infection of Swiss 3T3 fibroblasts with EPEC WT, Δ*espH*, or Δ*espH* complemented with EspH (Δ*espH*/pEspH) for 90 min. 200 actin pedestals were measured in triplicates using AxioVision 4.7 LE software (Zeiss). siRNA knockdown of Cdc42 in Δ*espH* mutant restores actin pedestal length to EPEC WT levels. Results are presented as a mean ± SD of three independent experiments. * ($P < 0.001$).**

3.4 Characterization of EPEC *tir* chromosomal mutants

Next, we hypothesized that EspH could amplify one of the Tir actin signaling pathways. In order to test this hypothesis, we constructed mutant EPEC strains chromosomally expressing Tir_{Y454A} (mutated at the IRSp53/IRTKS binding site) (termed Tir_{Y454A}), Tir_{Y474A} (mutated at the Nck-binding site) (termed Tir_{Y474A}) and $Tir_{Y454A/Y474A}$ (double mutant) (termed $Tir_{Y454A/Y474A}$). The mutants were constructed based on a lambda red mutagenesis strategy (Datsenko *et al.*, 2000, Crepin *et al.*, 2009) that involved insertion of a kanamycin cassette in the *tir-cesT* intergenic region (Figure 14A). A control mock mutant was also generated with the insertion of the kanamycin cassette, but without modification to the *tir* coding sequence (termed Tir_{WT}).

We first assessed ability of these Tir mutants to translocate Tir and induce actin polymerization by immunofluorescence microscopy of infected Swiss 3T3 fibroblasts. While Tir_{WT} and Tir_{Y454A} strains localized Tir beneath adherent bacteria and induced formation of actin pedestals (Figure 14B), Tir but not polymerized actin was detected underneath EPEC Tir_{Y474A} or $Tir_{Y454A/Y474A}$ strains. Neither Tir nor actin polymerization was observed under the attached Δ*tir* control strain (Figure 14B).

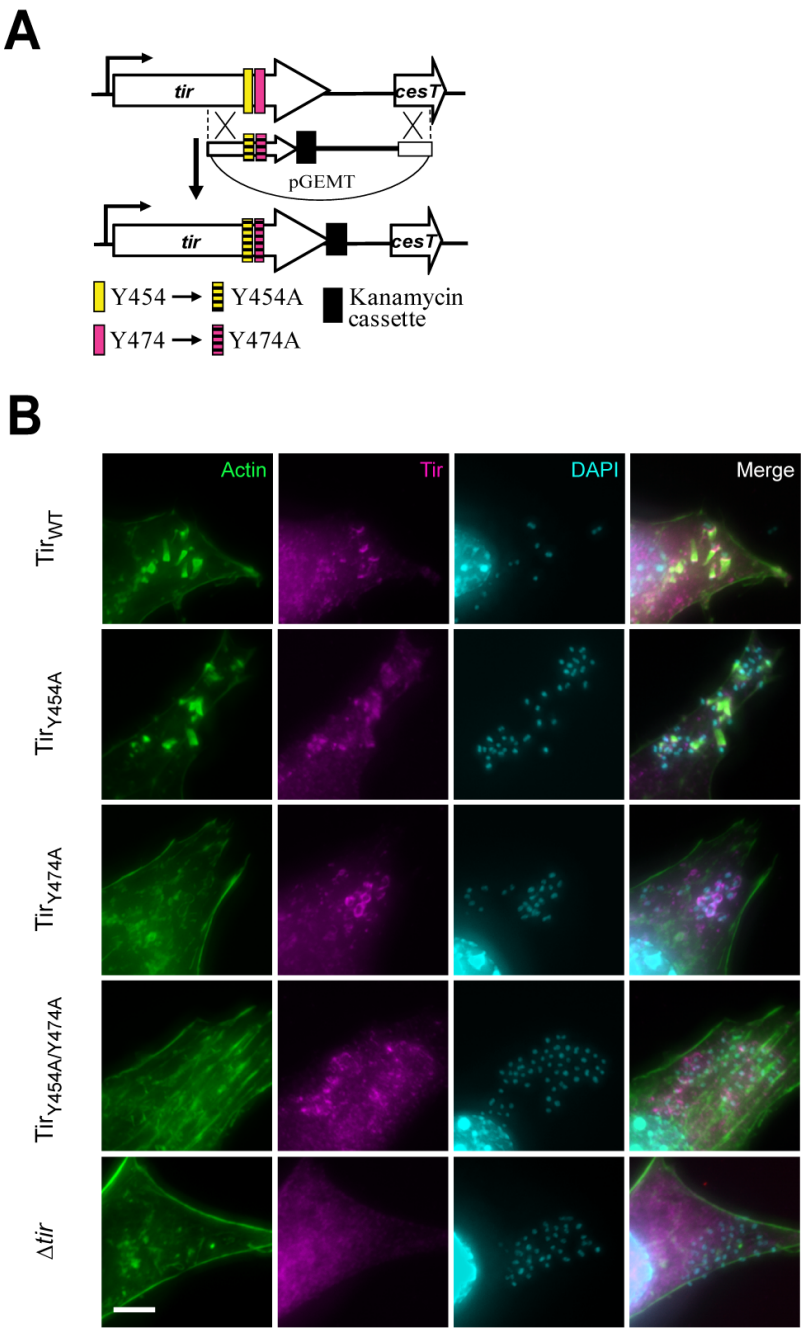


Figure 14. Construction and characterization of EPEC *tir* chromosomal point mutants.

(A) Schematic representation of tir_{EPEC} chromosomal mutagenesis strategy. Amplified fragments of recombinant pGEMT plasmids containing *tir* Y454 and/or Y474 mutations were used to introduce the mutations in tandem with an *aphT* kanamycin-resistance cassette into the endogenous tir_{EPEC} locus to generate EPEC Tir_{Y454A}, Tir_{Y474A} and $Tir_{Y454A/Y474A}$ mutants. As a control recombination of *tir*, an *aphT* kanamycin-resistance cassette with no mutations was inserted (Tir_{WT}).

(B) Infection of Swiss 3T3 fibroblasts with EPEC expressing Tir_{WT}, Tir_{Y454A}, Tir_{Y474A}, $Tir_{Y454A/Y474A}$ or Δ*tir*. Actin was stained with Oregon green phalloidin (green), Tir was detected with anti-Tir antibody (magenta) and bacteria were visualized with DAPI staining (cyan). Actin pedestals were detected in Tir_{WT}, Tir_{Y454A} mutants, but not $Tir_{Y454A/Y474A}$ or Δ*tir*. Bar = 5µm.

3.5 EspH promotes Tir-dependent actin polymerization independently of tyrosine residues 454 and 474

We then ectopically expressed HA-tagged EspH (pEspH-HA) in the same strains, and assessed its localization and impact on Tir-dependent actin polymerization. EspH was mainly localized to the membrane surrounding actin pedestals, as well as to the plasma membrane of infected cells. Expression of plasmid-encoded EspH did not significantly alter actin pedestal length in the EPEC Tir_{Y454A} mutant. Interestingly, expression of HA-tagged EspH triggered localized actin polymerization in EPEC expressing Tir_{Y474A} and $Tir_{Y454A/Y474A}$. EspH-mediated actin polymerization was different from that formed by Tir WT, as EPEC microcolonies appear to be surrounded by an actin 'coat', rather than distinctive pedestals (Figure 15A).

Quantification of EPEC microcolonies revealed that 38.5 ± 10.6% and 38.5 ± 10.9% of adherent EPEC co-expressing HA-EspH and Tir_{Y474A} or $Tir_{Y454A/Y474A}$ respectively were associated with actin (Figure 15B). EspH was mainly localized to the membrane surrounding F-actin, as well as to the plasma membrane of infected cells (Figure A). In contrast, neither actin polymerization nor EspH was detected beneath adherent E2348/69Δ*tir* expressing HA-tagged EspH (Figure 15A), indicating that recruitment of EspH and F-actin at the bacterial attachment site is Tir-dependent.

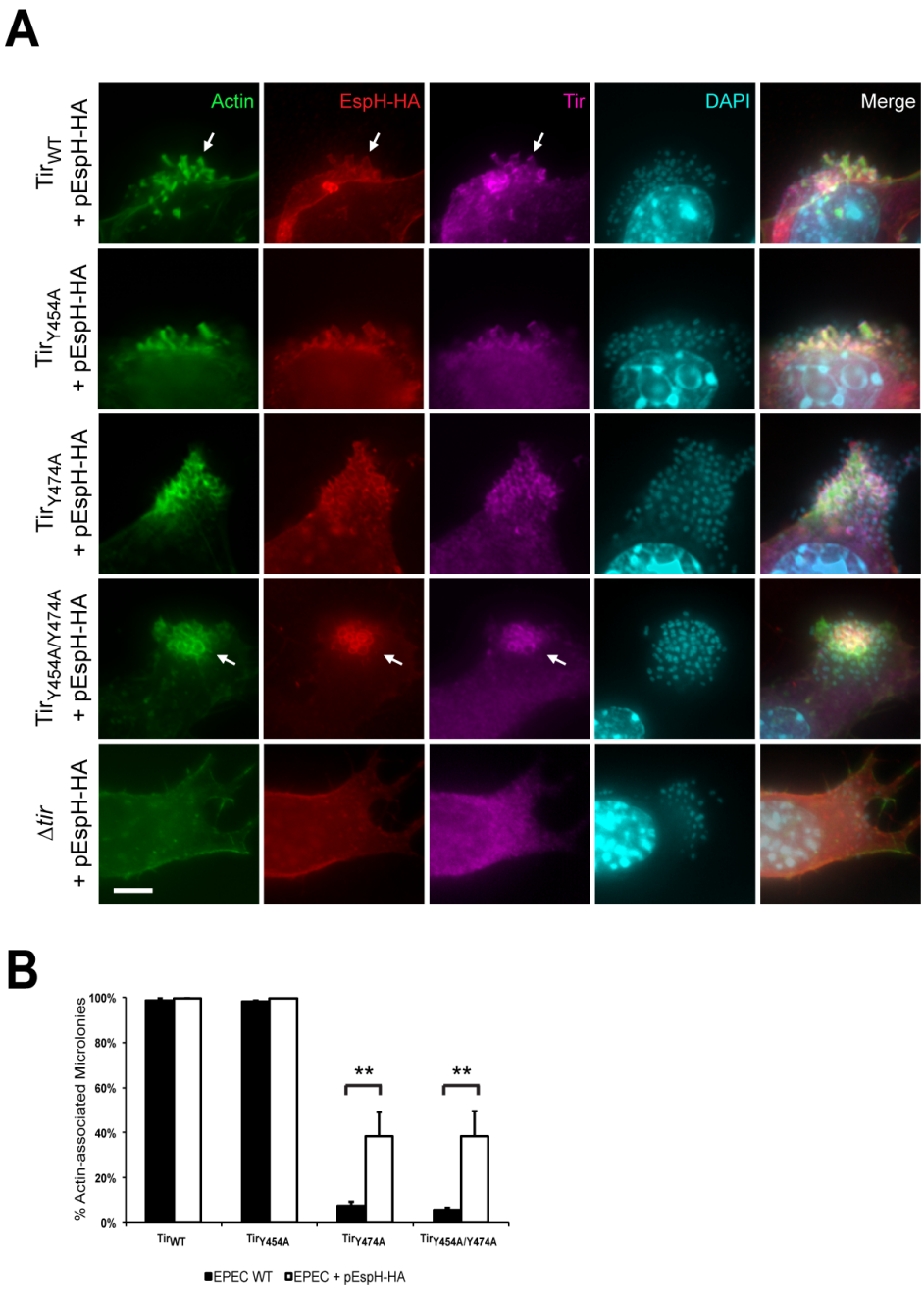


Figure 15. EspH promotes Tir-mediated actin polymerization independently of Tir Y454 and Y474.

(A) Infection of Swiss 3T3 fibroblasts with EPEC expressing Tir_{WT}, Tir_{Y454A}, Tir_{Y474A}, $Tir_{Y454A/Y474A}$ or Δ*tir* with plasmid-expressed haemagglutinin-tagged EspH (pEspH-HA). Actin was stained with Oregon green phalloidin (green), HA-tagged EspH was detected with anti-HA antibody (red), Tir was detected with anti-Tir antibody (magenta) and bacteria were visualized with DAPI staining (cyan). EspH localized to the pedestal membrane (arrows). Ectopic expression of EspH induced localized F-actin accumulation under EPEC expressing $Tir_{Y454A/Y474A}$ (arrows). No detection of actin was observed in EPEC $Tir_{Y454A/Y474A}$ alone or in Δ*tir* + pEspH. Bar = 5μm.

(B) Quantification of EPEC microcolonies associated with actin from (A). 100 microcolonies were counted in triplicates. Results are presented as a mean ± SD of three independent experiments. ** ($P < 0.01$).

3.6 N-WASP and Arp2 are recruited during EspH-mediated actin polymerization

To investigate the mechanism of EspH-mediated actin polymerization, I sought to determine which actin nucleation factors are recruited to the bacterial attachment sites. Following a 2 h infection, coverslips of Swiss 3T3 fibroblasts infected with Tir_{WT}, $Tir_{Y454A/Y474A}$ or $Tir_{Y454A/Y474A}$ strains + pEspH were fixed and stained for N-WASP and the Arp2 subunit of the Arp2/3 complex. N-WASP (Figure 16A) and the Arp2 subunit (Figure 16B) were both detected underneath Tir_{WT} and $Tir_{Y454A/Y474A}$ + pEspH. In contrast, only a few microcolonies of $Tir_{Y454A/Y474A}$ were associated with N-WASP and the Arp2 subunit. These results show that EspH promotes efficient recruitment of N-WASP and the Arp2/3 complex beneath EPEC microcolonies independently of Tir tyrosine residues Y454 and Y474.

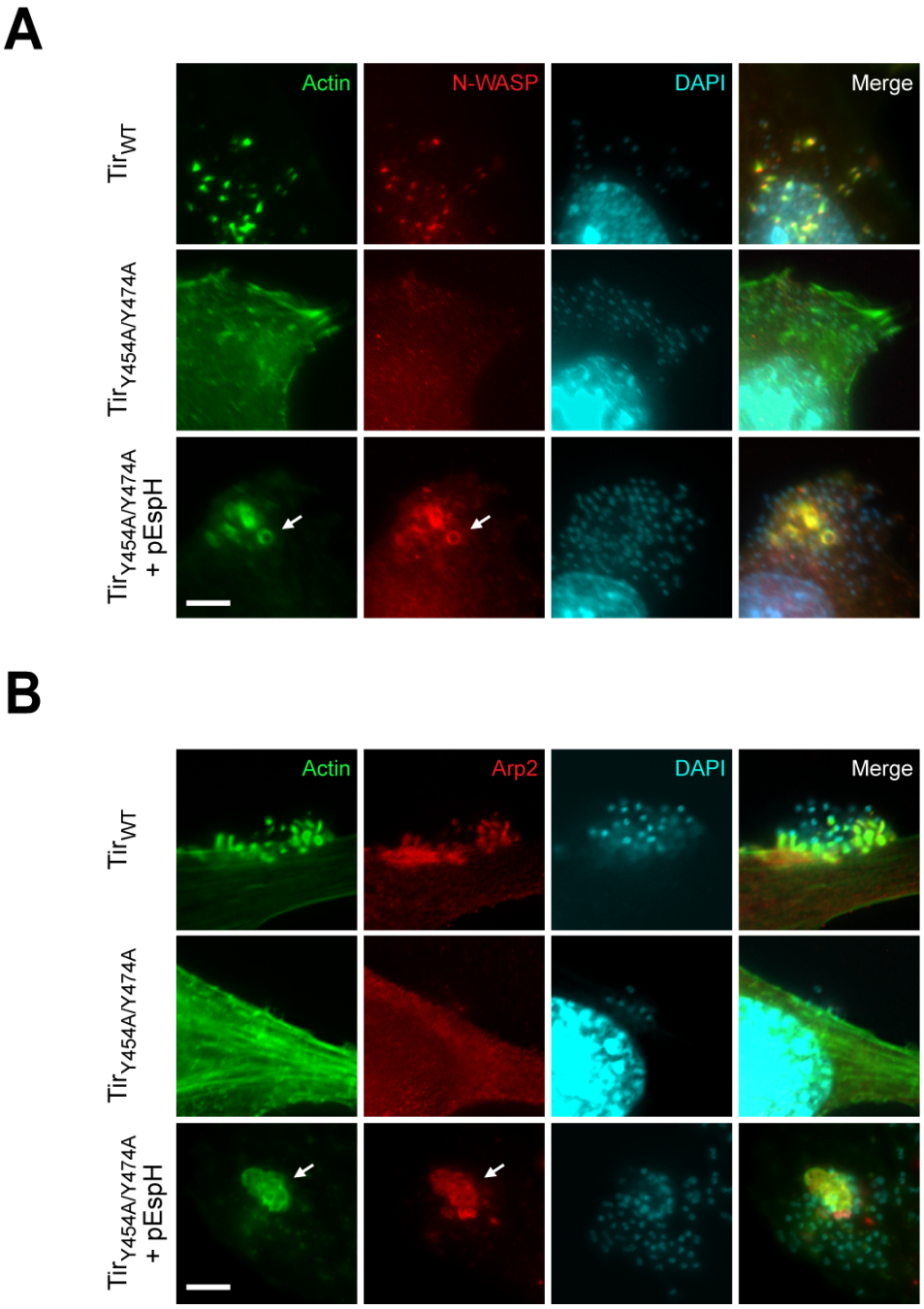


Figure 16. N-WASP and Arp2 are recruited during EspH-mediated actin polymerization.

Infection of Swiss 3T3 fibroblasts with EPEC expressing Tir_{WT}, $Tir_{Y454A/Y474A}$, or co-expressing $Tir_{Y454A/Y474A}$ and EspH ($Tir_{Y454A/Y474A}$ + pEspH). N-WASP (A) or the Arp2/3 complex (B) was detected with anti-N-WASP antibody or anti-Arp2 antibody respectively (red). Actin was stained with Oregon green phalloidin (green), and bacteria were visualized with DAPI staining (cyan). N-WASP (A) and the Arp2 subunit (B) were both detected under adherent EPEC expressing Tir_{WT} and EPEC $Tir_{Y454A/Y474A}$ + pEspH (arrows), but not $Tir_{Y454A/Y474A}$ alone. Bar = 5µm.

3.7 IRSp53 and WAVE2 are not recruited during EspH-mediated actin polymerization

To investigate if other actin promoting factors are recruited to the bacterial attachment sites, I also visualized IRSp53 and WAVE2 by transfection of their respective Myc-tagged constructs for 24 h, followed by infection with EPEC expressing Tir_{WT}, or $Tir_{Y454A/Y474A}$ or co-expressing $Tir_{Y454A/Y474A}$ and pEspH for 2 h. Staining of coverslips for Myc-tagged IRSp53 or WAVE2 revealed that they were not recruited to the bacterial attachment site (Figure 17). This indicates that neither IRSp53 nor WAVE2 are required for EspH-mediated actin polymerization.

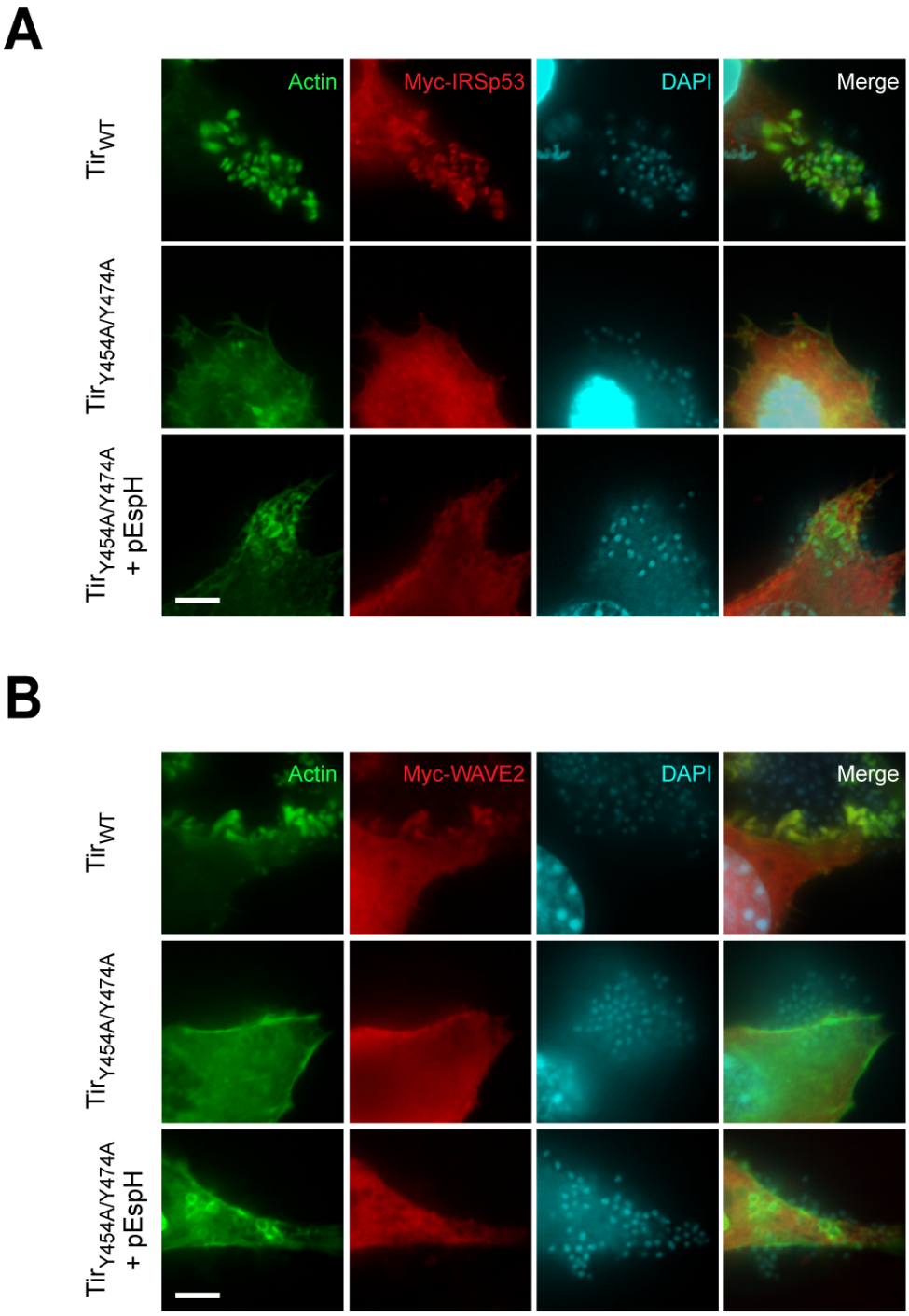


Figure 17. IRSp53 and WAVE2 are not recruited during EspH-mediated actin polymerization.

Swiss 3T3 fibroblasts were transfected with Myc-tagged IRSp53 or WAVE2, and infected with EPEC expressing Tir$_{WT}$, Tir$_{Y454A/Y474A}$, or co-expressing Tir$_{Y454A/Y474A}$ + pEspH. IRSp53 (A) or WAVE2 (B) were detected with anti-Myc antibody (red). Actin was stained with Oregon green phalloidin (green), and bacteria were visualized with DAPI staining (cyan). IRSp53 (A) and WAVE2 (B) were not detected under adherent Tir$_{Y454A/Y474A}$ + pEspH. Bar = 5µm.

3.7 Nck and Rho GTPases are not required for EspH-mediated actin polymerization

Although Tir_{Y474} recruits Nck during EPEC pedestal formation, this does not preclude its role during EspH-mediated actin polymerization. To determine if Nck plays a role in EspH-mediated actin polymerization, we infected Nck-deficient (Nck-/-) fibroblasts expressing Tir WT or $Tir_{Y454A/Y474A}$ strains, with or without pEspH-HA. Both EPEC expressing Tir WT and $Tir_{Y454A/Y474A}$ co-expressing EspH-HA strains were able to trigger localized actin polymerization in the Nck-/- fibroblasts, but not Tir WT or $Tir_{Y454A/Y474A}$ alone (Figure 18A). EspH-mediated actin polymerization is thus dependent on Tir but independent of Nck and the Tir tyrosine residues. To assess if the repression of Rho GTPases is involved in EspH-mediated actin polymerization, we performed siRNA knockdown of Cdc42, Rac1, and RhoA, and infected Swiss 3T3 fiboblasts with EPEC expressing $Tir_{Y454A/Y474A}$, with or without co-expression of EspH. Quantification of EPEC microcolonies revealed no difference in actin-associated microcolonies compared to the scrambled siRNA control (Figure 18B). This suggests that EspH-mediated actin polymerization is not a result of Rho GTPase inactivation.

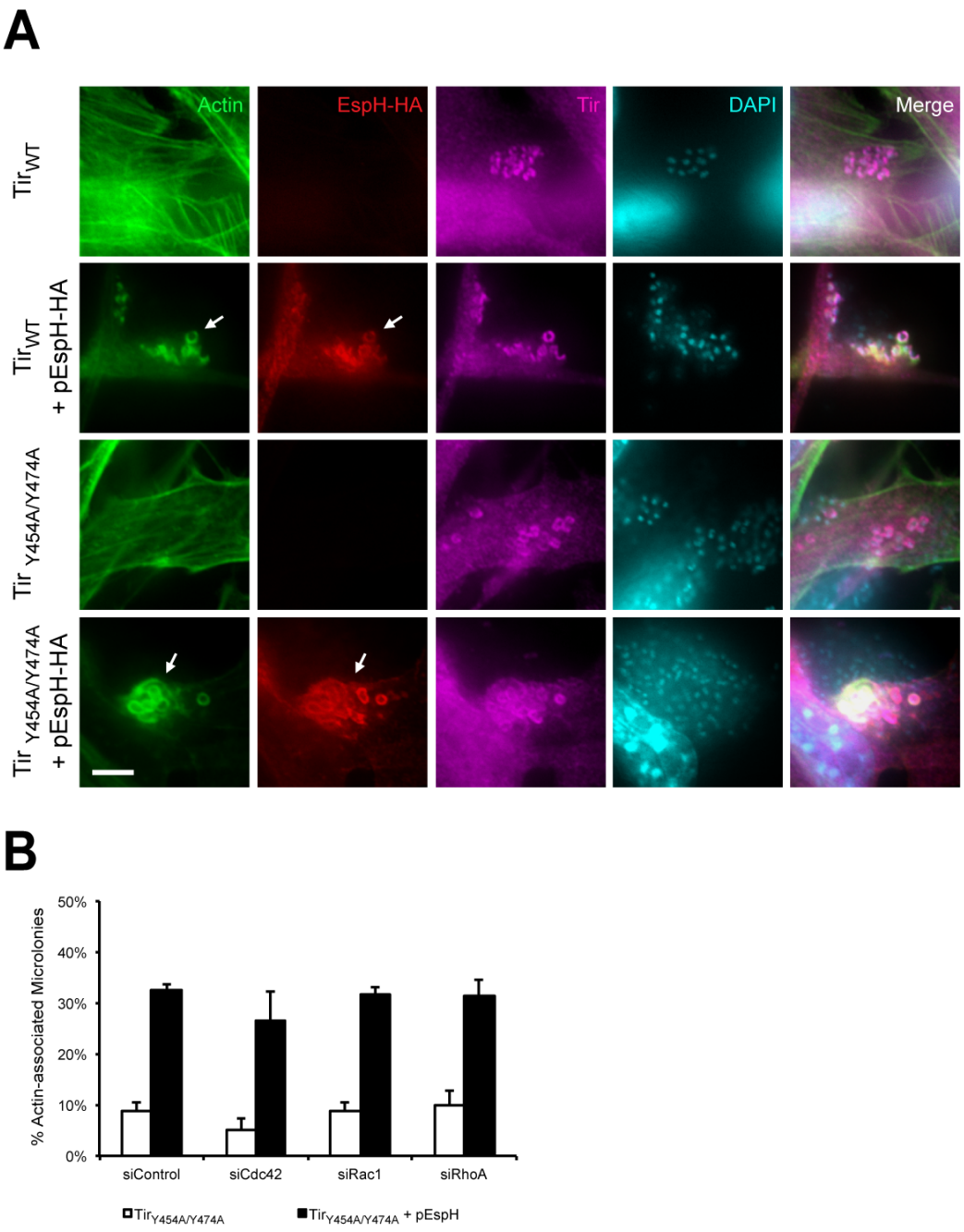


Figure 18. Nck and Rho GTPases are not required for EspH-mediated actin polymerization.

(A) Infection of Nck-deficient (Nck-/-) fibroblasts EPEC expressing Tir WT, $Tir_{Y454A/Y474A,}$ or co-expressing $Tir_{Y454A/Y474A}$ + pEspH. Actin was stained with Oregon green phalloidin (green), HA-tagged EspH was detected with anti-HA antibody (red), Tir was detected with anti-Tir antibody (magenta) and bacteria were visualized with DAPI staining (cyan). Expression of EspH induced localized actin polymerization in both Tir WT and $Tir_{Y454A/Y474A}$ (arrows). Bar = 5µm.

(B) Quantification of EPEC microcolonies associated with actin on siRNA-treated cells infected with EPEC expressing $Tir_{Y454A/Y474A}$, with or without EspH (pEspH). 100 microcolonies were counted in triplicates. Results are presented as a mean ± SD of three independent experiments.

3.8 EspH-mediated N-WASP recruitment is dependent on the C-terminus of Tir

We next determined which of the cytoplasmic Tir domains is involved in EspH-mediated N-WASP recruitment. Towards this end, we utilized a Tir complementation assay previously described (Campellone *et al.*, 2004b). We obtained an HA-tagged membrane-targeting Tir derivative that has its N-terminus replaced with the transmembrane domain of the Newcastle Disease Virus HN protein, followed by the intimin-binding extracellular loop and C-terminus of Tir (HA-TirMC), and a similar construct but with a point Y474F mutation (HA-TirMC$_{Y474F}$) (kindly provided by J. Leong). Using HA-TirMC as a template, we then deleted the C-terminus domain and inserted the N-terminus of Tir before the HN transmembrane domain to generate HA-TirNM (Figure 19A). With GFP as negative control, we transfected the Tir derivatives into Swiss 3T3 fibroblasts; 30 h later the cells were infected with Δ*tir* + pEspH for 2 hours. Triple staining of HA-tagged Tir, N-WASP, and intimin revealed that both HA-TirMC and HA-TirMC$_{Y474F}$, but not HA-TirNM, recruited N-WASP at the site of intimin-clustered Tir (Figure 19B). These results suggest that EspH-mediated recruitment of N-WASP is dependent on the C-terminus of Tir but independent of Y474.

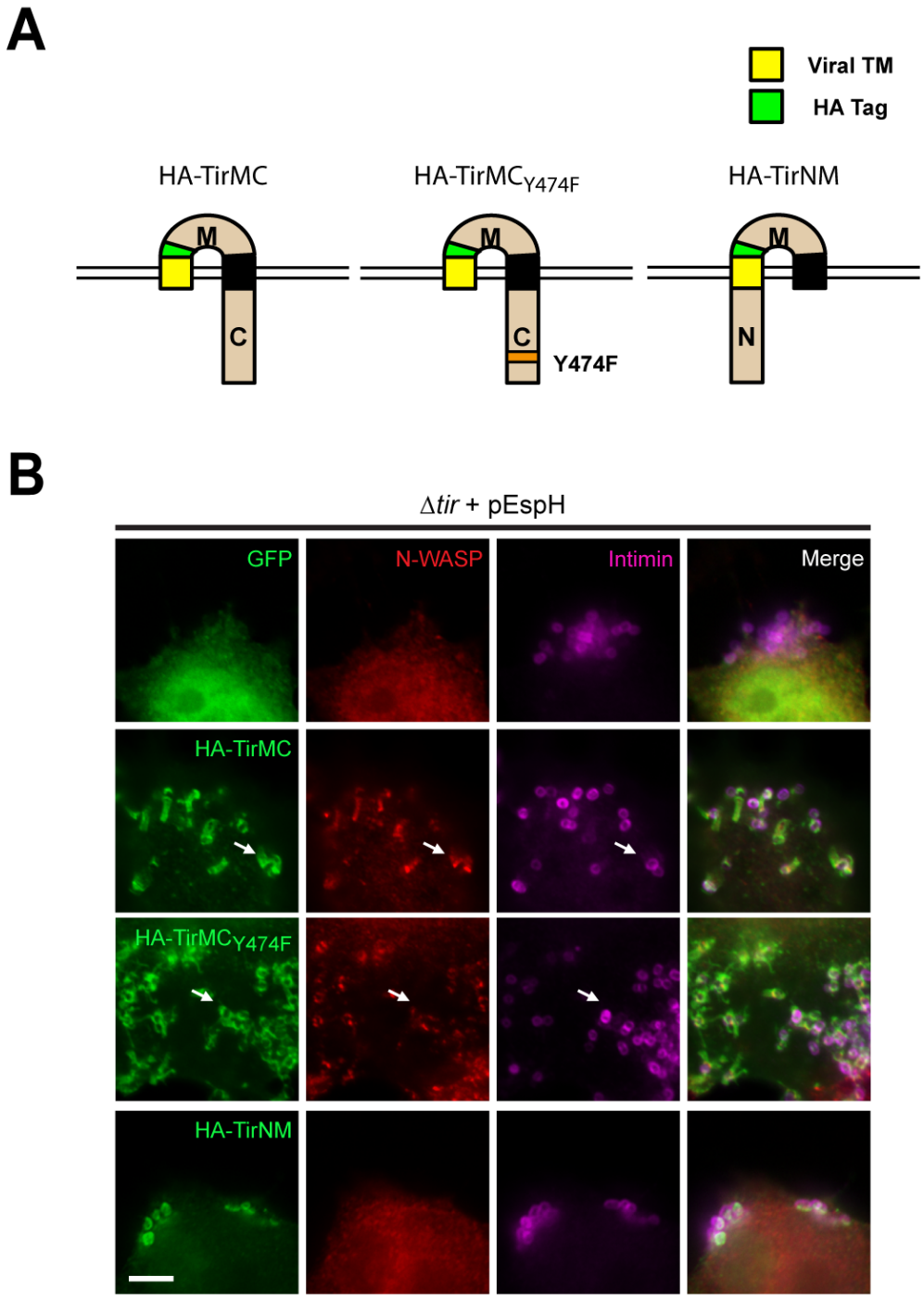


Figure 19. EspH-mediated N-WASP recruitment is dependent on the C-terminus of Tir.

(A) Schematic representation of Tir transfection derivatives comprising HA-TirMC, HA-TirMC$_{Y474F}$, and HA-TirNM.

(B) Swiss 3T3 fibroblasts were transfected with the Tir derivatives, or GFP as negative control and infected with EPEC Δ*tir* expressing EspH (Δ*tir* + pEspH). HA-tagged Tir was detected with anti-HA antibody (green), N-WASP was detected with an anti-N-WASP antibody (red) and bacteria were visualized with an anti-intimin antibody (magenta) to indicate positive Tir clustering. N-WASP was not detected beneath adherent microcolonies in cells transfected with GFP or HA-TirNM. Transfection of HA-TirMC or HA-TirMC$_{Y474F}$ complemented recruitment of N-WASP by Δ*tir* + pEspH (arrows). Bar = 5µm.

3.9 Expression of GFP-N-WASP deletion variants

As EspH promotes the recruitment of N-WASP, the NPF implicated in EPEC-induced actin pedestal formation, we wanted to further investigate the role of N-WASP in EspH-mediated actin polymerization. The N-terminus of N-WASP is modular and consists of WH1, B, GBD, PRD domains that bind numerous adaptor proteins and phosphoinositides (described in section 1.1.3). To identify the domain/s involved in EspH-mediated actin polymerization, we constructed several deletion variants of murine N-WASP fused to GFP by inverse PCR (Figure 20A), and transfected them into N-WASP-deficient (N-WASP-/-) mouse embryonic fibroblasts (MEFs). GFP alone was used as a control. Immunoblotting of N-WASP-/- MEF cell lysates with anti-GFP or anti-N-WASP antibodies indicated that the fusion proteins were expressed during transfection (Figure 20B).

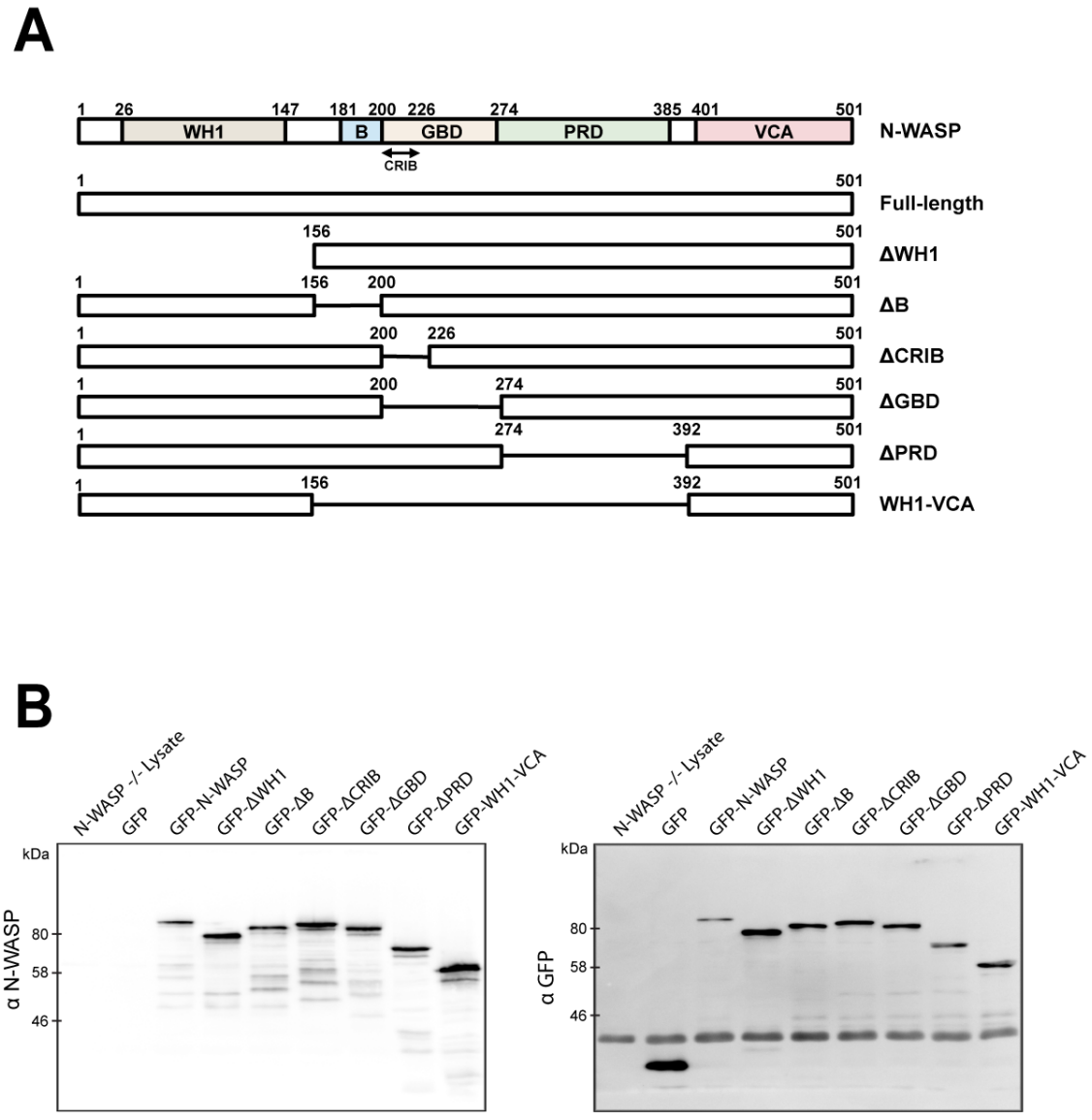


Figure 20. Construction and expression of GFP-N-WASP deletion variants.

(A) Schematic representation of GFP-N-WASP deletion variants GFP-ΔWH1, GFP-ΔB, GFP-ΔCRIB, GFP-ΔGBD, GFP-ΔPRD, and GFP-WH1-VCA.

(B) Lysates of N-WASP-/- mouse embryonic fibroblasts (MEFs) transfected with GFP or GFP-N-WASP deletion variants were immunoblotted and probed with anti-N-WASP or anti-GFP antibodies. GFP-N-WASP was detected as a ~ 90kDa protein; no N-WASP was detected on N-WASP-/- MEFs transfected with GFP alone. Ectopic expression of GFP-ΔWH1, GFP-ΔB, GFP-ΔCRIB, GFP-ΔGBD, GFP-ΔPRD, and GFP-WH1-VCA resulted in accumulation of intact fusion proteins.

3.10 EspH-mediated actin polymerization requires WH1 domain of N-WASP

N-WASP-/- MEFs transfected with the different GFP-N-WASP deletion variants were then infected with EPEC expressing Tir_{WT}, $Tir_{Y454A/Y474A}$ or $Tir_{Y454A/Y474A}$ + pEspH-HA. No polymerized actin was detected in GFP transfected MEFs infected with any of the EPEC strains (Figure 21). Transfection of GFP-N-WASP restored pedestal formation by EPEC expressing Tir_{WT} (Figure 21), with 91.9 ± 1.3% of microcolonies associated with polymerized actin (Figure 22). Only 10.8 ± 0.9% of microcolonies were associated with polymerized actin in the GFP-N-WASP transfected cells infected with EPEC expressing $Tir_{Y454A/Y474A}$ (Figure 22). However, infection of the GFP-N-WASP transfected cells with EPEC co-expressing $Tir_{Y454A/Y474A}$ and EspH resulted in 62.7 ± 5.0% of microcolonies associated with polymerized actin (Figure 22) and N-WASP recruitment to the site of bacterial adherence (Figure 21).

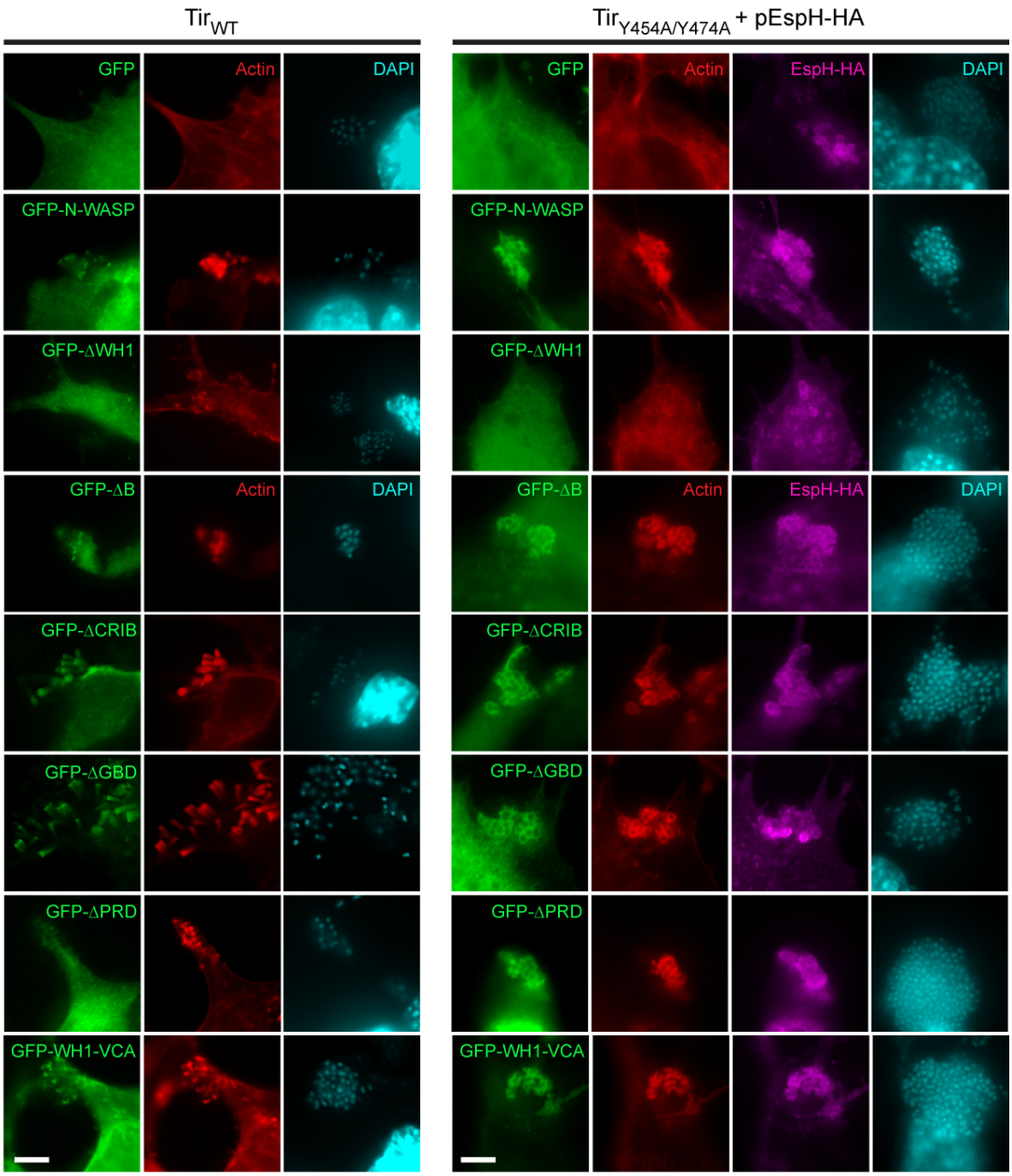


Figure 21. EspH-mediated actin polymerization requires WH1 domain of N-WASP.

N-WASP-/- MEFs transfected with different GFP-N-WASP deletion variants were infected with EPEC expressing Tir$_{WT}$ or co-expressing Tir$_{Y454A/Y474A}$ + pEspH-HA. HA-tagged EspH was detected with anti-HA antibody (green), actin was stained with TRITC phalloidin (red) and bacteria were visualized with DAPI staining (cyan). No actin was detected beneath adherent microcolonies in GFP-transfected cells. Actin polymerization was significantly impaired in GFP-ΔWH1-transfected cells infected with EPEC Tir$_{WT}$ or Tir$_{Y454A/Y474A}$ + pEspH-HA. Transfection with GFP-WH1-VCA was sufficient to restore actin polymerization in Tir$_{WT}$ and Tir$_{Y454A/Y474A}$ + pEspH-HA (arrow). Bar = 5µm.

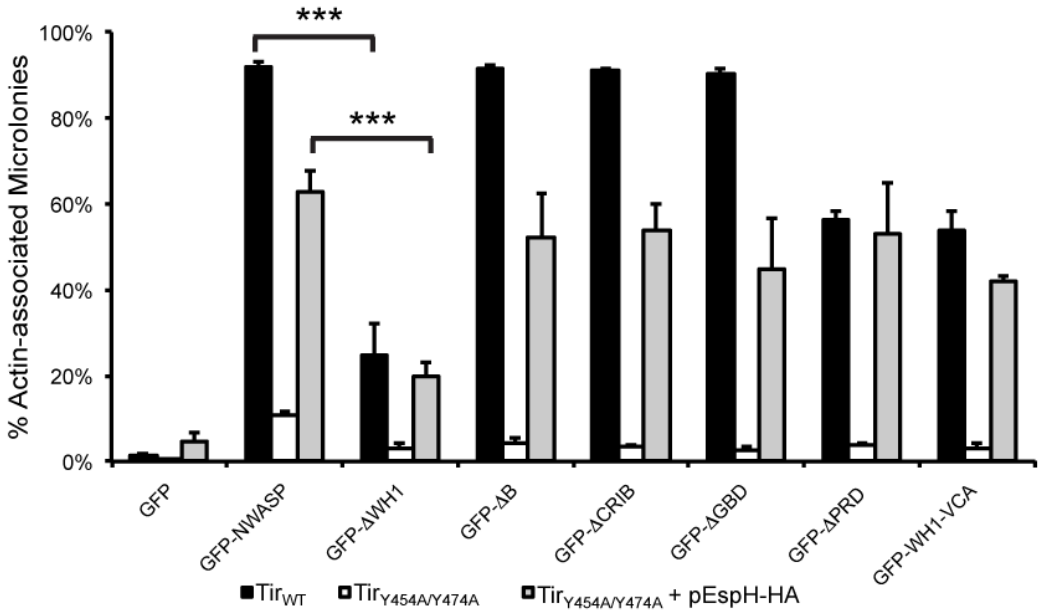


Figure 22. EspH-mediated actin polymerization requires WH1 domain of N-WASP.

Quantification of EPEC microcolonies associated with actin in N-WASP-/- MEFs expressing GFP-N-WASP deletion variants and infected with EPEC expressing Tir_{WT}, $Tir_{Y454A/Y474A}$, or co-expressing $Tir_{Y454A/Y474A}$ and EspH-HA (EPEC $Tir_{Y454A/Y474A}$ + pEspH-HA). 100 microcolonies were counted in triplicates. Results are presented as a mean ± SD of three independent experiments. * (P < 0.001).**

We then assessed the importance of the individual domains of N-WASP on EspH-mediated actin polymerization. Deletion of the WASP-homology 1 (GFP-ΔWH1) or proline-rich (GFP-ΔPRD) domains of N-WASP resulted in a marked decrease in pedestal formation by EPEC expressing Tir_{WT}, as 24.7 ± 7.3% and 56.1 ± 2.1% respectively of EPEC microcolonies were associated with polymerized actin (Figure 21/22). When the transfected MEFs were infected with EPEC expressing $Tir_{Y454A/Y474A}$ + pEspH, only the deletion of the WH1 domain of N-WASP (GFP-ΔWH1) showed a significant reduction, with 19.8 ± 3.2% of EPEC microcolonies associated with polymerized actin (Figure 21/22). Compared to full-length N-WASP, we did not observe a significant difference in actin polymerization triggered by EPEC Tir_{WT} or $Tir_{Y454A/Y474A}$ + pEspH-HA in N-WASP-/- MEFs expressing GFP-N-WASP deletions in Basic (GFP-ΔB), Cdc42/Rac-interactive binding (GFP-ΔCRIB), or

GTPase-binding (GFP-ΔGBD) domains (Figure 21/22). This suggests that PI(4,5)P_2 and Cdc42 are not involved in either actin pedestal formation or EspH-mediated actin polymerization.

In order to ascertain the role of the WH1 domain of N-WASP in EspH-mediated actin polymerization, we constructed an expression variant with the WH1 domain fused directly to the verprolin-central-acidic (VCA) domain which activates the Arp2/3 complex (GFP-WH1-VCA), and ectopically expressed this construct in N-WASP-/- MEFs. Infection with EPEC expressing Tir_{WT} revealed that the WH1 domain is sufficient for pedestal formation, but does not restore the intensity and frequency of actin polymerization to that of full-length N-WASP levels (Figure 21/22). In contrast, the GFP-WH1-VCA construct was as functional as the full-length N-WASP in the context of infection with EPEC expressing $Tir_{Y454A/Y474A}$ + pEspH-HA (Figure 21/22). Taken together, these results show that the WH1 domain of N-WASP is required for EspH-mediated actin polymerization, while both WH1 and PRD domains are required for efficient pedestal formation.

3.11 Dominant-negative of WIP abolishes EspH-mediated actin polymerization

WIP interacts with the WH1 domain of N-WASP via its WASP/N-WASP-binding domain (WBD). To investigate the role of WIP in triggering EspH-mediated actin polymerization, we transfected Swiss 3T3 fibroblasts with GFP or a GFP-WBD to determine if the latter exhibited a dominant-negative effect. Fluorescence microscopy of GFP-WBD transfected cells infected with EPEC expressing Tir_{WT} exhibited a marked reduction in actin pedestal formation (Figure 23A), as only 40.1 ± 5.2% of microcolonies formed pedestals (Figure 23B). In contrast, transfection of GFP-WBD severely attenuated EspH-mediated actin polymerization (Figure 23A), as only 3.4 ± 0.1% of EPEC expressing $Tir_{Y454A/Y474A}$ + pEspH-HA microcolonies were associated with polymerized actin (Figure 23B). This suggests that N-WASP recruitment during EspH-mediated actin polymerization is primarily mediated by WIP/N-WASP binding, while WIP recruitment of N-WASP accounts for approximately 60% of pedestal formation efficiency in cultured cells.

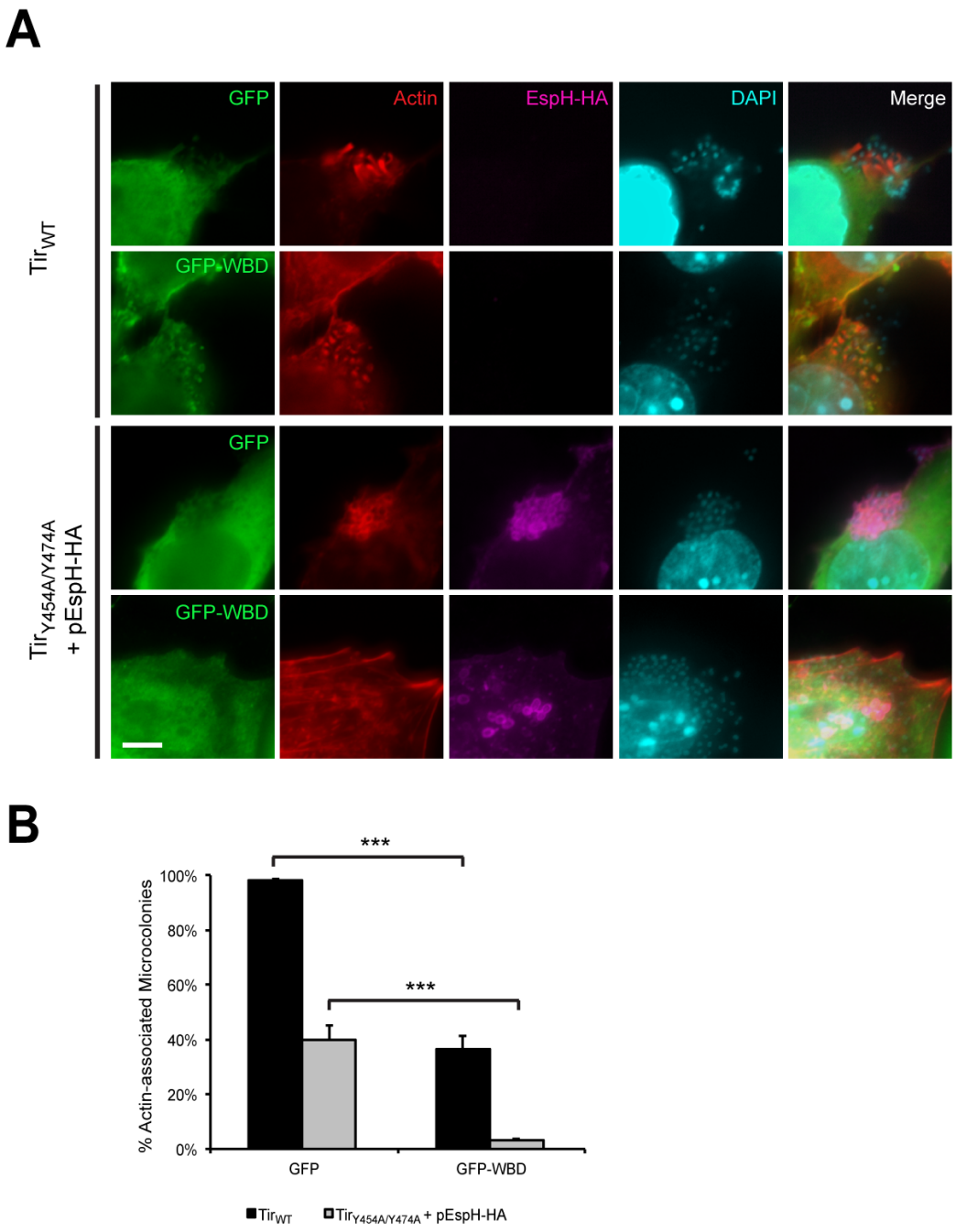


Figure 23. Disruption of WIP/N-WASP binding abolishes EspH-mediated actin polymerization.

(A) Swiss 3T3 fibroblasts transfected with GFP or GFP fused to the WASP binding domain of WIP (GFP-WBD), with infected with EPEC expressing Tir_{WT} or $Tir_{Y454A/Y474A}$ + pEspH-HA. Actin was stained with TRITC phalloidin (red), HA-tagged EspH was detected with anti-HA antibody (magenta), and bacteria were visualized with DAPI staining (cyan). Transfection with GFP-WBD diminished actin pedestal formation and elongation in EPEC Tir_{WT}, but completely abolishes EspH-mediated actin polymerization in $Tir_{Y454A/Y474A}$ + pEspH-HA (arrows). Bar = 5µm.

(B) Quantification of EPEC microcolonies associated with actin in transfected cells infected with EPEC Tir_{WT} or $Tir_{Y454A/Y474A}$ + pEspH-HA. 100 microcolonies were counted in triplicates. Results are presented as a mean ± SD of three independent experiments. * ($P < 0.001$).**

3.12 EspH recruits WIP independently of Tir-mediated actin polymerization pathways

The observation that both pedestal formation and EspH-mediated actin polymerization require WIP/N-WASP suggests that EPEC may utilize two distinct, yet synergistic, actin signaling pathways that converge on WIP. To test this hypothesis, we constructed a Δ*espH* $Tir_{Y454A/Y474A}$ triple mutant that is deficient in Nck-dependent, NPY-dependent, and EspH-mediated actin signaling pathways. We assessed WIP recruitment by either actin signaling pathways by transfecting GFP-WIP into Swiss 3T3 fibroblasts, and infecting them with EPEC Tir_{WT}, Δ*espH* $Tir_{Y454A/Y474A}$, or Δ*espH* $Tir_{Y454A/Y474A}$ complemented with either Tir or EspH. GFP-WIP was localized to the tip of the pedestal following infection with EPEC Tir_{WT} (Figure 24). Cells infected with Δ*espH* $Tir_{Y454A/Y474A}$ however showed neither WIP recruitment nor polymerized actin to the bacterial attachment site. Complementation of the Δ*espH* $Tir_{Y454A/Y474A}$ with Tir restored the recruitment of WIP and formation of short actin pedestals (Figure 24). Intriguingly, complementation of Δ*espH* $Tir_{Y454A/Y474A}$ with EspH induced intense actin rearrangement and formation of a protrusive structure with an actin core surrounded by GFP-WIP that is associated with EPEC microcolonies (Figure 24). Scanning electron microscopy revealed that these protrusive structures are associated with EPEC microcolonies, which we term 'macro-pedestals'. These results affirm our hypothesis that two distinct actin signaling pathways mediated by the Nck-dependent pathway and EspH are converged on WIP and N-WASP.

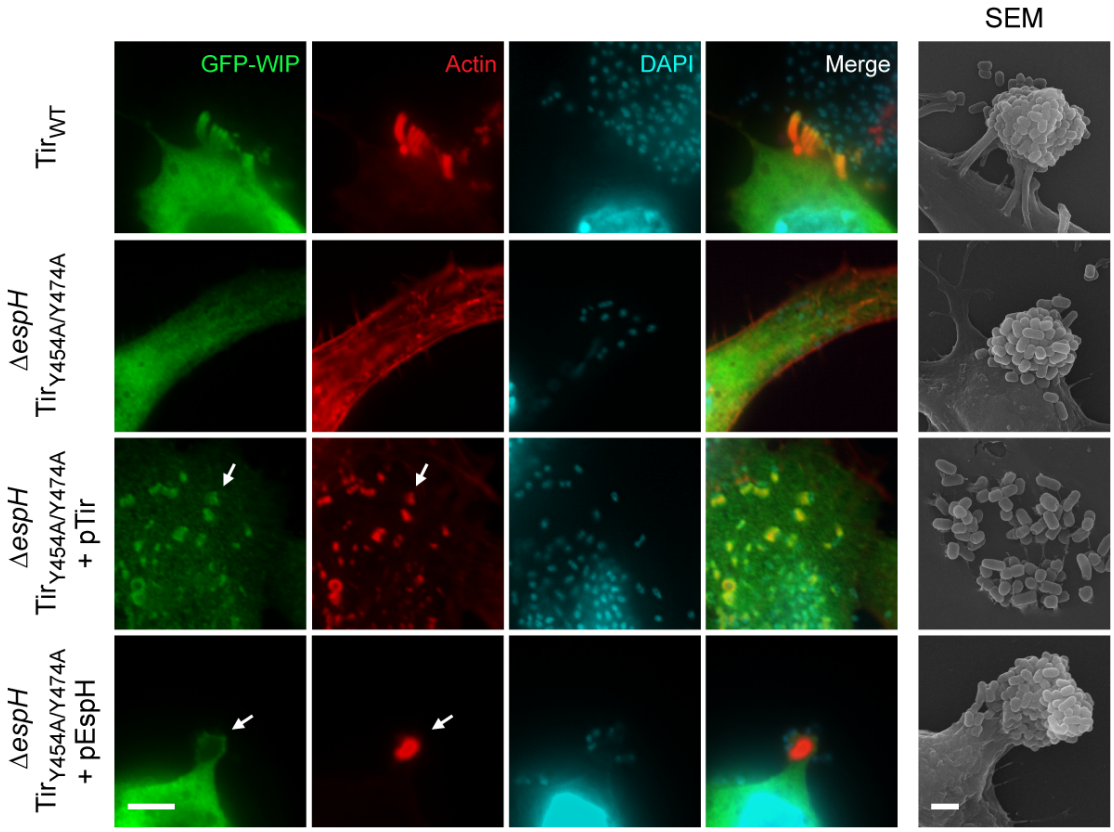


Figure 24. Tir-mediated actin polymerization pathways and EspH recruit WIP to bacterial attachment sites.

Swiss 3T3 fibroblasts transfected with GFP-WIP were infected with EPEC expressing Tir_{WT}, Δ*espH* expressing $Tir_{Y454A/Y474A}$, or Δ*espH*/$Tir_{Y454A/Y474A}$ complemented with either plasmid-expressed Tir (pTir) or EspH (pEspH). Actin was stained with TRITC phalloidin (red), and bacteria were visualized with DAPI staining (cyan). WIP is recruited to the tip of the pedestal in cells infected with EPEC expressing Tir_{WT}, but not Δ*espH* expressing $Tir_{Y454A/Y474A}$. Complementation of Δ*espH*/$Tir_{Y454A/Y474A}$ with either EPEC Tir or EspH restored the recruitment of WIP (arrows). Bar = 5µm. Scanning electron microscopy of the same experiment is displayed on the far right column (Magnification: X6000). Bar = 2µm.

3.13 N-WASP is required for WIP recruitment to bacterial attachment site

In cells WIP exists mainly in complex with N-WASP (Ho *et al.*, 2001). As both Nck-dependent pedestal formation and EspH-mediated actin polymerization recruit WIP and are dependent on N-WASP, we assessed if WIP can be recruited to the site of bacterial attachment independently of N-WASP. In order to test this, we transfected N-WASP-/- MEFs with GFP-WIP and then infected them with EPEC expressing Tir_{WT}, Δ*espH* $Tir_{Y454A/Y474A}$, or co-expressing Δ*espH* $Tir_{Y454A/Y474A}$ + pEspH. None of the strains recruited WIP in the absence of N-WASP (Figure 25), suggesting that WIP and N-WASP are recruited in complex to the site of bacterial attachment.

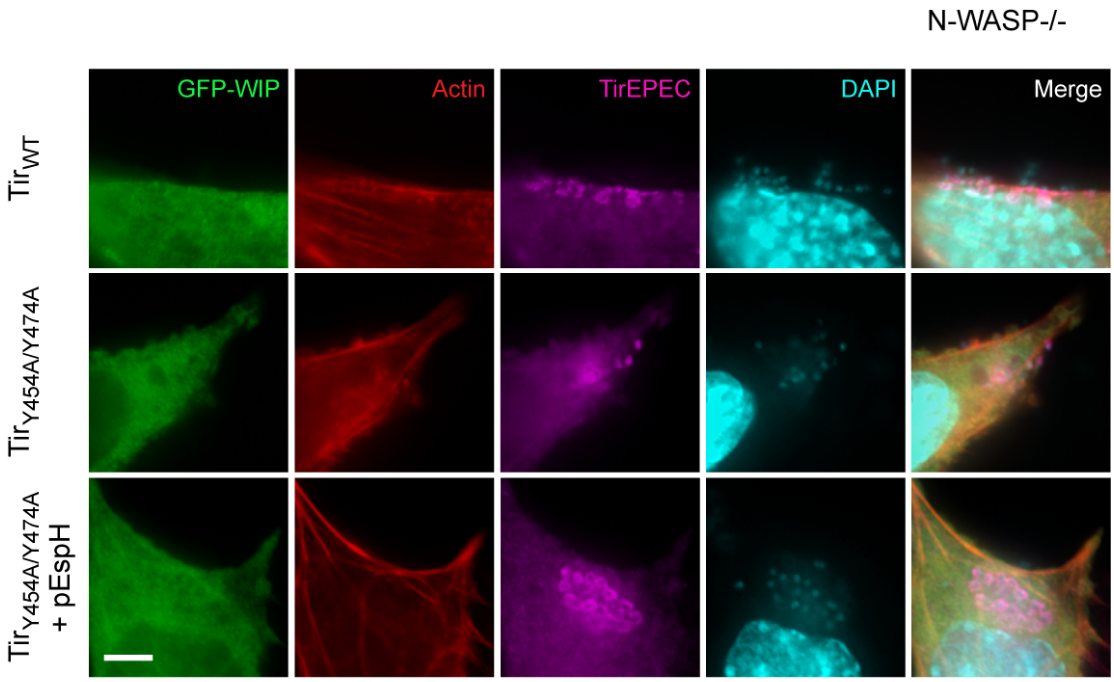


Figure 25. N-WASP is required for WIP recruitment to bacterial attachment site.

Infection of N-WASP-/- MEFs transfected with GFP-WIP with EPEC expressing Tir_{WT}, Δ*espH* expressing $Tir_{Y454A/Y474A}$, or Δ*espH*/$Tir_{Y454A/Y474A}$ + pEspH. Tir was detected with anti-TirEPEC antibody (magenta), actin was stained with TRITC phalloidin (red), and bacteria were visualized with DAPI staining (cyan). None of the strains were able to recruit WIP or trigger actin polymerization. Bar = 5µm.

3.14 Tir, EspH, WIP, N-WASP and cortactin are recruited to macro-pedestals

WIP has been shown to bind to cortactin, Nck and N-WASP (Anton *et al.*, 1998, Volkman *et al.*, 2002, Rohatgi *et al.*, 2001). To further characterize EspH-induced macro-pedestals, we transfected Swiss 3T3 fibroblasts with GFP-WIP and infected them with Δ*espH* $Tir_{Y454A/Y474A}$ complemented with EspH-HA. Cells were fixed and subsequently stained for Tir, EspH, N-WASP, cortactin and Nck. Immunofluoresence microscopy revealed that Tir, EspH, cortactin and N-WASP co-localized with WIP around the macro-pedestals (Figure 26A). Interestingly, although WIP can bind Nck *in vitro,* Nck was not localized to actin macro-pedestals (Figure 26A). As a control, we infected the GFP-WIP transfected cells with EPEC expressing Tir_{WT} or Δ*espH* expressing $Tir_{Y454A/Y474A}$. Tir, Nck, cortactin and N-WASP were all recruited beneath EPEC expressing Tir_{WT}, but only Tir was recruited beneath EPEC expressing Δ*espH* $Tir_{Y454A/Y474A}$ (Figure 26B). These results reaffirm that Nck is not required for EspH-mediated actin polymerization and that ectopic expression of EspH and WIP induces formation of macro-pedestals that are enriched with cortactin and N-WASP.

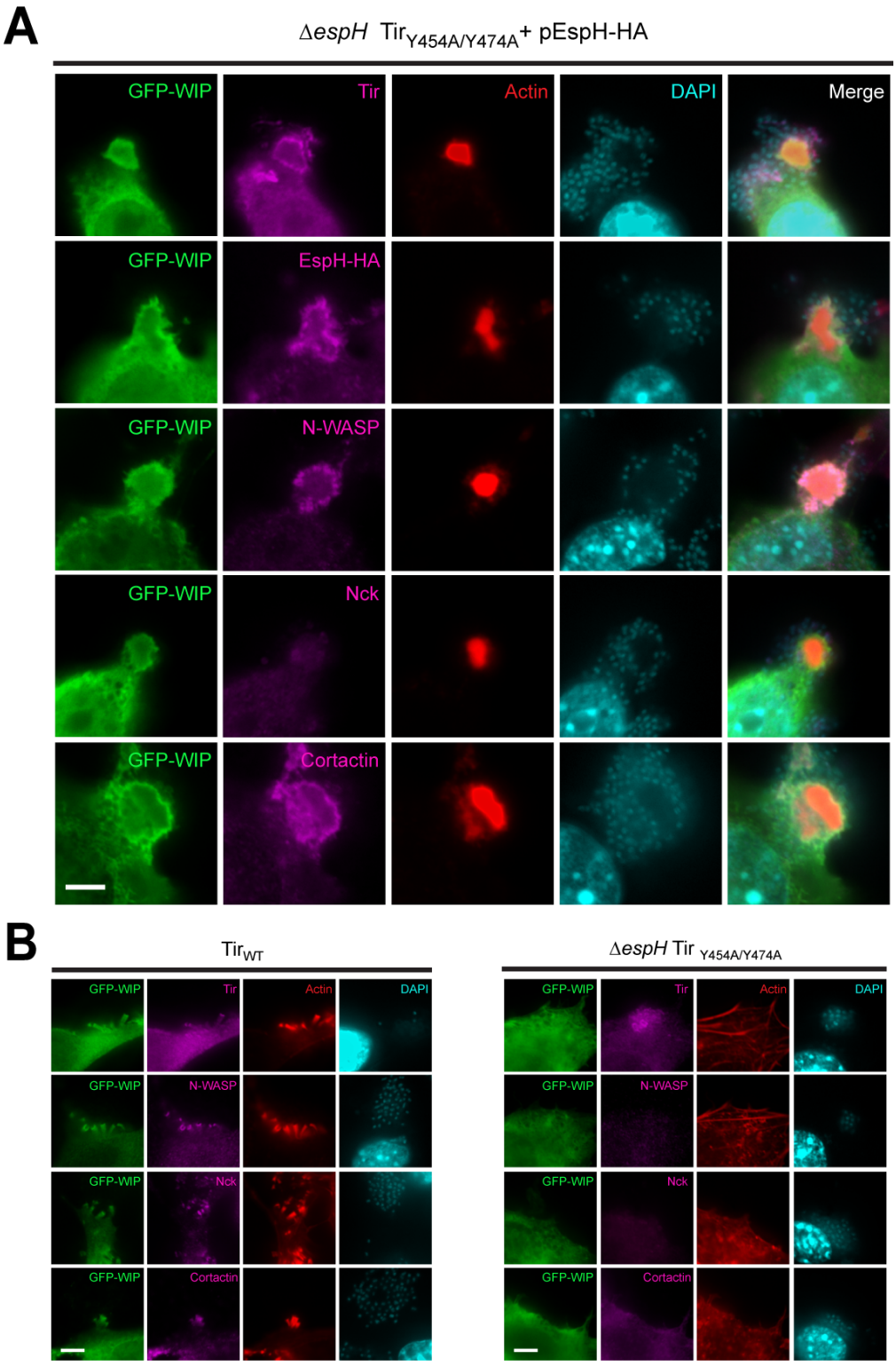


Figure 26. Tir, EspH, WIP, N-WASP and cortactin, but not Nck, are recruited to macro-pedestals.

(A) Swiss 3T3 fibroblasts transfected with GFP-WIP were infected with EPECΔ*espH* co-expressing $Tir_{Y454A/Y474A}$ and HA-tagged EspH (Δ*espH* $Tir_{Y454A/Y474A}$ + pEspH-HA). Tir, EspH-HA, N-WASP, Nck and cortactin were labeled with respective antibodies (magenta), actin was stained with TRITC phalloidin (red), and bacteria were visualized with DAPI staining (cyan). Tir, EspH, cortactin and N-WASP co-localized with WIP, but not Nck. Bar = 5µm.

(B) Swiss 3T3 fibroblasts transfected with GFP-WIP were infected with EPEC expressing Tir_{WT}, or Δ*espH* expressing $Tir_{Y454A/Y474A}$. Tir, N-WASP, cortactin and Nck were labeled with respective antibodies (magenta), actin was stained with TRITC phalloidin (red), and bacteria were visualized with DAPI staining (cyan). Tir, Nck, cortactin and N-WASP co-localizes with WIP at the tip of actin pedestals in Tir_{WT}. Bar = 5µm.

3.15 Tir:Nck, Tir:IRTKS/IRSp53 and EspH-mediated actin polymerization pathways are dispensable for colonization or A/E lesion formation *in vivo*

Construction of *C. rodentium* Δ*espH*/$Tir_{Y451A/Y471A}$ mutant and *in vivo* experiments were performed by Dr. Valerie Crepin. Stool samples of mice infected with *C. rodentium* WT (Nal^R) or *C. rodentium* Δ*espH*/$Tir_{Y451A/Y471A}$ (Cm/Kn^R) mutant were collected and viable count was assessed by selective agar plating. Quantification of bacterial colonies formed per gram of stool showed no significant difference in colonization at the peak of infection (day 8). Moreover, no difference in terms of bacterial clearance was seen for up to day 18 post-infection (Figure 27A/B). Immunofluorescence microscopy of colonic sections taken at day 8 also showed no difference in terms of bacterial colonization and A/E lesion formation (Figure 27C). Taken together, the results show that the Tir:Nck, Tir:IRTKS/IRSp53, and EspH-mediated actin polymerization pathways are not required for bacterial colonization and A/E lesion formation *in vivo*.

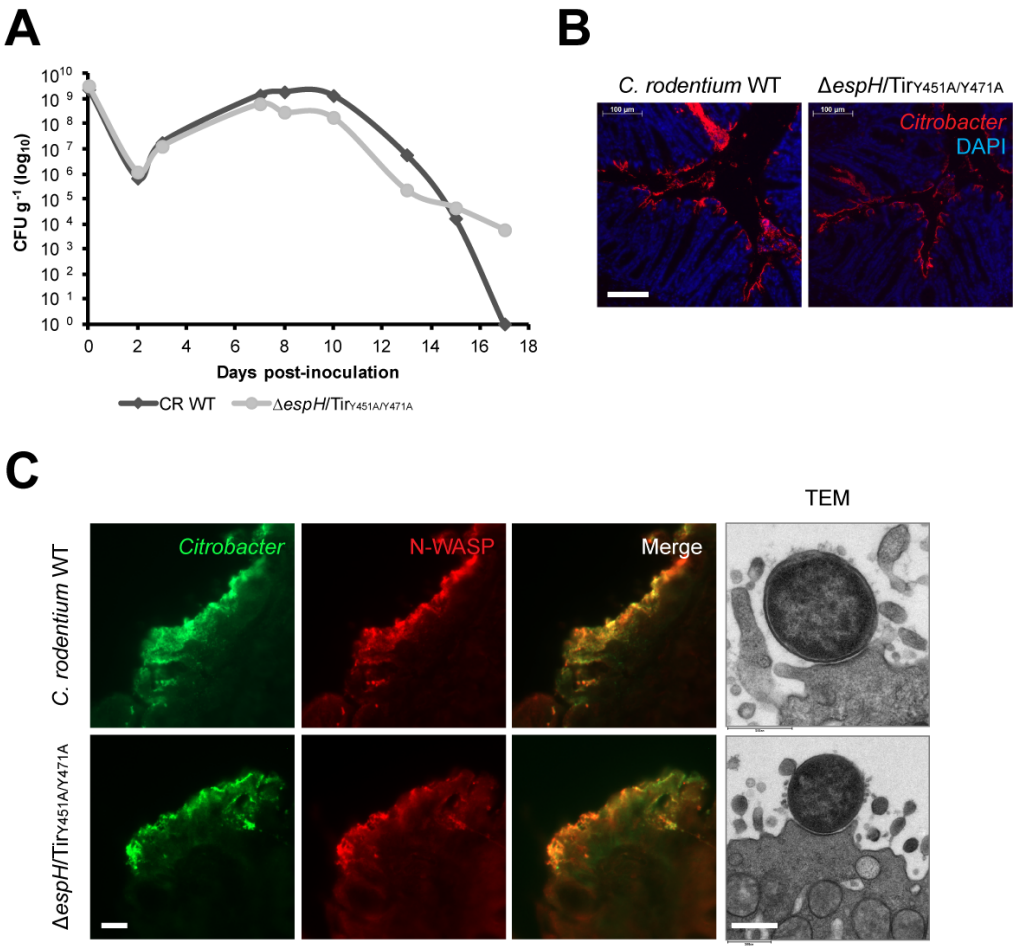


Figure 27. Tir:Nck, Tir:IRTKS/IRSp53 and EspH-mediated actin polymerization pathways are not required for colonization or A/E lesion formation in vivo.

(A) Female C57BL/6 mice were inoculated with *C. rodentium* WT (ICC169) or Δ*espH* expressing $Tir_{Y454A/Y474A}$. Stool samples were collected and viable colonies per gram (CFU g^{-1}) of stool determined by selective agar plating. Δ*espH* expressing $Tir_{Y454A/Y474A}$ did not show a difference in colonization over the course of infection compared to WT.

(B) Indirect immunofluorescence assay was performed on formalin-fixed colon sections taken at day 8 from mice inoculated with *C. rodentium* WT or Δ*espH* expressing $Tir_{Y454A/Y474A}$. *C. rodentium* was visualized with anti-*Citrobacter* antibody (red) and cell nuclei were stained with DAPI (blue). No difference in colonization levels was observed by indirect immunofluorescence assay. Bar = 10µm.

(C) Indirect immunofluorescence assay was performed on colon cryosections taken at day 8 from mice inoculated with *C. rodentium* WT or Δ*espH* expressing $Tir_{Y454A/Y474A}$. *C. rodentium* and N-WASP was visualized with anti-*Citrobacter* (green) and anti-EVH1 antibodies (red). N-WASP was recruited to bacterial attachment sites in the absence of Tir:Nck, Tir:IRTKS/IRSp53 and EspH-mediated actin polymerization pathways. Bar = 10µm. Transmission electron micrograph of respective colon samples indicates no difference in A/E lesion morphology. Bar = 500nm.

To determine if N-WASP was recruited to the site of bacterial attachment *in vivo*, cryosections of mice colon infected with *C. rodentium* WT or *C. rodentium* Δ*espH*/Tir$_{Y451A/Y471A}$ mutant were also taken by Dr. Valerie Crepin, and processed for immunofluorescence microscopy. This revealed that N-WASP was recruited to the site of bacterial attachment in the Δ*espH*/Tir$_{Y451A/Y471A}$ mutant, thus demonstrating that Tir:Nck, Tir:IRTKS/IRSp53, and EspH-mediated actin polymerization pathways are dispensable for N-WASP recruitment *in vivo*. Proccesing of tissue samples for transmission electron microscopy by Dr. Artemis Kosta further revealed no differences in A/E lesions formed by either *C. rodentium* WT or the mutant. This demonstrates that Tir:Nck, Tir:IRTKS/IRSp53, and EspH-mediated actin pathways are dispensable for A/E lesion formation *in vivo*.

3.16 Discussion

In this chapter, we show that EspH mediates Tir-dependent actin polymerization via a novel pathway. We found that EspH promotes N-WASP recruitment and Arp2/3-mediated actin polymerization independently of Tir residues Y454 and Y474 and by extension the Tir:Nck and Tir:IRTKS/IRSp53 actin signaling pathways. Accordingly EPEC triggers localized actin polymerization by parallel mechanisms that eventually converge on WIP and N-WASP.

Tir-induced pedestal formation and EspH-mediated actin polymerization both require the WH1 domain of N-WASP. Lommel *et al*. (2001) previously reported that WIP is found throughout the pedestal length (Lommel *et al.*, 2001). However, we observed that WIP mainly localizes to the tip of pedestals together with Tir, Nck and N-WASP,

suggesting that WIP might have an active role at the site of actin nucleation. In addition, we found that WIP plays an important role in mediating pedestal dynamics as expression of a dominant-negative WIP markedly reduced pedestal formation and elongation. Consistent with the observation that Cdc42 inhibition compensates for the absence of EspH and restores actin pedestal length, WIP inhibits Cdc42-induced filopodia formation (Martinez-Quiles *et al.*, 2001). As N-WASP is required for WIP recruitment to the bacterial attachment site, both proteins appear to be recruited in complex. Since WIP also binds Nck (Anton *et al.*, 1998, Rohatgi *et al.*, 2001), our results give further evidence for a model whereby the Tir:Nck pathway recruits a WIP/N-WASP complex via both Nck/WIP and Nck/N-WASP interactions that synergistically trigger actin polymerization in a process similar to Vaccinia virus actin-based motility (Moreau *et al.*, 2000).

Ectopic expression of WIP also appears to induce extensive actin cytoskeletal rearrangements at the site of bacterial attachment of EPEC overexpressing EspH. This unique actin structure is characterized by the recruitment of Tir, EspH, WIP, and N-WASP around an actin core which we termed "macro-pedestals". WIP over-expression has previously been reported to increase F-actin content and induce formation of subcortical actin clusters in human B cell lines (Ramesh *et al.*, 1997). Although we observed stronger F-actin staining in GFP-WIP transfected Swiss 3T3 fibroblasts (data not shown), we did not observe the formation of macro-pedestals in either EPEC expressing Tir WT or Δ*espH* $Tir_{Y454A/Y474A}$–infected cells, suggesting that this phenotype requires high levels of EspH. Interestingly, while Nck is recruited during EPEC pedestal formation, we could not observe Nck recruitment at the site of

macro-pedestals. This suggests that other adaptor protein/s are involved in the EspH-mediated actin signaling upstream of WIP.

A question that remains unanswered is why endogenous levels of EspH are insufficient to trigger localized actin polymerization during EPEC infection. This question is not limited to EspH as phenotypes of other cytoskeletal-modulating T3SS effectors, e.g. EspV (Arbeloa *et al.*, 2011), EspT (Bulgin *et al.*, 2009b) and EspM (Arbeloa *et al.*, 2008), could only be seen using *in vitro* cell models following over-expression. Indeed, the original report showing that EspH enhances EHEC pedestal elongation was based on expression of EspH above endogenous levels (Tu *et al.*, 2003). This might reflect the existence of a complex regulatory mechanism of effectors expression and translocation *in vivo*, which we do not yet understand, that the cell culture conditions do not mimic. Alternatively, over-expression of EspH may simply shorten the length of time needed by EPEC to initiate EspH-mediated actin polymerization which endogenous levels could only achieve beyond the viability of the infected monolayer. Nonetheless, our data show that just as TccP/EspF$_u$ in EHEC (Garmendia *et al.*, 2004, Campellone *et al.*, 2004a, Garmendia *et al.*, 2006, Sallee *et al.*, 2008, Cheng *et al.*, 2008) and EPEC lineage 2 (Whale *et al.*, 2006) strains are able to amplify the inefficient Tir:IRTKS/IRSp53 actin polymerization pathway, EspH capable of intensifying actin polymerization pathways in a mechanism that is dependent on the C-terminus of Tir. Importantly, while Tir:Nck, Tir:IRTKS/IRSp53 and EspH-mediated actin polymerization pathways are conserved in A/E pathogens, they are not important for colonization or A/E lesion formation *in vivo*. This demonstrates that other mechanisms must be involved. Our lack of understanding at

the molecular level is also underscored by the observation that N-WASP is recruited independently of all three actin polymerization pathways *in vivo*.

The mechanism by which EspH recruits the WIP/N-WASP complex to the bacterial attachment site remains elusive. As we were unable to co-immunoprecipitate EspH with WIP or N-WASP (data not shown), it is unlikely that EspH directly binds WIP/N-WASP. However, the observation that EspH induces co-localization of cortactin with Tir, WIP and N-WASP could entail an exciting prospect where the class II NPF binds WIP to synergistically trigger Arp2/3-mediated actin polymerization in tandem with N-WASP. Alternatively, EspH also localizes to the plasma membrane and promiscuously binds DH-PH containing RhoGEFs (Dong *et al.*, 2010), which contain other domains such as regulator of G-protein signaling (RGS) and Src-homology 3 (SH3) domains (Rossman *et al.*, 2005). It is thus possible that EspH could recruit WIP/N-WASP complex via interactions with specific RhoGEFs. Interestingly, previous studies also demonstrate that the WIP/N-WASP complex can localize and trigger actin polymerization dependent on the curvature of the membrane (Takano *et al.*, 2008). EspH could thus trigger actin polymerization at the plasma membrane as an indirect result of its ability to induce dramatic changes to cell shape (Tu *et al.*, 2003, Dong *et al.*, 2010). Further work is required to determine if membrane dynamics play a role in modulating EspH-mediated actin remodeling.

Chapter 4 – Bacterial RhoGEFs and EspH in modulating actin dynamics, adhesion and cell death

Chapter 4 – Bacterial RhoGEFs and EspH in modulating actin dynamics, adhesion, and cell death

4.1 EspH induces detachment, cytotoxicity and FA disassembly

Inhibition of Rho GTPase signaling is a trigger for apoptosis (Hippenstiel *et al.*, 2002, Qa'Dan *et al.*, 2002). As EspH is known to induce actin cytoskeletal disruption and cell rounding (Tu *et al.*, 2003, Dong *et al.*, 2010), we further characterized EspH-induced cytotoxicity by assessing the levels of cell rounding, cell detachment and lactate dehydrogenase (LDH) release. Myc-tagged EspH (Myc-EspH), or GFP (Myc-GFP) as a control, were ectopically expressed from a pRK5myc vector for 24 h, and the levels of cell rounding quantified by immunofluorescence microscopy. Cells transfected with Myc-EspH showed a marked increase in cell rounding compared to Myc-GFP (Figure 28A).

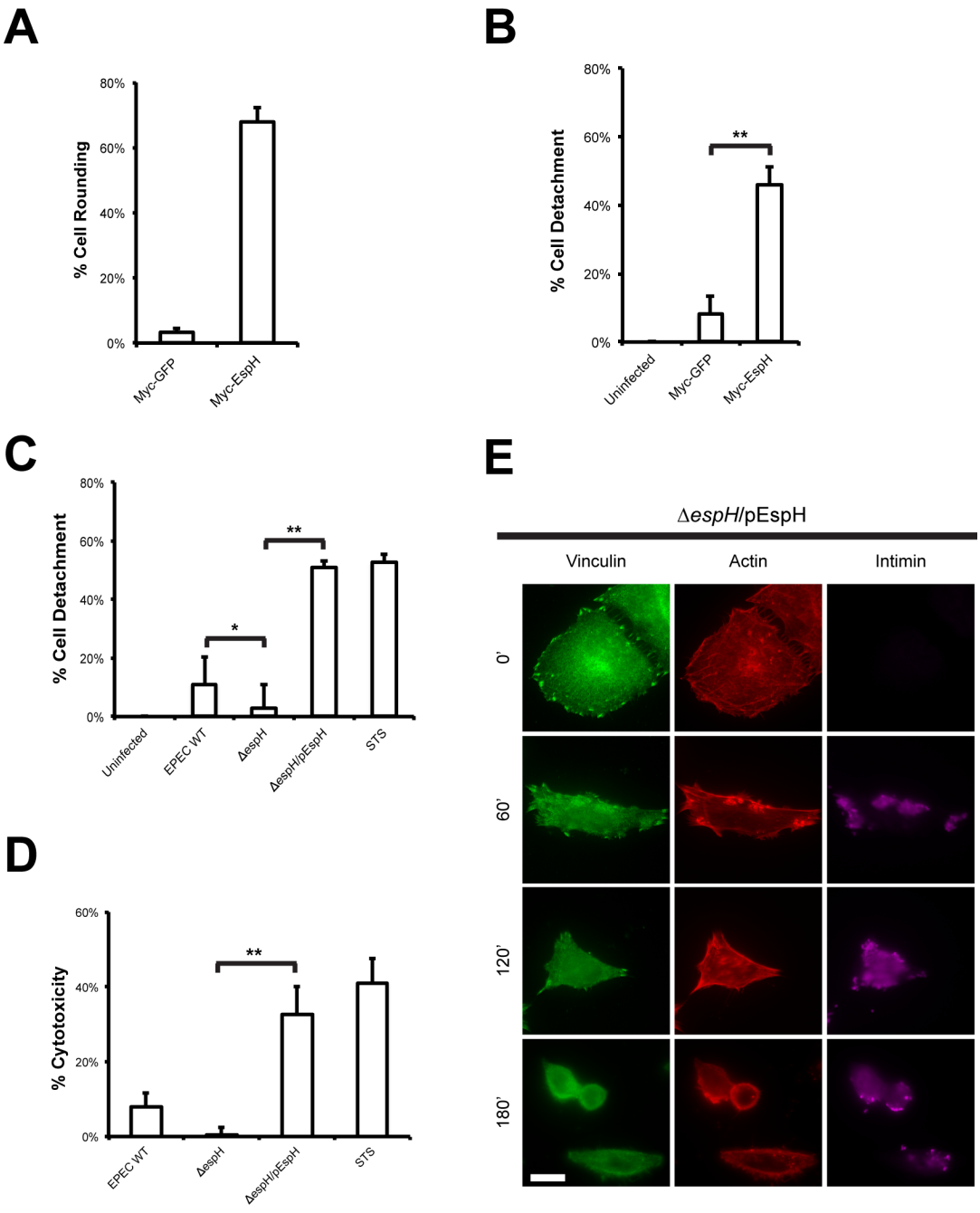


Figure 28. EspH induces cell detachment, cytotoxicity and FA disassembly.

(A) Quantification of cell rounding of HeLa cells transfected with Myc-GFP or My-EspH for 24 h. 100 transfected cells were counted in triplicates. Ectopic expression of EspH induced a significant increase in cell rounding compared to GFP. Results are presented as a mean ± SD of three independent experiments.

(B) Quantification of detachment levels of HeLa cells transfected with Myc-GFP or My-EspH for 24 h. Ectopic expression of EspH induced a significant increase in cell detachment compared to GFP. Results are presented as a mean ± SD of three independent experiments. ** ($p < 0.01$).

(C) Quantification of detachment levels of HeLa cells infected with EPEC WT, Δ*espH*, or Δ*espH* complemented with EspH (Δ*espH*/pEspH) for 1 h, then incubated with gentamicin for 3 h. STS treatment of HeLa cells for 5 h was used as a positive control. Cell detachment was expressed as a percentage of uninfected cells. Cell detachment was reduced in the Δ*espH* mutant compared to

EPEC WT. Complementation with EspH increased cell detachment to STS levels. Results are presented as a mean ± SD of three independent experiments. * ($p < 0.05$), ** ($p < 0.01$).

(D) Quantification of cytotoxicity to HeLa cells infected with EPEC WT, Δ*espH*, or Δ*espH* complemented with EspH (Δ*espH*/pEspH) for 30 min, then incubated with gentamicin for 4 h. STS treatment of HeLa cells for 5 h was used as a positive control. Cytotoxicity was assayed by quantifying the levels of LDH release into the culture supernatant from cells 4 h post-infection. Results are presented as a mean ± SD of three independent experiments.

(E) Immunofluorescence microscopy of HeLa cells infected with Δ*espH* complemented with EspH (Δ*espH*/pEspH) for 0, 60, 120, and 180 min. Bacteria were visualized with anti-intimin antibody (magenta), vinculin was detected with anti-vinculin antibody (green), and actin was stained with TRITC-phalloidin (red). Infection with Δ*espH*/pEspH progressively induced focal adhesion disassembly, as cells were rounded after 180 min infection. Bar = 10 µm.

The level of cell detachment following Myc-EspH or Myc-GFP expression was measured and quantified as the percentage of total cells. Myc-EspH was found to induce 45.8 ± 5.5 % cell detachment, compared to 8.2 ± 5.0 % cell detachment in Myc-GFP control (Figure 28B). A cell detachment assay was also performed to assess the role of EspH during EPEC infection. HeLa cells were infected with wild type EPEC (EPEC WT), Δ*espH*, or Δ*espH* complemented with EspH (Δ*espH*/pEspH) for 1 h, then incubated for a further 3 h with gentamicin to stop bacterial replication. Treatment of cells with the apoptotic inducer staurosporine (STS) for 5 h was used as a positive control. Quantification of cells post-infection showed that 11.0 ± 9.5 % of cells infected with wild type EPEC detached (Figure 28C). In contrast, only 2.9 ± 8.7 % of cells detached following infection with Δ*espH*. Complementation of the mutant with a plasmid-encoded EspH dramatically increased the level of cell detachment to the STS control, as 51.1 ± 1.8 % of cells infected with Δ*espH*/pEspH detached.

The contribution of EspH to cytotoxicity during EPEC infection was also measured by lactate dehydrogenase (LDH) release, which results from plasma membrane damage. Treatment of cells with STS for 5 h was used as a positive control. Infection with wild type EPEC resulted in a slightly higher LDH release compared to the

Δ*espH* mutant (Figure 28D). Complementation of the Δ*espH* mutant significantly increased LDH release to levels comparable with the STS control. EspH is thus a potent inducer of cytotoxicity and cell detachment.

The phenotype of cell rounding and cell detachment led us to examine whether EspH had an effect on focal adhesions. To investigate this, we performed a time-course of HeLa cells infected with Δ*espH*/pEspH by fixing coverslips hourly for 3 h. Using vinculin as a marker for focal adhesions, immunofluorescence microscopy revealed that EspH progressively induces disassembly of focal adhesions concomitantly with actin disruption; no focal adhesions were observed when cells were rounded at the end of infection (Figure 28E).

4.2 EspH mediates FA disassembly in a caspase-independent manner

Inhibition of Rho GTPase signaling is also a trigger for caspase activation and apoptosis (Fiorentini *et al.*, 1998) and the EspH-mediated focal adhesion disassembly observed could therefore be a result of caspase-mediated cleavage of focal adhesion proteins (Gervais *et al.*, 1998).

The ability of EspH to induce caspase-3 activation was tested by infecting HeLa cells with EPEC WT, Δ*espH*, or Δ*espH*/pEspH for 1 h, and incubation for a further 3 h in the presence of gentamicin. Treatment of cells with STS for 5 h was used as a positive control and cleaved caspase 3 detected by immunoflourescence microscopy. 61.1 ± 0.8 % of STS-treated cells stained positive for active caspase-3, whereas only 2.9 ± 0.5 % of untreated cells stained positive (Figure 29A/B). 16.9 ± 3.7 % of EPEC WT infected cells stained positive for caspase-3 activation compared to 9.7 ± 2.1 % of

cells infected with the Δ*espH* mutant (Figure 29A/B). Complementation of the Δ*espH* mutant with plasmid-encoded EspH significantly increased caspase-3 activation, as 29.0 ± 1.6 % of cells infected with Δ*espH*/pEspH stained positive for active caspase-3 (Figure 29A/B).

To determine if EspH alone was sufficient to induce caspase-3 activation, cleaved caspase 3 was detected in cells ectopically expressing EspH (Myc-EspH) or Myc-tagged GFP (Myc-GFP) for 24 h. We observed that while 35.9 ± 8.7 % of cells expressing EspH stained positive for active caspase-3 only 1.9 ± 0.8 % of GFP-expressing cells exhibited the presence of cleaved caspase-3 (Figure 29C/D).

We then used the pan-caspase inhibitor zVAD-fmk to assess the levels of cell detachment following infection with Δ*espH*/pEspH (Figure 29E). STS was again used as a control and as expected, STS-induced cell detachment was inhibited by zVAD-fmk as it is caspase-mediated (cell detachment was reduced from 53.9 ± 3.1 % to 11.6 ± 2.6 % in the presence of zVAD-fmk). However, treatment with zVAD-fmk did not diminish cell detachment induced by infection with Δ*espH*/pEspH (62.3 ± 3.1 % cell detachment without and 53.0 ± 2.2 % cell detachment with zVAD-fmk) (Figure 29E).

Immunofluorescence microscopy of Δ*espH*/pEspH-infected cells treated with zVAD-fmk further showed that cells were still rounded and no focal adhesions (vinculin) were observed after a 3 h infection (Figure 29F). These results suggest that EspH-induced cell detachment was a result of FA disassembly rather than caspase activation.

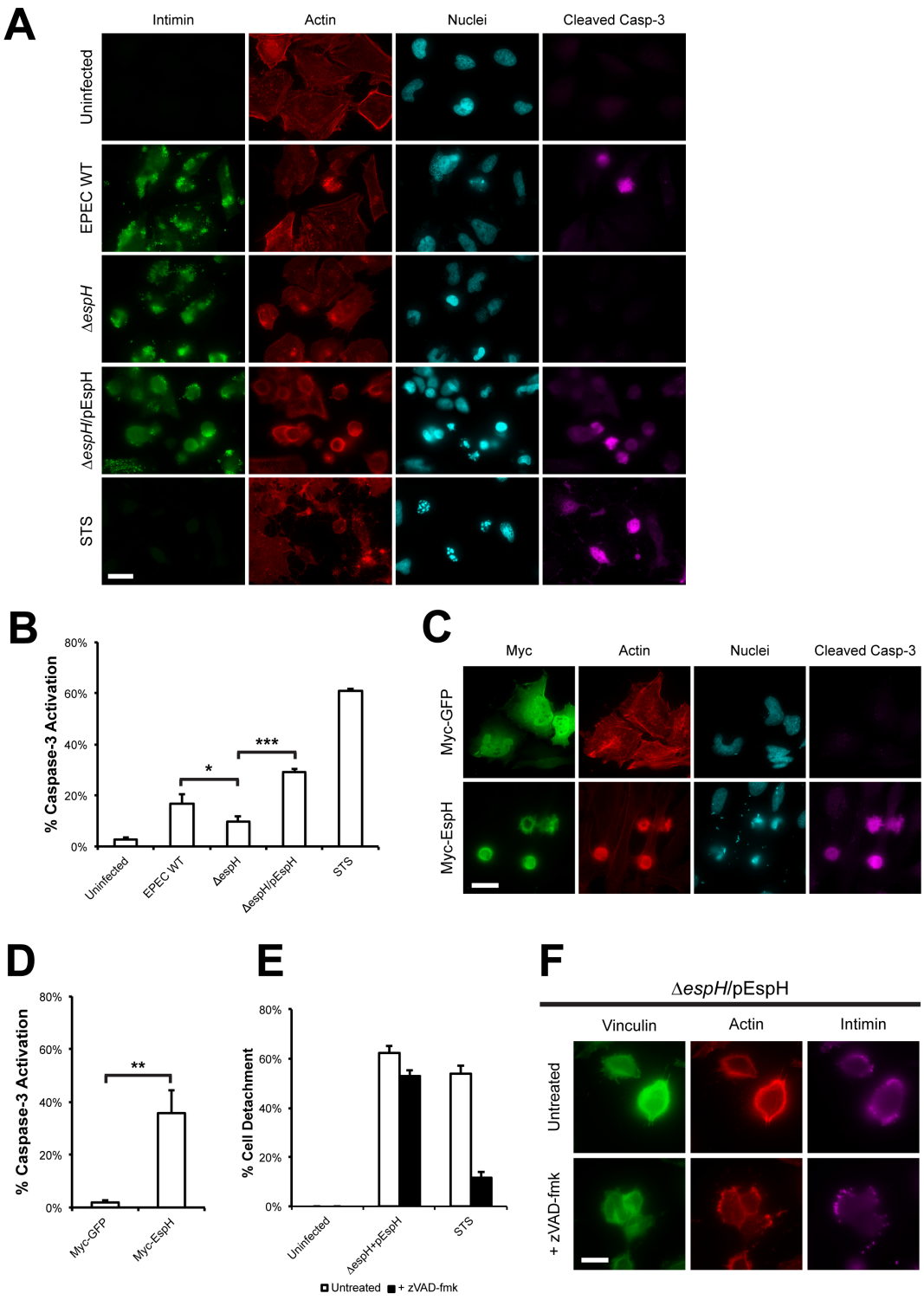


Figure 29. EspH mediates FA disassembly in a caspase-independent manner.

(A) Immunofluorescence microscopy of uninfected HeLa cells or cells infected with EPEC WT, Δ*espH*, or Δ*espH* complemented with EspH (Δ*espH*/pEspH) for 1 h, then incubated with gentamicin for 3 h. Bacteria were visualized with anti-intimin antibody (green), active caspase-3 was detected with anti-caspase-3 (cleaved) antibody (magenta), actin was stained with TRITC-phalloidin (red) and cell nuclei were stained with DAPI (cyan). The Δ*espH* mutant induced reduced levels of caspase-3 activation compared to EPEC WT. Complementation with EspH resulted in a marked increase in caspase-3 activation when compared to Δ*espH* alone. Bar = 20 µm.

(B) Quantification of caspase-3 activation of infected cells from (A). STS treatment of HeLa cells for 5 h was used as a positive control. 100 infected cells were counted in triplicates. Results are presented as a mean ± SD of three independent experiments. * ($p < 0.05$), * ($p < 0.001$).**

(C) Immunofluorescence microscopy of HeLa cells transfected with Myc-GFP or Myc-EspH. Myc-tagged proteins were visualized with anti-Myc antibody (green), active caspase-3 was detected with anti-caspase-3 (cleaved) antibody (magenta), actin was stained with TRITC-phalloidin (red) and nuclei were stained with DAPI (cyan). Ectopic expression of EspH, but not GFP, induced caspase-3 activation. Bar = 20 µm.

(D) Quantification of caspase-3 activation of transfected cells from (C). STS treatment of HeLa cells for 5 h was used as a positive control. 100 transfected cells were counted in triplicates. Results are presented as a mean ± SD of three independent experiments. ** ($p < 0.01$).

(E) Quantification of detachment levels of HeLa cells, with or without zVAD-fmk treatment, infected with Δ*espH* complemented with EspH (Δ*espH*/pEspH) for 1 h, then incubated with gentamicin for 3 h. STS treatment of HeLa cells for 5 h was used as a positive control. Cell detachment was expressed as a percentage of uninfected cells. Treatment with zVAD-fmk inhibited STS-induced cell detachment, but not cell detachment following infection with Δ*espH*/pEspH. Results are presented as a mean ± SD of three independent experiments.

(F) Immunofluorescence microscopy of HeLa cells infected with Δ*espH* complemented with EspH (Δ*espH*/pEspH) for 180 min, with or without zVAD-fmk treatment. Bacteria were visualized with anti-intimin antibody (magenta), vinculin was detected with anti-vinculin antibody (green), and actin was stained with TRITC-phalloidin (red). Treatment with zVAD-fmk did not prevent focal adhesion disassembly. Bar = 10 µm.

4.3 FAK is involved in EspH-induced cell rounding, detachment and caspase-3 activation

As FAK regulates localized Rho GTPase activity and focal adhesion dynamics (Mitra *et al.*, 2005), we investigated if FAK is involved in EspH-induced cell rounding and caspase-3 activation. FAK-null (FAK-/-) and FAK-reconstituted (FAK+/+) fibroblasts were transfected with Myc-tagged EspH or Myc-tagged GFP as a control, and stained for F-actin and cleaved caspase-3. Immunofluorescence microscopy revealed that EspH induced cell rounding and caspase-3 activation in FAK+/+ fibroblasts (Figure 30A-C). In contrast, FAK-/- fibroblasts exhibited reduced levels of cell rounding and little caspase-3 activation (Figure 30A-C).

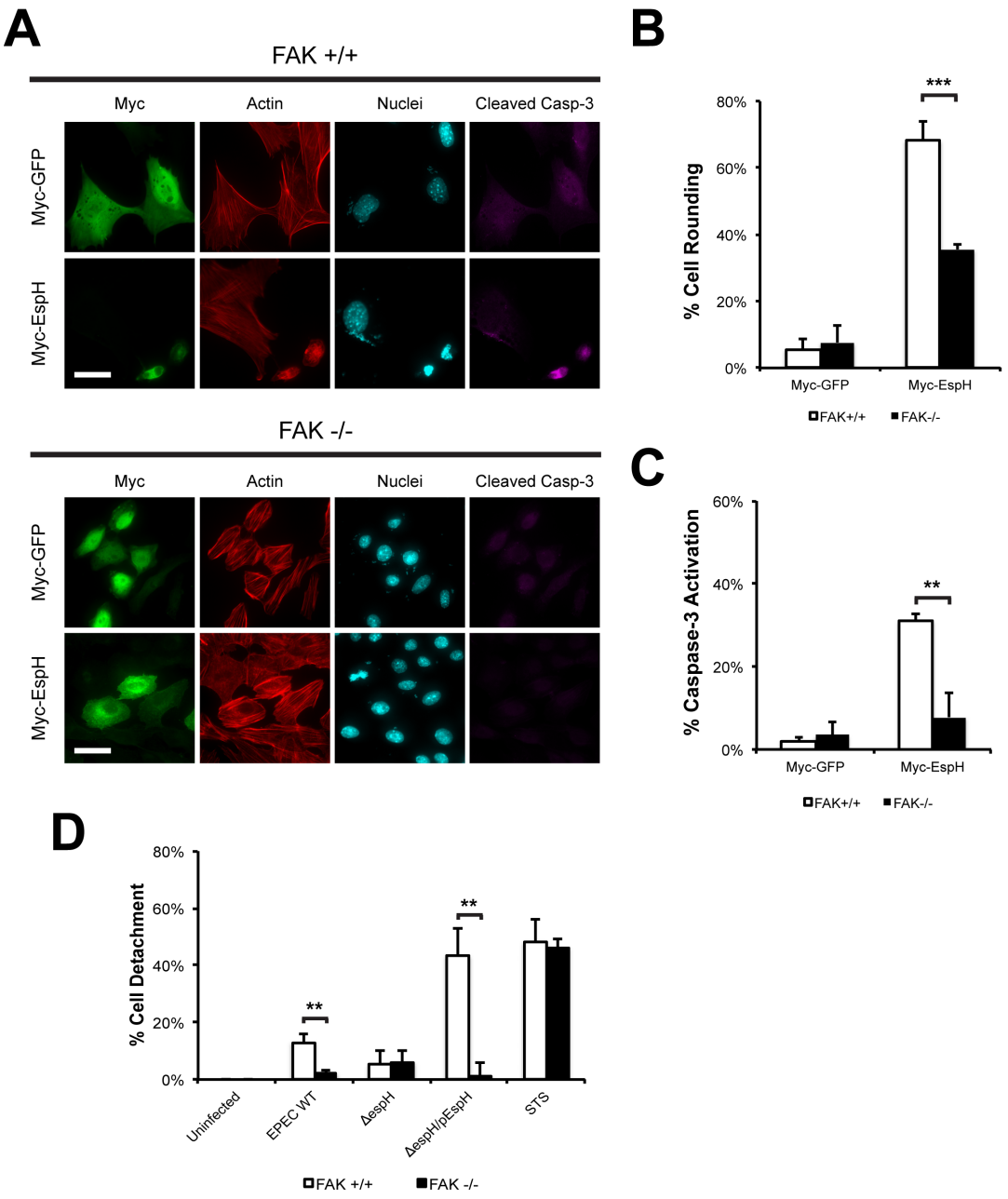


Figure 30. FAK is involved in EspH-induced cell rounding, detachment and caspase-3 activation.

(A) Immunofluorescence microscopy of FAK+/+ or FAK-/- fibroblasts transfected with Myc-GFP or Myc-EspH. Myc-tagged proteins were visualized with anti-Myc antibody (green), active caspase-3 was detected with anti-caspase-3 (cleaved) antibody (magenta), actin was stained with TRITC-phalloidin (red) and cell nuclei were stained with DAPI (cyan). Ectopic expression of EspH induced cell rounding, nuclear condensation and caspase-3 activation in FAK+/+ cells, but not FAK-/- fibroblasts. Bar = 20 µm.

(B) Quantification of cell rounding of FAK+/+ or FAK-/- fibroblasts transfected with Myc-GFP or Myc-EspH. 100 transfected cells were counted in triplicates. Results are presented as a mean ± SD of three independent experiments. * ($p < 0.001$).**

(C) Quantification of caspase-3 activation of FAK+/+ or FAK-/- fibroblasts transfected with Myc-GFP or Myc-EspH. 100 transfected cells were counted in triplicates. Results are presented as a mean ± SD of three independent experiments. ** ($p < 0.01$).

(D) Quantification of detachment levels of FAK+/+ or FAK-/- fibroblasts infected with EPEC WT, Δ*espH*, or Δ*espH* complemented with EspH (Δ*espH*/pEspH) for 1 h, then incubated with 200 μg ml^{-1} gentamicin for 3 h. 1 μM staurosporine (STS) treatment of HeLa cells for 5 h was used as a positive control. Cell detachment was expressed as a percentage of uninfected cells. Cell detachment was drastically reduced in FAK-/- fibroblasts infected with EPEC WT or Δ*espH*/pEspH when compared to FAK+/+ fibroblasts. Results are presented as a mean ± SD of three independent experiments. ** ($p < 0.01$).

As FAK-/- fibroblasts were resistant to EspH-induced cell rounding, the role of FAK on cell adhesion during EPEC infection was examined. FAK-/- and FAK+/+ fibroblasts were assessed for levels of cell detachment following infection with wild type EPEC, Δ*espH*, or Δ*espH*/pEspH. STS treatment was used as a control and showed similar levels of cell detachment in FAK-/- and FAK+/+ fibroblasts (Figure 30D). Consistent with our previous result, FAK-/- fibroblasts did not show any significant levels of cell detachment after infection with any of the strains (Figure 30D). In contrast, 43.2 ± 9.5 % of cells detached following infection of FAK+/+ fibroblasts with Δ*espH*/pEspH (Figure 30D). Taken together, our results show that FAK is an important mediator of EspH-induced cell rounding and cell detachment, and suggest that defects in focal adhesion disassembly diminishes the ability of EspH to induce cell rounding and caspase-3 activation.

4.4 Bacterial RhoGEFs are active in the presence of EspH

We next investigated if in addition to blocking mammalian DH-PH RhoGEFs, EspH also inhibits the activity of bacterial RhoGEFs. HeLa cells transfected with Myc-tagged EspH or Myc-tagged GFP, were infected with Δ*map*/pMap for 30 min, EPEC/pEspT or EPEC/pEspM2 for 90 min and assessed for filopodia, lamellipodia and stress fiber formation, respectively. As EspT and EspM are not found in the prototypical EPEC E2348/69 strain, we deleted endogenous *map* so that all three

effectors were expressed from inducible genes for consistency. Staining with F-actin revealed that EPEC expressing the WxxxE effectors were able to induce formation of their respective actin structures in cells transfected with either GFP or EspH (Figure 31). This suggests that EspH does not inhibit the activity of the WxxxE-family RhoGEFs during EPEC infection.

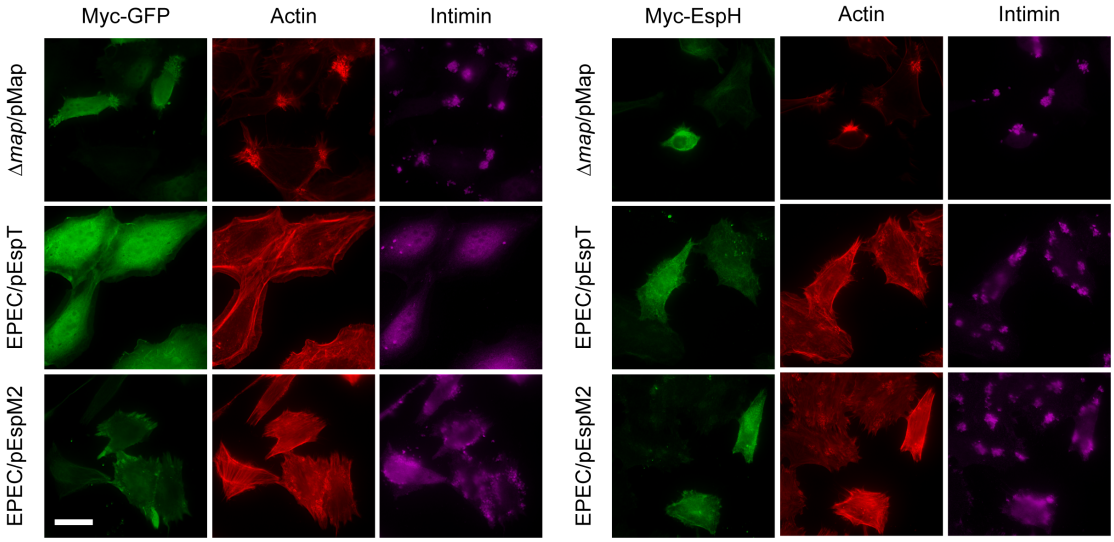


Figure 31. Ectopic expression of EspH does not inhibit WxxxE effectors during EPEC infection.

Immunofluorescence microscopy of HeLa cells transfected with Myc-GFP or Myc-EspH, then infected with Δ*map* complemented with Map (Δ*map*/pMap) for 30 min, or EPEC expressing EspT (EPEC/pEspT) or EspM2 (EPEC/pEspM2) for 90 min. Myc-tagged proteins were visualized with anti-Myc antibody (green), bacteria were visualized with anti-intimin antibody (magenta), and actin was stained with TRITC-phalloidin (red). Ectopic expression of EspH did not inhibit the formation of filopodia (Map), lamellipodia (EspT) or stress fibres (EspM2). Bar = 20 µm.

To affirm this observation, RFP or RFP-EspH were co-transfected with Myc-tagged Map, EspT, EspM2, or the catalytic region of SopE ($SopE_{78-240}$). Co-transfection with Myc-tagged p115-RhoGEF, a mammalian RhoA GEF which has been shown to bind EspH (Dong *et al.*, 2010), was used as a control. After staining for F-actin we observed that EspH was able to inhibit stress fiber formation by p115-RhoGEF, and the co-transfected cells were rounded (Figure 32A). In contrast, co-transfection of

RFP-EspH with Map, EspT, EspM2 or $SopE_{78-240}$ did not abrogate formation of filopodia (Map), lamellipodia (EspT/SopE) or stress fibers (EspM2) respectively (Figure 32A). When co-transfected with RFP the RhoA GEFs p115-RhoGEF and EspM2 induced stress fiber formation in 79.7 ± 3.3 % and 90.6 ± 1.1 % of cells respectively (Figure 32B). When co-transfected with RFP-EspH p115-RhoGEF showed markedly reduced stress fiber formation with only 14.5 ± 2.8 % of cells displaying stress fibers (Figure 32B). In contrast, only a modest decrease in stress fiber formation was observed in cells co-transfected with EspM2 and RFP-EspH as 76.5 ± 2.1 % of cells were positive for stress fibers (Figure 32B). Taken together, these results demonstrate that bacterial RhoGEFs are insensitive to EspH.

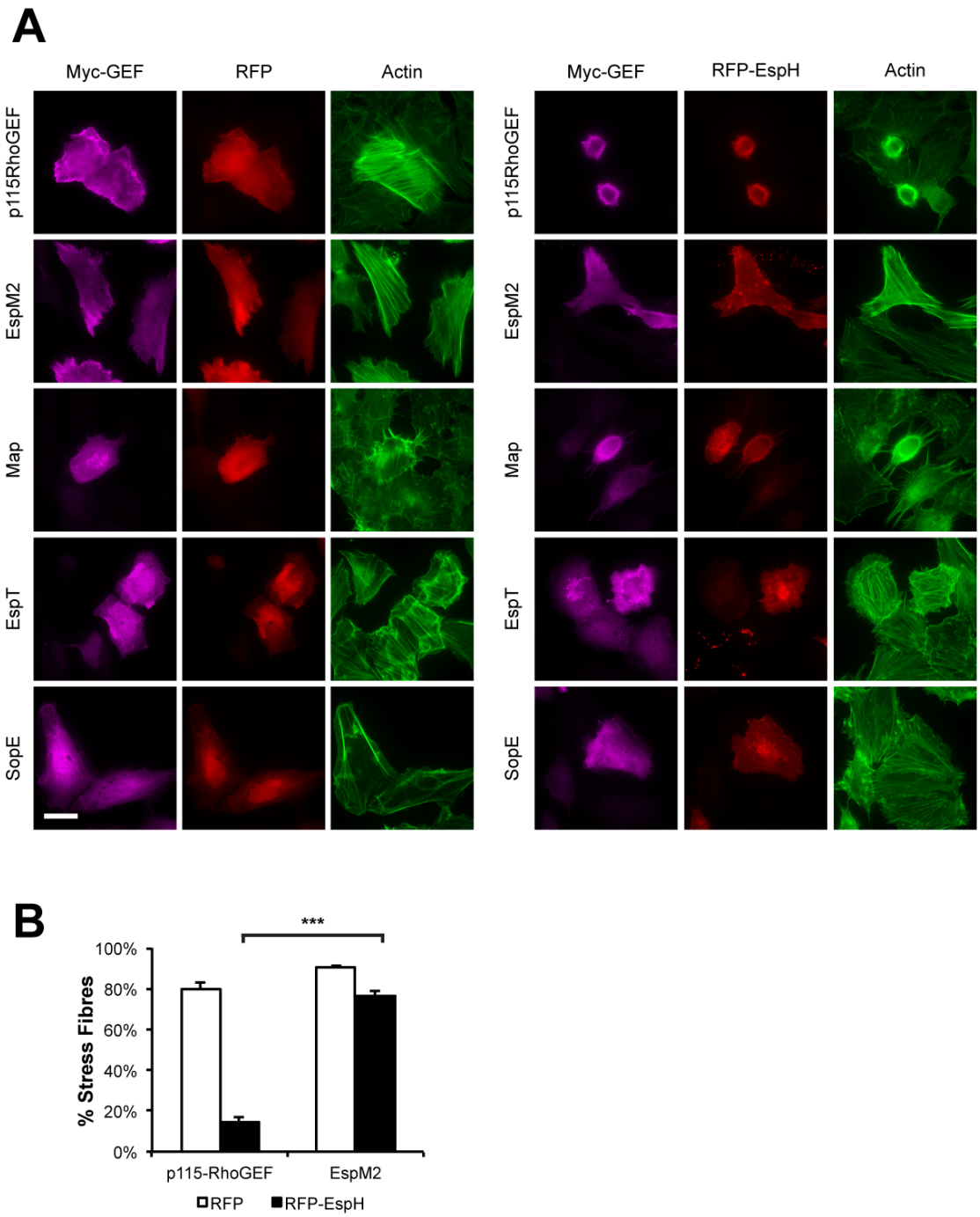


Figure 32. Bacterial RhoGEFs are active when co-expressed with EspH.

(A) Immunofluorescence microscopy of HeLa cells co-transfected with Myc-p115RhoGEF, Myc-EspM2, Myc-Map, Myc-EspT, Myc-SopE$_{78-240}$, and RFP or RFP-EspH (red). Myc-tagged proteins were visualized with anti-Myc antibody (magenta) and actin was stained with Oregon Green phalloidin (green). Co-transfection of Myc-p115RhoGEF and RFP-EspH drastically reduced stress fibre formation, but not Myc-EspM2 and RFP-EspH. Filopodia (Map) and lamellipodia (EspT/SopE) were also evident in the presence of RFP-EspH. Bar = 20 µm.

(B) Quantification of stress fibres formation in HeLa cells co-transfected with Myc-p115RhoGEF or Myc-EspM2, and RFP or RFP-EspH. 100 co-transfected cells were counted in triplicates. Results are presented as a mean ± SD of three independent experiments. * ($p < 0.001$).**

4.5 EspT, EspM2 and SopE block EspH-induced detachment and FA disassembly

Next, we determined if the bacterial RhoGEFs could mitigate the detrimental effects of EspH. To investigate if bacterial RhoGEFs could block EspH-induced cell detachment, we transfected HeLa cells with Myc-tagged bacterial RhoGEFs or their respective Rho GTPase dominant positives as controls, and then infected them with Δ*espH*/pEspH for 1 h, followed by gentamicin treatment for a further 3 h. No construct induced significant levels of cell detachment by transfection alone when compared to the Myc-GFP control (Figure 33A). Infection of Myc-GFP transfected cells with Δ*espH*/pEspH resulted in 55.6 ± 5.1 % of detachment (Figure 33A). Interestingly, cells transfected with the Rac1-activating effectors EspT and $SopE_{78-240}$, and dominant-positive Rac1 (Rac1L61) showed a significant reduction in cell detachment following infection with Δ*espH*/pEspH, as only 30.3 ± 6.7 %, 30.6 ± 2.8 % and 34.4 ± 4.2% of cells detached respectively (Figure 33A). We also observed an intermediate reduction in cell detachment of cells transfected with dominant positive RhoA (RhoAL63) and its corresponding GEF EspM2, as 43.1 ± 2.7 % and 35.0 ± 6.4 % of cells detached respectively (Figure 33A). Neither the Cdc42 GEF Map nor dominant positive Cdc42 (Cdc42L61) could inhibit cell detachment following infection with Δ*espH*/pEspH, as 53.7 ± 11.2 % and 52.7% ± 4.9 % of cells detached respectively (Figure 33A). These results imply that Cdc42 activation alone is unable to block EspH-induced cell detachment.

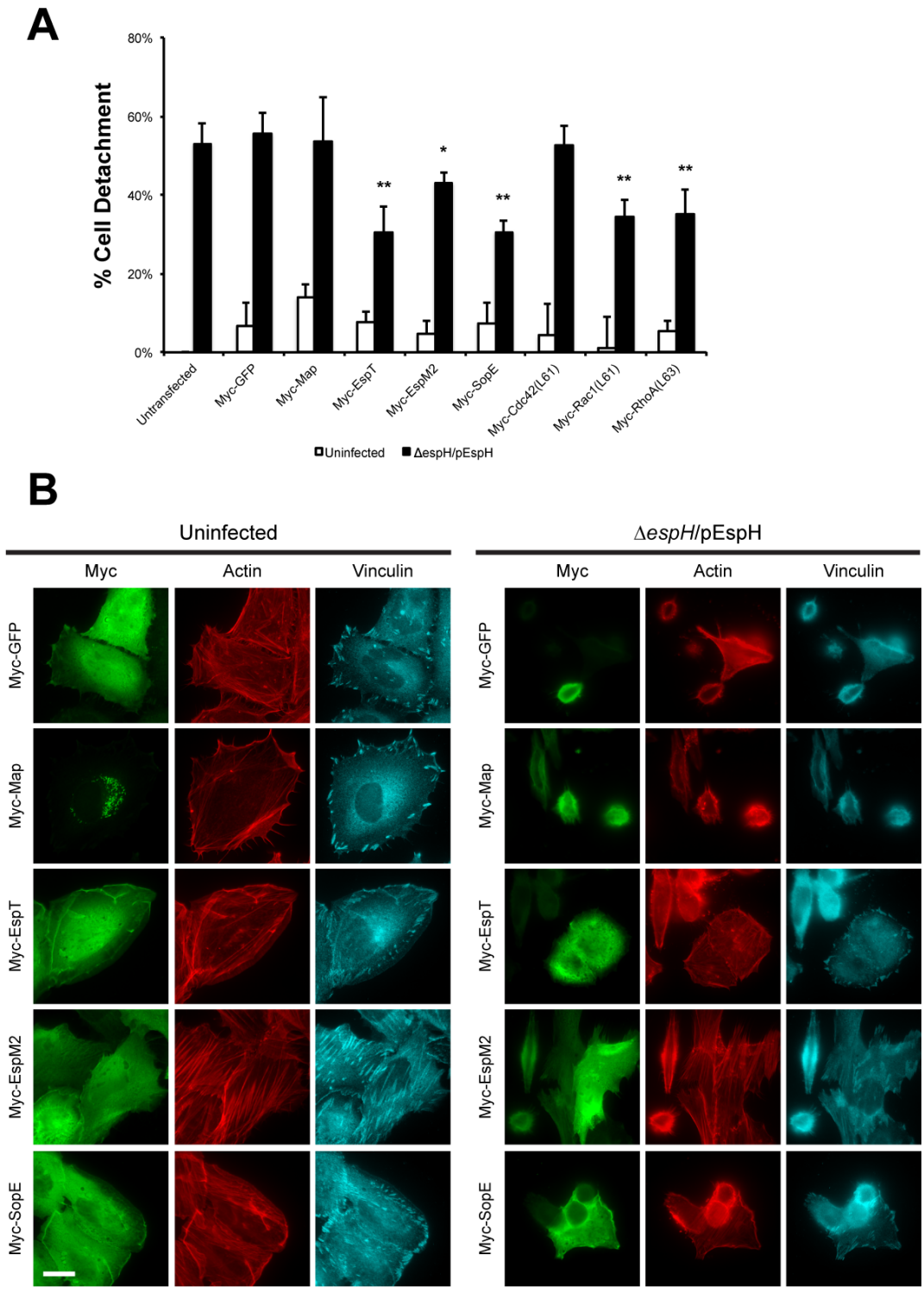


Figure 33. EspT, EspM2 and SopE block EspH-induced detachment and FA disassembly.

(A) Quantification of detachment levels of HeLa cells transfected with Myc-GFP or Myc-tagged bacterial RhoGEFs, uninfected or infected with Δ*espH* complemented with EspH (Δ*espH*/pEspH) for 1 h, followed by incubation with 200 µg ml^{-1} gentamicin for 3 h. Transfection of dominant-positives of Cdc42 (Cdc42L61), Rac1 (Rac1L61) and RhoA (RhoAL63) were used as positive controls. Cell detachment was expressed as a percentage of non-transfected/infected cells. Ectopic expression of Myc-tagged EspT, EspM2 or SopE$_{78-240}$ showed reduced cell detachment following infection with Δ*espH*/pEspH, but not Myc-tagged GFP or Map. Results are presented as a mean ± SD of three independent experiments. Statistical significance is based on a student's t-test compared to Myc-GFP control. * ($p < 0.05$), ** ($p < 0.01$).

(B) Immunofluorescence microscopy of HeLa cells transfected with Myc-GFP or Myc-tagged bacterial RhoGEFs, uninfected or infected with ΔespH complemented with EspH (ΔespH/pEspH) for 1 h, followed by incubation with 200 µg ml-1 gentamicin for 3 h. Myc-tagged proteins were visualized with anti-Myc antibody (green), vinculin was detected with anti-vinculin antibody (cyan) and actin was stained with TRITCphalloidin (red). Ectopic expression of Myc-tagged EspT, EspM2 or SopE retained focal adhesions following infection with ΔespH/pEspH, but not Myc-tagged GFP or Map. Bar = 20 µm.

We next examined if EspT, EspM2 and SopE also inhibited EspH-induced focal adhesion disassembly. In contrast to GFP and Map transfected cells, EspT and $SopE_{78-240}$ transfected cells blocked EspH-induced cell rounding, and vinculin staining revealed large focal adhesions were still present in a radial pattern following infection with Δ*espH*/pEspH (Figure 33B). EspM2-transfected cells also retained stress fiber-associated focal adhesions following infection with Δ*espH*/pEspH (Figure 33B). These results suggest that Rac1 and RhoA activation are critical for inhibition of EspH-induced cell detachment and focal adhesion disassembly.

4.6 EspT, EspM2 and SopE inhibit EspH-induced caspase-3 activation

We next investigated if the bacterial RhoGEFs could also block EspH-induced caspase-3 activation. Using the same transfection-infection delivery strategy as above, Δ*espH*/pEspH induced caspase activation in 33.0 ± 8.5 % of cells transfected with the GFP control (Figure 34A/B). Map was unable to inhibit EspH-induced caspase-3 activation, as 32.1 ± 6.7 % of transfected cells were positive for caspase-3 activation (Figure 34A/B). In contrast, EspT, EspM2 and $SopE_{78-240}$ inhibited EspH-induced caspase-3 activation, as only 8.3 ± 2.8 %, 13.9 ± 3.3 %, and 9.2 ± 2.2 % of transfected cells respectively were positive for caspase-3 activation (Figure 34A/B).

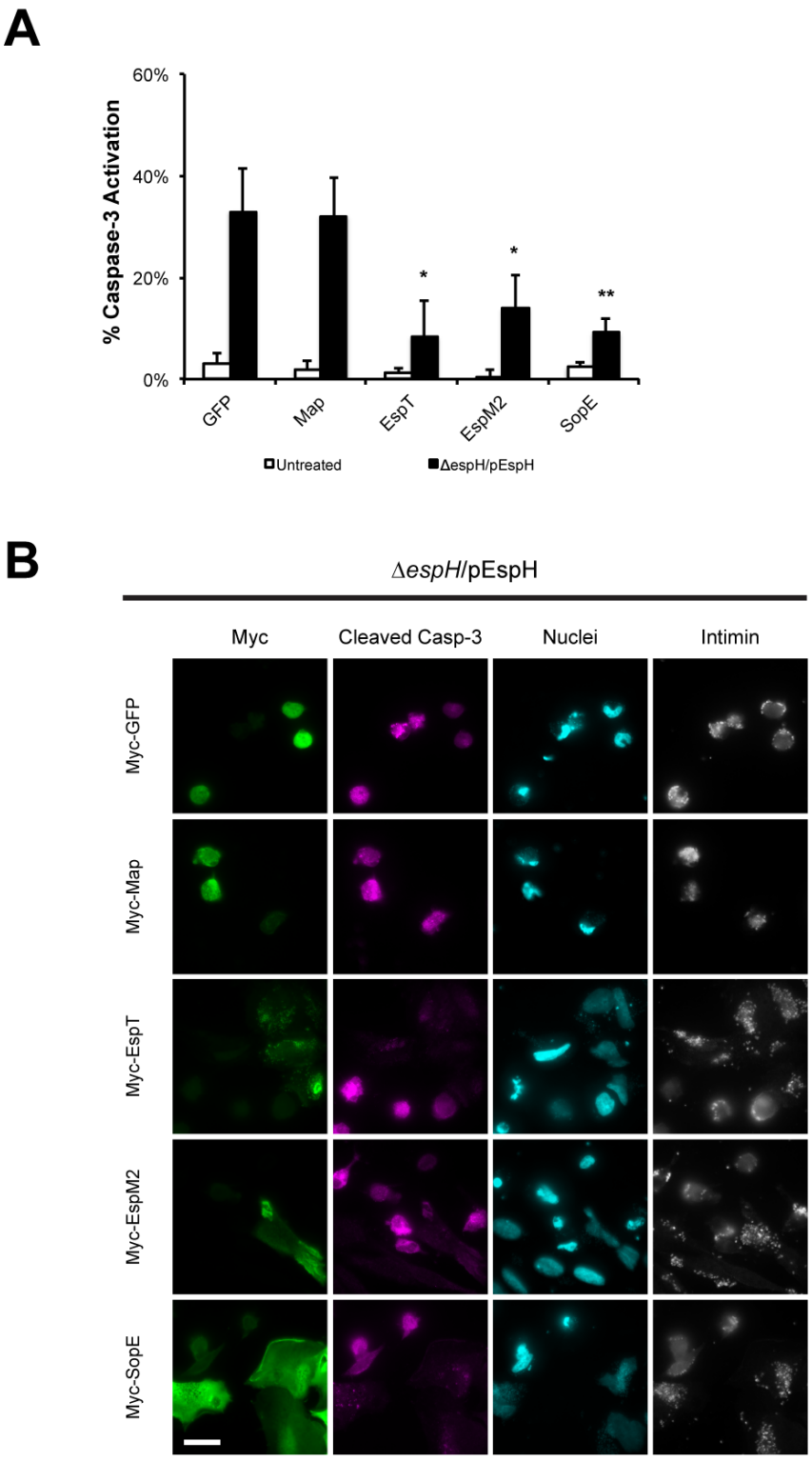


Figure 34. EspT, EspM2 and SopE inhibit EspH-induced caspase-3 activation.

(A) Quantification of caspase-3 activation of HeLa cells transfected with Myc-GFP or Myc-tagged bacterial RhoGEFs, uninfected or infected with Δ*espH* complemented with EspH (Δ*espH*/pEspH) for 1 h, followed by incubation with 200 µg/ml gentamicin for 3 h. 100 transfected cells were counted in triplicates. Ectopic expression of Myc-tagged EspT, EspM2 or $SopE_{78-240}$ markedly reduced caspase-3 activation in cells infected with Δ*espH*/pEspH, but not Myc-tagged GFP or Map. Results are presented as a mean ± SD of three independent

experiments. Statistical significance is based on a student's t-test compared to Myc-GFP control. * ($p < 0.05$), ** ($p < 0.01$).

(B) Immunofluorescence microscopy of HeLa cells transfected with Myc-GFP or Myc-tagged bacterial RhoGEFs, uninfected or infected with ΔespH complemented with EspH (ΔespH/pEspH) for 1 h, followed by incubation with 200 µg/ml gentamicin for 3 h. Myc-tagged proteins were visualized with anti-Myc antibody (green), active caspase-3 was detected with anti-caspase-3 (cleaved) antibody (magenta), and cell nuclei were stained with DAPI (cyan). Bar = 20 µm.

4.7 EspT, EspM2 and SopE inhibit staurosporine-induced caspase-3 activation

As Rho GTPases play a role in cell survival (Hall, 1998), we investigated if the bacterial RhoGEFs could play an additional role in inhibiting apoptosis. To investigate this, we transfected HeLa cells with Myc-tagged Map, EspT, EspM2 and $SopE_{78-240}$, and treated them with STS for 5 h. Transfection of anti-apoptotic Myc-tagged NleH1, which inhibits caspase-3 activation induced by STS (Hemrajani *et al.*, 2010), was used as a control. Quantification of cleaved caspase-3 by immunofluorescence revealed that cells transfected with the Myc-GFP control or Map displayed high levels of cleaved caspase-3 (Figure 35A/B). In contrast, cells transfected with Myc-tagged EspT, EspM2 or $SopE_{78-240}$ all showed a marked reduction in levels of cleaved caspase-3 similar to cells transfected with anti-apoptotic effector NleH (Figure 35A/B). Rac1 and RhoA activating bacterial RhoGEFs are thus able to inhibit EspH-induced and STS-induced caspase-3 activation.

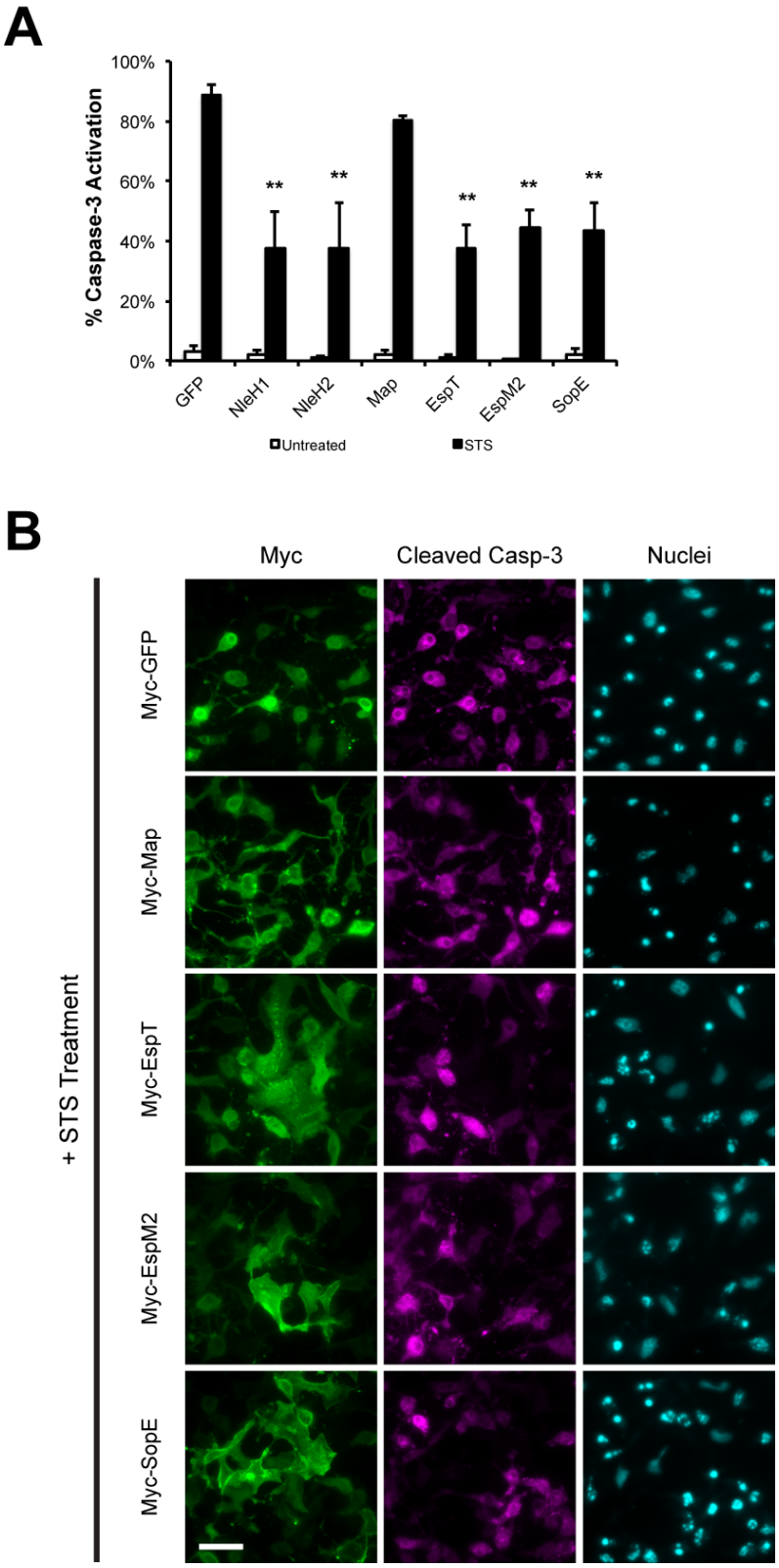


Figure 35. EspT, EspM2 and SopE inhibit staurosporine-induced caspase-3 activation.

(A) Quantification of caspase-3 activation of HeLa cells transfected with Myc-GFP or Myc-tagged bacterial RhoGEFs, then treated with 1 µM staurosporine (STS) for 5 hours. Transfection of Myc-NleH1 and Myc-NleH2 were used as positive controls. 100 transfected cells were counted in triplicates. Ectopic expression of Myc-tagged EspT, EspM2 or SopE78-240 markedly reduced caspase-3 activation in cells treated with STS to that of NleH effectors, but not Myc-tagged GFP

or Map. Results are presented as a mean ± SD of three independent experiments. Statistical significance is based on a student's t-test compared to Myc-GFP control. ** ($p < 0.01$).

(B) Immunofluorescence microscopy of HeLa cells transfected with Myc-GFP or Myc-tagged bacterial RhoGEFs, then treated with 1 µM staurosporine (STS) for 5 hours. Myc-tagged proteins were visualized with anti-Myc antibody (green), active caspase-3 was detected with anti-caspase-3 (cleaved) antibody (magenta), and nuclei were stained with DAPI (cyan). Bar = 50 µm.

4.8 EspT and EspM2 can compensate for NleH in inhibiting caspase-3 activation, detachment and cytotoxicity

The observation that EspT and EspM2 could all inhibit cleaved caspase-3 activation towards different cytotoxic stimuli suggests that EspT and EspM2 could compensate for NleH effectors in promoting cell survival during EPEC infection. In order to test this hypothesis, we infected HeLa cells with EPEC WT, Δ*nleH1*Δ*nleH2*, or Δ*nleH1*Δ*nleH2* expressing plasmid-encoded NleH1, NleH2, EspT, EspT(W63A) (defective in Rac1 activation), EspM2, or EspM2(W70A) (defective in RhoA activation), and processed them for immunofluorescence microscopy. Quantification of caspase-3 activation showed that, consistent with a previous report, both NleH1 and NleH2 were able to partially complement the Δ*nleH1*Δ*nleH2* mutant in inhibiting caspase-3 activation (Figure 36A/B). Interestingly, expression of plasmid-encoded EspT or EspM2 partially compensated for NleH effectors in inhibiting caspase-3 activation during EPEC infection. This is dependent on Rac1 or RhoA activation as expression of defective EspT(W63A) or EspM2(W70A) point mutants in the Δ*nleH1*Δ*nleH2* mutant could not inhibit caspase-3 activation (Figure 36A/B).

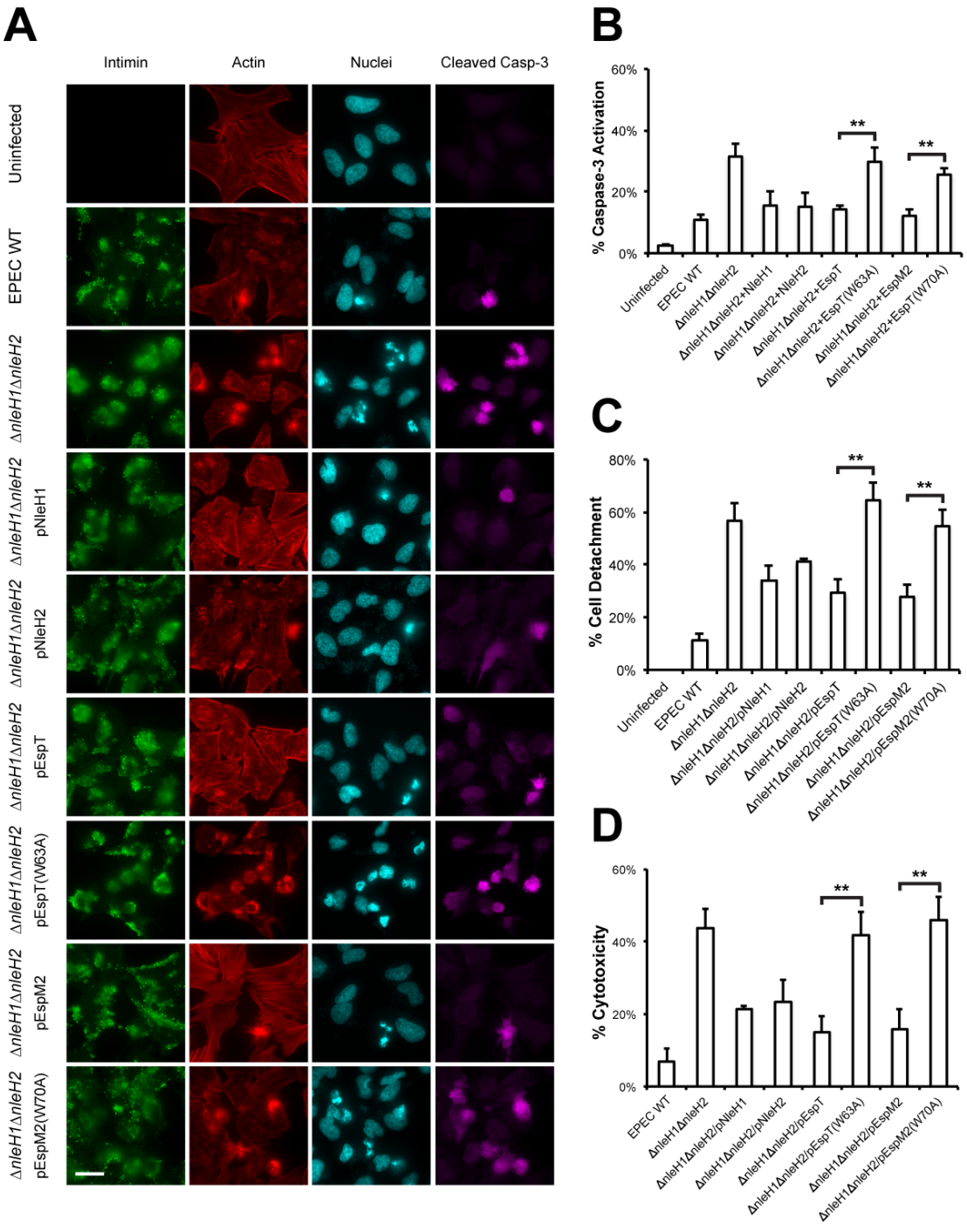


Figure 36. EspT and EspM2 can compensate for NleH in inhibiting caspase-3 activation, detachment and cytotoxicity.

(A) Immunofluorescence microscopy of HeLa cells infected with EPEC WT, Δ*nleH1*Δ*nleH2*, or Δ*nleH1*Δ*nleH2* expressing NleH1, NleH2 EspT, EspT(W63A), EspM2 or EspM2(W70A) for 1 h, then incubated with 200 µg ml^{-1} gentamicin for 3 h. Bacteria were visualized with anti-intimin antibody (green), active caspase-3 was detected with anti-caspase-3 (cleaved) antibody (magenta), actin was stained with TRITC-phalloidin (red) and cell nuclei were stained with DAPI (cyan). Complementation with NleH1 or NleH2, or expression of EspT or EspM2 significantly reduced caspase-3 activation induced by the Δ*nleH1*Δ*nleH2* mutant. This is dependent on an intact WxxxE motif as expression of point mutants EspT(W63A) and EspM2(W70A) did not reduce caspase-3 activation. Bar = 20 µm.

(B) Quantification of caspase-3 activation of HeLa cells infected with EPEC WT, Δ*nleH1*Δ*nleH2*, or Δ*nleH1*Δ*nleH2* expressing NleH1, NleH2 EspT, EspT(W63A), EspM2 or EspM2(W70A) for 1 h, then incubated with 200 µg ml^{-1} gentamicin for 3 h. 100 infected cells were counted in triplicates. Results are presented as a mean ± SD of three independent experiments. ** ($p < 0.01$).

(C) Quantification of detachment levels of HeLa cells infected with EPEC WT, Δ*nleH1*Δ*nleH2*, or Δ*nleH1*Δ*nleH2* expressing NleH1, NleH2 EspT, EspT(W63A), EspM2 or EspM2(W70A) for 1 h, then incubated with 200 µg ml^{-1} gentamicin for 3 h. Cell detachment was expressed as a percentage of uninfected cells. Expression of EspT and EspM2 significantly reduced cell detachment induced by the Δ*nleH1*Δ*nleH2* mutant to the extent of NleH complementation, dependent on an intact WxxxE motif. Results are presented as a mean ± SD of three independent experiments. ** ($p < 0.01$).

(D) Quantification of cytotoxicity to HeLa cells infected with EPEC WT, Δ*nleH1*Δ*nleH2*, or Δ*nleH1*Δ*nleH2* expressing NleH1, NleH2 EspT, EspT(W63A), EspM2 or EspM2(W70A) for 30 min, then incubated with 200 µg ml^{-1} gentamicin for 4 h. Cytotoxicity was assayed by quantifying the levels of LDH release into the culture supernatant from cells 4 hours post-infection. Expression of EspT and EspM2 significantly reduced cytotoxicity of the Δ*nleH1*Δ*nleH2* mutant to the extent of NleH complementation, dependent on an intact WxxxE motif. Results are presented as a mean ± SD of three independent experiments. ** ($p < 0.01$).

To further characterize the role of EspT and EspM2 in promoting cell survival, we also assessed the ability of EspT to EspM2 to functionally compensate for NleH effectors in blocking cell detachment and cytotoxicity. Processing HeLa cells infected with the above strains for cell detachment (Figure 36C) and cytotoxicity assays (Figure 36D) revealed that, similar to the pattern observed during caspase-3 activation, EspT and EspM2 were able to partially rescue the Δ*nleH1*Δ*nleH2* double mutant to the extent of a single NleH complementation in a Rac1-dependent and RhoA-dependent manner respectively. Taken together, our results demonstrate that the bacterial RhoGEFs EspT and EspM2 are able to functionally compensate for NleH effectors to promote cell survival during EPEC infection.

4.9 Screening for additional T3SS effectors that block EspH-induced cell detachment

The observation that EspT, EspM2 and NleH could counteract EspH cytotoxicity suggests that other prosurvival T3SS effectors might be able to do the same. To

identify them, a transfection-infection delivery screen was performed using several different T3SS effectors to assess their ability to counteract EspH-induced cell detachment. NleH was used as a control.

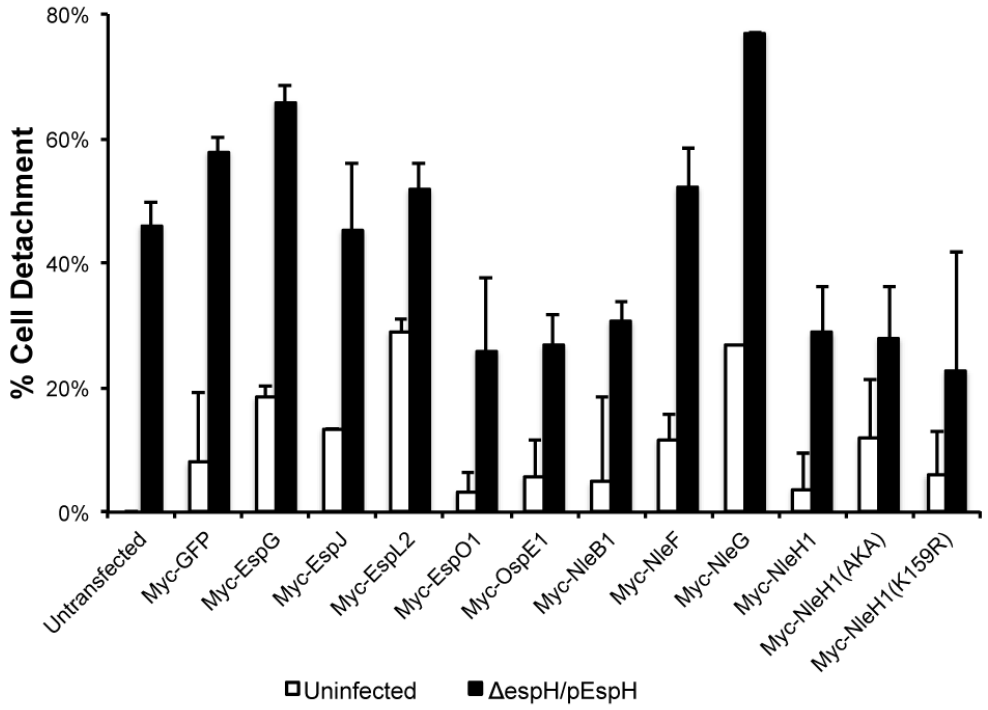


Figure 37. Screening for T3SS effectors that block EspH-induced cell detachment.

Quantification of detachment levels of HeLa cells transfected with Myc-GFP or Myc-tagged bacterial effectors, uninfected or infected with Δ*espH* complemented with EspH (Δ*espH*/pEspH) for 1 h, followed by incubation with 200 µg ml^{-1} gentamicin for 3 h. Cell detachment was expressed as a percentage of non-transfected/infected cells. Ectopic expression of Myc-tagged EspO1, OspE1, NleB1, NleH1 and NleH1 point mutants showed reduced cell detachment following infection with Δ*espH*/pEspH compared to Myc-tagged GFP. Results are presented as a mean ± SD of three independent experiments.

Screening for additional effectors revealed that NleB1 and EspO1/OspE1 were all able to inhibit EspH-induced cell detachment to the extent of NleH, suggesting that they might also play a role in promoting cell survival during EPEC infection (Figure 37). In addition, the expression of PDZ-negative (NleH1$_{AKA}$) and kinase-dead (NleH1$_{K159R}$) mutants of NleH1 was also able to inhibit EspH-induced cell

detachment to the same extent, suggesting the PDZ-binding motif and kinase domain of NleH are dispensable for its ability to inhibit EspH-induced cell detachment.

4.10 Discussion

Several roles have been ascribed for SopE and the WxxxE-family bacterial RhoGEFs, including actin remodeling, bacterial invasion, innate host cell response, and tight junction disruption (reviewed in (Bulgin *et al.*, 2010)). In this chapter, we expand the repertoire of bacterial RhoGEF functions to include promotion of cell adhesion and survival. We also found that bacterial RhoGEFs are resistant to the DH-PH mammalian RhoGEF inhibitor EspH. EPEC and EHEC are thus able to neutralize mammalian RhoGEFs while translocating their own bacterial RhoGEFs to hijack Rho GTPase signaling for the proprietary benefit of the pathogen.

While EPEC and EHEC translocate several WxxxE RhoGEFs, thus far no effector with RhoGAP activity has been identified (Wong *et al.*, 2011). Instead, EPEC uses a novel strategy by which EspH globally inhibits mammalian DH-PH RhoGEFs (Dong *et al.*, 2010). As Map was still able to induce filopodia in the presence of EspH, it is unlikely that EspH directly affects Map GEF activity towards Cdc42. Rather, we hypothesize that EspH inhibits Map-induced filopodia by inhibiting the RhoA/ROCK pathway, which has been implicated in the stabilization of Map-induced filopodia (Berger *et al.*, 2009). This indirect effect could be attributed to the fact that ROCK regulates the activity of cofilin, and thus could enhance actin depolymerization that is induced by Map to promote actin pedestal formation triggered by Tir.

Indeed, the ability of EspH to induce cell rounding, focal adhesion disassembly and caspase-3 activation is reminiscent of *Clostridial* toxin B (TcdB) intoxication (Fiorentini *et al.*, 1998). This is not surprising given the fact that EspH, like TcdB, inactivates Rho GTPases, although TcdB directly targets Rho GTPases and inactivates them by glucosylation of Thr-37 (reviewed in (Voth *et al.*, 2005)). Significantly, we show that the ability of EPEC to antagonize EspH is mediated by the WxxxE effectors EspT and EspM2, and that neither Map nor Cdc42 activation was able to block EspH-induced cell detachment or caspase-3 activation. While it was previously reported that Map induces mitochondrial dysfunction (Ma *et al.*, 2006), we did not observe any significant Map-induced cell detachment or caspase-3 activation by transfection. Consistent with our findings that Rac1 and RhoA activation are sufficient to inhibit EspH-induced cell detachment and caspase-3 activation, we also found that FAK, which coordinates the activities of Rac1 and RhoA to regulate focal adhesion dynamics, is an important mediator of EspH-induced cell rounding, cell detachment and caspase-3 activation. As EspT and SopE are unable to trigger lamellipodia formation in FAK-/- fibroblasts (data not shown), our results support a model where EPEC and EHEC utilize EspH and bacterial RhoGEFs to mediate focal adhesion dynamics through subversion of FAK signaling pathways.

Intriguingly, EspT, EspM2 and SopE (but not Map) can also inhibit STS-induced caspase-3 activation to the same extent as anti-apoptotic effector NleH. This suggests that bacterial RhoGEFs play an additional role in promoting host cell survival during infection. Furthermore, EspT and EspM2 can compensate for NleH effectors in inhibiting caspase-3 activation, cell detachment and cytotoxicity during EPEC infection. This demonstrates the extraordinary redundancy in effector function, where

A/E pathogens can utilize NleH, EspT and EspM2 to maintain host cell survival, and thus enhance multiplication and dissemination. Importantly, EspT and EspM2 protection is dependent on Rac1 and RhoA activation, while NleH protection is dependent on Bax-inhibitor 1 (Hemrajani *et al.*, 2010). This suggests that these effectors function through remarkably distinct mechanisms to achieve the same outcome of host cell survival. Indeed, several reports have demonstrated that Rac1 and RhoA-activating RhoGEFs are able to activate mitogen-activated protein kinase (MAPK) and NF-κB pathways (Fukazawa *et al.*, 2008, Bruno *et al.*, 2009, Raymond *et al.*, 2011), which have pivotal roles in the regulation of cell survival (Karin *et al.*, 2002, Wada *et al.*, 2004). As FAK-mediated signaling cascades are also involved in the regulation of cell survival by bacterial RhoGEFs, more work is required to dissect the mechanisms by which WxxxE-family effectors are able to modulate the cell death response. Thus, in assessing the interplay of EspH and bacterial RhoGEFs in modulating actin dynamics, adhesion and cell death, we find that A/E pathogens have evolved sophisticated mechanisms to hijack multiple signaling pathways in a functionally coordinated manner.

Chapter 5 – General Discussion

Chapter 5 – General discussion

5.1 EspH as a modulator of actin pedestal dynamics

Previous work on EspH has demonstrated two distinct yet related phenotypes. In a localized context, EspH is able to promote actin pedestal elongation at the site of bacterial attachment; in a global context, EspH binds to DH-PH RhoGEFs to inhibit cellular Rho GTPase signaling and phagocytosis. My work has focused on the further characterization of both phenotypes. In Chapter 3, I demonstrated that EspH was able to recruit WIP independently of Tir-mediated actin polymerization pathways, and that WIP plays an important role in the modulation of actin pedestal formation and elongation. In Chapter 4, I characterized the impact of EspH-mediated DH-PH RhoGEF inhibition on the cell, and showed that EspH disrupted the actin cytoskeleton, induced focal adhesion disassembly, and activated caspase-3. EspH is thus a multifunctional T3SS effector that modulates several signaling pathways of the mammalian cell.

While the mechanisms involved in actin pedestal formation *in vitro* are not required for A/E lesion formation *in vivo*, a *C. rodentium* $Tir_{Y451A/Y471A}$ mutant deficient in both Tir:Nck and Tir:IRTKS/IRSp53 pathways is rapidly outcompeted by wild-type *C. rodentium*, thus showing that these conserved cascades confer a competitive advantage to the bacterium *in vivo* (Crepin *et al.*, 2009). Understanding the molecular mechanism of actin pedestal formation also serves as a useful tool to study fundamental biological mechanisms in the mammalian cell. While EspH is not required for actin pedestal formation, it has been shown to promote pedestal formation and elongation. As Map-induced filopodia forms before pedestal formation

and that deletion of Tir results in persistence of localized filopodia, two general hypotheses can be formed – (1) EspH promotes filopodia withdrawal and therefore indirectly promotes pedestal formation, or (2) EspH directly contributes to pedestal formation, and therefore represses filopodia formation.

Evidences supporting hypothesis (1) is the observation that global inactivation of Rho GTPases induces a modest increase in pedestal length in an indirect manner (Ben-Ami *et al.*, 1998). EspH could also promiscuously bind to mammalian RhoGEFs or even directly to Map to promote filopodia withdrawal. On the other hand, several evidences suggest that hypothesis (2) is more valid. Firstly, inhibition of Cdc42, but not Rac1 or RhoA, compensates for the absence of EspH in terms of pedestal elongation, thus showing specificity for the activity of EspH. Secondly, EspH does not inhibit the activity of Map. Thirdly, EspH is able to recruit the WIP/N-WASP complex independently of Nck, as well as Cdc42 (deletion of CRIB or GBD of N-WASP does not alter EspH-mediated N-WASP recruitment). Fourthly, WIP has been shown to inhibit Cdc42-induced filopodia formation, thus suggesting EspH-induced filopodial downregulation. Finally, we show that WIP plays a role in modulating both actin pedestal formation and elongation.

In light of all the results, a plausible model for EspH in mediating filopodia:pedestal dynamics at the site of bacterial attachment is proposed as follows. Map induces transient filopodia formation. EspH could destabilize Map-induced filopodia by downregulation of the RhoA/ROCK/cofilin pathway. In addition, EspH indirectly recruits WIP which inhibits Cdc42-induced filopodia formation, but also stimulate Tir-dependent actin pedestal formation and elongation following the initiation of

Tir:Nck and Tir:IRTKS/IRSp53 pathways. Therefore, the molecular mechanism for actin pedestal formation involves distinct Tir-mediate actin signaling cascades that converge on the WIP/N-WASP complex to synergistically trigger actin pedestal formation (Figure 38).

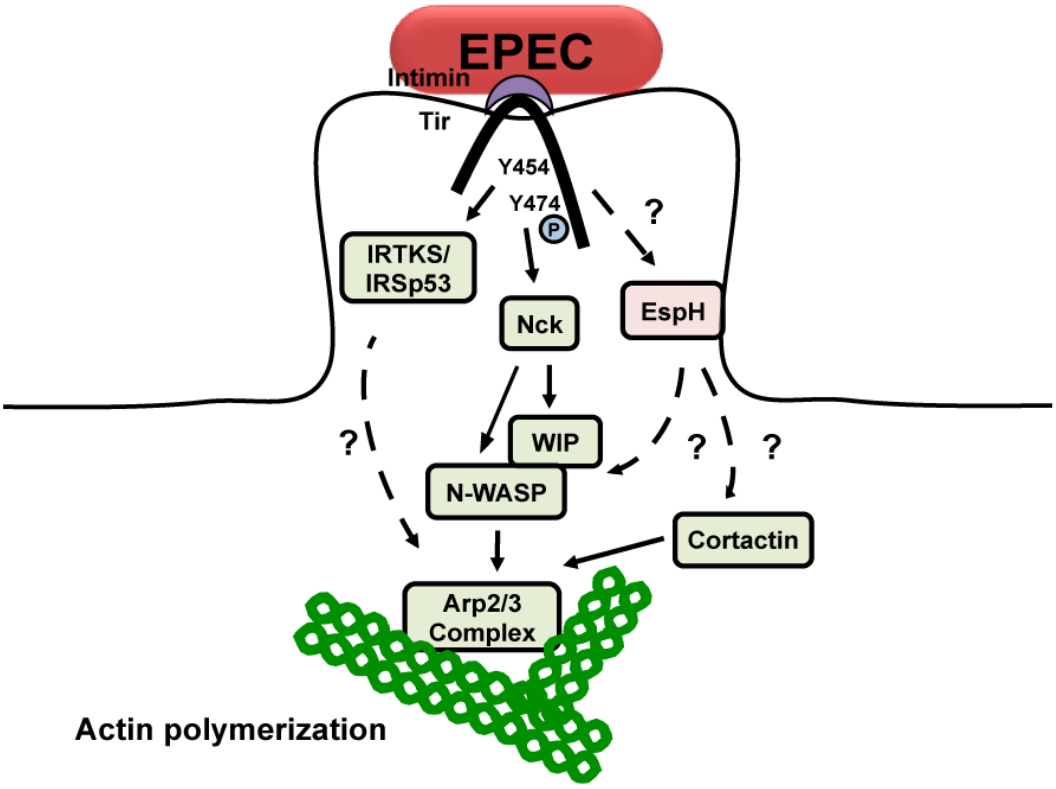


Figure 38. A model for EPEC actin polymerization pathways.

EPEC recruits and activates the WIP/N-WASP complex via distinct, convergent and synergistic actin signaling cascades. Details are described in section 5.1.

Admittedly, the current model lacks a clear mechanism for EspH-mediated WIP recruitment, as well as a mechanism for WIP-mediated inhibition of Cdc42. In addition, the role of the class II NPF cortactin in EspH-mediated actin polymerization and actin pedestal formation is also not clear. Inactivation of cortactin inhibits pedestal formation (Cantarelli *et al.*, 2002); recruitment of cortactin to the site of bacterial attachment has however been shown to either require the N-terminus of Tir,

or require the Tir:Nck pathway (Cantarelli *et al.*, 2000, Nieto-Pelegrin *et al.*, 2009). However, my work has shown that the recruitment of cortactin, like WIP, is mediated either by the Tir:Nck pathway or EspH. As cortactin can also trigger activation of the Arp2/3 complex, future work will also need to address the role of cortactin in the overall context of EPEC actin pedestal dynamics.

The existence of multiple actin polymerization signaling cascades is also not limited to EPEC. Indeed, *Vaccinia* virus particles encode the transmembrane protein A36R that also mimics receptor tyrosine kinase (RTK) signaling in a similar manner to Tir. A36R is phosphorylated on tyrosine residues Y112 and Y132, which then recruit the adaptor proteins Grb2 and Nck respectively (Frischknecht, 1999, Scaplehorn *et al.*, 2002). Nck in turn recruits the WIP/N-WASP complex, while Grb2 also binds the PRD domain of N-WASP to enhance actin polymerization, but only prior to the recruitment of the WIP/N-WASP complex initiated by Nck. This "primary" and "secondary" form of cooperative signaling is evident in EPEC, as EspH indirectly recruits the WIP/N-WASP complex via the WH1 domain, but is unable to generate actin pedestals in the absence of the Tir:Nck pathway. Although Tir Y454 does not bind Grb2, it has been suggested that may mimic the function of A36R Y112 as it is also phosphorylated (Campellone *et al.*, 2005). However, IRTKS/IRSp53 binding does not appear to require phosphorylation (Vingadassalom *et al.*, 2009, Weiss *et al.*, 2009). Furthermore, phosphorylated Y454 can also bind PI3K to mediate phosphoinositide signaling at the plasma membrane (Sason *et al.*, 2009). As phosphoinotisides are upstream regulators of actin cytoskeletal components, these studies of Tir and A36R clearly demonstrate that RTK signaling in general is far more complex than binary phosphorylation states.

To address the question of the relative contributions of Nck, WIP, and cortactin in mediating actin pedestal dynamics, one interesting technique would be to use fluorescent recovery after photobleacing (FRAP) analysis to assess the turnover rates of each protein during actin pedestal formation. Using FRAP analysis, it was shown that Grb2, WIP, Nck and N-WASP do not form a stable complex beneath *Vaccinia*, thus proving that the interactions between them are inherently dynamic and transient; the higher the exchange rate of N-WASP, the faster *Vaccinia* moves but the shorter the actin comet tail (Weisswange *et al.*, 2009). In the case where EspH enhances EPEC actin pedestal formation and elongation, adapting the same approach to study EPEC and comparing turnover rates in the presence or absence of Tir:Nck, Tir:IRTKS/IRSp53 or EspH-mediated pathways would likely yield exciting quantititative results that will not only elucidate the intricacies of actin pedestal formation, but how different mechanisms of N-WASP activation affect the outcome of formation of higher-order actin structures.

5.2 EspH as a modulator of host cell adhesion and survival

In addition to mediating actin pedestal dynamics at the site of bacterial attachment, EspH also plays a role in cell adhesion and survival. We show that EspH induces cell rounding, FA disassembly, and caspase-3 activation. Coupled with the observation that cell nuclei were markedly denser and showed signs of fragmentation, EspH most likely triggers the apoptotic cascade. To investigate the order of appearance for the different phenotypes, we utilized FAK-deficient fibroblasts that exhibit excessive stress fiber and focal adhesions. FAK-deficient fibroblasts significantly showed reduced cell rounding and caspase-3 activation, and also appear to adhere normally in

the presence of EspH. Consistently, we show that focal adhesions disassemble independently of caspase-3 activation. Thus it is most plausible that EspH, by globally inhibiting mammalian RhoGEFs, first induces loss of stress fibers and focal adhesion disassembly, and subsequently initiates the execution pathway of apoptosis.

How does EspH trigger apoptosis? Owing to the myriad of cellular signals that are terminated upon Rho GTPase inactivation, it is almost impossible to study the relative contribution of individual signaling pathways to apoptosis, and we cannot exclude the possibility that apoptosis may still occur at later stages even without focal adhesion disassembly or caspase activation. However, as focal adhesions play a significant role during EspH-induced caspase-3 activation, its role cannot be ignored. Mechanistically, mammalian RhoGEFs and RhoGAPs are recruited by FAK during cell migration (Tomar *et al.*, 2009b). As such, inhibition of RhoGEFs by EspH could cause disruption to this coordination and hence hinder regular FA turnover, leading to the loss of adhesion signaling cascades that consequently trigger apoptotic signals.

Apart from the actin cytoskeleton, studies of anoikis (apoptosis induced by the loss of integrin-dependent survival signals due to either inadequacy or the binding of inappropriate ligands) implicate the downregulation of two major downstream integrin-dependent signaling pathways during its induction – the PI3K/Akt signaling pathway and MAPK signaling pathways (Gilmore, 2005). PI3K is recruited to focal adhesions via FAK or Src, and facilitates the localized interaction of Rac GTPases and WAVE2 complexes at focal adhesions (Chang *et al.*, 2007). While MAPK signaling pathways are downstream pathways of PI3K/Akt pathway, ERK and JNK have both been implicated in the regulation of focal adhesion assembly and calpain-

mediated FA disassembly, thus exerting an effect on FA turnover (Mitra *et al.*, 2005). As Rho GTPases play a role in the regulation of these signaling pathways, it would be interesting to investigate the effect of EspH on them, and the relevance of these pathways in the induction of focal adhesion disassembly.

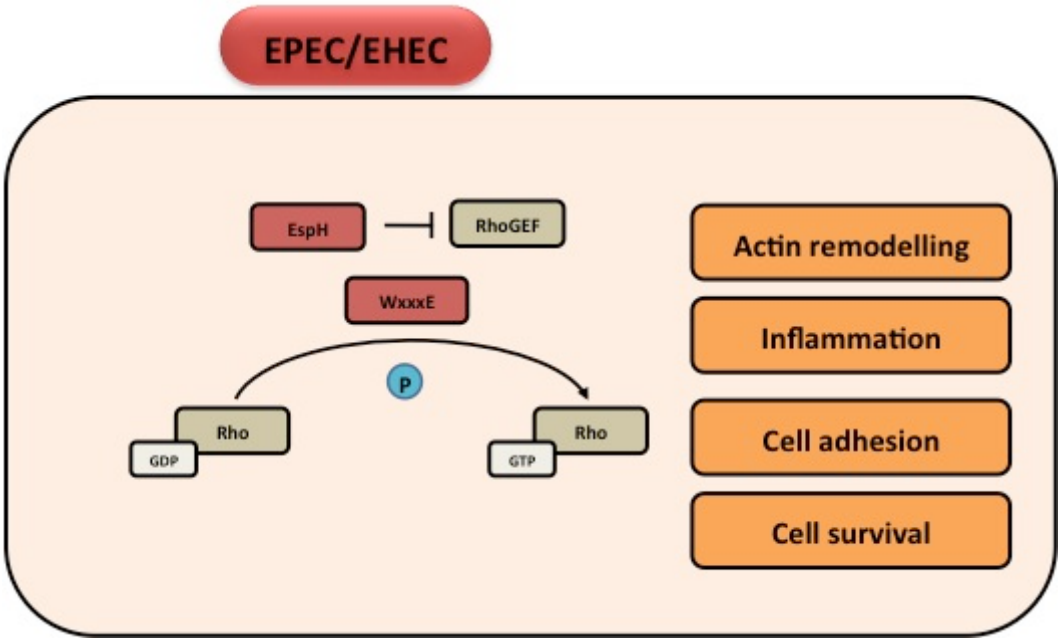


Figure 39. EspH and WxxxE bacterial RhoGEFs mediate diverse cellular processes.

Importantly, several reports have demonstrated that Rac1 and RhoA-activating bacterial RhoGEFs are also able to activate mitogen-activated protein kinase (MAPK) and NF-κB pathways (Fukazawa *et al.*, 2008, Bruno *et al.*, 2009, Raymond *et al.*, 2011) to induce pro-inflammatory responses. Investigating the impact of EspH on inflammation is therefore another aspect that has not been explored. Hypothetically, the inhibition of Rho GTPases may exert an anti-inflammatory effect owing to the downregulation of Rho GTPase signaling (Figure 39). How this may affect the overall infection cycle of EPEC/EHEC is however unclear. While inflammatory responses have pivotal roles in the regulation of cell survival and immune defense (Karin *et al.*,

2002, Wada *et al.*, 2004), several reports have also suggested that specialized bacterial pathogens may also modulate the inflammatory response as a mechanism of gaining a competitive advantage in colonization against resident gut microflora utilize (Sekirov *et al.*, 2010). This host-pathogen dichotomy is reflected in seperate *in vivo* studies of EspH which has yielded inconsistent results; studies on the murine model using *C. rodentium espH* mutants do not affect colonization, but studies on the leporine model using EHEC *espH* mutants showed a significant attenuation in colonization (Mundy *et al.*, 2004, Ritchie *et al.*, 2005). Importantly, EspT, which overrides EspH and triggers inflammatory responses, is present in *C. rodentium*, but not in EHEC. Thus, one explanation could be that attenuated effects of EspH are masked by EspT in *C. rodentium*, but is apparent in EHEC. More work is warranted to establish the role of EspH in the context of inflammation and outcome of infection.

5.3 Coordination of Rho GTPase subversion by bacterial pathogens

As described in section 1.6.4, several bacterial pathogens are known to independently co-evolve sophisticated strategies to exploit host cell Rho GTPase signaling. While structural and biochemical studies have elucidated a detailed picture of the molecular mechanisms of many of these effector proteins, the coordination of these effectors during infection *in vivo* are still not well understood. Spatial and temporal forms of Rho GTPase coordination have been identified. One is that of *Salmonella enterica* serovar Typhimurium, which temporally regulates Cdc42 and Rac1 by delivering SopE and SptP. SopE activates Cdc42/Rac1 to induce the "trigger mechanism" of bacterial invasion, but is quickly degraded (Kubori *et al.*, 2003). SptP exhibits GAP activity but slower degradation kinetics, thus allowing recovery from SopE-induced membrane ruffling (Kubori *et al.*, 2003). Another example of temporal regulation is

that of *E. coli* CNF1, which constitutively activates Rho GTPases but also increases its susceptibility to ubiquitination and consequent degradation (Doye *et al.*, 2002). The other is that of EPEC, in which the Cdc42 GEF Map triggers transient filopodia formation at the site of bacterial attachment (Kenny *et al.*, 2002) before re-localizing to the mitochondria via its N-terminal mitochondrial targeting sequence (Ma *et al.*, 2006). Filopodia dynamics are spatially regulated by Map interaction, through its carboxy-terminal PSD-95/Disk-large/ZO-1 (PDZ)-binding motif (DTRL), with the scaffold proteins sodium/hydrogen exchanger regulatory factor 1 and 2 (NHERF1/2) at the cell surface (Simpson *et al.*, 2006, Alto *et al.*, 2006, Martinez *et al.*, 2010).

In the case of EspH and bacterial RhoGEFs, a novel example is described in terms of functional coordination, where EPEC/EHEC utilizes EspH to globally silence mammalian Rho GTPase signaling, but also translocate their own bacterial RhoGEFs which are insensitive to EspH and thus exploit Rho GTPase signaling in an exclusive manner. These examples provide insights into how bacterial effectors may coordinate their activity during infection; not only is it important to characterize the mechanism of effector activity, additional parameters such as translocation hierarchy, translocated protein levels, effector stability, scaffolding of effectors, as well as target exclusivity of effectors must also be taken into account before we can have a global understanding of the subversion of Rho GTPases during bacterial infection.

These parameters do not apply solely for *Salmonella* SopE/SptP, or EPEC/EHEC WxxxE/EspH. In the case of *Yersinia*, three T3SS effectors are known to subvert Rho GTPase signaling. YopT has been shown to be target the CAAX motif of Rho GTPases, and acts as a cysteine protease that cleaves the CAAX motif, thus

abolishing membrane localization of Rho GTPases leading to its loss of function (Shao *et al.*, 2002, Shao *et al.*, 2003). YopE possesses a RhoGAP-like domain (Andor *et al.*, 2001, Aili *et al.*, 2006). YpkA/YopO possesses a GDI-like domain, and is able to bind and sequester both Rac1 and RhoA (Prehna *et al.*, 2006). In this case, all 3 effectors appear to inhibit Rho GTPase activity. However, YopO and YopT could operate independently of YopE functions, as they target both GDP- and GTP-bound Rho GTPases, while YopE only targets GTP-bound Rho GTPases. Yet, the context of their biochemical activity during infection cannot be considered well-defined without additional knowledge of spatiotemporal restrictions or binding targets.

Interestingly, *Salmonella* and EPEC/EHEC possess effectors that activate or disable Rho GTPases, thus giving them exquisite overall control over them. However, we do not know if this is more the exception or the rule as other bacterial pathogens, notably *Yersinia* and *C. difficile* only express effector proteins that covalently inhibit Rho GTPases. On the other hand, *Shigella* expresses the WxxxE effectors IpgB1 and IpgB2 which activate Rho GTPases, but no Rho disabling activity has been ascribed thus far. How these latter pathogens negatively regulate or indirectly offset the effects of their own Rho GTPase subversion is still not known, although we cannot ignore the possibility that such effectors have not been identified, or that these effectors are regulated by protein degradation kinetics.

5.4 Effector interplay: an emerging theme

Given the multifunctional and redundant nature of T3SS effectors, previous work has endeavoured to explore the different functions of T3SS effectors, e.g. Tir, EspF, EspT and Map. In this study, the interplay between EspH and different T3SS effectors is

explored and characterized. EspH and Tir play a role in modulating Arp2/3-mediated actin pedestals at the site of bacterial attachment. On the other hand, EspH and WxxxE effectors play a role in modulating actin dynamics, cell adhesion and cell death through Rho GTPase signaling. Other studies of NleB/NleC/NleD/NleE/NleH also reveal their ability to inhibit inflammatory responses of the TNF pathway (reviewed in (Wong *et al.*, 2011)). In these cases, the work is centred on how different T3SS effectors affect the same cellular signaling cascades, and understanding the synergistic, antagonistic and functional redundancy among these effectors. The result of this is the expansion of the functional network of effectors with diverse functions across different cellular processes.

Despite the recent advances in our knowledge of effector interplay, one prospect that has not been examined yet is the interplay between effectors that influence different signaling pathways. This aspect of interplay is particularly complex and challenging, as the intersections between different signaling pathways have not been thoroughly characterized in cell biology. By conducting a screen of T3SS effectors that could counteract EspH cytotoxicity, I have identified EspO/NleB/NleH as positive targets. Unlike EspO which binds integrin-linked kinase (ILK) to stabilize focal adhesions (Kim *et al.*, 2009), no obvious mechansistic relation to Rho GTPase signaling has been described for NleB or NleH. In the case of NleH, this activity is most likely mediated by the ability of NleH to bind Bax-inhibitor 1 (BI-1) (Hemrajani *et al.*, 2010), as the kinase domain which is required for NF-κB suppression is not involved in inhibition of EspH cytotoxicity (Gao *et al.*, 2009, Wan *et al.*, 2011). BI-1 is most associated with suppression of ER stress-mediated apoptosis, but has also recently been shown to possess actin bundling activity *in vitro* (Lee *et al.*, 2010), thus

suggesting a link to the actin cytoskeleton. Therefore, studying the interplay between NleH and EspH could uncover novel findings that would refine our understanding of the intersections between the cellular pathways of intrinsic apoptosis and Rho GTPases.

Another factor that cannot be overlooked is also the distribution of effectors in question across A/E pathogens. During this study, we found that NleH, EspM2 and EspT are all able to inhibit EspH-induced caspase-3 activation, detachment and cytoxicity. One would therefore assume that EspM2 and EspT should be positively selected for, owing to its pro-survival properties. Paradoxically, NleH is conserved across A/E pathogens, EspM is found in ~50% of EPEC/EHEC isolates screened, while EspT is not found in EHEC, and is found in only ~2% of EPEC isolates (Arbeloa *et al.*, 2009). This plasticity in effector repertoire across A/E pathogens may reflect the existence of a tradeoff in T3SS-mediated virulence strategies; EspT but not EspM induces EPEC invasion (Bulgin *et al.*, 2009a) and inflammatory responses (Raymond *et al.*, 2011), while NleH1 also binds RPS3 to inhibit NF-κB-mediated inflammation (Gao *et al.*, 2009, Wan *et al.*, 2011). These additional factors may level the advantage of increased host cell adhesion and survival when we consider that A/E pathogens are mainly extracellular and so utilize pro- and anti-inflammatory responses to enhance their colonization among resident gut microflora (Sekirov *et al.*, 2010). In the case of *Salmonella*, it has been proposed that SopE plays a role in promoting intracellular bacterial survival in addition to bacterial invasion (Hashim *et al.*, 2000, Mukherjee *et al.*, 2001); in this context we suggest that SopE could also contribute to host cell survival by inhibiting cell death, thus facilitating intracellular bacterial replication and persistence following bacterial entry.

5.5 Concluding remarks

This thesis has presented two studies focusing on the conserved LEE effector EspH and its interplay with other T3SS effectors. The first study highlights the role of EspH in mediating Tir-dependent actin pedestal formation. EspH promotes an actin polymerization pathway that is distinct of the Tir:Nck and Tir:IRTKS/IRSp53 pathways, and that this pathway requires the the recruitment of the WIP/N-WASP complex. Disruption of WIP recruitment results in the decrease in actin pedestal formation and elongation, while overexpression of WIP and EspH during EPEC infection induces extensive actin cytoskeletal rearrangements at the bacterial attachment site, forming a protrusive actin patch that is associated with EPEC microcolonies, termed "macro-pedestals". This study shows the complex intricacies of EPEC actin pedestal formation that involves convergent, redundant and synergistic signaling cascades. The second study highlights the functional coordination that exists with EspH as a mammalan RhoGEF inhibitor, and bacterial WxxxE RhoGEFs that are insensitive to EspH inhibition and therefore counteract the cytotoxic effects of EspH. In addition, bacterial RhoGEFs also play a role in promoting cell adhesion and survival. This study expands the role of bacterial RhoGEFs to include cell adhesion and survival, and demonstrates a unique strategy by which A/E pathogens subvert Rho GTPase signaling. Thus, EspH is a multifunctional effector that is able to subvert host cell function in a localized and global context during EPEC infection.

References

Abercrombie, M., Heaysman, J.E. and Pegrum, S.M. (1970a). The locomotion of fibroblasts in culture. I. Movements of the leading edge. *Exp Cell Res* **59,** 393-398.

Abercrombie, M., Heaysman, J.E. and Pegrum, S.M. (1970b). The locomotion of fibroblasts in culture. II. "RRuffling". *Exp Cell Res* **60,** 437-444.

Abul-Milh, M., Wu, Y., Lau, B., Lingwood, C.A. and Barnett Foster, D. (2001). Induction of epithelial cell death including apoptosis by enteropathogenic *Escherichia coli* expressing bundle-forming pili. *Infect Immun* **69,** 7356-7364.

Aili, M., Isaksson, E.L., Hallberg, B., Wolf-Watz, H. and Rosqvist, R. (2006). Functional analysis of the YopE GTPase-activating protein (GAP) activity of *Yersinia pseudotuberculosis*. *Cell Microbiol* **8,** 1020-1033.

Akeda, Y. and Galan, J. (2004). Genetic analysis of the Salmonella enterica type III secretion-associated ATPase InvC defines discrete functional domains. *J Bacteriol* **186,** 2402-2412.

Alto, N.M., Shao, F., Lazar, C.S., Brost, R.L., Chua, G., Mattoo, S.*, et al.* (2006). Identification of a bacterial type III effector family with G protein mimicry functions. *Cell* **124,** 133-145.

Alto, N.M., Weflen, A.W., Rardin, M.J., Yarar, D., Lazar, C.S., Tonikian, R.*, et al.* (2007). The type III effector EspF coordinates membrane trafficking by the spatiotemporal activation of two eukaryotic signaling pathways. *J Cell Biol* **178,** 1265-1278.

Andor, A., Trulzsch, K., Essler, M., Roggenkamp, A., Wiedemann, A., Heesemann, J. and Aepfelbacher, M. (2001). YopE of *Yersinia*, a GAP for Rho GTPases, selectively modulates Rac-dependent actin structures in endothelial cells. *Cell Microbiol* **3,** 301-310.

Anton, I.M., Jones, G.E., Wandosell, F., Geha, R. and Ramesh, N. (2007). WASP-interacting protein (WIP): working in polymerisation and much more. *Trends Cell Biol* **17,** 555-562.

Anton, I.M., Lu, W., Mayer, B.J., Ramesh, N. and Geha, R.S. (1998). The Wiskott-Aldrich syndrome protein-interacting protein (WIP) binds to the adaptor protein Nck. *J Biol Chem* **273,** 20992-20995.

Arbeloa, A., Blanco, M., Moreira, F.C., Bulgin, R., Lopez, C., Dahbi, G.*, et al.* (2009). Distribution of espM and espT among enteropathogenic and enterohaemorrhagic *Escherichia coli*. *J Med Microbiol* **58,** 988-995.

Arbeloa, A., Bulgin, R.R., MacKenzie, G., Shaw, R.K., Pallen, M.J., Crepin, V.F.*, et al.* (2008). Subversion of actin dynamics by EspM effectors of attaching and effacing bacterial pathogens. *Cell Microbiol* **10,** 1429-1441.

Arbeloa, A., Garnett, J., Lillington, J., Bulgin, R.R., Berger, C.N., Lea, S.M.*, et al.* (2010). EspM2 is a RhoA guanine nucleotide exchange factor. *Cell Microbiol* **12,** 654-664.

Arbeloa, A., Oates, C.V., Marches, O., Hartland, E.L. and Frankel, G. (2011). Enteropathogenic and enterohemorrhagic *Escherichia coli* type III secretion effector EspV induces radical morphological changes in eukaryotic cells. *Infect Immun* **79,** 1067-1076.

Ashkenazi, A. and Dixit, V.M. (1998). Death receptors: signaling and modulation. *Science* **281,** 1305-1308.

Aspenstrom, P. (2002). The WASP-binding protein WIRE has a role in the regulation of the actin filament system downstream of thmn nm e platelet-derived growth factor receptor. *Exp Cell Res* **279,** 21-33.

Backert, S. and Selbach, M. (2005). Tyrosine-phosphorylated bacterial effector proteins: the enemies within. *Trends Microbiol.* **13,** 476-484.

Bamburg, J.R. (1999). Proteins of the ADF/cofilin family: essential regulators of actin dynamics. *Annu Rev Cell Dev Biol* **15,** 185-230.

Barbieri, J.T. and Sun, J. (2004). *Pseudomonas aeruginosa* ExoS and ExoT. *Rev Physiol Biochem Pharmacol* **152,** 79-92.

Barrett, T., Xiao, B., Dodson, E.J., Dodson, G., Ludbrook, S.B., Nurmahomed, K.*, et al.* (1997). The structure of the GTPase-activating domain from p50rhoGAP. *Nature* **385,** 458-461.

Baruch, K., Gur-Arie, L., Nadler, C., Koby, S., Yerushalmi, G., Ben-Neriah, Y.*, et al.* (2011). Metalloprotease type III effectors that specifically cleave JNK and NF-kappaB. *EMBO J* **30,** 221-231.

Batchelor, M., Guignot, J., Patel, A., Cummings, N., Cleary, J., Knutton, S.*, et al.* (2004). Involvement of the intermediate filament protein cytokeratin-18 in actin pedestal formation during EPEC infection. *EMBO Rep* **5,** 219.

Batchelor, M., Prasannan, S., Daniell, S., Reece, S., Connerton, I., Bloomberg, G.*, et al.* (2000). Structural basis for recognition of the translocated intimin receptor (Tir) by intimin from enteropathogenic *Escherichia coli*. *EMBO J* **19,** 2452-2464.

Ben-Ami, G., Ozeri, V., Hanski, E., Hofmann, F., Aktories, K., Hahn, K.M.*, et al.* (1998). Agents that inhibit Rho, Rac, and Cdc42 do not block formation of actin pedestals in HeLa cells infected with enteropathogenic *Escherichia coli*. *Infect Immun* **66,** 1755-1758.

Berger, C.N., Crepin, V.F., Jepson, M.A., Arbeloa, A. and Frankel, G. (2009). The mechanisms used by enteropathogenic *Escherichia coli* to control filopodia dynamics. *Cell Microbiol* **11,** 309-322.

Bernet-Camard, M.F., Coconnier, M.H., Hudault, S. and Servin, A.L. (1996). Pathogenicity of the diffusely adhering strain Escherichia coli C1845: F1845 adhesin-decay accelerating factor interaction, brush border microvillus injury, and actin disassembly in cultured human intestinal epithelial cells. *Infect Immun* **64,** 1918-1928.

Blanchoin, L., Amann, K.J., Higgs, H.N., Marchand, J.B., Kaiser, D.A. and Pollard, T.D. (2000). Direct observation of dendritic actin filament networks nucleated by Arp2/3 complex and WASP/Scar proteins. *Nature* **404,** 1007-1011.

Bommarius, B., Maxwell, D., Swimm, A., Leung, S., Corbett, A., Bornmann, W. and Kalman, D. (2007). Enteropathogenic *Escherichia coli* Tir is an SH2/3 ligand that recruits and activates tyrosine kinases required for pedestal formation. *Mol Microbiol* **63,** 1748-1768.

Bosch, M., Le, K.H., Bugyi, B., Correia, J.J., Renault, L. and Carlier, M.F. (2007). Analysis of the function of Spire in actin assembly and its synergy with formin and profilin. *Mol Cell* **28,** 555-568.

Brady, M.J., Campellone, K.G., Ghildiyal, M. and Leong, J.M. (2007). Enterohaemorrhagic and enteropathogenic *Escherichia coli* Tir proteins trigger a common Nck-independent actin assembly pathway. *Cell Microbiol* **9,** 2242-2253.

Breitbach, K., Rottner, K., Klocke, S., Rohde, M., Jenzora, A., Wehland, J. and Steinmetz, I. (2003). Actin-based motility of *Burkholderia pseudomallei* involves the Arp 2/3 complex, but not N-WASP and Ena/VASP proteins. *Cell Microbiol* **5,** 385-393.

Brenner, B., Koppenhoefer, U., Weinstock, C., Linderkamp, O., Lang, F. and Gulbins, E. (1997). Fas- or ceramide-induced apoptosis is mediated by a Rac1-regulated activation of Jun N-terminal kinase/p38 kinases and GADD153. *J Biol Chem* **272,** 22173-22181.

Brown, M.D., Bry, L., Li, Z. and Sacks, D.B. (2008). Actin pedestal formation by enteropathogenic *Escherichia coli* is regulated by IQGAP1, calcium, and calmodulin. *J Biol Chem* **283,** 35212-35222.

Bruno, V.M., Hannemann, S., Lara-Tejero, M., Flavell, R.A., Kleinstein, S.H. and Galan, J.E. (2009). Salmonella Typhimurium type III secretion effectors stimulate innate immune responses in cultured epithelial cells. *PLoS pathog* **5,** e1000538.

Budihardjo, I., Oliver, H., Lutter, M., Luo, X. and Wang, X. (1999). Biochemical pathways of caspase activation during apoptosis. *Annu Rev Cell Dev Biol* **15,** 269-290.

Bulgin, R., Arbeloa, A., Goulding, D., Dougan, G., Crepin, V.F., Raymond, B. and Frankel, G. (2009a). The T3SS effector EspT defines a new category of invasive enteropathogenic *E. coli* (EPEC) which form intracellular actin pedestals. *PLoS Pathog* **5,** e1000683.

Bulgin, R., Raymond, B., Garnett, J.A., Frankel, G., Crepin, V.F., Berger, C.N. and Arbeloa, A. (2010). Bacterial guanine nucleotide exchange factors SopE-like and WxxxE effectors. *Infect Immun* **78,** 1417-1425.

Bulgin, R.R., Arbeloa, A., Chung, J.C. and Frankel, G. (2009b). EspT triggers formation of lamellipodia and membrane ruffles through activation of Rac-1 and Cdc42. *Cell Microbiol* **11,** 217-229.

Buss, C., Muller, D., Ruter, C., Heusipp, G. and Schmidt, M.A. (2009). Identification and characterization of Ibe, a novel type III effector protein of A/E pathogens targeting human IQGAP1. *Cell Microbiol* **11,** 661-677.

Cai, J., Yang, J. and Jones, D.P. (1998). Mitochondrial control of apoptosis: the role of cytochrome c. *Biochim Biophys Acta* **1366,** 139-149.

Campellone, K., Robbins, D. and Leong, J. (2004a). EspF(U) is a translocated EHEC effector that interacts with Tir and N-WASP and promotes Nck-independent actin assembly. *Dev Cell* **7,** 217-228.

Campellone, K.G., Brady, M.J., Alamares, J.G., Rowe, D.C., Skehan, B.M., Tipper, D.J. and Leong, J.M. (2006). Enterohaemorrhagic *Escherichia coli* Tir requires a C-terminal 12-residue peptide to initiate EspFu-mediated actin assembly and harbours N-terminal sequences that influence pedestal length. *Cell Microbiol* **8,** 1488-1503.

Campellone, K.G., Cheng, H.C., Robbins, D., Siripala, A.D., McGhie, E.J., Hayward, R.D.*, et al.* (2008). Repetitive N-WASP-binding elements of the enterohemorrhagic *Escherichia coli* effector EspF(U) synergistically activate actin assembly. *PLoS Pathog* **4,** e1000191.

Campellone, K.G., Giese, A., Tipper, D.J. and Leong, J.M. (2002). A tyrosine-phosphorylated 12-amino-acid sequence of enteropathogenic *Escherichia coli* Tir binds the host adaptor protein Nck and is required for Nck localization to actin pedestals. *Mol Microbiol* **43,** 1227-1241.

Campellone, K.G. and Leong, J.M. (2005). Nck-independent actin assembly is mediated by two phosphorylated tyrosines within enteropathogenic *Escherichia coli* Tir. *Mol Microbiol* **56,** 416-432.

Campellone, K.G., Rankin, S., Pawson, T., Kirschner, M.W., Tipper, D.J. and Leong, J.M. (2004b). Clustering of Nck by a 12-residue Tir phosphopeptide is sufficient to trigger localized actin assembly. *J Cell Biol* **164,** 407-416.

Campellone, K.G. and Welch, M.D. (2010). A nucleator arms race: cellular control of actin assembly. *Nat Rev Mol Cell Biol* **11,** 237-251.

Cantarelli, V.V., Kodama, T., Nijstad, N., Abolghait, S.K., Nada, S., Okada, M.*, et al.* (2007). Tyrosine phosphorylation controls cortactin binding to two enterohaemorrhagic *Escherichia coli* effectors: Tir and EspFu/TccP. *Cell Microbiol* **9,** 1782-1795.

Cantarelli, V.V., Takahashi, A., Akeda, Y., Nagayama, K. and Honda, T. (2000). Interaction of enteropathogenic or enterohemorrhagic *Escherichia coli* with HeLa cells results in translocation of cortactin to the bacterial adherence site. *Infect Immun* **68,** 382-386.

Cantarelli, V.V., Takahashi, A., Yanagihara, I., Akeda, Y., Imura, K., Kodama, T.*, et al.* (2001). Talin, a host cell protein, interacts directly with the translocated intimin receptor, Tir, of enteropathogenic *Escherichia coli*, and is essential for pedestal formation. *Cell Microbiol* **3,** 745-751.

Cantarelli, V.V., Takahashi, A., Yanagihara, I., Akeda, Y., Imura, K., Kodama, T.*, et al.* (2002). Cortactin is necessary for F-actin accumulation in pedestal structures induced by enteropathogenic *Escherichia coli* infection. *Infect Immun* **70,** 2206-2209.

Carlier, M.F., Nioche, P., Broutin-L'Hermite, I., Boujemaa, R., Le Clainche, C., Egile, C.*, et al.* (2000). GRB2 links signaling to actin assembly by enhancing interaction of neural Wiskott-Aldrich syndrome protein (N-WASp) with actin-related protein (ARP2/3) complex. *J Biol Chem* **275,** 21946-21952.

Chang, F., Lemmon, C.A., Park, D. and Romer, L.H. (2007). FAK potentiates Rac1 activation and localization to matrix adhesion sites: a role for betaPIX. *Mol Biol Cell* **18,** 253-264.

Charpentier, X. and Oswald, E. (2004). Identification of the secretion and translocation domain of the enteropathogenic and enterohemorrhagic *Escherichia coli* effector Cif, using TEM-1 beta-lactamase as a new fluorescence-based reporter. *J Bacteriol* **186,** 5486-5495.

Cheng, H.C., Skehan, B.M., Campellone, K.G., Leong, J.M. and Rosen, M.K. (2008). Structural mechanism of WASP activation by the enterohaemorrhagic *E. coli* effector EspF(U). *Nature* **454,** 1009-1013.

Chikumi, H., Fukuhara, S. and Gutkind, J.S. (2002). Regulation of G protein-linked guanine nucleotide exchange factors for Rho, PDZ-RhoGEF, and LARG by tyrosine phosphorylation: evidence of a role for focal adhesion kinase. *J Biol Chem* **277,** 12463-12473.

Christie, P.J. and Cascales, E. (2005). Structural and dynamic properties of bacterial type IV secretion systems (review). *Mol Membr Biol* **22,** 51-61.

Chuang, T.H., Bohl, B.P. and Bokoch, G.M. (1993). Biologically active lipids are regulators of Rac.GDI complexation. *J Biol Chem* **268,** 26206-26211.

Clements, A., Smollett, K., Lee, S.F., Hartland, E.L., Lowe, M. and Frankel, G. (2011). EspG of enteropathogenic and enterohemorrhagic *E. coli* binds the Golgi matrix protein GM130 and disrupts the Golgi structure and function. *Cell Microbiol* **13,** 1429-1439.

Coleman, M.L. and Olson, M.F. (2002). Rho GTPase signalling pathways in the morphological changes associated with apoptosis. *Cell Death Differ* **9,** 493-504.

Coleman, M.L., Sahai, E.A., Yeo, M., Bosch, M., Dewar, A. and Olson, M.F. (2001). Membrane blebbing during apoptosis results from caspase-mediated activation of ROCK I. *Nat Cell Biol* **3,** 339-345.

Condeelis, J. (2001). How is actin polymerization nucleated in vivo? *Trends Cell Biol* **11,** 288-293.

Cookson, S.T. and Nataro, J.P. (1996). Characterization of HEp-2 cell projection formation induced by diffusely adherent *Escherichia coli*. *Microb Pathog* **21,** 421-434.

Cornelis, G.R. (2006). The type III secretion injectisome. *Nat Rev Microbiol* **4,** 811-825.

Cossart, P. and Sansonetti, P.J. (2004). Bacterial invasion: the paradigms of enteroinvasive pathogens. *Science* **304,** 242-248.

Cote, J.F. and Vuori, K. (2007). GEF what? Dock180 and related proteins help Rac to polarize cells in new ways. *Trends Cell Biol* **17,** 383-393.

Cotter, T.G., Lennon, S.V., Glynn, J.M. and Green, D.R. (1992). Microfilament-disrupting agents prevent the formation of apoptotic bodies in tumor cells undergoing apoptosis. *Cancer Res* **52,** 997-1005.

Cramer, L.P., Siebert, M. and Mitchison, T.J. (1997). Identification of novel graded polarity actin filament bundles in locomoting heart fibroblasts: implications for the generation of motile force. *J Cell Biol* **136,** 1287-1305.

Crane, J.K., Majumdar, S. and Pickhardt, D.F., 3rd (1999). Host cell death due to enteropathogenic *Escherichia coli* has features of apoptosis. *Infect Immun* **67,** 2575-2584.

Crane, J.K., McNamara, B.P. and Donnenberg, M.S. (2001). Role of EspF in host cell death induced by enteropathogenic *Escherichia coli*. *Cell Microbiol* **3,** 197-211.

Crepin, V.F., Girard, F., Schuller, S., Phillips, A.D., Mousnier, A. and Frankel, G. (2009). Dissecting the role of the Tir:Nck and Tir:IRTKS/IRSp53 signalling pathways in vivo. *Mol Microbiol* **75,** 308-323.

Crepin, V.F., Prasannan, S., Shaw, R.K., Wilson, R.K., Creasey, E., Abe, C.M.*, et al.* (2005a). Structural and functional studies of the enteropathogenic *Escherichia coli* type III needle complex protein EscJ. *Mol Microbiol* **55,** 1658-1670.

Crepin, V.F., Shaw, R.K., Abe, C.M., Knutton, S. and Frankel, G. (2005b). Polarity of enteropathogenic *Escherichia coli* EspA filament assembly and protein secretion. *J bacteriol* **187,** 2881-2889.

Croft, D.R., Coleman, M.L., Li, S., Robertson, D., Sullivan, T., Stewart, C.L. and Olson, M.F. (2005). Actin-myosin-based contraction is responsible for apoptotic nuclear disintegration. *J Cell Biol* **168,** 245-255.

Cui, J., Yao, Q., Li, S., Ding, X., Lu, Q., Mao, H.*, et al.* (2010). Glutamine deamidation and dysfunction of ubiquitin/NEDD8 induced by a bacterial effector family. *Science* **329,** 1215-1218.

Currie, M.G., Fok, K.F., Kato, J., Moore, R.J., Hamra, F.K., Duffin, K.L. and Smith, C.E. (1992). Guanylin: an endogenous activator of intestinal guanylate cyclase. *Proc Natl Acad Sci U S A* **89,** 947-951.

Daniell, S.J., Delahay, R.M., Shaw, R.K., Hartland, E.L., Pallen, M.J., Booy, F.*, et al.* (2001). The coiled coil domain of Enteropathogenic *E. coli* type III secreted protein EspD is involved in EspA filament-mediated cell attachment and haemolysis. *Infect Immun* **69,** 4055-4064.

Daniell, S.J., Kocsis, E., Morris, E., Knutton, S., Booy, F.P. and Frankel, G. (2003). 3D structure of EspA filaments from enteropathogenic *Escherichia coli*. *Mol Microbiol* **49,** 301-308.

Datsenko, K.A. and Wanner, B.L. (2000). One-step inactivation of chromosomal genes in *Escherichia coli* K-12 using PCR products. *Proc Natl Acad Sci U S A* **97,** 6640-6645.

Dautin, N. and Bernstein, H.D. (2007). Protein secretion in gram-negative bacteria via the autotransporter pathway. *Annu Rev Microbiol* **61,** 89-112.

de Grado, M., Abe, A., Gauthier, A., Steele-Mortimer, O., DeVinney, R. and Finlay, B.B. (1999). Identification of the intimin binding domain of Tir of enteropathogenic *Escherichia coli*. *Cell Microbiol* **1,** 7-18.

de la Fuente, M.A., Sasahara, Y., Calamito, M., Anton, I.M., Elkhal, A., Gallego, M.D.*, et al.* (2007). WIP is a chaperone for Wiskott-Aldrich syndrome protein (WASP). *Proc Natl Acad Sci U S A* **104,** 926-931.

Dean, P. and Kenny, B. (2004). Intestinal barrier dysfunction by enteropathogenic *Escherichia coli* is mediated by two effector molecules and a bacterial surface protein. *Mol Microbiol* **54,** 665-675.

Dean, P. and Kenny, B. (2009). The effector repertoire of enteropathogenic *E. coli*: ganging up on the host cell. *Curr Opin Microbiol* **12,** 101-109.

Dean, P., Maresca, M., Schuller, S., Phillips, A.D. and Kenny, B. (2006). Potent diarrheagenic mechanism mediated by the cooperative action of three enteropathogenic *Escherichia coli*-injected effector proteins. *Proc Natl Acad Sci U S A* **103,** 1876-1881.

Dean, P., Scott, J.A., Knox, A.A., Quitard, S., Watkins, N.J. and Kenny, B. (2010). The enteropathogenic *E. coli* effector EspF targets and disrupts the nucleolus by a process regulated by mitochondrial dysfunction. *PLoS Pathog* **6,** e1000961.

Deborah Chen, H. and Frankel, G. (2005). Enteropathogenic *Escherichia coli*: unravelling pathogenesis. *FEMS Microbiol Rev* **29,** 83-98.

Deng, W., Puente, J.L., Gruenheid, S., Li, Y., Vallance, B.A., Vazquez, A.*, et al.* (2004). Dissecting virulence: systematic and functional analyses of a pathogenicity island. *Proc Natl Acad Sci U S A* **101,** 3597-3602.

Derivery, E., Lombard, B., Loew, D. and Gautreau, A. (2009). The Wave complex is intrinsically inactive. *Cell Motil Cytoskel* **66,** 777-790.

DerMardirossian, C., Schnelzer, A. and Bokoch, G.M. (2004). Phosphorylation of RhoGDI by Pak1 mediates dissociation of Rac GTPase. *Mol Cell* **15,** 117-127.

Dong, N., Liu, L. and Shao, F. (2010). A bacterial effector targets host DH-PH domain RhoGEFs and antagonizes macrophage phagocytosis. *EMBO J* **29,** 1363-1376.

Dovas, A. and Couchman, J.R. (2005). RhoGDI: multiple functions in the regulation of Rho family GTPase activities. *Biochem J* **390,** 1-9.

Doye, A., Mettouchi, A., Bossis, G., Clement, R., Buisson-Touati, C., Flatau, G.*, et al.* (2002). CNF1 exploits the ubiquitin-proteasome machinery to restrict Rho GTPase activation for bacterial host cell invasion. *Cell* **111,** 553-564.

Du, C., Fang, M., Li, Y., Li, L. and Wang, X. (2000). Smac, a mitochondrial protein that promotes cytochrome c-dependent caspase activation by eliminating IAP inhibition. *Cell* **102,** 33-42.

Eden, S., Rohatgi, R., Podtelejnikov, A.V., Mann, M. and Kirschner, M.W. (2002). Mechanism of regulation of WAVE1-induced actin nucleation by Rac1 and Nck. *Nature* **418,** 790-793.

Elliott, S.J., Wainwright, L.A., McDaniel, T.K., Jarvis, K.G., Deng, Y., Lai, L.*, et al.* (1998). The complete sequence of the locus of enterocyte effacement (LEE) from enteropathogenic *Escherichia coli* E2348/69. *Mol Microbiol* **28,** 1-4.

Elmore, S. (2007). Apoptosis: a review of programmed cell death. *Toxicol Pathol* **35,** 495-516.

Enari, M., Sakahira, H., Yokoyama, H., Okawa, K., Iwamatsu, A. and Nagata, S. (1998). A caspase-activated DNase that degrades DNA during apoptosis, and its inhibitor ICAD. *Nature* **391,** 43-50.

Etienne-Manneville, S. and Hall, A. (2002). Rho GTPases in cell biology. *Nature* **420,** 629-635.

Filloux, A. (2004). The underlying mechanisms of type II protein secretion. *Biochim Biophys Acta* **1694,** 163-179.

Filloux, A., Hachani, A. and Bleves, S. (2008). The bacterial type VI secretion machine: yet another player for protein transport across membranes. *Microbiology* **154,** 1570-1583.

Fiorentini, C., Fabbri, A., Falzano, L., Fattorossi, A., Matarrese, P., Rivabene, R. and Donelli, G. (1998). *Clostridium difficile* toxin B induces apoptosis in intestinal cultured cells. *Infect Immun* **66,** 2660-2665.

Flatau, G., Lemichez, E., Gauthier, M., Chardin, P., Paris, S., Fiorentini, C. and Boquet, P. (1997). Toxin-induced activation of the G protein p21 Rho by deamidation of glutamine. *Nature* **387,** 729-733.

Frankel, G., Lider, O., Hershkoviz, R., Mould, A.P., Kachalsky, S.G., Candy, D.C.*, et al.* (1996). The cell-binding domain of intimin from enteropathogenic *Escherichia coli* binds to beta1 integrins. *J Biol Chem* **271,** 20359-20364.

Frankel, G., Phillips, A.D., Trabulsi, L.R., Knutton, S., Dougan, G. and Matthews, S. (2001). Intimin and the host cell - is it bound to end in Tir(s)? *Trends Microbiol* **9,** 214-218.

Freeman, N.L., Zurawski, D.V., Chowrashi, P., Ayoob, J.C., Huang, L., Mittal, B.*, et al.* (2000). Interaction of the enteropathogenic *Escherichia coli* protein, translocated intimin receptor (Tir), with focal adhesion proteins. *Cell Motil Cytoskeleton* **47,** 307-318.

Frischknecht, F., Moreau, V., Rottger, S., Gonfloni, S., Reckmann, I., Superti-Furga, G., and Way, M. (1999). Actin-based motility of vaccinia virus mimics receptor tyrosine kinase signalling. *Nature* **401,** 926-929.

Fronzes, R., Christie, P.J. and Waksman, G. (2009). The structural biology of type IV secretion systems. *Nat Rev Microbiol* **7,** 703-714.

Fu, Y. and Galan, J.E. (1998). The Salmonella typhimurium tyrosine phosphatase SptP is translocated into host cells and disrupts the actin cytoskeleton. *Mol Microbiol* **27,** 359-368.

Fukazawa, A., Alonso, C., Kurachi, K., Gupta, S., Lesser, C.F., McCormick, B.A. and Reinecker, H.C. (2008). GEF-H1 mediated control of NOD1 dependent NF-kappaB activation by *Shigella* effectors. *PLoS pathog* **4,** e1000228.

Galan, J.E., Ginocchio, C. and Costeas, P. (1992). Molecular and functional characterization of the Salmonella invasion gene invA: homology of InvA to members of a new protein family. *J Bacteriol* **174,** 4338-4349.

Gao, X., Wan, F., Mateo, K., Callegari, E., Wang, D., Deng, W.*, et al.* (2009). Bacterial effector binding to ribosomal protein s3 subverts NF-kappaB function. *PLoS Pathog* **5,** e1000708.

Garmendia, J., Carlier, M.F., Egile, C., Didry, D. and Frankel, G. (2006). Characterization of TccP-mediated N-WASP activation during enterohaemorrhagic *Escherichia coli* infection. *Cell Microbiol* **8,** 1444-1455.

Garmendia, J., Phillips, A.D., Carlier, M.F., Chong, Y., Schuller, S., Marches, O.*, et al.* (2004). TccP is an enterohaemorrhagic *Escherichia coli* O157:H7 type III effector protein that couples Tir to the actin-cytoskeleton. *Cell Microbiol* **6,** 1167-1183.

Gauthier, A., Puente, J. and Finlay, B. (2003). Secretin of the enteropathogenic *Escherichia coli* type III secretion system requires components of the type III apparatus for assembly and localization. *Infect Immun* **71,** 3310-3319.

Gautreau, A., Ho, H.Y., Li, J., Steen, H., Gygi, S.P. and Kirschner, M.W. (2004). Purification and architecture of the ubiquitous Wave complex. *Proc Natl Acad Sci U S A* **101,** 4379-4383.

Genth, H., Gerhard, R., Maeda, A., Amano, M., Kaibuchi, K., Aktories, K. and Just, I. (2003). Entrapment of Rho ADP-ribosylated by *Clostridium botulinum* C3 exoenzyme in the Rho-guanine nucleotide dissociation inhibitor-1 complex. *J Biol Chem* **278,** 28523-28527.

Gerhard, R., Nottrott, S., Schoentaube, J., Tatge, H., Olling, A. and Just, I. (2008). Glucosylation of Rho GTPases by *Clostridium difficile* toxin A triggers apoptosis in intestinal epithelial cells. *J Med Microbiol* **57,** 765-770.

Gervais, F.G., Thornberry, N.A., Ruffolo, S.C., Nicholson, D.W. and Roy, S. (1998). Caspases cleave focal adhesion kinase during apoptosis to generate a FRNK-like polypeptide. *J Biol Chem* **273,** 17102-17108.

Gilmore, A.P. (2005). Anoikis. *Cell Death Differ* **12 (2),** 1473-1477.

Girard, F., Crepin, V.F. and Frankel, G. (2009). Modelling of infection by enteropathogenic *Escherichia coli* strains in lineages 2 and 4 ex vivo and in vivo by using *Citrobacter rodentium* expressing TccP. *Infect Immun* **77,** 1304-1314.

Girard, F., Dziva, F., van Diemen, P., Phillips, A.D., Stevens, M.P. and Frankel, G. (2007). Adherence of enterohemorrhagic *Escherichia coli* O157, O26, and O111 strains to bovine intestinal explants ex vivo. *Appl Environ Microbiol* **73,** 3084-3090.

Girard, F., Oswald, I.P., Taranu, I., Helie, P., Appleyard, G.D., Harel, J. and Fairbrother, J.M. (2005). Host immune status influences the development of attaching and effacing lesions in weaned pigs. *Infect Immun* **73,** 5514-5523.

Goley, E.D., Rodenbusch, S.E., Martin, A.C. and Welch, M.D. (2004). Critical conformational changes in the Arp2/3 complex are induced by nucleotide and nucleation promoting factor. *Mol Cell* **16,** 269-279.

Goosney, D.L., DeVinney, R., Pfuetzner, R.A., Frey, E.A., Strynadka, N.C. and Finlay, B.B. (2000). Enteropathogenic *E. coli* translocated intimin receptor, Tir, interacts directly with alpha-actinin. *Curr Biol* **10,** 735-738.

Gosser, Y.Q., Nomanbhoy, T.K., Aghazadeh, B., Manor, D., Combs, C., Cerione, R.A. and Rosen, M.K. (1997). C-terminal binding domain of Rho GDP-dissociation inhibitor directs N-terminal inhibitory peptide to GTPases. *Nature* **387,** 814-819.

Gouin, E., Egile, C., Dehoux, P., Villiers, V., Adams, J., Gertler, F.*, et al.* (2004). The RickA protein of *Rickettsia conorii* activates the Arp2/3 complex. *Nature* **427,** 457-461.

Grant, S.R., Fisher, E.J., Chang, J.H., Mole, B.M. and Dangl, J.L. (2006). Subterfuge and manipulation: type III effector proteins of phytopathogenic bacteria. *Annu Rev Microbiol* **60,** 425-449.

Green, D.R. and Kroemer, G. (2004). The pathophysiology of mitochondrial cell death. *Science* **305,** 626-629.

Grimm, S., Stanger, B.Z. and Leder, P. (1996). RIP and FADD: two "death domain"-containing proteins can induce apoptosis by convergent, but dissociable, pathways. *Proc Natl Acad Sci U S A* **93,** 10923-10927.

Grizot, S., Faure, J., Fieschi, F., Vignais, P.V., Dagher, M.C. and Pebay-Peyroula, E. (2001). Crystal structure of the Rac1-RhoGDI complex involved in nadph oxidase activation. *Biochemistry* **40,** 10007-10013.

Gruenheid, S., DeVinney, R., Bladt, F., Goosney, D., Gelkop, S., Gish, G.D.*, et al.* (2001). Enteropathogenic *E. coli* Tir binds Nck to initiate actin pedestal formation in host cells. *Nat Cell Biol* **3,** 856-859.

Gruenheid, S., Sekirov, I., Thomas, N.A., Deng, W., O'Donnell, P., Goode, D.*, et al.* (2004). Identification and characterization of NleA, a non-LEE-encoded type III translocated virulence factor of enterohaemorrhagic *Escherichia coli* O157:H7. *Mol Microbiol* **51,** 1233-1249.

Guttman, J.A., Li, Y., Wickham, M.E., Deng, W., Vogl, A.W. and Finlay, B.B. (2006). Attaching and effacing pathogen-induced tight junction disruption in vivo. *Cell Microbiol* **8,** 634-645.

Haglund, C.M., Choe, J.E., Skau, C.T., Kovar, D.R. and Welch, M.D. (2010). *Rickettsia* Sca2 is a bacterial formin-like mediator of actin-based motility. *Nat Cell Biol* **12,** 1057-1063.

Hall, A. (1998). Rho GTPases and the actin cytoskeleton. *Science* **279,** 509-514.

Hamaguchi, M., Hamada, D., Suzuki, K.N., Sakata, I. and Yanagihara, I. (2008). Molecular basis of actin reorganization promoted by binding of enterohaemorrhagic *Escherichia coli* EspB to alpha-catenin. *FEBS J* **275,** 6260-6267.

Hardt, W.D., Chen, L.M., Schuebel, K.E., Bustelo, X.R. and Galan, J.E. (1998). S. typhimurium encodes an activator of Rho GTPases that induces membrane ruffling and nuclear responses in host cells. *Cell* **93,** 815-826.

Hardwidge, P.R., Deng, W., Vallance, B.A., Rodriguez-Escudero, I., Cid, V.J., Molina, M. and Finlay, B.B. (2005). Modulation of host cytoskeleton function by the enteropathogenic *Escherichia coli* and *Citrobacter rodentium* effector protein EspG. *Infect Immun* **73,** 2586-2594.

Harlander, R.S., Way, M., Ren, Q., Howe, D., Grieshaber, S.S. and Heinzen, R.A. (2003). Effects of ectopically expressed neuronal Wiskott-Aldrich syndrome protein domains on *Rickettsia rickettsii* actin-based motility. *Infect Immun* **71,** 1551-1556.

Hartland, E.L., Batchelor, M., Delahay, R.M., Hale, C., Matthews, S., Dougan, G*., et al.* (1999). Binding of intimin from enteropathogenic *Escherichia coli* to Tir and to host cells. *Mol Microbiol* **32,** 151-158.

Hartwig, J.H., Bokoch, G.M., Carpenter, C.L., Janmey, P.A., Taylor, L.A., Toker, A. and Stossel, T.P. (1995). Thrombin receptor ligation and activated Rac uncap actin filament barbed ends through phosphoinositide synthesis in permeabilized human platelets. *Cell* **82,** 643-653.

Hashim, S., Mukherjee, K., Raje, M., Basu, S.K. and Mukhopadhyay, A. (2000). Live Salmonella modulate expression of Rab proteins to persist in a specialized compartment and escape transport to lysosomes. *J Biol Chem* **275,** 16281-16288.

Heasman, S.J. and Ridley, A.J. (2008). Mammalian Rho GTPases: new insights into their functions from in vivo studies. *Nat Rev Mol Cell Biol* **9,** 690-701.

Hemrajani, C., Berger, C.N., Robinson, K.S., Marches, O., Mousnier, A. and Frankel, G. (2010). NleH effectors interact with Bax inhibitor-1 to block apoptosis during enteropathogenic Escherichia coli infection. *Proc Natl Acad Sci U S A* **107,** 3129-3134.

Hemrajani, C., Marches, O., Wiles, S., Girard, F., Dennis, A., Dziva, F*., et al.* (2008). Role of NleH, a type III secreted effector from attaching and effacing pathogens, in colonization of the bovine, ovine, and murine gut. *Infect Immun* **76,** 4804-4813.

Hertzog, M., van Heijenoort, C., Didry, D., Gaudier, M., Coutant, J., Gigant, B*., et al.* (2004). The beta-thymosin/WH2 domain; structural basis for the switch from inhibition to promotion of actin assembly. *Cell* **117,** 611-623.

Hippenstiel, S., Schmeck, B., N'Guessan, P.D., Seybold, J., Krull, M., Preissner, K*., et al.* (2002). Rho protein inactivation induced apoptosis of cultured human endothelial cells. *Am J Physiol Lung Cell Mol Physiol* **283,** L830-838.

Hirao, M., Sato, N., Kondo, T., Yonemura, S., Monden, M., Sasaki, T*., et al.* (1996). Regulation mechanism of ERM (ezrin/radixin/moesin) protein/plasma membrane association: possible involvement of phosphatidylinositol turnover and Rho-dependent signaling pathway. *J Cell Biol* **135,** 37-51.

Ho, H.Y., Rohatgi, R., Lebensohn, A.M., Le, M., Li, J., Gygi, S.P. and Kirschner, M.W. (2004). Toca-1 mediates Cdc42-dependent actin nucleation by activating the N-WASP-WIP complex. *Cell* **118,** 203-216.

Ho, H.Y., Rohatgi, R., Ma, L. and Kirschner, M.W. (2001). CR16 forms a complex with N-WASP in brain and is a novel member of a conserved proline-rich actin-binding protein family. *Proc Natl Acad Sci U S A* **98,** 11306-11311.

Hodges, K., Alto, N.M., Ramaswamy, K., Dudeja, P.K. and Hecht, G. (2008). The enteropathogenic *Escherichia coli* effector protein EspF decreases sodium hydrogen exchanger 3 activity. *Cell Microbiol* **10,** 1735-1745.

Hoffman, G.R., Nassar, N. and Cerione, R.A. (2000). Structure of the Rho family GTP-binding protein Cdc42 in complex with the multifunctional regulator RhoGDI. *Cell* **100,** 345-356.

Holland, I.B., Schmitt, L. and Young, J. (2005). Type 1 protein secretion in bacteria, the ABC-transporter dependent pathway (review). *Mol Membr Biol* **22,** 29-39.

Hood, R.D., Singh, P., Hsu, F., Guvener, T., Carl, M.A., Trinidad, R.R.*, et al.* (2010). A type VI secretion system of *Pseudomonas aeruginosa* targets a toxin to bacteria. *Cell Host Microbe* **7,** 25-37.

Hsu, H., Xiong, J. and Goeddel, D.V. (1995). The TNF receptor 1-associated protein TRADD signals cell death and NF-kappa B activation. *Cell* **81,** 495-504.

Huang, Z., Sutton, S.E., Wallenfang, A.J., Orchard, R.C., Wu, X., Feng, Y.*, et al.* (2009). Structural insights into host GTPase isoform selection by a family of bacterial GEF mimics. *Nat Struct Mol Biol* **16,** 853-860.

Hussain, N.K., Jenna, S., Glogauer, M., Quinn, C.C., Wasiak, S., Guipponi, M.*, et al.* (2001). Endocytic protein intersectin-l regulates actin assembly via Cdc42 and N-WASP. *Nat Cell Biol* **3,** 927-932.

Iguchi, A., Thomson, N.R., Ogura, Y., Saunders, D., Ooka, T., Henderson, I.R.*, et al.* (2009). Complete genome sequence and comparative genome analysis of enteropathogenic *Escherichia coli* O127:H6 strain E2348/69. *J Bacteriol* **191,** 347-354.

Iizumi, Y., Sagara, H., Kabe, Y., Azuma, M., Kume, K., Ogawa, M.*, et al.* (2007). The enteropathogenic *E. coli* effector EspB facilitates microvillus effacing and antiphagocytosis by inhibiting myosin function. *Cell Host Microbe* **2,** 383-392.

Ilic, D., Furuta, Y., Kanazawa, S., Takeda, N., Sobue, K., Nakatsuji, N.*, et al.* (1995). Reduced cell motility and enhanced focal adhesion contact formation in cells from FAK-deficient mice. *Nature* **377,** 539-544.

Innocenti, M., Zucconi, A., Disanza, A., Frittoli, E., Areces, L.B., Steffen, A.*, et al.* (2004). Abi1 is essential for the formation and activation of a WAVE2 signalling complex. *Nat Cell Biol* **6,** 319-327.

Jaffe, A.B. and Hall, A. (2005). Rho GTPases: biochemistry and biology. *Annu Rev Cell Dev Biol* **21,** 247-269.

Jewett, T.J., Fischer, E.R., Mead, D.J. and Hackstadt, T. (2006). Chlamydial TARP is a bacterial nucleator of actin. *Proc Natl Acad Sci U S A* **103,** 15599-15604.

Joza, N., Susin, S.A., Daugas, E., Stanford, W.L., Cho, S.K., Li, C.Y.*, et al.* (2001). Essential role of the mitochondrial apoptosis-inducing factor in programmed cell death. *Nature* **410,** 549-554.

Jubelin, G., Taieb, F., Duda, D.M., Hsu, Y., Samba-Louaka, A., Nobe, R.*, et al.* (2010). Pathogenic bacteria target NEDD8-conjugated cullins to hijack host-cell signaling pathways. *PLoS Pathog* **6**.

Just, I., Selzer, J., Wilm, M., von Eichel-Streiber, C., Mann, M. and Aktories, K. (1995). Glucosylation of Rho proteins by *Clostridium difficile* toxin B. *Nature* **375,** 500-503.

Kaper, J.B. (1996). Defining EPEC. *Rev Microbiol* **Sao Paulo,** 130-133.

Kaper, J.B., Nataro, J.P. and Mobley, H.L. (2004). Pathogenic *Escherichia coli*. *Nat Rev Microbiol* **2,** 123-140.

Karch, H., Tarr, P.I. and Bielaszewska, M. (2005). Enterohaemorrhagic *Escherichia coli* in human medicine. *Int J Med Microbiol* **295,** 405-418.

Karin, M. and Lin, A. (2002). NF-kappaB at the crossroads of life and death. *Nat Immunol* **3,** 221-227.

Katoh, K., Kano, Y., Amano, M., Onishi, H., Kaibuchi, K. and Fujiwara, K. (2001). Rho-kinase--mediated contraction of isolated stress fibers. *J Cell Biol* **153,** 569-584.

Keep, N.H., Barnes, M., Barsukov, I., Badii, R., Lian, L.Y., Segal, A.W.*, et al.* (1997). A modulator of rho family G proteins, rhoGDI, binds these G proteins via an immunoglobulin-like domain and a flexible N-terminal arm. *Structure* **5,** 623-633.

Kenny, B. (1999). Phosphorylation of tyrosine 474 of the enteropathogenic *Escherichia coli* (EPEC) Tir receptor molecule is essential for actin nucleating activity and is preceded by additional host modifications. *Mol Microbiol* **31,** 1229-1241.

Kenny, B., DeVinney, R., Stein, M., Reinscheid, D.J., Frey, E.A. and Finlay, B.B. (1997). Enteropathogenic *E. coli* (EPEC) transfers its receptor for intimate adherence into mammalian cells. *Cell* **91,** 511-520.

Kenny, B., Ellis, S., Leard, A.D., Warawa, J., Mellor, H. and Jepson, M.A. (2002). Co-ordinate regulation of distinct host cell signalling pathways by multifunctional enteropathogenic *Escherichia coli* effector molecules. *Mol Microbiol* **44,** 1095-1107.

Kenny, B. and Jepson, M. (2000). Targeting of an enteropathogenic *Escherichia coli* (EPEC) effector protein to host mitochondria. *Cell Microbiol* **2,** 579-590.

Kerr, J.F., Wyllie, A.H. and Currie, A.R. (1972). Apoptosis: a basic biological phenomenon with wide-ranging implications in tissue kinetics. *B J Canc*er **26,** 239-257.

Kim, A.S., Kakalis, L.T., Abdul-Manan, N., Liu, G.A. and Rosen, M.K. (2000). Autoinhibition and activation mechanisms of the Wiskott-Aldrich syndrome protein. *Nature* **404,** 151-158.

Kim, J., Thanabalasuriar, A., Chaworth-Musters, T., Fromme, J.C., Frey, E.A., Lario, P.I.*, et al.* (2007). The bacterial virulence factor NleA inhibits cellular protein secretion by disrupting mammalian COPII function. *Cell Host Microbe* **2,** 160-171.

Kim, M., Ogawa, M., Fujita, Y., Yoshikawa, Y., Nagai, T., Koyama, T.*, et al.* (2009). Bacteria hijack integrin-linked kinase to stabilize focal adhesions and block cell detachment. *Nature* **459,** 578-582.

Kimura, K., Ito, M., Amano, M., Chihara, K., Fukata, Y., Nakafuku, M.*, et al.* (1996). Regulation of myosin phosphatase by Rho and Rho-associated kinase (Rho-kinase). *Science* **273,** 245-248.

Kischkel, F.C., Hellbardt, S., Behrmann, I., Germer, M., Pawlita, M., Krammer, P.H. and Peter, M.E. (1995). Cytotoxicity-dependent APO-1 (Fas/CD95)-associated proteins form a death-inducing signaling complex (DISC) with the receptor. *EMBO J* **14,** 5579-5588.

Klink, B.U., Barden, S., Heidler, T.V., Borchers, C., Ladwein, M., Stradal, T.E.*, et al.* (2010). Structure of *Shigella* IpgB2 in complex with human RhoA: implications for the mechanism of bacterial guanine nucleotide exchange factor mimicry. *J Biol Chem* **285,** 17197-17208.

Knappstein, S., Ide, T., Schmidt, M.A. and Heusipp, G. (2004). Alpha 1-antitrypsin binds to and interferes with functionality of EspB from atypical and typical enteropathogenic *Escherichia coli* strains. *Infect Immun* **72,** 4344-4350.

Knutton, S., Lloyd, D.R. and McNeish, A.S. (1987). Adhesion of enteropathogenic *Escherichia coli* to human intestinal enterocytes and cultured human intestinal mucosa. *Infect Immun* **55,** 69-77.

Kodama, T., Akeda, Y., Kono, G., Takahashi, A., Imura, K., Iida, T. and Honda, T. (2002). The EspB protein of enterohaemorrhagic *Escherichia coli* interacts directly with alpha-catenin. *Cell Microbiol* **4,** 213-222.

Kook, S., Shim, S.R., Choi, S.J., Ahnn, J., Kim, J.I., Eom, S.H., *et al.* (2000). Caspase-mediated cleavage of p130cas in etoposide-induced apoptotic Rat-1 cells. *Mol Biol Cell* **11,** 929-939.

Kornberg, L., Earp, H.S., Parsons, J.T., Schaller, M. and Juliano, R.L. (1992). Cell adhesion or integrin clustering increases phosphorylation of a focal adhesion-associated tyrosine kinase. *J Biol Chem* **267,** 23439-23442.

Kornberg, L.J., Earp, H.S., Turner, C.E., Prockop, C. and Juliano, R.L. (1991). Signal transduction by integrins: increased protein tyrosine phosphorylation caused by clustering of beta 1 integrins. *Proc Natl Acad Sci U S A* **88,** 8392-8396.

Koronakis, V., Eswaran, J. and Hughes, C. (2004). Structure and function of TolC: the bacterial exit duct for proteins and drugs. *Annu Rev Biochem* **73,** 467-489.

Kresse, A.U., Rohde, M. and Guzman, C.A. (1999). The EspD protein of enterohemorrhagic *Escherichia coli* is required for the formation of bacterial surface appendages and is incorporated in the cytoplasmic membranes of target cells. *Infect Immun* **67,** 4834-4842.

Kubori, T. and Galan, J.E. (2003). Temporal regulation of salmonella virulence effector function by proteasome-dependent protein degradation. *Cell* **115,** 333-342.

Kurushima, J., Nagai, T., Nagamatsu, K. and Abe, A. (2010). EspJ effector in enterohemorrhagic *E. coli* translocates into host mitochondria via an atypical mitochondrial targeting signal. *Microbiol Immunol* **54,** 371-379.

Kuwana, T., Bouchier-Hayes, L., Chipuk, J.E., Bonzon, C., Sullivan, B.A., Green, D.R. and Newmeyer, D.D. (2005). BH3 domains of BH3-only proteins differentially regulate Bax-mediated mitochondrial membrane permeabilization both directly and indirectly. *Mol Cell* **17,** 525-535.

Lambrechts, A., Gevaert, K., Cossart, P., Vandekerckhove, J. and Van Troys, M. (2008). Listeria comet tails: the actin-based motility machinery at work. *Trends Cell Biol* **18,** 220-227.

Lang, A.E., Schmidt, G., Schlosser, A., Hey, T.D., Larrinua, I.M., Sheets, J.J., *et al.* (2010). Photorhabdus luminescens toxins ADP-ribosylate actin and RhoA to force actin clustering. *Science* **327,** 1139-1142.

Lazarides, E. and Burridge, K. (1975). Alpha-actinin: immunofluorescent localization of a muscle structural protein in nonmuscle cells. *Cell* **6,** 289-298.

LeClaire, L.L., 3rd, Baumgartner, M., Iwasa, J.H., Mullins, R.D. and Barber, D.L. (2008). Phosphorylation of the Arp2/3 complex is necessary to nucleate actin filaments. *J Cell Biol* **182,** 647-654.

Lee, G.H., Ahn, T., Kim, D.S., Park, S.J., Lee, Y.C., Yoo, W.H., *et al.* (2010). Bax inhibitor 1 increases cell adhesion through actin polymerization: involvement of calcium and actin binding. *Mol Cell Biol* **30,** 1800-1813.

Lee, S.F., Kelly, M., McAlister, A., Luck, S.N., Garcia, E.L., Hall, R.A., *et al.* (2008). A C-terminal class I PDZ binding motif of EspI/NleA modulates the virulence of attaching and effacing *Escherichia coli* and *Citrobacter rodentium*. *Cell Microbiol* **10,** 499-513.

Leung, T., Manser, E., Tan, L. and Lim, L. (1995). A novel serine/threonine kinase binding the Ras-related RhoA GTPase which translocates the kinase to peripheral membranes. *J Biol Chem* **270,** 29051-29054.

Leung, Y., Ally, S. and Goldberg, M.B. (2008). Bacterial actin assembly requires toca-1 to relieve N-wasp autoinhibition. *Cell Host Microbe* **3,** 39-47.

Levine, M.M., Berquist, E.J., Nalin, D.R., Waterman, D.H., Hornick, R.B., Young, C.R., *et al.* (1978). *Escherichia coli* that cause diarrhoea but do not produce heat-labile or heat-stable enterotoxins and are non-invasive. *Lancet* **i,** 119-122.

Levkau, B., Herren, B., Koyama, H., Ross, R. and Raines, E.W. (1998). Caspase-mediated cleavage of focal adhesion kinase pp125FAK and disassembly of focal adhesions in human endothelial cell apoptosis. *J Exp Med* **187,** 579-586.

Li, F. and Higgs, H.N. (2005). Dissecting requirements for auto-inhibition of actin nucleation by the formin, mDia1. *J Biol Chem* **280,** 6986-6992.

Li, L.Y., Luo, X. and Wang, X. (2001). Endonuclease G is an apoptotic DNase when released from mitochondria. *Nature* **412,** 95-99.

Lim, Y., Lim, S.T., Tomar, A., Gardel, M., Bernard-Trifilo, J.A., Chen, X.L., *et al.* (2008). PyK2 and FAK connections to p190Rho guanine nucleotide exchange factor regulate RhoA activity, focal adhesion formation, and cell motility. *J Cell Biol* **180,** 187-203.

Liu, X., Wang, H., Eberstadt, M., Schnuchel, A., Olejniczak, E.T., Meadows, R.P., *et al.* (1998). NMR structure and mutagenesis of the N-terminal Dbl homology domain of the nucleotide exchange factor Trio. *Cell* **95,** 269-277.

Liverman, A.D., Cheng, H.C., Trosky, J.E., Leung, D.W., Yarbrough, M.L., Burdette, D.L., *et al.* (2007). Arp2/3-independent assembly of actin by *Vibrio* type III effector VopL. *Proc Natl Acad Sci U S A* **104,** 17117-17122.

Lommel, S., Benesch, S., Rohde, M., Wehland, J. and Rottner, K. (2004). Enterohaemorrhagic and enteropathogenic *Escherichia coli* use different mechanisms for actin pedestal formation that converge on N-WASP. *Cell Microbiol* **6,** 243-254.

Lommel, S., Benesch, S., Rottner, K., Franz, T., Wehland, J. and Kuhn, R. (2001). Actin pedestal formation by enteropathogenic *Escherichia coli* and intracellular motility of *Shigella flexneri* are abolished in N-WASP-defective cells. *EMBO Rep* **2,** 850-857.

Luo, X., Budihardjo, I., Zou, H., Slaughter, C. and Wang, X. (1998). Bid, a Bcl2 interacting protein, mediates cytochrome c release from mitochondria in response to activation of cell surface death receptors. *Cell* **94,** 481-490.

Luo, Y., Frey, E.A., Pfuetzner, R.A., Creagh, A.L., Knoechel, D.G., Haynes, C.A., *et al.* (2000). Crystal structure of enteropathogenic *Escherichia coli* intimin-receptor complex. *Nature* **405,** 1073-1077.

Ma, C., Wickham, M.E., Guttman, J.A., Deng, W., Walker, J., Madsen, K.L., *et al.* (2006). *Citrobacter rodentium* infection causes both mitochondrial dysfunction and intestinal epithelial barrier disruption in vivo: role of mitochondrial associated protein (Map). *Cell Microbiol* **8,** 1669-1686.

Machesky, L.M., Atkinson, S.J., Ampe, C., Vandekerckhove, J. and Pollard, T.D. (1994). Purification of a cortical complex containing two unconventional actins from Acanthamoeba by affinity chromatography on profilin-agarose. *J Cell Biol* **127,** 107-115.

Marches, O., Batchelor, M., Shaw, R.K., Patel, A., Cummings, N., Nagai, T.*, et al.* (2006). EspF of enteropathogenic *Escherichia coli* binds sorting nexin 9. *J Bacteriol* **188,** 3110-3115.

Marches, O., Covarelli, V., Dahan, S., Cougoule, C., Bhatta, P., Frankel, G. and Caron, E. (2008). EspJ of enteropathogenic and enterohaemorrhagic *Escherichia coli* inhibits opsono-phagocytosis. *Cell Microbiol* **10,** 1104-1115.

Marches, O., Ledger, T.N., Boury, M., Ohara, M., Tu, X., Goffaux, F.*, et al.* (2003). Enteropathogenic and enterohaemorrhagic *Escherichia coli* deliver a novel effector called Cif, which blocks cell cycle G2/M transition. *Mol Microbiol* **50,** 1553-1567.

Marches, O., Wiles, S., Dziva, F., La Ragione, R.M., Schuller, S., Best, A.*, et al.* (2005). Characterization of two non-locus of enterocyte effacement-encoded type III-translocated effectors, NleC and NleD, in attaching and effacing pathogens. *Infect Immun* **73,** 8411-8417.

Martinez, E., Schroeder, G.N., Berger, C.N., Lee, S.F., Robinson, K.S., Badea, L.*, et al.* (2010). Binding to Na(+) /H(+) exchanger regulatory factor 2 (NHERF2) affects trafficking and function of the enteropathogenic *Escherichia coli* type III secretion system effectors Map, EspI and NleH. *Cell Microbiol* **12,** 1718-1731.

Martinez-Quiles, N., Rohatgi, R., Anton, I.M., Medina, M., Saville, S.P., Miki, H.*, et al.* (2001). WIP regulates N-WASP-mediated actin polymerization and filopodium formation. *Nat Cell Biol* **3,** 484-491.

Matsuzawa, T., Kuwae, A., Yoshida, S., Sasakawa, C. and Abe, A. (2004). Enteropathogenic *Escherichia coli* activates the RhoA signaling pathway via the stimulation of GEF-H1. *EMBO J* **23,** 3570-3582.

McDaniel, T.K., Jarvis, K.G., Donnenberg, M.S. and Kaper, J.B. (1995). A genetic locus of enterocyte effacement conserved among diverse enterobacterial pathogens. *Proc Natl Acad Sci USA* **92,** 1664-1668.

McNamara, B.P., Koutsouris, A., O'Connell, C.B., Nougayrede, J.P., Donnenberg, M.S. and Hecht, G. (2001). Translocated EspF protein from enteropathogenic *Escherichia coli* disrupts host intestinal barrier function. *J Clin Invest* **107,** 621-629.

Meller, N., Merlot, S. and Guda, C. (2005). CZH proteins: a new family of Rho-GEFs. *J Cell Sci* **118,** 4937-4946.

Mitra, S.K., Hanson, D.A. and Schlaepfer, D.D. (2005). Focal adhesion kinase: in command and control of cell motility. *Nat Rev Mol Cell Biol* **6,** 56-68.

Miyahara, A., Nakanishi, N., Ooka, T., Hayashi, T., Sugimoto, N. and Tobe, T. (2009). Enterohemorrhagic *Escherichia coli* Effector EspL2 Induces Actin Microfilament Aggregation through Annexin 2 Activation. *Cell Microbiol* **11,** 337-350.

Moreau, V., Frischknecht, F., Reckmann, I., Vincentelli, R., Rabut, G., Stewart, D. and Way, M. (2000). A complex of N-WASP and WIP integrates signalling cascades that lead to actin polymerization. *Nat Cell Biol* **2,** 441-448.

Morikawa, H., Kim, M., Mimuro, H., Punginelli, C., Koyama, T., Nagai, S.*, et al.* (2010). The bacterial effector Cif interferes with SCF ubiquitin ligase function by inhibiting deneddylation of Cullin1. *Biochem Biophys Res Commun* **401,** 268-274.

Morita-Ishihara, T., Terajima, J., Watanabe, H. and Izumiya, H. (2009). Interaction between enterohemorrhagic *Escherichia coli* O157:H7 EspFu and IRSp53 induces dynamic membrane remodeling in epithelial cells. *Jpn J Infect Dis* **62,** 351-355.

Moss, D.K., Betin, V.M., Malesinski, S.D. and Lane, J.D. (2006). A novel role for microtubules in apoptotic chromatin dynamics and cellular fragmentation. *J Cell Sci* **119,** 2362-2374.

Mougous, J.D., Cuff, M.E., Raunser, S., Shen, A., Zhou, M., Gifford, C.A*., et al.* (2006). A virulence locus of *Pseudomonas aeruginosa* encodes a protein secretion apparatus. *Science* **312,** 1526-1530.

Mounier, J., Laurent, V., Hall, A., Fort, P., Carlier, M.F., Sansonetti, P.J. and Egile, C. (1999). Rho family GTPases control entry of *Shigella flexneri* into epithelial cells but not intracellular motility. *J Cell Sci* **112 (13),** 2069-2080.

Muehlen, S., Ruchaud-Sparagano, M.H. and Kenny, B. (2010). Proteasome-independent degradation of canonical NF{kappa}B complex components by the NleC protein of pathogenic *E.coli. J Biol Chem* **In press**.

Mukherjee, K., Parashuraman, S., Raje, M. and Mukhopadhyay, A. (2001). SopE acts as an Rab5-specific nucleotide exchange factor and recruits non-prenylated Rab5 on Salmonella-containing phagosomes to promote fusion with early endosomes. *J Biol Chem* **276,** 23607-23615.

Muller, M. (2005). Twin-arginine-specific protein export in *Escherichia coli. Res Microbiol* **156,** 131-136.

Mundy, R., MacDonald, T.T., Dougan, G., Frankel, G. and Wiles, S. (2005). *Citrobacter rodentium* of mice and man. *Cell Microbiol* **7,** 1697-1706.

Mundy, R., Petrovska, L., Smollett, K., Simpson, N., Wilson, R.K., Yu, J*., et al.* (2004). Identification of a novel Citrobacter rodentium type III secreted protein, EspI, and roles of this and other secreted proteins in infection. *Infect Immun* **72,** 2288-2302.

Muza-Moons, M.M., Schneeberger, E.E. and Hecht, G.A. (2004). Enteropathogenic *Escherichia coli* infection leads to appearance of aberrant tight junctions strands in the lateral membrane of intestinal epithelial cells. *Cell Microbiol* **6,** 783-793.

Nadler, C., Baruch, K., Kobi, S., Mills, E., Haviv, G., Farago, M*., et al.* (2010). The Type III Secretion Effector NleE Inhibits NF-kappaB Activation. *PLoS Pathog* **6,** e1000743.

Nataro, J.P., Deng, Y., Maneval, D.R., German, A.L., Martin, W.C. and Levine, M.M. (1992). Aggregative adherence fimbriae I of enteroaggregative *Escherichia coli* mediate adherence to HEp-2 cells and hemagglutination of human erythrocytes. *Infect Immun* **60,** 2297-2304.

Nataro, J.P. and Kaper, J.B. (1998). Diarrheagenic *Escherichia coli*. *Clin Microbiol Rev* **11,** 142-201.

Naylor, S.W., Low, J.C., Besser, T.E., Mahajan, A., Gunn, G.J., Pearce, M.C*., et al.* (2003). Lymphoid follicle-dense mucosa at the terminal rectum is the principal site of colonization of enterohemorrhagic *Escherichia coli* O157:H7 in the bovine host. *Infect Immun* **71,** 1505-1512.

Newton, H.J., Pearson, J.S., Badea, L., Kelly, M., Lucas, M., Holloway, G*., et al.* (2010). The type III effectors NleE and NleB from enteropathogenic *E. coli* and OspZ from *Shigella* block nuclear translocation of NF-kappaB p65. *PLoS Pathog* **6,** e1000898.

Nieto-Pelegrin, E. and Martinez-Quiles, N. (2009). Distinct phosphorylation requirements regulate cortactin activation by TirEPEC and its binding to N-WASP. *Cell Commun Signal* **7,** 11.

Nobes, C.D. and Hall, A. (1995). Rho, rac, and cdc42 GTPases regulate the assembly of multimolecular focal complexes associated with actin stress fibers, lamellipodia, and filopodia. *Cell* **81,** 53-62.

Nobes, C.D. and Hall, A. (1999). Rho GTPases control polarity, protrusion, and adhesion during cell movement. *J Cell Biol* **144,** 1235-1244.

Nolen, B.J., Littlefield, R.S. and Pollard, T.D. (2004). Crystal structures of actin-related protein 2/3 complex with bound ATP or ADP. *Proc Natl Acad Sci U S A* **101,** 15627-15632.

Noriega, F.R., Liao, F.M., Formal, S.B., Fasano, A. and Levine, M.M. (1995). Prevalence of *Shigella* enterotoxin 1 among Shigella clinical isolates of diverse serotypes. *J Infect Dis* **172,** 1408-1410.

Nougayrede, J.P. and Donnenberg, M.S. (2004). Enteropathogenic *Escherichia coli* EspF is targeted to mitochondria and is required to initiate the mitochondrial death pathway. *Cell Microbiol* **6,** 1097-1111.

Nougayrede, J.P., Foster, G.H. and Donnenberg, M.S. (2007). Enteropathogenic *Escherichia coli* effector EspF interacts with host protein Abcf2. *Cell Microbiol* **9,** 680-693.

O'Connell, C.B., Creasey, E.A., Knutton, S., Elliott, S., Crowther, L.J., Luo, W.*, et al.* (2004). SepL, a protein required for enteropathogenic *Escherichia coli* type III translocation, interacts with secretion component SepD. *Mol Microbiol* **52,** 1613-1625.

Ogura, Y., Ooka, T., Whale, A., Garmendia, J., Beutin, L., Tennant, S.*, et al.* (2007). TccP2 of O157:H7 and non-O157 enterohemorrhagic *Escherichia coli* (EHEC): challenging the dogma of EHEC-induced actin polymerization. *Infect Immun* **75,** 604-612.

Ohashi, K., Nagata, K., Maekawa, M., Ishizaki, T., Narumiya, S. and Mizuno, K. (2000). Rho-associated kinase ROCK activates LIM-kinase 1 by phosphorylation at threonine 508 within the activation loop. *J Biol Chem* **275,** 3577-3582.

Otomo, T., Tomchick, D.R., Otomo, C., Panchal, S.C., Machius, M. and Rosen, M.K. (2005). Structural basis of actin filament nucleation and processive capping by a formin homology 2 domain. *Nature* **433,** 488-494.

Owen, K.A., Pixley, F.J., Thomas, K.S., Vicente-Manzanares, M., Ray, B.J., Horwitz, A.F.*, et al.* (2007). Regulation of lamellipodial persistence, adhesion turnover, and motility in macrophages by focal adhesion kinase. *J Cell Biol* **179,** 1275-1287.

Papanikou, E., Karamanou, S. and Economou, A. (2007). Bacterial protein secretion through the translocase nanomachine. *Nat Rev Microbiol* **5,** 839-851.

Papatheodorou, P., Domanska, G., Oxle, M., Mathieu, J., Selchow, O., Kenny, B. and Rassow, J. (2006). The enteropathogenic *Escherichia coli* (EPEC) Map effector is imported into the mitochondrial matrix by the TOM/Hsp70 system and alters organelle morphology. *Cell Microbiol* **8,** 677-689.

Papayannopoulos, V., Co, C., Prehoda, K.E., Snapper, S., Taunton, J. and Lim, W.A. (2005). A polybasic motif allows N-WASP to act as a sensor of PIP(2) density. *Mol Cell* **17,** 181-191.

Patel, A., Cummings, N., Batchelor, M., Hill, P.J., Dubois, T., Mellits, K.H.*, et al.* (2006). Host protein interactions with enteropathogenic Escherichia coli (EPEC): 14-3-3tau binds Tir and has a role in EPEC-induced actin polymerization. *Cell Microbiol* **8,** 55-71.

Pearson, J.S., Riedmaier, P., Marches, O., Frankel, G. and Hartland, E.L. (2011). A type III effector protease NleC from enteropathogenic Escherichia coli targets NF- κ B for degradation *Mol Microbiol* **doi:10.1111/j.1365-2958.2011.07568.x**.

Peck, J., Douglas, G.t., Wu, C.H. and Burbelo, P.D. (2002). Human RhoGAP domain-containing proteins: structure, function and evolutionary relationships. *FEBS letters* **528,** 27-34.

Peiffer, I., Bernet-Camard, M.F., Rousset, M. and Servin, A.L. (2001). Impairments in enzyme activity and biosynthesis of brush border-associated hydrolases in human intestinal Caco-2/TC7 cells infected by members of the Afa/Dr family of diffusely adhering *Escherichia coli*. *Cell Microbiol* **3,** 341-357.

Peiffer, I., Servin, A.L. and Bernet-Camard, M.F. (1998). Piracy of decay-accelerating factor (CD55) signal transduction by the diffusely adhering strain *Escherichia coli* C1845 promotes cytoskeletal F-actin rearrangements in cultured human intestinal INT407 cells. *Infect Immun* **66,** 4036-4042.

Pellegrin, S. and Mellor, H. (2007). Actin stress fibres. *J Cell Sci* **120,** 3491-3499.

Peralta-Ramirez, J., Hernandez, J.M., Manning-Cela, R., Luna-Munoz, J., Garcia-Tovar, C., Nougayrede, J.P*., et al.* (2008). EspF Interacts with nucleation-promoting factors to recruit junctional proteins into pedestals for pedestal maturation and disruption of paracellular permeability. *Infect Immun* **76,** 3854-3868.

Perna, N.T., Plunkett, G., 3rd, Burland, V., Mau, B., Glasner, J.D., Rose, D.J*., et al.* (2001). Genome sequence of enterohaemorrhagic *Escherichia coli* O157:H7. *Nature* **409,** 529-533.

Peterson, F.C., Deng, Q., Zettl, M., Prehoda, K.E., Lim, W.A., Way, M. and Volkman, B.F. (2007). Multiple WASP-interacting protein recognition motifs are required for a functional interaction with N-WASP. *J Biol Chem* **282,** 8446-8453.

Petty, N.K., Bulgin, R., Crepin, V.F., Cerdeno-Tarraga, A.M., Schroeder, G.N., Quail, M.A*., et al.* (2010). The *Citrobacter rodentium* genome sequence reveals convergent evolution with human pathogenic *Escherichia coli*. *J Bacteriol* **192,** 525-538.

Phillips, A.D. and Frankel, G. (2000a). Intimin-mediated tissue specificity in enteropathogenic Escherichia coli interaction with human intestinal organ cultures. *J Infect Dis* **181,** 1496-1500.

Phillips, A.D., Navabpour, S., Hicks, S., Dougan, G., Wallis, T. and Frankel, G. (2000b). Enterohaemorrhagic *Escherichia coli* O157:H7 target Peyer's patches in humans and cause attaching/effacing lesions in both human and bovine intestine. *Gut* **47,** 377-381.

Phillips, N., Hayward, R.D. and Koronakis, V. (2004). Phosphorylation of the enteropathogenic E. coli receptor by the Src-family kinase c-Fyn triggers actin pedestal formation. *Nat Cell Biol* **6,** 618-625.

Pollard, T.D. (1986). Rate constants for the reactions of ATP- and ADP-actin with the ends of actin filaments. *J Cell Biol* **103,** 2747-2754.

Pollard, T.D. and Borisy, G.G. (2003). Cellular motility driven by assembly and disassembly of actin filaments. *Cell* **112,** 453-465.

Prehna, G., Ivanov, M.I., Bliska, J.B. and Stebbins, C.E. (2006). Yersinia virulence depends on mimicry of host Rho-family nucleotide dissociation inhibitors. *Cell* **126,** 869-880.

Price, L.S., Langeslag, M., ten Klooster, J.P., Hordijk, P.L., Jalink, K. and Collard, J.G. (2003). Calcium signaling regulates translocation and activation of Rac. *J Biol Chem* **278,** 39413-39421.

Pukatzki, S., Ma, A.T., Revel, A.T., Sturtevant, D. and Mekalanos, J.J. (2007). Type VI secretion system translocates a phage tail spike-like protein into target cells where it cross-links actin. *Proc Natl Acad Sci U S A* **104,** 15508-15513.

Qa'Dan, M., Ramsey, M., Daniel, J., Spyres, L.M., Safiejko-Mroczka, B., Ortiz-Leduc, W. and Ballard, J.D. (2002). Clostridium difficile toxin B activates dual caspase-dependent and caspase-independent apoptosis in intoxicated cells. *Cell Microbiol* **4,** 425-434.

Qualmann, B. and Kessels, M.M. (2009). New players in actin polymerization--WH2-domain-containing actin nucleators. *Trends Cell Biol* **19,** 276-285.

Quinlan, M.E., Heuser, J.E., Kerkhoff, E. and Mullins, R.D. (2005). Drosophila Spire is an actin nucleation factor. *Nature* **433,** 382-388.

Quitard, S., Dean, P., Maresca, M. and Kenny, B. (2006). The enteropathogenic *Escherichia coli* EspF effector molecule inhibits PI-3 kinase-mediated uptake independently of mitochondrial targeting. *Cell Microbiol* **8,** 972-981.

Ramesh, N., Anton, I.M., Hartwig, J.H. and Geha, R.S. (1997). WIP, a protein associated with wiskott-aldrich syndrome protein, induces actin polymerization and redistribution in lymphoid cells. *Proc Natl Acad Sci U S A* **94,** 14671-14676.

Rao, L., Perez, D. and White, E. (1996). Lamin proteolysis facilitates nuclear events during apoptosis. *J Cell Biol* **135,** 1441-1455.

Rasko, D.A., Webster, D.R., Sahl, J.W., Bashir, A., Boisen, N., Scheutz, F.*, et al.* (2011). Origins of the E. coli strain causing an outbreak of hemolytic-uremic syndrome in Germany. *N Engl J Med* **365,** 709-717.

Raymond, B., Crepin, V.F., Collins, J.W. and Frankel, G. (2011). The WxxxE effector EspT triggers expression of immune mediators in anErk/JNK and NF-kappaB-dependent manner. *Cell Microbiol*

Ren, X.D., Kiosses, W.B., Sieg, D.J., Otey, C.A., Schlaepfer, D.D. and Schwartz, M.A. (2000). Focal adhesion kinase suppresses Rho activity to promote focal adhesion turnover. *J Cell Sci* **113 (20),** 3673-3678.

Ridley, A.J. (2006). Rho GTPases and actin dynamics in membrane protrusions and vesicle trafficking. *Trends Cell Biol* **16,** 522-529.

Riedl, S.J. and Shi, Y. (2004). Molecular mechanisms of caspase regulation during apoptosis. *Nat Rev Mol Cell Biol* **5,** 897-907.

Ritchie, J.M., Brady, M.J., Riley, K.N., Ho, T.D., Campellone, K.G., Herman, I.M.*, et al.* (2008). EspFU, a type III-translocated effector of actin assembly, fosters epithelial association and late-stage intestinal colonization by E. coli O157:H7. *Cell Microbiol* **10,** 836-847.

Ritchie, J.M. and Waldor, M.K. (2005). The locus of enterocyte effacement-encoded effector proteins all promote enterohemorrhagic *Escherichia coli* pathogenicity in infant rabbits. *Infect Immun* **73,** 1466-1474.

Rittinger, K., Walker, P.A., Eccleston, J.F., Nurmahomed, K., Owen, D., Laue, E.*, et al.* (1997a). Crystal structure of a small G protein in complex with the GTPase-activating protein rhoGAP. *Nature* **388,** 693-697.

Rittinger, K., Walker, P.A., Eccleston, J.F., Smerdon, S.J. and Gamblin, S.J. (1997b). Structure at 1.65 A of RhoA and its GTPase-activating protein in complex with a transition-state analogue. *Nature* **389,** 758-762.

Robinson, K.S., Mousnier, A., Hemrajani, C., Fairweather, N., Berger, C.N. and Frankel, G. (2010). The enteropathogenic *Escherichia coli* effector NleH inhibits apoptosis induced by Clostridium difficile toxin B. *Microbiology* **156,** 1815-1823.

Robinson, R.C., Turbedsky, K., Kaiser, D.A., Marchand, J.B., Higgs, H.N., Choe, S. and Pollard, T.D. (2001). Crystal structure of Arp2/3 complex. *Science* **294,** 1679-1684.

Rodriguez-Escudero, I., Hardwidge, P.R., Nombela, C., Cid, V.J., Finlay, B.B. and Molina, M. (2005). Enteropathogenic *Escherichia coli* type III effectors alter cytoskeletal function and signalling in *Saccharomyces cerevisiae*. *Microbiology* **151,** 2933-2945.

Rohatgi, R., Ho, H.Y. and Kirschner, M.W. (2000). Mechanism of N-WASP activation by CDC42 and phosphatidylinositol 4, 5-bisphosphate. *J Cell Biol* **150,** 1299-1310.

Rohatgi, R., Nollau, P., Ho, H.Y., Kirschner, M.W. and Mayer, B.J. (2001). Nck and phosphatidylinositol 4,5-bisphosphate synergistically activate actin polymerization through the N-WASP-Arp2/3 pathway. *J Biol Chem* **276,** 26448-26452.

Romero, S., Le Clainche, C., Didry, D., Egile, C., Pantaloni, D. and Carlier, M.F. (2004). Formin is a processive motor that requires profilin to accelerate actin assembly and associated ATP hydrolysis. *Cell* **119,** 419-429.

Rosenshine, I., Ruschkowski, S., Stein, M., Reinscheid, D.J., Mills, S.D. and Finlay, B.B. (1996). A pathogenic bacterium triggers epithelials signals to form a functionnal bacterial receptor that mediates actin pseudopod formation. *EMBO J* **15,** 2613-2624.

Rossman, K.L., Der, C.J. and Sondek, J. (2005). GEF means go: turning on RHO GTPases with guanine nucleotide-exchange factors. *Nat Rev Mol Cell Biol* **6,** 167-180.

Rouiller, I., Xu, X.P., Amann, K.J., Egile, C., Nickell, S., Nicastro, D.*, et al.* (2008). The structural basis of actin filament branching by the Arp2/3 complex. *J Cell Biol* **180,** 887-895.

Royan, S.V., Jones, R.M., Koutsouris, A., Roxas, J.L., Falzari, K., Weflen, A.W.*, et al.* (2010). Enteropathogenic *E. coli* non-LEE encoded effectors NleH1 and NleH2 attenuate NF-kappaB activation. *Mol Microbiol* **78,** 1232-1245.

Rubin, E.J., Gill, D.M., Boquet, P. and Popoff, M.R. (1988). Functional modification of a 21-kilodalton G protein when ADP-ribosylated by exoenzyme C3 of Clostridium botulinum. *Mol Cell Biol* **8,** 418-426.

Rudel, T. and Bokoch, G.M. (1997). Membrane and morphological changes in apoptotic cells regulated by caspase-mediated activation of PAK2. *Science* **276,** 1571-1574.

Russell, A.B., Hood, R.D., Bui, N.K., LeRoux, M., Vollmer, W. and Mougous, J.D. (2011). Type VI secretion delivers bacteriolytic effectors to target cells. *Nature* **475,** 343-347.

Sakahira, H., Enari, M. and Nagata, S. (1998). Cleavage of CAD inhibitor in CAD activation and DNA degradation during apoptosis. *Nature* **391,** 96-99.

Sallee, N.A., Rivera, G.M., Dueber, J.E., Vasilescu, D., Mullins, R.D., Mayer, B.J. and Lim, W.A. (2008). The pathogen protein EspF(U) hijacks actin polymerization using mimicry and multivalency. *Nature* **454,** 1005-1008.

Samba-Louaka, A., Nougayrede, J.P., Watrin, C., Jubelin, G., Oswald, E. and Taieb, F. (2008). Bacterial cyclomodulin Cif blocks the host cell cycle by stabilizing the cyclin-dependent kinase inhibitors p21 and p27. *Cell Microbiol* **10,** 2496-2508.

Samba-Louaka, A., Nougayrede, J.P., Watrin, C., Oswald, E. and Taieb, F. (2009). The enteropathogenic *Escherichia coli* effector Cif induces delayed apoptosis in epithelial cells. *Infect Immun* **77,** 5471-5477.

Sason, H., Milgrom, M., Weiss, A.M., Melamed-Book, N., Balla, T., Grinstein, S.*, et al.* (2009). Enteropathogenic *Escherichia coli* subverts phosphatidylinositol 4,5-bisphosphate and phosphatidylinositol 3,4,5-trisphosphate upon epithelial cell infection. *Mol Biol Cell* **20,** 544-555.

Savarino, S.J., Fasano, A., Watson, J., Martin, B.M., Levine, M.M., Guandalini, S. and Guerry, P. (1993). Enteroaggregative *Escherichia coli* heat-stable enterotoxin 1 represents another subfamily of E. coli heat-stable toxin. *Proc Natl Acad Sci U S A* **90,** 3093-3097.

Scaffidi, C., Fulda, S., Srinivasan, A., Friesen, C., Li, F., Tomaselli, K.J.*, et al.* (1998). Two CD95 (APO-1/Fas) signaling pathways. *EMBO J* **17,** 1675-1687.

Scaplehorn, N., Holmstrom, A., Moreau, V., Frischknecht, F., Reckmann, I. and Way, M. (2002). Grb2 and Nck act cooperatively to promote actin-based motility of *Vaccinia* virus. *Curr Biol* **12,** 740-745.

Schaller, M.D., Hildebrand, J.D., Shannon, J.D., Fox, J.W., Vines, R.R. and Parsons, J.T. (1994). Autophosphorylation of the focal adhesion kinase, pp125FAK, directs SH2-dependent binding of pp60src. *Mol Cel Biol* **14,** 1680-1688.

Scheffzek, K., Ahmadian, M.R., Kabsch, W., Wiesmuller, L., Lautwein, A., Schmitz, F. and Wittinghofer, A. (1997). The Ras-RasGAP complex: structural basis for GTPase activation and its loss in oncogenic Ras mutants. *Science* **277,** 333-338.

Schirenbeck, A., Bretschneider, T., Arasada, R., Schleicher, M. and Faix, J. (2005). The Diaphanous-related formin dDia2 is required for the formation and maintenance of filopodia. *Nat Cell Biol* **7,** 619-625.

Schlosser-Silverman, E., Elgrably-Weiss, M., Rosenshine, I., Kohen, R. and Altuvia, S. (2000). Characterization of *Escherichia coli* DNA lesions generated within J774 macrophages. *J Bacteriol* **182,** 5225-5230.

Schmidt, G., Sehr, P., Wilm, M., Selzer, J., Mann, M. and Aktories, K. (1997). Gln 63 of Rho is deamidated by *Escherichia coli* cytotoxic necrotizing factor-1. *Nature* **387,** 725-729.

Schuller, S., Chong, Y., Lewin, J., Kenny, B., Frankel, G. and Phillips, A.D. (2007). Tir phosphorylation and Nck/N-WASP recruitment by enteropathogenic and enterohaemorrhagic *Escherichia coli* during ex vivo colonization of human intestinal mucosa is different to cell culture models. *Cell Microbiol* **9,** 1352-1364.

Schurmann, A., Mooney, A.F., Sanders, L.C., Sells, M.A., Wang, H.G., Reed, J.C. and Bokoch, G.M. (2000). p21-activated kinase 1 phosphorylates the death agonist bad and protects cells from apoptosis. *Mol Cell Biol* **20,** 453-461.

Sebbagh, M., Renvoize, C., Hamelin, J., Riche, N., Bertoglio, J. and Breard, J. (2001). Caspase-3-mediated cleavage of ROCK I induces MLC phosphorylation and apoptotic membrane blebbing. *Nat Cell Biol* **3,** 346-352.

Sekine, A., Fujiwara, M. and Narumiya, S. (1989). Asparagine residue in the rho gene product is the modification site for botulinum ADP-ribosyltransferase. *J Biol Chem* **264,** 8602-8605.

Sekirov, I., Russell, S.L., Antunes, L.C. and Finlay, B.B. (2010). Gut microbiota in health and disease. *Physiol Rev* **90,** 859-904.

Selyunin, A.S., Sutton, S.E., Weigele, B.A., Reddick, L.E., Orchard, R.C., Bresson, S.M*., et al.* (2011). The assembly of a GTPase-kinase signalling complex by a bacterial catalytic scaffold. *Nature* **469,** 107-111.

Serio, A.W., Jeng, R.L., Haglund, C.M., Reed, S.C. and Welch, M.D. (2010). Defining a core set of actin cytoskeletal proteins critical for actin-based motility of *Rickettsia*. *Cell Host Microbe* **7,** 388-398.

Shames, S.R., Deng, W., Guttman, J.A., de Hoog, C.L., Li, Y., Hardwidge, P.R*., et al.* (2010). The pathogenic *E. coli* type III effector EspZ interacts with host CD98 and facilitates host cell prosurvival signalling. *Cell Microbiol*.

Shao, F., Merritt, P.M., Bao, Z., Innes, R.W. and Dixon, J.E. (2002). A *Yersinia* effector and a Pseudomonas avirulence protein define a family of cysteine proteases functioning in bacterial pathogenesis. *Cell* **109,** 575-588.

Shao, F., Vacratsis, P.O., Bao, Z., Bowers, K.E., Fierke, C.A. and Dixon, J.E. (2003). Biochemical characterization of the *Yersinia* YopT protease: cleavage site and recognition elements in Rho GTPases. *Proc Natl Acad Sci U S A* **100,** 904-909.

Shaw, R.K., Cleary, J., Murphy, M.S., Frankel, G. and Knutton, S. (2005a). Interaction of enteropathogenic *Escherichia coli* with human intestinal mucosa: role of effector proteins in brush border remodeling and formation of attaching and effacing lesions. *Infect Immun* **73,** 1243-1251.

Shaw, R.K., Smollett, K., Cleary, J., Garmendia, J., Straatman-Iwanowska, A., Frankel, G. and Knutton, S. (2005b). Enteropathogenic *Escherichia coli* type III effectors EspG and EspG2 disrupt the microtubule network of intestinal epithelial cells. *Infect Immun* **73,** 4385-4390.

Sheikh, J., Czeczulin, J.R., Harrington, S., Hicks, S., Henderson, I.R., Le Bouguenec, C*., et al.* (2002). A novel dispersin protein in enteroaggregative *Escherichia coli*. *J Clin Invest* **110,** 1329-1337.

Simpson, N., Shaw, R., Crepin, V.F., Mundy, R., FitzGerald, A.J., Cummings, N.*, et al.* (2006). The enteropathogenic *Escherichia coli* type III secretion system effector Map binds EBP50/NHERF1: implication for cell signalling and diarrhoea. *Mol Microbiol* **60,** 349-363.

Sinclair, J.F. and O'Brien, A.D. (2004). Intimin types alpha, beta, and gamma bind to nucleolin with equivalent affinity but lower avidity than to the translocated intimin receptor. *J Biol Chem* **279,** 33751-33758.

Sitthidet, C., Stevens, J.M., Field, T.R., Layton, A.N., Korbsrisate, S. and Stevens, M.P. (2010). Actin-based motility of *Burkholderia thailandensis* requires a central acidic domain of BimA that recruits and activates the cellular Arp2/3 complex. *J Bacteriol* **192,** 5249-5252.

Snapper, S.B., Takeshima, F., Anton, I., Liu, C.H., Thomas, S.M., Nguyen, D.*, et al.* (2001). N-WASP deficiency reveals distinct pathways for cell surface projections and microbial actin-based motility. *Nat Cell Biol* **3,** 897-904.

Spangler, B.D. (1992). Structure and function of cholera toxin and the related *Escherichia coli* heat-labile enterotoxin. *Microbiol Rev* **56,** 622-647.

Stamm, L.M., Pak, M.A., Morisaki, J.H., Snapper, S.B., Rottner, K., Lommel, S. and Brown, E.J. (2005). Role of the WASP family proteins for *Mycobacterium marinum* actin tail formation. *Proc Natl Acad Sci U S A* **102,** 14837-14842.

Stebbins, C.E. and Galan, J.E. (2000). Modulation of host signaling by a bacterial mimic: structure of the Salmonella effector SptP bound to Rac1. *Mol Cell* **6,** 1449-1460.

Steffen, A., Faix, J., Resch, G.P., Linkner, J., Wehland, J., Small, J.V.*, et al.* (2006). Filopodia formation in the absence of functional WAVE- and Arp2/3-complexes. *Mol Biol Cell* **17,** 2581-2591.

Stevens, J.M., Galyov, E.E. and Stevens, M.P. (2006). Actin-dependent movement of bacterial pathogens. *Nat Rev Microbiol* **4,** 91-101.

Stevens, M.P., Stevens, J.M., Jeng, R.L., Taylor, L.A., Wood, M.W., Hawes, P.*, et al.* (2005). Identification of a bacterial factor required for actin-based motility of *Burkholderia pseudomallei*. *Mol Microbiol* **56,** 40-53.

Suetsugu, S., Hattori, M., Miki, H., Tezuka, T., Yamamoto, T., Mikoshiba, K. and Takenawa, T. (2002). Sustained activation of N-WASP through phosphorylation is essential for neurite extension. *Dev Cell* **3,** 645-658.

Suetsugu, S., Kurisu, S., Oikawa, T., Yamazaki, D., Oda, A. and Takenawa, T. (2006). Optimization of WAVE2 complex-induced actin polymerization by membrane-bound IRSp53, PIP(3), and Rac. *J Cell Biol* **173,** 571-585.

Suzuki, T., Mimuro, H., Miki, H., Takenawa, T., Sasaki, T., Nakanishi, H.*, et al.* (2000). Rho family GTPase Cdc42 is essential for the actin-based motility of *Shigella* in mammalian cells. *J Exp Med* **191,** 1905-1920.

Swimm, A., Bommarius, B., Li, Y., Cheng, D., Reeves, P., Sherman, M.*, et al.* (2004). Enteropathogenic *Escherichia coli* use redundant tyrosine kinases to form actin pedestals. *Mol Biol Cell* **15,** 3520-3529.

Taieb, F., Nougayrede, J.P., Watrin, C., Samba-Louaka, A. and Oswald, E. (2006). Escherichia coli cyclomodulin Cif induces G2 arrest of the host cell cycle without activation of the DNA-damage checkpoint-signalling pathway. *Cell Microbiol* **8,** 1910-1921.

Takano, K., Toyooka, K. and Suetsugu, S. (2008). EFC/F-BAR proteins and the N-WASP-WIP complex induce membrane curvature-dependent actin polymerization. *EMBO J* **27,** 2817-2828.

Takenawa, T. and Suetsugu, S. (2007). The WASP-WAVE protein network: connecting the membrane to the cytoskeleton. *Nat Rev Mol Cell Biol* **8,** 37-48.

Tam, V.C., Suzuki, M., Coughlin, M., Saslowsky, D., Biswas, K., Lencer, W.I.*, et al.* (2010). Functional analysis of VopF activity required for colonization in *Vibrio cholerae*. *MBio* **1,** e00289-10.

Taylor, R.C., Cullen, S.P. and Martin, S.J. (2008). Apoptosis: controlled demolition at the cellular level. *Nat Rev Mol Cell Biol* **9,** 231-241.

Thanabalasuriar, A., Koutsouris, A., Weflen, A., Mimee, M., Hecht, G. and Gruenheid, S. (2010). The bacterial virulence factor NleA is required for the disruption of intestinal tight junctions by enteropathogenic *Escherichia coli*. *Cell Microbiol* **12,** 31-41.

Thanbichler, M. and Shapiro, L. (2008). Getting organized--how bacterial cells move proteins and DNA. *Nat Rev Microbiol* **6,** 28-40.

Tobe, T., Beatson, S.A., Taniguchi, H., Abe, H., Bailey, C.M., Fivian, A.*, et al.* (2006). An extensive repertoire of type III secretion effectors in *Escherichia coli* O157 and the role of lambdoid phages in their dissemination. *Proc Natl Acad Sci U S A* **103,** 14941-14946.

Tomar, A., Lim, S.T., Lim, Y. and Schlaepfer, D.D. (2009a). A FAK-p120RasGAP-p190RhoGAP complex regulates polarity in migrating cells. *J Cell Sci* **122,** 1852-1862.

Tomar, A. and Schlaepfer, D.D. (2009b). Focal adhesion kinase: switching between GAPs and GEFs in the regulation of cell motility. *Curr Opin Cell Biol* **21,** 676-683.

Tomson, F.L., Viswanathan, V.K., Kanack, K.J., Kanteti, R.P., Straub, K.V., Menet, M.*, et al.* (2005). Enteropathogenic *Escherichia coli* EspG disrupts microtubules and in conjunction with Orf3 enhances perturbation of the tight junction barrier. *Mol Microbiol* **56,** 447-464.

Touze, T., Hayward, R.D., Eswaran, J., Leong, J.M. and Koronakis, V. (2004). Self-association of EPEC intimin mediated by the beta-barrel-containing anchor domain: a role in clustering of the Tir receptor. *Mol Microbiol* **51,** 73-87.

Tripathi, R., Singh Naorem, S., Dureja, C., Haldar, S., Mondal, A.K. and Raychaudhuri, S. (2010). VopF, a type III effector protein from a non-O1, non-O139 *Vibrio cholerae* strain, demonstrates toxicity in a *Saccharomyces cerevisiae* model. *J Med Microbiol* **59,** 17-24.

Tu, X., Nisan, I., Yona, C., Hanski, E. and Rosenshine, I. (2003). EspH, a new cytoskeleton-modulating effector of enterohaemorrhagic and enteropathogenic *Escherichia coli*. *Mol Microbiol* **47,** 595-606.

Van Kirk, L.S., Hayes, S.F. and Heinzen, R.A. (2000). Ultrastructure of Rickettsia rickettsii actin tails and localization of cytoskeletal proteins. *Infect Immun* **68,** 4706-4713.

van Loo, G., van Gurp, M., Depuydt, B., Srinivasula, S.M., Rodriguez, I., Alnemri, E.S.*, et al.* (2002). The serine protease Omi/HtrA2 is released from mitochondria during apoptosis. Omi interacts with caspase-inhibitor XIAP and induces enhanced caspase activity. *Cell Death Differ* **9,** 20-26.

Vega, F.M. and Ridley, A.J. (2007). SnapShot: Rho family GTPases. *Cell* **129,** 1430.

Vingadassalom, D., Campellone, K.G., Brady, M.J., Skehan, B., Battle, S.E., Robbins, D.*, et al.* (2010). Enterohemorrhagic *E. coli* requires N-WASP for efficient type III translocation but not for EspFU-mediated actin pedestal formation. *PLoS Pathog* **6,** e1001056.

Vingadassalom, D., Kazlauskas, A., Skehan, B., Cheng, H.C., Magoun, L., Robbins, D.*, et al.* (2009). Insulin receptor tyrosine kinase substrate links the *E. coli* O157:H7 actin assembly effectors Tir and EspF(U) during pedestal formation. *Proc Natl Acad Sci U S A* **106,** 6754-6759.

Viswanathan, V.K., Lukic, S., Koutsouris, A., Miao, R., Muza, M.M. and Hecht, G. (2004). Cytokeratin 18 interacts with the enteropathogenic *Escherichia coli* secreted protein F (EspF) and is redistributed after infection. *Cell Microbiol* **6,** 987-997.

Volkman, B.F., Prehoda, K.E., Scott, J.A., Peterson, F.C. and Lim, W.A. (2002). Structure of the N-WASP EVH1 domain-WIP complex: insight into the molecular basis of Wiskott-Aldrich Syndrome. *Cell* **111,** 565-576.

Vossenkamper, A., Marches, O., Fairclough, P.D., Warnes, G., Stagg, A.J., Lindsay, J.O*., et al.* (2010). Inhibition of NF-kappaB signaling in human dendritic cells by the enteropathogenic *Escherichia coli* effector protein NleE. *J Immunol* **185,** 4118-4127.

Voth, D.E. and Ballard, J.D. (2005). *Clostridium difficile* toxins: mechanism of action and role in disease. *Clin Microbiol Rev* **18,** 247-263.

Wada, T. and Penninger, J.M. (2004). Mitogen-activated protein kinases in apoptosis regulation. *Oncogene* **23,** 2838-2849.

Wan, F., Weaver, A., Gao, X., Bern, M., Hardwidge, P.R. and Lenardo, M.J. (2011). IKKbeta phosphorylation regulates RPS3 nuclear translocation and NF-kappaB function during infection with *Escherichia coli* strain O157:H7. *Nat Immunol* **12,** 335-343.

Watanabe, N., Madaule, P., Reid, T., Ishizaki, T., Watanabe, G., Kakizuka, A*., et al.* (1997). p140mDia, a mammalian homolog of *Drosophila* diaphanous, is a target protein for Rho small GTPase and is a ligand for profilin. *EMBO J* **16,** 3044-3056.

Webb, D.J., Parsons, J.T. and Horwitz, A.F. (2002). Adhesion assembly, disassembly and turnover in migrating cells -- over and over and over again. *Nat Cell Biol* **4,** E97-100.

Weiss, S.M., Ladwein, M., Schmidt, D., Ehinger, J., Lommel, S., Stading, K*., et al.* (2009). IRSp53 links the enterohemorrhagic *E. coli* effectors Tir and EspFU for actin pedestal formation. *Cell Host Microbe* **5,** 244-258.

Weisswange, I., Newsome, T.P., Schleich, S. and Way, M. (2009). The rate of N-WASP exchange limits the extent of ARP2/3-complex-dependent actin-based motility. *Nature* **458,** 87-91.

Welch, M.D., and Mullins, R.D. (2002). Cellular control of actin nucleation. *Annu Rev Cell Dev Biol* **18,** 247-288.

Welch, M.D., Rosenblatt, J., Skoble, J., Portnoy, D.A. and Mitchison, T.J. (1998). Interaction of human Arp2/3 complex and the Listeria monocytogenes ActA protein in actin filament nucleation. *Science* **281,** 105-108.

Whale, A.D., Garmendia, J., Gomes, T.A. and Frankel, G. (2006). A novel category of enteropathogenic *Escherichia coli* simultaneously utilizes the Nck and TccP pathways to induce actin remodelling. *Cell Microbiol* **8,** 999-1008.

Whale, A.D., Hernandes, R.T., Ooka, T., Beutin, L., Schuller, S., Garmendia, J*., et al.* (2007). TccP2-mediated subversion of actin dynamics by EPEC 2 - a distinct evolutionary lineage of enteropathogenic *Escherichia coli*. *Microbiology* **153,** 1743-1755.

Wiles, S., Clare, S., Harker, J., Huett, A., Young, D., Dougan, G. and Frankel, G. (2004). Organ specificity, colonization and clearance dynamics in vivo following oral challenges with the murine pathogen *Citrobacter rodentium*. *Cell Microbiol* **6,** 963-972.

Willis, S.N., Fletcher, J.I., Kaufmann, T., van Delft, M.F., Chen, L., Czabotar, P.E*., et al.* (2007). Apoptosis initiated when BH3 ligands engage multiple Bcl-2 homologs, not Bax or Bak. *Science* **315,** 856-859.

Wilson, R.K., Shaw, R.K., Daniell, S., Knutton, S. and Frankel, G. (2001). Role of EscF, a putative needle complex protein, in the type III protein translocation system of enteropathogenic *Escherichia coli*. *Cell Microbiol* **3,** 753-762.

Wolf, M.K. (1997). Occurrence, distribution, and associations of O and H serogroups, colonization factor antigens, and toxins of enterotoxigenic Escherichia coli. *Clin Microbiol Rev* **10,** 569-584.

Wong, A.R., Pearson, J.S., Bright, M.D., Munera, D., Robinson, K.S., Lee, S.F.*, et al.* (2011). Enteropathogenic and enterohaemorrhagic *Escherichia coli*: even more subversive elements. *Mol Microbiol* **80,** 1420-1438.

Wood, M.W., Rosqvist, R., Mullan, P.B., Edwards, M.H. and Galyov, E.E. (1996). SopE, a secreted protein of Salmonella *dublin*, is translocated into the target eukaryotic cell via a sip-dependent mechanism and promotes bacterial entry. *Mol Microbiol* **22,** 327-338.

Worthylake, D.K., Rossman, K.L. and Sondek, J. (2000). Crystal structure of Rac1 in complex with the guanine nucleotide exchange region of Tiam1. *Nature* **408,** 682-688.

Wu, B., Skarina, T., Yee, A., Jobin, M.C., Dileo, R., Semesi, A.*, et al.* (2010). NleG Type 3 effectors from enterohaemorrhagic *Escherichia coli* are U-Box E3 ubiquitin ligases. *PLoS Pathog* **6,** e1000960.

Yamamoto, T., Kaneko, M., Changchawalit, S., Serichantalergs, O., Ijuin, S. and Echeverria, P. (1994). Actin accumulation associated with clustered and localized adherence in *Escherichia coli* isolated from patients with diarrhea. *Infect Immun* **62,** 2917-2929.

Yang, E., Zha, J., Jockel, J., Boise, L.H., Thompson, C.B. and Korsmeyer, S.J. (1995). Bad, a heterodimeric partner for Bcl-XL and Bcl-2, displaces Bax and promotes cell death. *Cell* **80,** 285-291.

Yang, J., Zhang, Z., Roe, S.M., Marshall, C.J. and Barford, D. (2009). Activation of Rho GTPases by DOCK exchange factors is mediated by a nucleotide sensor. *Science* **325,** 1398-1402.

Yarbrough, M.L., Li, Y., Kinch, L.N., Grishin, N.V., Ball, H.L. and Orth, K. (2009). AMPylation of Rho GTPases by *Vibrio* VopS disrupts effector binding and downstream signaling. *Science* **323,** 269-272.

Yen, H., Ooka, T., Iguchi, A., Hayashi, T., Sugimoto, N. and Tobe, T. (2010). NleC, a type III secretion protease, compromises NF-kappaB activation by targeting p65/RelA. *PLoS Pathog* **6,** e1001231.

Youle, R.J. and Strasser, A. (2008). The BCL-2 protein family: opposing activities that mediate cell death. *Nat Rev Mol Cell Biol* **9,** 47-59.

Yu, B., Cheng, H.C., Brautigam, C.A., Tomchick, D.R. and Rosen, M.K. (2011). Mechanism of actin filament nucleation by the bacterial effector VopL. *Nat Struct Mol Biol* **18,** 1068-1074.

Zaidel-Bar, R., Ballestrem, C., Kam, Z. and Geiger, B. (2003). Early molecular events in the assembly of matrix adhesions at the leading edge of migrating cells. *J Cell Sci* **116,** 4605-4613.

Zettl, M. and Way, M. (2002). The WH1 and EVH1 domains of WASP and Ena/VASP family members bind distinct sequence motifs. *Curr Biol* **12,** 1617-1622.

Zha, J., Harada, H., Yang, E., Jockel, J. and Korsmeyer, S.J. (1996). Serine phosphorylation of death agonist BAD in response to survival factor results in binding to 14-3-3 not BCL-X(L). *Cell* **87,** 619-628.

Zhai, J., Lin, H., Nie, Z., Wu, J., Canete-Soler, R., Schlaepfer, W.W. and Schlaepfer, D.D. (2003). Direct interaction of focal adhesion kinase with p190RhoGEF. *J Biol Chem* **278,** 24865-24873.

Zigmond, S.H. (2004a). Beginning and ending an actin filament: control at the barbed end. *Curr Top Dev Biol* **63,** 145-188.

Zigmond, S.H. (2004b). Formin-induced nucleation of actin filaments. *Curr Opin Cell Biol* **16,** 99-105.

Zuchero, J.B., Coutts, A.S., Quinlan, M.E., Thangue, N.B. and Mullins, R.D. (2009). p53-cofactor JMY is a multifunctional actin nucleation factor. *Nat Cell Biol* **11,** 451-459.

Appendices

Research Publications

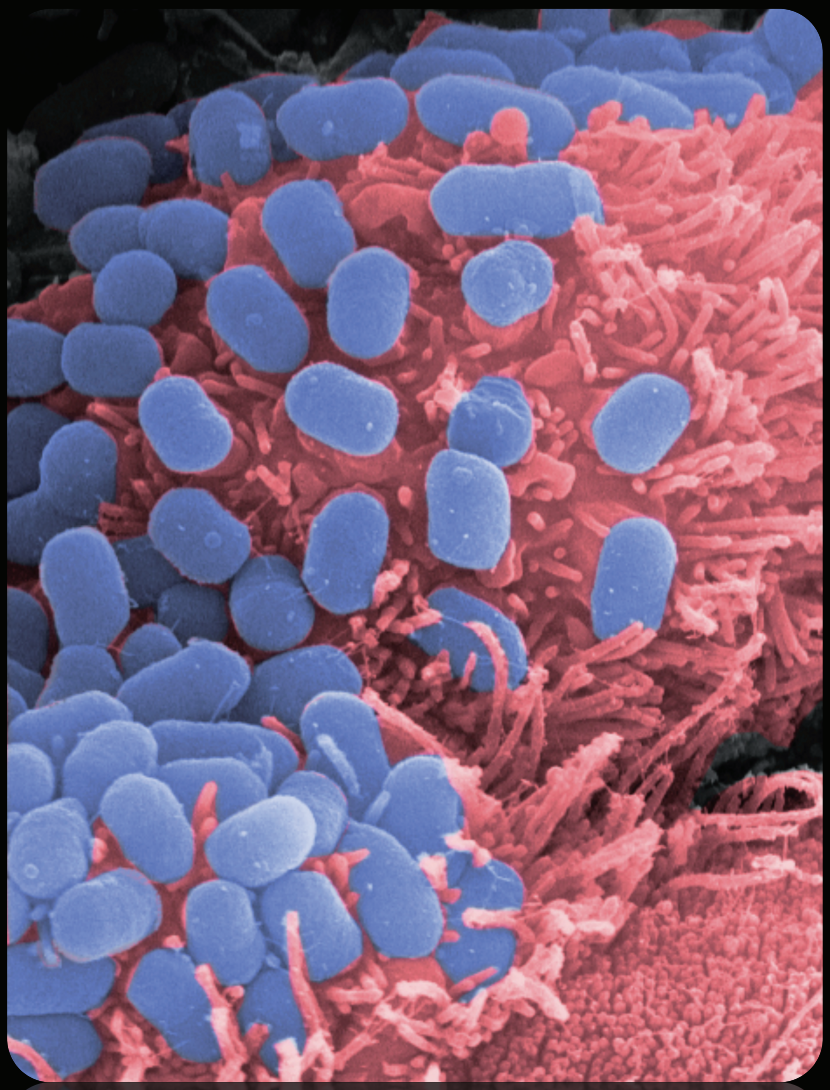
Wong, A. R. C., Pearson, J. S., Bright, M. D., Munera, D., Robinson, K. S., Lee, S. F., Frankel, G. and Hartland, E. L. (2011). Enteropathogenic and enterohaemorrhagic *Escherichia coli*: even more subversive elements. *Mol Microbiol* **80**, 1420-1438.

Wong, A. R. C., Clements, A., Raymond, B., Crepin, V. F. and Frankel, G. (2012). The interplay between the *E. coli* Rho guanine nucleotide exchange factor (GEF) effectors and mammalian RhoGEF inhibitor EspH. *MBio* **3,** e00250-11.

Wong, A. R. C., Raymond, B., Collins, J. W., Crepin, V. F. and Frankel, G. (2012). The enteropathogenic *E. coli* effector EspH promotes actin pedestal formation and elongation via WASP-interacting protein (WIP). *Cell Microbiol*. *In press.*

VOLUME 80 | NUMBER 6 | JUNE 2011 | ISSN 0950-382X | www.mol-micro.com

molecular microbiology



On the cover:
Type III secretion effectors of EPEC and EHEC

Iron uptakes systems in *Listeria monocytogenes*

Integration of virulence gene regulatory cascades in *Salmonella*

Cell division in *Caulobacter*

WILEY-BLACKWELL

Molecular Microbiology (2011) 80(6), 1420–1438 ■
doi:10.1111/j.1365-2958.2011.07661.x
First published online 5 May 2011

MicroReview

Enteropathogenic and enterohaemorrhagic *Escherichia coli*: even more subversive elements

Alexander R. C. Wong,[1] Jaclyn S. Pearson[2], Michael D. Bright,[1] Diana Munera,[1] Keith S. Robinson,[1] Sau Fung Lee,[2] Gad Frankel[1] and Elizabeth L. Hartland[2]*

[1]*Centre for Molecular Microbiology and Infection, Division of Cell and Molecular Biology, Imperial College London, London SW7 2AZ, UK.*

[2]*Department of Microbiology and Immunology, University of Melbourne, Melbourne, Vic. 3010, Australia.*

Summary

The human pathogens enteropathogenic and enterohemorrhagic *Escherichia coli* (EPEC and EHEC) share a unique mechanism of colonization that results from the concerted action of effector proteins translocated into the host cell by a type III secretion system (T3SS). EPEC and EHEC not only induce characteristic attaching and effacing (A/E) lesions, but also subvert multiple host cell signalling pathways during infection. Our understanding of the mechanisms by which A/E pathogens hijack host cell signalling has advanced dramatically in recent months with the identification of novel activities for many effectors. In addition to further characterization of established effectors (Tir, EspH and Map), new effectors have emerged as important mediators of virulence through activities such as mimicry of Rho guanine nucleotide exchange factors (Map and EspM), inhibition of apoptosis (NleH and NleD), interference with inflammatory signalling pathways (NleB, NleC, NleE and NleH) and phagocytosis (EspF, EspH and EspJ). The findings have highlighted the multifunctional nature of the effectors and their ability to participate in redundant, synergistic or antagonistic relationships, acting in a co-ordinated spatial and temporal manner on different host organelles and cellular pathways during infection.

Accepted 5 April, 2011. *For correspondence. E-mail hartland@unimelb.edu.au; Tel. (+61) 3 8344 8041; Fax (+61) 3 9347 1540.

© 2011 Blackwell Publishing Ltd

Introduction

Attaching and effacing (A/E) pathogens are a family of diarrhoeagenic pathogens that induce histopathological lesions, termed A/E lesions on the apical surface of host enterocytes (Fig. 1). This group includes the human pathogens enteropathogenic *Escherichia coli* (EPEC) and enterohemorrhagic *E. coli* (EHEC), reviewed in (Nataro and Kaper, 1998; Robins-Browne and Hartland, 2002), and a number of animal pathogens such as the mouse-specific pathogen *Citrobacter rodentium* and rabbit-specific enteropathogenic *E. coli* (REPEC) (Barthold *et al.*, 1978; Schauer and Falkow, 1993; Robins-Browne *et al.*, 1994). EPEC is a cause of gastroenteritis in infants less than 2 years of age while EHEC causes bloody diarrhoea in children and the elderly. EHEC is distinguished from EPEC by the production of Shiga toxins that can cause severe kidney damage leading to the haemolytic uremic syndrome, a form of acute renal failure (Nataro and Kaper, 1998; Robins-Browne and Hartland, 2002). REPEC causes severe diarrhoea in susceptible animals, showing the same clinicopathological features, host, age and tissue specificity as strains of EPEC which infect humans (Robins-Browne *et al.*, 1994). By contrast, diarrhoea is not a strong feature of *C. rodentium* infection; rather *C. rodentium* causes mucosal hyperplasia where mortality results from secondary inflammatory responses and, in severe cases, rectal prolapse (Barthold *et al.*, 1978). These A/E pathogens all have distinct fimbrial and non-fimbrial adhesins that allow the bacteria to adhere to the gut surface to initiate A/E lesions.

Attaching and effacing lesions are a striking ultrastructural feature of infection where the bacteria adhere intimately to the host cell plasma membrane, destroy the enterocyte microvilli and induce cytoskeletal rearrangements beneath adherent bacteria, reviewed in (Frankel *et al.*, 1998). All A/E pathogens carry a pathogenicity island, the locus of enterocyte effacement (LEE) (Elliott *et al.*, 1998) (Fig. 1) that encodes gene regulators (Elliott *et al.*, 2000; Deng *et al.*, 2004), the adhesin, intimin (Jerse *et al.*, 1990), a type III secretion system (T3SS)

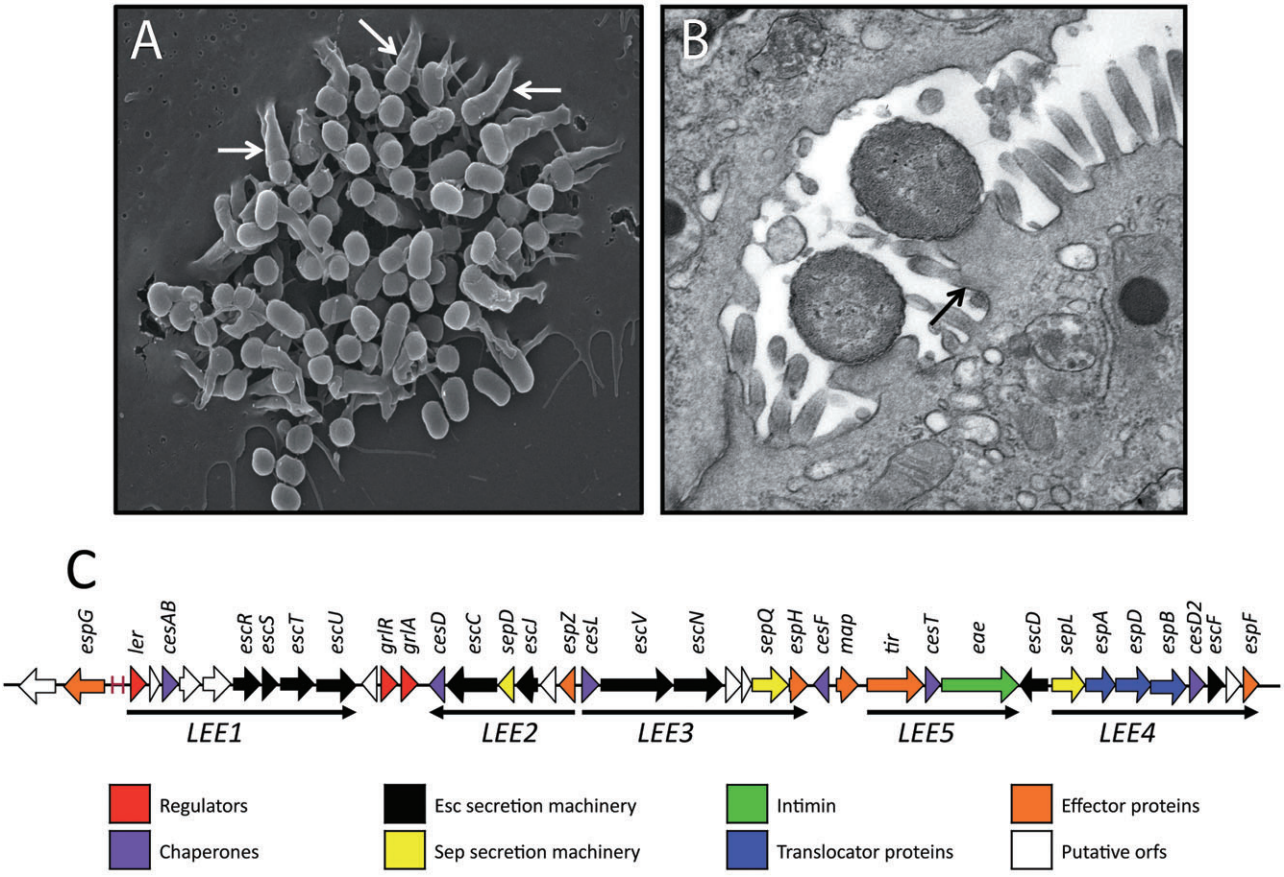


Fig. 1. Distinct histopathological lesions induced by attaching and effacing (A/E) pathogens.
A. Scanning electron micrograph of pedestals induced by adherent bacteria (arrows).
B. Transmission electron micrograph showing intestinal A/E lesions (arrow).
C. Diagram illustrating the genetic organization of the locus of enterocyte effacement (LEE) region from EPEC E2348/69.

(Jarvis *et al*., 1995; Elliott *et al*., 1998), chaperones (Abe *et al*., 1999; Elliott *et al*., 1999; Younis *et al*., 2010) and several secreted proteins, including the translocated intimin receptor, Tir (Kenny *et al*., 1997; Deibel *et al*., 1998; Elliott *et al*., 1999). Although there is some small variation among the LEE regions from different A/E pathogens, overall organization and gene content is highly conserved. Together with the T3SS apparatus itself, the secreted proteins, EspA, EspB and EspD form a translocon that is essential for protein secretion and the translocation of multiple LEE-encoded and non-LEE encoded effectors into the host cell (Knutton *et al*., 1998; Wachter *et al*., 1999; Hartland *et al*., 2000; Ide *et al*., 2001).

While the bacteria remain mostly extracellular in the lumen of the gut, the T3SS effectors of A/E pathogens access and manipulate the intracellular environment of host cells. The effectors subvert various host cell processes, which enable the bacteria to colonize, multiply and cause disease. A group of 21 core effectors, including all those encoded within LEE and a number of non-LEE effectors, are shared by all A/E pathogens (Iguchi *et al*., 2009). However, the repertoire of the remaining non-LEE effectors varies widely in different EPEC and EHEC serotypes, suggesting that different isolates employ distinct, strain-specific infection strategies. Identifying and characterizing the biochemical functions of T3SS effectors and understanding how effector activity is co-ordinated is therefore critical to appreciating the molecular basis of host-pathogen interactions. The repertoire of EPEC/EHEC effectors, their localization, interacting partners and homologues are summarized in Table 1.

Effector co-ordination: hierarchy of expression, secretion and translocation

The complexity of the T3SS requires tight regulation to ensure functional spatial and temporal expression, secretion and translocation of the different components. Most of the LEE genes are organized in 5 operons (*LEE1-5*) (Fig. 1), expression of which is controlled through

Table 1. The T3SS translocome of A/E pathogens.

T3SS effector	Presence[a] EPEC O127:H6 E2348/69	EHEC O157:H7 Sakai	CR[b] ICC168	Subcellular localization	Putative and known host binding partners/ substrates	Homologues [BLASTp]	Cellular function	References
LEE encoded effectors								
EspB	1	1	1	Cytosol, PM[c]	α_1-antitrypsin, α-catenin, Myosin-1c	YopD	Translocation pore component, AJ disruption, binds myosins to inhibit phagocytosis	(Kodama *et al.*, 2002; Knappstein *et al.*, 2004; Iizumi *et al.*, 2007; Hamaguchi *et al.*, 2008)
Tir	1	1	1	PM	14-3-3tau, α-actinin, cortactin, CK18, IQGAP1, IRTKS, IRSp53, Nck, PI3K, Talin, Vinculin	None known	Receptor for the adhesion intimin, actin pedestal formation, downregulates Map-dependent filopodia formation, SGLT-1 inactivation	(Freeman *et al.*, 2000; Goosney *et al.*, 2000; Gruenheid *et al.*, 2001; Kenny *et al.*, 2002; Batchelor *et al.*, 2004; Dean *et al.*, 2006; Patel *et al.*, 2006; Cantarelli *et al.*, 2007; Brown *et al.*, 2008; Berger *et al.*, 2009; Nieto-Pelegrin and Martinez-Quiles, 2009; Sason *et al.*, 2009; Selbach *et al.*, 2009; Vingadassalom *et al.*, 2009; Weiss *et al.*, 2009)
EspF	1	1	1	Mitochondria, Cytosol, Nucleus, TJ[d], Apical membrane, Lateral membrane	14-3-3zeta, ABCF2, actin, Arp2, CK18, N-WASP, Profilin, SNX9, ZO-1/ZO-2	TccP/EspFu	Mitochondrial disruption, NHE3 inactivation, SGLT-1 inactivation, TJ disruption, disrupts nucleolus, disrupts intermediate filaments, activates SNX9 to induce membrane remodelling, binds and activates N-WASP, inhibits PI3K-dependent phagocytosis	(McNamara *et al.*, 2001; Dean and Kenny, 2004; Muza-Moons *et al.*, 2004; Viswanathan *et al.*, 2004; Dean *et al.*, 2006; 2010; Guttman *et al.*, 2006; Quitard *et al.*, 2006; Marches *et al.*, 2006; Alto *et al.*, 2007; Nougayrede *et al.*, 2007; Hodges *et al.*, 2008; Peralta-Ramirez *et al.*, 2008; Thanabalasuriar *et al.*, 2010a)
Map	1	1	1	Mitochondria	EBP50 (NHERF1), NHERF2, Cdc42	IpgB, SopE	Cdc42 GEF that induces transient filopodia formation, mitochondrial disruption, SGLT-1 inactivation, TJ disruption	(Dean and Kenny, 2004; Alto *et al.*, 2006; Dean *et al.*, 2006; Ma *et al.*, 2006; Papatheodorou *et al.*, 2006; Simpson *et al.*, 2006; Huang *et al.*, 2009; Martinez *et al.*, 2010)
EspG	2	1	1	Cytosol, Golgi	Tubulin, Arf1/6, PAK1/2/3	VirA	Disrupts microtubules, blocks ARF GTPase signalling and stimulates PAKs to inhibit endomembrane trafficking	(Matsuzawa *et al.*, 2004; Hardwidge *et al.*, 2005; Shaw *et al.*, 2005; Tomson *et al.*, 2005; Germane and Spiller, 2011; Selyunin *et al.*, 2011)
EspH	1	1	1	PM, Pedestal	DH-PH RhoGEFs	None known	Blocks Rho GTPase signalling and FCγR-mediated phagocytosis, promotes actin pedestal length	(Tu *et al.*, 2003; Dong *et al.*, 2010)
EspZ	1	1	1	PM	CD98	None known	Enhances β1-integrin and FAK signalling to inhibit apoptosis and cellular cytotoxicity	(Shames *et al.*, 2010)
Non-LEE encoded effectors								
EspI/NleA	1	1	1	Golgi, PM	Syntrophin, Sec23/24, MALS3, PDZK11, SNX27, TCOF1, EBP50 (NHERF1), NHERF2, MAGI-3, SAP97, SAP102, PSD-95	None known	Inhibits COPII-dependent protein export from ER, TJ disruption	(Gruenheid *et al.*, 2004; Kim *et al.*, 2007; Lee *et al.*, 2008; Thanabalasuriar *et al.*, 2010a)
EspJ	1	1	1	Cytosol, Mitochondria	Unknown	HopF	Inhibits FCγR-mediated and CR3-mediated *trans*-phagocytosis	(Marches *et al.*, 2008; Kurushima *et al.*, 2010)
EspK	0	1	1	Unknown	Unknown	GogB	Unknown	
EspL	3 (2)	4 (1)	1	Pedestal	Annexin 2	OspD	Enhances F-actin bundling activity of Annexin 2	(Miyahara *et al.*, 2009)

© 2011 Blackwell Publishing Ltd,

© 2011 Blackwell Publishing Ltd, *Molecular Microbiology*, **80**, 1420–1438

Table 1. *cont.*

T3SS effector	Presence[a] EPEC O127:H6 E2348/69	EHEC O157:H7 Sakai	CR[b] ICC168	Subcellular localization	Putative and known host binding partners/ substrates	Homologues [BLASTp]	Cellular function	References
EspM	0	2	3 (1)	Cytosol	RhoA	IpgB, SopE	RhoA GEF that induces stress fibre formation	(Arbeloa *et al.*, 2008; 2010)
EspN	0	1	3 (2)	Unknown	Unknown	SARI_01330, SARI_01464, SeAg_B1500, CNF1	Unknown	
EspO	1 (1)	2	1	Unknown	Integrin-linked kinase (ILK)	OspE	Unknown	(Kim *et al.*, 2009)
EspR	0	4 (1)	0	Unknown	Unknown	SF1757	Unknown	
EspS	0	0	1	Unknown	Unknown	OspB	Unknown	
EspT	0	0	1	Mitochondria	Unknown	IpgB, SopE	Activates Cdc42 and Rac1 that induces membrane ruffles and lammelipodia, promotes intracellular bacterial uptake via trigger mechanism	(Bulgin *et al.*, 2009, 2010)
EspV	0	1 (1)	1	Cytosol	Unknown	AvrA1	Modulates cytoskeleton	(Arbeloa *et al.*, 2011)
EspW	0	1	0	Unknown	Unknown	HopPmaA, HopW1	Unknown	
EspX	0	7 (1)	1	Unknown	Unknown	Sd1012_0237, SSON_0027	Unknown	
EspY	0	5 (1)	0	Unknown	Unknown	SopD	Unknown	
NleB	3 (1)	3 (1)	2 (1)	Cytosol	Unknown	SseK	Inhibits TNF-induced NF-κB activation	(Nadler *et al.*, 2010; Newton *et al.*, 2010)
NleC	1	1	1	Cytosol, Nucleus	p65 (RelA), p50, c-Rel, IκB	AIP56	Metalloprotease that cleaves p65 (RelA), c-Rel, p50 and IκB to inhibit NF-κB activation	(Yen *et al.*, 2010; Baruch *et al.*, 2011; Muehlen *et al.*, 2011; Pearson *et al.*, 2011)
NleD	1	1	2	Cytosol	JNK	HopAP1, HopH1	Metalloprotease that cleaves JNK to inhibit AP-1 activation	(Baruch *et al.*, 2011)
NleE	2	1	1	Cytosol	Unknown	OspZ	Blocks IκB degradation to inhibit NF-κB activation	(Nadler *et al.*, 2010; Newton *et al.*, 2010; Vossenkamper *et al.*, 2010)
NleF	1	1	1	Unknown	Unknown	None known	Unknown	
NleG/NleI	1	14 (5)	5 (2)	Cytosol	UBE2D2	STY1076	U-box E3 ubiquitin ligase	(Wu *et al.*, 2010)
NleH	3 (1)	2	1	ER[e], PM, Cytosol	Bax-inhibitor 1, NHERF2, RPS3	OspG	Binds Bax-inhibitor 1 to block apoptosis, sequesters RPS3 to inhibit NF-κB signalling	(Gao *et al.*, 2009; Hemrajani *et al.*, 2010; Martinez *et al.*, 2010; Royan *et al.*, 2010; Wan *et al.*, 2011)
NleK	0	0	1	Unknown	Unknown	STY1628	Unknown	
Cif	1 (1)	0	0	Nucleus	NEDD8, Ubiquitin	CHBP, Plu2515, Ypk19711, Pha4011	Inhibits CRL activity via NEDD8 deamidation to induce p21 and p27 accumulation and G(2)/G(1) cell cycle arrest	(Cui *et al.*, 2010; Jubelin *et al.*, 2010; Morikawa *et al.*, 2010)
Ibe	0	0	0	Cytosol	IQGAP1	OspB	Enhances pedestal formation	(Buss *et al.*, 2009)
TccP/EspFu	0	2 (1)	0	Cytosol	N-WASP, IRTKS, IRSp53, Cortactin	EspF	Relieves N-WASP autoinhibition to trigger actin pedestal formation	(Campellone *et al.*, 2004b; Garmendia *et al.*, 2004; 2006; Cantarelli *et al.*, 2007; Campellone *et al.*, 2008; Cheng *et al.*, 2008; Sallee *et al.*, 2008; Morita-Ishihara *et al.*, 2009; Vingadassalom *et al.*, 2009; Weiss *et al.*, 2009)
Total	27 (6)	62 (12)	35 (6)					

a. Number of effector genes present in EPEC O127:H6 strain E2348/69, EHEC O157:H7 strain Sakai and *C. rodentium* strain ICC168 () indicates pseudogene.
b. *Citrobacter rodentium.*
c. PM, plasma membrane.
d. TJ, tight junction.
e. ER, endoplasmic reticulum.

complicated regulatory cascades involving cross-talk between bacterial, host and environmental factors (Hughes and Sperandio, 2008). The LEE-encoded regulator (Ler) is the main transcriptional regulator that by functioning as a repressor of *LEE1* and activator of *LEE2–LEE5* creates a negative feedback loop (Elliott *et al*., 2000; Bustamante *et al*., 2001; Berdichevsky *et al*., 2005). The level of Ler within the bacterial cell is controlled by other transcriptional regulators that are activated in response to different environmental stimuli (Iyoda *et al*., 2006; Russell *et al*., 2007). Contact of EPEC/EHEC with host cells upregulates T3SS expression (Roe *et al*., 2004; Brutinel and Yahr, 2008). Although the factors and mechanisms that mediate contact-dependent LEE gene expression are not clear, the fact that Hfq negatively regulates the T3SS of a variety of pathogens suggests that Hfq/sRNA complexes enable the bacterium to respond rapidly to changing environmental conditions such as interaction with the host plasma membrane (Shakhnovich *et al*., 2009).

Upon cell contact the LEE-encoded translocators EspB and EspD are inserted into the plasma membrane of the host cell, forming a translocation pore (Hartland *et al*., 2000; Daniell *et al*., 2001; Ide *et al*., 2001; Buttner and Bonas, 2002). The fact that EspB and EspD are required for the translocation of all the EPEC/EHEC effectors suggests a secretion hierarchy whereby translocators are directed to, and secreted by, the T3SS machinery prior to the effectors. T3SS substrates typically contain two secretion signals: a short (*c*. 20 amino acids) N-terminal motif and a chaperone-binding domain (Gauthier and Finlay, 2003; Ghosh, 2004). Importantly, the N-terminal secretion signal of effectors, as well as that of translocators, is both necessary and sufficient for the secretion and translocation of reporter proteins (Charpentier and Oswald, 2004; Munera *et al*., 2010). Although it is unclear how the T3SS distinguishes between effectors and translocators, the LEE-encoded proteins SepD and SepL play a major role in this process. SepD and SepL form a complex at the bacterial inner membrane and may sense and respond to certain environmental signals such as low calcium (Creasey *et al*., 2003; O'Connell *et al*., 2004; Deng *et al*., 2005). EPEC *sepD* and *sepL* mutants exhibit aberrant secretion profiles where translocators are absent and effectors are over-secreted. This suggests that the SepL/D complex functions as a checkpoint allowing translocation of effector proteins only once the translocon is fully assembled and functional (Deng *et al*., 2005).

Translocation of different effectors into the host cell must also be tightly timed and co-ordinated. This is achieved at different levels, from the magnitude and timing of gene expression in the bacterial cell to a hierarchy of effector protein translocation. Indeed, real-time analysis of LEE-encoded effectors has revealed a distinct order of protein translocation (Mills *et al*., 2008). Importantly, the concentration of the effectors within the bacterial cell, their interaction with intracellular chaperones and bacterial attachment to the host cell are all important parameters that regulate translocation efficiencies (Mills *et al*., 2008). Moreover, since the activities of effectors can complement or antagonize each other, their spatial and temporal activity must also be controlled from within the host cells. Ubiquitination followed by proteasomal degradation (Kubori and Galan, 2003), protein phosphorylation (Kenny, 1999) and exploitation of scaffold proteins as intracellular distribution hubs (Martinez *et al*., 2010) are a few examples by which bacterial pathogens co-ordinate spatial and temporal effector function in the host cell environment.

Re-programming actin dynamics

Tir-mediated actin polymerization and A/E lesion formation

Subversion of the host-cell actin cytoskeleton is central to the theme of T3SS-mediated virulence. EPEC/EHEC translocate the translocated intimin receptor (Tir) which, following integration into the plasma membrane, binds the bacterial outer membrane adhesin, intimin, through a surface exposed 55-amino-acid intimin binding domain (Kenny *et al*., 1997; Hartland *et al*., 1999; Kenny, 1999). *In vitro* studies have shown that Tir:intimin interaction results in Tir clustering and the initiation of downstream signalling events leading to the formation of actin-rich pedestals (Campellone *et al*., 2004a). In EPEC, phosphorylation of Tir tyrosine residue 474 (Y_{474}) by redundant host cell tyrosine kinases c-Fyn (Phillips *et al*., 2004), Abl, Arg and Etk (Swimm *et al*., 2004; Bommarius *et al*., 2007) generates a binding site for the host cell adaptor protein Nck (Gruenheid *et al*., 2001). Although it was originally believed that Nck then activates the neural Wiskott-Aldrich syndrome protein (N-WASP) to stimulate Arp2/3-mediated actin polymerization (Kenny, 1999; Gruenheid *et al*., 2001) by binding to the proline-rich domain (PRD) (Rohatgi *et al*., 2001), Lommel *et al*. have shown that in fact the PRD domain of N-WASP is dispensable for pedestal formation (Lommel *et al*., 2001). Instead, another domain, the WASP-homology 1 (WH1) domain of N-WASP is essential for EPEC pedestal formation *in vitro* (Lommel *et al*., 2001). WASP-interacting protein (WIP) (Ramesh *et al*., 1997), a cytoskeletal protein that binds Nck and the WH1 domain of N-WASP (Fig. 2) (Anton *et al*., 1998) has been proposed as the linker between Nck and N-WASP. However, dominant-negative WIP constructs do not abrogate pedestal formation (Lommel *et al*., 2001). While the possible involvement of other unknown host cell adaptors or T3SS effectors cannot be excluded, our current understanding supports a model where the

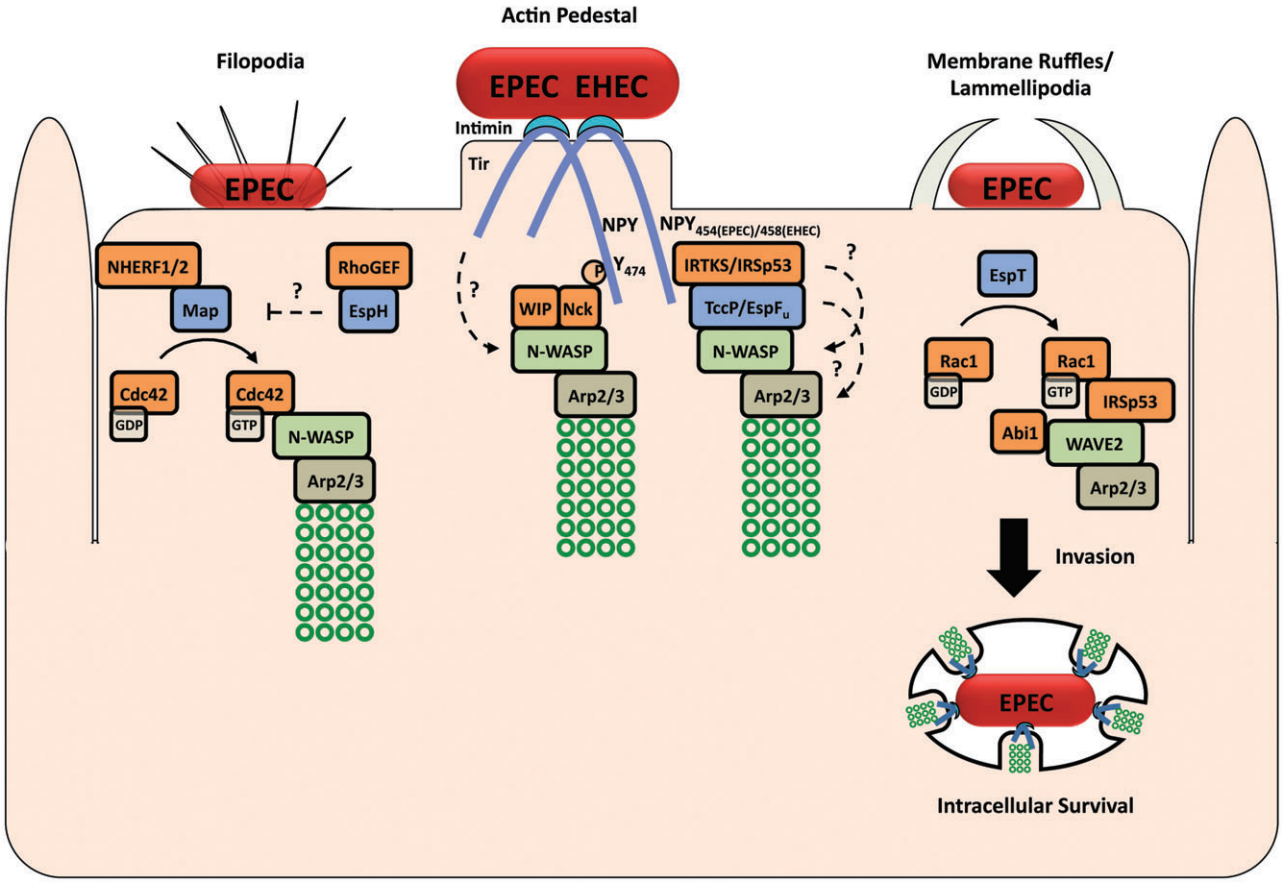


Fig. 2. Diagram summarizing the effect of a subset of T3SS effectors from A/E pathogens on host cytoskeletal pathways and structures. See text for explanation. Green circles represent actin filaments.

Tir:Nck pathway recruits N-WASP via both WIP/WH1 and Nck/PRD interactions to synergistically trigger actin assembly, a process that is analogous to Vaccinia virus actin-based motility (Fig. 2) (Moreau *et al.*, 2000; Zettl and Way, 2002; Weisswange *et al.*, 2009).

EHEC Tir lacks Y_{474}, and instead utilizes a conserved Asn-Pro-Tyr (NPY_{458}) motif, which is also found in EPEC Tir as NPY_{454}, to recruit the IRSp53/MIM proteins, IRTKS (Vingadassalom *et al.*, 2009) and IRSp53 (Campellone and Leong, 2005; Brady *et al.*, 2007; Weiss *et al.*, 2009). The Tir:IRTKS/IRSp53 complex induces inefficient Nck-independent pedestal formation in EPEC (Campellone and Leong, 2005). This pathway is amplified in EHEC by the non-LEE effector TccP/$EspF_U$, which contains an N-terminal secretion signal followed by multiple almost identical 47-amino-acid proline-rich repeats that bind IRTKS/IRSp53 (Vingadassalom *et al.*, 2009) and the GTPase-binding domain (GBD) of N-WASP (Garmendia *et al.*, 2004; Campellone *et al.*, 2004b) (Fig. 2). Rather than mimicking Cdc42 activation, each TccP/$EspF_U$ repeat mimics an auto-inhibitory element within the GBD, thus competitively binding to the GBD to relieve N-WASP auto-inhibition, triggering actin polymerization via the Arp2/3 complex (Cheng *et al.*, 2008; Sallee *et al.*, 2008). While a minimum of 2 proline-rich repeat is required for pedestal formation, additional repeats act synergistically to enhance N-WASP activation and actin polymerization (Garmendia *et al.*, 2006; Campellone *et al.*, 2008). Interestingly, the Tir:IRTKS/IRSp53:TccP/$EspF_U$ pathway is also able to trigger Arp2/3-mediated actin polymerization independently of N-WASP (Vingadassalom *et al.*, 2010), implying that additional host cell factors must also play a role in actin polymerization.

The Tir:Nck and Tir:IRTKS/IRSp53:TccP/$EspF_U$ pathways are conserved in EPEC belonging to lineage 1 and EHEC O157 respectively (Ogura *et al.*, 2007; Whale *et al.*, 2007). Somewhat unexpectedly, both pathways are active in most non-O157 EHEC strains and in EPEC strains belonging to lineage 2 as well as EPEC O119:H6 (Ogura *et al.*, 2007; Whale *et al.*, 2007), implying functional redundancy, reviewed in (Frankel and Phillips, 2008). Importantly, although Tir is essential for A/E lesion formation on mucosal surfaces and the pathways responsible for actin polymerization in cell lines *in vitro* appear to

be under intense selective pressure, neither the Tir:Nck nor Tir:IRTKS/IRSp53:TccP/EspF$_u$ signalling complexes are necessary for A/E lesion formation or N-WASP recruitment during *C. rodentium* infection of mice (Crepin *et al*., 2010), or EPEC infection of human intestinal *in vitro* organ cultures (IVOC) (Schuller *et al*., 2007; Crepin *et al*., 2010). In addition, TccP/EspF$_u$ contributes to colonization efficiency of EHEC in rabbits and gnotobiotic piglets, but is not essential for the development of A/E lesions (Ritchie *et al*., 2008). Overall, these studies highlight the fact that our understanding of Tir-mediated actin signalling pathways *in vivo* is far from complete.

There is also increasing evidence that Tir-mediated actin signalling pathways are modulated by phosphoinositide (PI) metabolism, and this can be co-ordinated via additional Tir residues. Sason *et al*. (2009) revealed that EPEC Tir induces a shift from phosphatidylinositol 4,5-bisphosphate [PI(4,5)P_2] to phosphatidylinositol 3,4,5-trisphosphate [PI(3,4,5)P_3] at the bacterial attachment site, and that this is dependent on the recruitment of phosphoinositide 3-kinase (PI3K) via its phosphorylation of Y_{454} (Sason *et al*., 2009; Selbach *et al*., 2009). Recent work by Smith *et al*. (2010) showed that Tir tyrosine residues Y_{483}/Y_{511}, which resemble immunoreceptor tyrosine-based inhibition motifs (ITIMs), recruit inositol-5-phosphatase SHIP2 to dephosphorylate PI(3,4,5)P_3 to make PI(3,4)P_2. Point mutations on Y_{483}/Y_{511} or depletion of SHIP2 resulted in accumulation of PI(3,4,5)P_3, and a dramatic change in pedestal morphology to induce a 'Medusa phenotype' that is characterized by the formation of multiple irregular elongated pedestals under each bacterium (Smith *et al*., 2010). Interestingly, EHEC possesses a similar ITIM, but does not recruit SHIP2 (Smith *et al*., 2010). The role of phosphoinositide metabolism *in vivo* has also not been defined, and future work is warranted to further our understanding of the interplay between actin dynamics and membrane remodelling at the site of bacterial attachment.

Modulation of Rho GTPases

The recent characterization of the T3SS effectors, mitochondrial-associated protein (Map), EspM and EspT, has deepened our understanding of actin cytoskeletal manipulation by EPEC/EHEC beyond pedestal formation (Alto *et al*., 2006; Bulgin *et al*., 2010). Map, EspM and EspT belong to the WxxxE family of effectors also found in *Shigella* (IpgB1 and IpgB2) and *Salmonella* (SifA) (Alto *et al*., 2006; Arbeloa *et al*., 2008; Bulgin *et al*., 2009). While carriage of *map* is completely conserved among EPEC and EHEC strains, a screen of ~1000 clinical and environmental isolates showed that *espM* is found in 50% of EPEC and EHEC strains while *espT* is found in less than 2% of EPEC and none of the EHEC strains tested (Arbeloa *et al*., 2009). Map and EspM exhibit guanine exchange factor (GEF) activity towards Cdc42 (Huang *et al*., 2009) and RhoA (Arbeloa *et al*., 2010), respectively, thereby triggering formation of filopodia (Map) and stress fibres (EspM) (Alto *et al*., 2006; Arbeloa *et al*., 2008; Bulgin *et al*., 2009). EspT activates both Cdc42 and Rac1 which trigger membrane ruffles and lamellipodia and EPEC-induced invasion (Bulgin *et al*., 2009). By activating Cdc42, Map induces transient filopodia formation at bacterial attachment sites during the early stages of EPEC infection (Kenny *et al*., 2002; Berger *et al*., 2009). Filopodia retraction is dependent on Tir, either via a putative GTPase-activating protein (GAP)-like arginine finger motif (GLXR) present in the C-terminus, and/or by activation of Tir actin polymerization cascades (Kenny *et al*., 2002; Berger *et al*., 2009). The relevance of Map-mediated filopodia formation on cultured cells to *in vivo* infection is not yet known. The T3SS effector EspH is also implicated in modulating filopodia and pedestal dynamics. Deletion of *espH* results in prolonged filopodia formation concomitant with delayed pedestal formation, while overexpression of EspH results in pedestal elongation (Tu *et al*., 2003). Recently, Dong *et al*. reported that EspH inactivates endogenous Dbl-homology and pleckstrin-homology (DH-PH) RhoGEFs by competitively binding to tandem DH-PH domains which inhibit Rho activation (Dong *et al*., 2010). As bacterial GEFs do not share any sequence homology to DH-PH domains, and ectopic expression of EspH does not inhibit the activity of the translocated WxxxE EPEC/EHEC RhoGEFs (A.W., unpubl. data), it is tempting to speculate that EPEC/EHEC neutralizes endogenous RhoGEFs while injecting their own bacterial GEFs to hijack Rho GTPase signalling for the exclusive benefit of the pathogen.

EspT exemplifies this by utilizing the 'trigger' mechanism to promote EPEC invasion into non-phagocytic cells via Rac1-dependent membrane ruffle formation (Bulgin *et al*., 2009). Intriguingly, internalized EPEC mobilizes Tir to the vacuolar membrane, forming intracellular actin rich-pedestals that contribute to intracellular bacterial survival (Bulgin *et al*., 2009) (Fig. 2). EspT thus defines an invasive group of EPEC through its ability to manipulate Rho GTPase signalling pathways. EspV is the latest T3SS effector reported to modulate actin dynamics (Arbeloa *et al*., 2011). *espV* is present in ~16% of EPEC and EHEC strains and expression of EspV in mammalian cells leads to drastic and unique morphological alterations, which are characterized by nuclear condensation, cell rounding and formation of actin-rich, dendrite-like projections (Arbeloa *et al*., 2011). Thus, it appears that EspV modulates the actin cytoskeleton by a unique mechanism that is still undefined, and expands the activities of cytoskeleton-

targeting T3SS effectors beyond Rho GTPase signalling and pedestal formation.

Cross-talk between cytoskeletal networks

There is growing evidence of cross-talk between cytoskeletal networks other than actin during EPEC/EHEC infection. A prime example is the intermediate filaments CK8 and CK18, which are both recruited to the site of bacterial attachment (Batchelor *et al*., 2004). Tir interacts with both CK18 (Batchelor *et al*., 2004) and the 14-3-3tau isoform (Patel *et al*., 2006), an adaptor protein that also binds CK18. Formation of the Tir:CK18:14-3-3tau complex is essential, as depletion of either CK18 or 14-3-3tau impaired pedestal formation (Batchelor *et al*., 2004; Patel *et al*., 2006). Interestingly, CK18 and the 14-3-3zeta isoform also bind EspF (Viswanathan *et al*., 2004) and although EspF activates actin assembly, the functional significance of this is unknown (Alto *et al*., 2007).

Another example of cross-talk is given by the effectors EspG/EspG2 which, along with the *Shigella* homologue VirA, belong to a class of proteins involved in localized microtubule disruption during infection (Yoshida *et al*., 2002; Matsuzawa *et al*., 2004; Hardwidge *et al*., 2005; Shaw *et al*., 2005; Tomson *et al*., 2005). By destabilizing microtubules, EspG triggers the release of GEF-H1 into the cytosol, where it activates the RhoA-ROCK signalling pathway, resulting in the formation of actin stress fibres (Matsuzawa *et al*., 2004). Intriguingly, EspG appears to possess a dual function where it forms a GTPase–kinase signalling complex with ARF1/6 and PAKs to regulate endomembrane trafficking (Germane and Spiller, 2011; Selyunin *et al*., 2011), demonstrating the extraordinary multi-functionality of T3SS effectors. In summary, our current understanding of EPEC/EHEC infection supports a model of cytoskeletal restructuring at the site of bacterial attachment where actin and intermediate filament components accumulate while microtubule components are depleted.

Regulation of cell survival and apoptosis

During infection of intestinal epithelial cells, surface properties of EPEC/EHEC induce extrinsic apoptotic pathways (Abul-Milh *et al*., 2001), while T3SS effectors such as EspF, Map and Cycle inhibitory factor (Cif) trigger intrinsic apoptotic pathways. EspF induces mitochondrial lysis, opens tight junctions and promotes degradation of anti-apoptotic proteins (McNamara *et al*., 2001; Nougayrede and Donnenberg, 2004; Nougayrede *et al*., 2007). Map disrupts tight junctions, triggers mitochondrial dysfunction and inactivates the sodium-dependent glucose co-transporter SGLT-1, affecting enterocyte fluid uptake (Kenny and Jepson, 2000; Dean and Kenny, 2004; Dean *et al*., 2006; Ma *et al*., 2006). Cif arrests the host cell cycle at G1/S and G2/M, inhibits protein ubiquitination and stabilizes cell cycle inhibitory proteins $p21^{waf1}$ and $p27^{kip1}$, thereby inducing a delayed form of apoptosis (Marches *et al*., 2003; Taieb *et al*., 2006; Samba-Louaka *et al*., 2008; 2009). Interestingly, although EPEC/EHEC-mediated cell death exhibits early-stage apoptosis (exposure of phosphatidylserine on the cell surface and DNA cleavage), late-stage apoptotic features (membrane blebbing, cell shrinkage, nuclear condensation) are not evident (Crane *et al*., 1999; 2001; Hemrajani *et al*., 2010).

The antagonism of pro-apoptotic effects by EPEC/EHEC is mediated by the translocation of anti-apoptotic effectors such as NleH and NleD. EPEC/EHEC harbour two NleH effectors, NleH1 and NleH2, which share a high degree of similarity, including a conserved kinase active site and a PDZ-binding motif that interacts with the PDZ domain of NHERF2 (Perna *et al*., 2001; Hemrajani *et al*., 2008; Gao *et al*., 2009; Iguchi *et al*., 2009; Martinez *et al*., 2010; Petty *et al*., 2010). Overexpression of NHERF2 appears to sequester NleH and hinder its anti-apoptotic capacity. Indeed, NHERF2 also binds the PDZ motifs of EspI and Map, suggesting that it acts as a cellular hub at the plasma membrane for effector distribution (Martinez *et al*., 2010). Remarkably, both NleH effectors block multiple intrinsic apoptotic pathways, including cell death induced by the global kinase inhibitor staurosporine and *Clostridium difficile* toxin B (Hemrajani *et al*., 2010; Robinson *et al*., 2010). This ability appears to be largely due to the interaction of NleH1 and NleH2 with the anti-apoptotic protein, Bax inhibitor-1 (BI-1) (Hemrajani *et al*., 2010) (BI-1 is reviewed in Robinson *et al*., 2011) (Fig. 3). The NleH effectors therefore promote overall cell survival and inhibit enterocyte loss to promote sustained colonization by EPEC/EHEC.

Recently, NleD was described as a zinc metalloprotease that cleaves JNK, thereby compromising activity of the transcriptional regulator, AP-1, which regulates cell death, differentiation and proliferation (Baruch *et al*., 2011). NleD-mediated cleavage of JNK influences inflammatory responses (see below), but also inhibits the pro-apoptotic activity of JNK. Thus, NleD may complement the activities of NleH to protect infected cells from the activation of pro-death pathways.

EspZ is an additional effector that promotes cell survival and maintenance of the epithelium. Infection of cell monolayers with an EPEC Δ*espZ* mutant results in strong cytotoxicity. EspZ interacts with the host cell protein CD98, which enhances β1-integrin and focal adhesion kinase (FAK) signalling (Shames *et al*., 2010). *In vivo*, *C. rodentium* Δ*espZ* mutants are severely attenuated exhibiting markedly reduced colonization (Deng *et al*., 2004).

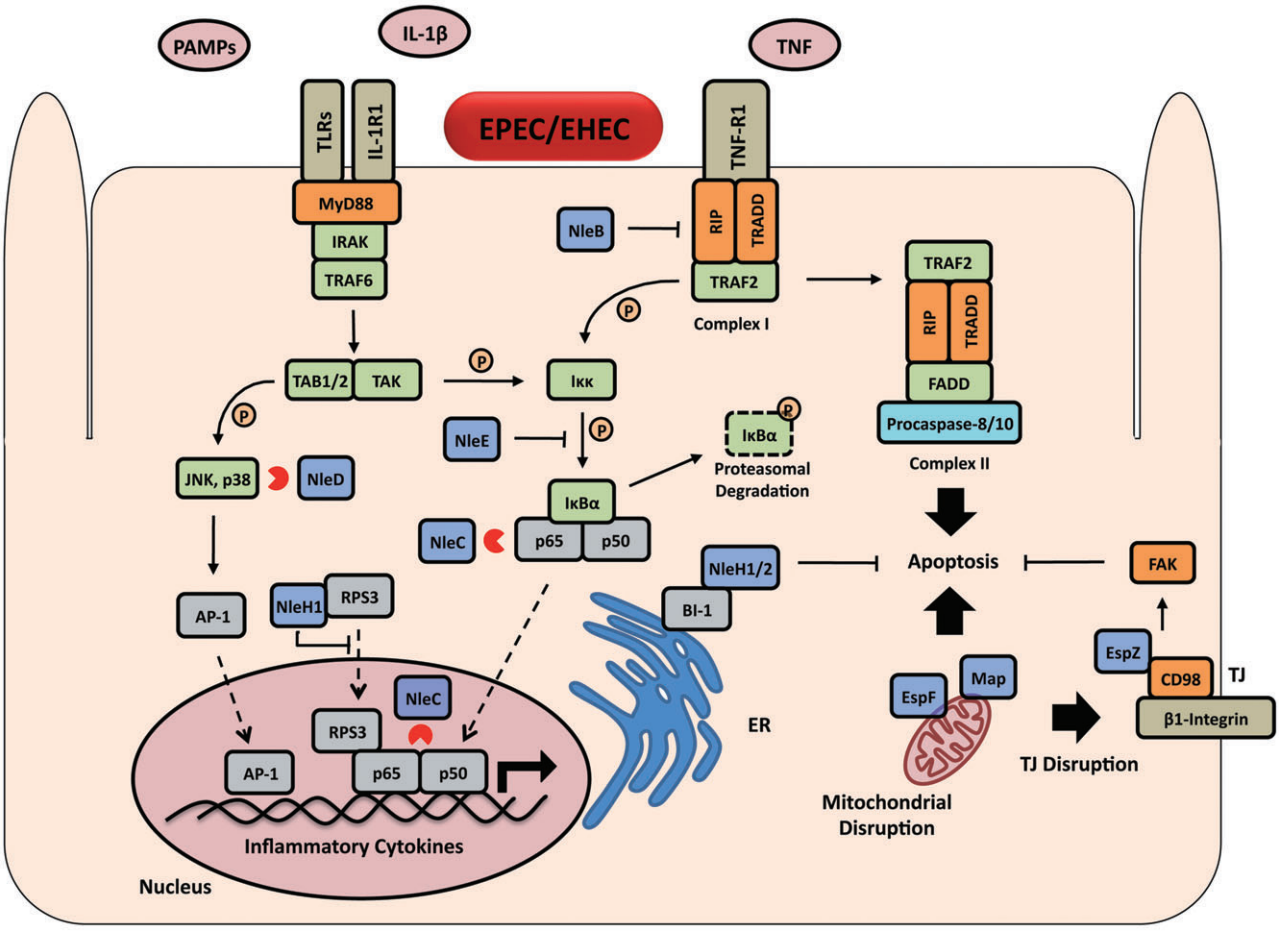


Fig. 3. Diagram summarizing the effect of a subset of T3SS effectors from A/E pathogens on host cell signalling pathways, including inflammation and apoptosis. See text for explanation. TJ is tight junction, ER is endoplasmic reticulum.

Therefore, the role of EspZ may be to stabilize the epithelium during bacterial colonization, thereby reducing the cytotoxic effect of bacterial infection (Shames *et al.*, 2010). Interestingly, the *Shigella flexneri* effector OspE, which shares homology with EPEC/EHEC EspO, has been shown to promote host cell adherence by interacting with integrin-linked kinase (ILK) to stabilize focal adhesions (Kim *et al.*, 2009). In concert with the EPEC/EHEC anti-apoptotic effectors, effectors such as EspZ and EspO that promote cell adherence and epithelial integrity are emerging as fundamentally important in pathogenesis.

Counteracting phagocytosis

Phagocytosis is the process by which cells of the immune system internalize and destroy bacteria and other targets. The best characterized phagocytic pathways are via the FCγ receptor (FCγR) or complement receptor (CR3), which mediate the phagocytosis of particles opsonized with immunoglobulin G (IgG) or the complement protein fragment C3bi respectively (Caron and Hall, 1998). Non-opsonized microorganisms can also be phagocytosed via diverse receptors including Toll like receptor 2 (TLR2) (Shen *et al.*, 2010), the scavenger and mannose receptors (Zhang *et al.*, 2005) and $P2X_7$ (Gu *et al.*, 2010). Infection of macrophages with EPEC/EHEC inhibits uptake of non-opsonized bacteria and IgG or C3bi-opsonized particles, suggesting that EPEC/EHEC infection paralyses general phagocytic mechanisms.

Although EspB plays a critical role as a component of the T3SS translocon, the effector itself is also translocated (Taylor *et al.*, 1998). EspB targets myosin function by binding the actin binding domains of multiple myosin family members (Iizumi *et al.*, 2007). Myosins are believed to provide force for phagosome closure during phagocytosis and multiple isoforms associate with phagocytic cups (Cox *et al.*, 2002; Diakonova *et al.*, 2002). EPEC expressing EspB lacking the myosin-binding domain lose their ability to inhibit their own uptake (Iizumi *et al.*, 2007). Another effector considered to be indispensable for inhibiting the phagocytosis of non-opsonized bacteria is EspF. EPEC *espF* mutants are phagocytosed to

the same extent as EPEC lacking a functional T3SS (Quitard *et al*., 2006; Marches *et al*., 2008). While the mechanism of EspF inhibition of phagocytosis remains elusive, some functions can be inferred from EspF binding partners. The anti-phagocytic activity of EspF lies within the N-terminal 101 residues (Quitard *et al*., 2006). Within this region are binding sites for actin, profilin and sorting nexin 9 (SNX9) (Alto *et al*., 2007; Peralta-Ramirez *et al*., 2008). The importance of actin for phagocytosis is well established, and profilin is an actin binding protein that is recruited to FCγR-mediated phagocytic cups (Coppolino *et al*., 2001). However, EspF does not inhibit opsonophagocytosis (Marches *et al*., 2008), which requires these host cell components, so these interactions are probably not key to the antiphagocytic mechanism of EspF. In fact, paradoxically, the interaction of EspF with SNX9 promotes the formation of membrane tubules, membrane remodelling and bacterial invasion of epithelial cells (Weflen *et al*., 2010). Whether the EspF–SNX9 interaction inhibits uptake by phagocytes remains to be determined.

EspH has emerged recently as an inhibitor of phagocytosis, most likely mediated by its ability to bind and inhibit DH-PH domain-containing Rho GEFs (Dong *et al*., 2010). Rho GTPases control cytoskeletal remodelling during phagocytosis and contribute to FCγR- and CR3-mediated uptake (Caron and Hall, 1998). EPEC *espH* mutants lose their ability to inhibit phagocytosis through the FCγR (Dong *et al*., 2010). Uniquely, EspJ inhibits both FCγR and CR3-mediated pathways (Marches *et al*., 2008). EPEC *espJ* mutants are unable to block opsonophagocytosis, although uptake of non-opsonized bacteria is still inhibited. The mechanism by which EspJ inhibits phagocytosis is unknown, and host interacting partners remain to be defined. While translocated EspJ localizes to mitochondria (Kurushima *et al*., 2010), this does not preclude a role for EspJ at the phagocytic cup. For example, EspF mainly localizes to mitochondria, but also has a function at bacterial attachment sites (Quitard *et al*., 2006). The apparent targeting of multiple uptake pathways suggests the anti-phagocytic effectors cooperate to exclude EPEC/EHEC from the intracellular environment in professional phagocytes. A key aspect of future work should address how the anti-phagocytic EPEC/EHEC effectors cooperate and whether they modulate the localization or activity of functionally similar host proteins.

Disarming the inflammatory response

EPEC and EHEC infection ultimately results in the induction of an inflammatory response via host recognition of pathogen-associated molecular patterns (PAMPs), most predominantly flagellin (Khan *et al*., 2008; Schuller *et al*., 2009). As a result, TLR signalling is initiated followed by activation of inflammatory signalling factors such as nuclear factor-kappaB (NF-κB) reviewed in (Li and Verma, 2002). The most abundant form of activated NF-κB in mammalian tissues is a dimer of p50 and p65, which is held in an inactive form in the cytoplasm by a family of inhibitory proteins called inhibitors of NF-κB (IκB). Activation of NF-κB occurs upon phosphorylation of IκB by the IκB kinase complex (Iκκ), and the subsequent ubiquitination and degradation of IκB by the cell proteasome (Perkins, 2007). This releases the p65/p50 dimer which translocates to the nucleus and binds NF-κB consensus sites thereby activating the expression of multiple cytokine genes including *IL8*, encoding interleukin-8 (IL-8) (Li and Verma, 2002).

In the initial stages of infection, EPEC/EHEC inhibit inflammatory cytokine production and NF-κB activation (Sharma *et al*., 2006; Ruchaud-Sparagano *et al*., 2007; Nobe *et al*., 2009). Recent work has demonstrated that EPEC encodes a set of effector proteins (NleE, NleB, NleC, NleD and NleH) that specifically target components of inflammatory signalling. The concerted activity of the effectors prevents host cells from mounting an effective inflammatory response (Nadler *et al*., 2010; Newton *et al*., 2010; Vossenkamper *et al*., 2010; Yen *et al*., 2010; Baruch *et al*., 2011; Muehlen *et al*., 2011; Pearson *et al*., 2011)

NleE is a highly conserved 27 kDa effector of A/E pathogens that is shared by *Shigella* where it is termed OspZ (Zurawski *et al*., 2008). NleE plays a key role in modulating the innate immune response during EPEC and EHEC infection by specifically blocking the translocation of activated NF-κB to the host cell nucleus, thereby causing a decrease in the expression and production of IL-8. This effect is seen in both epithelial cells and dendritic cells (Nadler *et al*., 2010; Newton *et al*., 2010; Vossenkamper *et al*., 2010). Although the mechanism by which p65 nuclear translocation is blocked is not clear, NleE prevents IκB degradation in response to tumour necrosis factor α (TNF) or IL-1β suggesting that the effector targets components shared by these inflammatory signalling pathways. One proposed mechanism is that NleE prevents Iκκ phosphorylation, although a direct interaction is yet to be shown (Nadler *et al*., 2010) (Fig. 3). A 6-amino-acid motif $IDSYMK_{209–214}$ is critical for the immunosuppressive function of NleE, but whether this motif is involved in direct interactions with NF-κB signalling factors is yet to be determined (Newton *et al*., 2010).

The NleB family of effectors are found on two pathogenicity islands (IE6 and PP4) encoding genes for *nleB1* and *nleB2* respectively. NleB1 and NleB2 are 38 kDa proteins conserved across A/E pathogens, with the exception of *C. rodentium* which carries only a single copy of the gene (Kelly *et al*., 2006; Petty *et al*., 2010). NleB1 from EPEC appears as effective as NleE at inhibiting NF-κB activation in response to TNF but not IL-1β, suggesting that NleB1

and NleE act at different points in the NF-κB signalling pathway (Newton *et al*., 2010) (Fig. 3). Similar to NleE, the mechanism by which NleB1 inhibits the TNF pathway is unknown. Given the high degree of similarity between NleB1 and NleB2 from EHEC and EPEC, it would be surprising if these effectors were not functionally conserved; however, this has not yet been investigated.

NleC was recently identified as an effector protease of EPEC and EHEC that cleaves and inactivates the NF-κB p65 subunit (Yen *et al*., 2010; Baruch *et al*., 2011; Muehlen *et al*., 2011; Pearson *et al*., 2011). Ectopically expressed NleC or NleC translocated by the T3SS degrade p65, p50 and c-Rel but not STAT1 or Erk, suggesting specificity for the Rel family of signalling components (Baruch *et al*., 2011; Pearson *et al*., 2011). NleC contains a consensus zinc metalloprotease motif $_{183}$HEIIH$_{187}$ that is responsible for the proteolytic activity of the enzyme. Mutagenesis of the motif abrogates the ability of NleC to degrade p65 and p50 (Yen *et al*., 2010; Baruch *et al*., 2011; Muehlen *et al*., 2011; Pearson *et al*., 2011). NleC appears to follow the activity of NleE, as p65 degradation in HeLa cells by wild-type EPEC is not seen until 6 hours after infection (Pearson *et al*., 2011). In addition, the activity of NleC appears to be largely in the nucleus where p65/p50 is translocated upon release from IκB (Baruch *et al*., 2011) (Fig. 3). While infection with an EPEC Δ*nleC* mutant does not result in increased IL-8 production, presumably due to functional redundancy with NleE (Baruch *et al*., 2011; Pearson *et al*., 2011), infection with an EPEC Δ*nleEC* double mutant or an EPEC Δ*nleBEC* triple mutant results in significantly higher IL-8 production by host cells compared with infection with EPEC Δ*nleE* or EPEC Δ*nleBE* alone (Baruch *et al*., 2011; Pearson *et al*., 2011). Thus, NleC appears to complement the activities of NleE and NleB by eliminating unbound and activated p65/p50 that would positively influence target gene transcription. The apparent redundancy in function between NleE and NleC may also explain why previous reports have failed to find a strong phenotype associated with either an *nleE* or *nleC* mutant during *C. rodentium* infection of mice (Marches *et al*., 2005; Kelly *et al*., 2006; Wickham *et al*., 2007). NleD also harbours a consensus zinc metalloprotease motif, $_{142}$HELLH$_{146}$. The NleD protease effector specifically cleaves JNK and p38 MAP kinases, thereby inactivating the AP-1 transcription factor, which regulates multiple cell processes including, inflammation, differentiation, proliferation and apoptosis (Baruch *et al*., 2011). Infection with an EPEC *nleBECD* quadruple deletion mutant results in increased IL-8 production compared with an *nleBEC* triple mutant and this is partially restored upon complementation with *nleD* (Baruch *et al*., 2011).

NleH1 and NleH2 have clear roles in inhibiting host cell apoptosis; however, these effectors also suppress NF-κB activation. The recently discovered non-Rel NF-κB subunit, RPS3, a KH domain protein that regulates NF-κB dependent transcription is a newly described binding partner of NleH (Wan *et al*., 2007; 2011; Gao *et al*., 2009). NleH1 but not NleH2 reduces the nuclear abundance of RPS3 with no effect on other NF-κB signalling factors. In fact, the N-terminal region of NleH1 is sufficient to perform this function (Gao *et al*., 2009). The NleH effectors also share significant sequence similarity with the *Shigella* effector OspG, a Ser/Thr protein kinase which prevents ubiquitination and subsequent degradation of phospho-IκB and downstream activation of NF-κB (Kim *et al*., 2005). Similar to OspG, NleH1 and NleH2 are autophosphorylated Ser/Thr protein kinases; however, their kinase activity is independent of their interaction with RPS3 (Gao *et al*., 2009). NleH1 and NleH2 also suppress TNF-induced IκBα degradation by interfering with phospho-IκB ubiquitination, which is dependent on conserved lysine residues K159 and K169 in NleH1 and NleH2 from EPEC respectively (Royan *et al*., 2010) (Fig. 3). Together, NleE, NleB, NleC, NleD and NleH implement a complex but co-ordinated attack on inflammatory signalling, which presumably allows the bacteria to establish infection and avoid immediate elimination by the host innate immune response.

EPEC/EHEC-induced diarrhoea

The precise mechanisms by which EPEC and EHEC cause diarrhoea are elusive but the development of diarrhoea is closely related to bacterial load and disease probably results from a combination of factors, including microvillus effacement, dysregulated ion and glucose transport, inhibition of water absorption channels (aquaporins), disruption of epithelial tight junctions and inflammatory changes in the gut (reviewed in Viswanathan *et al*., 2009). Several effector proteins have been implicated in the ability of EPEC and EHEC to alter ion transport in the gut and disrupt epithelial barrier function, including Map, EspF and EspG (Viswanathan *et al*., 2009) and more recently EspM and EspI (Simovitch *et al*., 2010; Thanabalasuriar *et al*., 2010a). The effect of EPEC and EHEC on tight junctions and ion transport is probably the result of effector activity on diverse cellular processes such as protein secretion and membrane trafficking (EspI, EspG), cytoskeletal function (Map, EspM) and/or direct inhibition of ion transport (EspF) (Kim *et al*., 2007; Hodges *et al*., 2008; Simovitch *et al*., 2010; Thanabalasuriar *et al*., 2010a; Selyunin *et al*., 2011). The mechanism of EspI-dependent disruption of tight junctions is likely related to the ability of EspI to bind Sec24 and inhibit COPII vesicle function and therefore protein secretion (Kim *et al*., 2007; Lee *et al*., 2008); however, the EspI PDZ-binding motif is dispensable for this activity (Thanabalasuriar *et al*.,

2010b). EspF-dependent diarrhoea has been attributed to the down regulation of sodium hydrogen exchanger 3 (NHE) activity which is independent of SNX9 binding or the role of EspF in apoptosis (Hodges *et al*., 2008). Notably, few of the effector proteins have been studied *in vivo* using REPEC infection of rabbits, the most representative small animal model of A/E pathogen-induced diarrhoea (Robins-Browne *et al*., 1994). Hence the combined activity of the effectors and their contribution to diarrhoea is incompletely understood and warrants further research using appropriate models of disease.

Conclusions

Recent advances in characterizing the biochemical functions of T3SS effectors from A/E pathogens have revealed a highly evolved bacterium that exerts exquisite control over its host, targeting multiple pathways and structures in an organized and deliberate manner. While inflicting this co-ordinated assault, a subset of the effectors ensures that infected cells, and thus their associated bacteria, remain alive. This cellular protection is central to successful multiplication and colonization by the pathogen. Until recently, the biochemical functions of only a handful of T3SS effectors were known, mainly those involved in cytoskeletal reorganization and disruption of tight junctions. It is now evident that A/E pathogens are remarkably versatile pathogens that target numerous cell organelles and pathways to gain an advantage over the host. Diverse effector complements allow individual EPEC and EHEC strains to deploy varied infection strategies, enabling A/E pathogens to infect different tissues and hosts and survive in diverse environments and animal reservoirs. A/E pathogen-induced disease is thus the cumulative outcome of a repertoire of effector proteins that perturb different facets of host physiology.

Acknowledgements

This work was supported by grants awarded to E.L.H. from the Australian National Health and Medical Research Council (NHMRC) and to G.F. from the Wellcome Trust and Medical Research Council (MRC). E.L.H. is supported by an Australian Research Council (ARC) Future Fellowship. J.S.P. is supported by an Australian Postgraduate Award.

References

Abe, A., de Grado, M., Pfuetzner, R.A., Sanchez-Sanmartin, C., Devinney, R., Puente, J.L., *et al*. (1999) Enteropathogenic *Escherichia coli* translocated intimin receptor, Tir, requires a specific chaperone for stable secretion. *Mol Microbiol* **33:** 1162–1175.

Abul-Milh, M., Wu, Y., Lau, B., Lingwood, C.A., and Barnett Foster, D. (2001) Induction of epithelial cell death including apoptosis by enteropathogenic *Escherichia coli* expressing bundle-forming pili. *Infect Immun* **69:** 7356–7364.

Alto, N.M., Shao, F., Lazar, C.S., Brost, R.L., Chua, G., Mattoo, S., *et al*. (2006) Identification of a bacterial type III effector family with G protein mimicry functions. *Cell* **124:** 133–145.

Alto, N.M., Weflen, A.W., Rardin, M.J., Yarar, D., Lazar, C.S., Tonikian, R., *et al*. (2007) The type III effector EspF coordinates membrane trafficking by the spatiotemporal activation of two eukaryotic signaling pathways. *J Cell Biol* **178:** 1265–1278.

Anton, I.M., Lu, W., Mayer, B.J., Ramesh, N., and Geha, R.S. (1998) The Wiskott-Aldrich syndrome protein-interacting protein (WIP) binds to the adaptor protein Nck. *J Biol Chem* **273:** 20992–20995.

Arbeloa, A., Bulgin, R.R., MacKenzie, G., Shaw, R.K., Pallen, M.J., Crepin, V.F., *et al*. (2008) Subversion of actin dynamics by EspM effectors of attaching and effacing bacterial pathogens. *Cell Microbiol* **10:** 1429–1441.

Arbeloa, A., Blanco, M., Moreira, F.C., Bulgin, R., Lopez, C., Dahbi, G., *et al*. (2009) Distribution of espM and espT among enteropathogenic and enterohaemorrhagic *Escherichia coli*. *J Med Microbiol* **58:** 988–995.

Arbeloa, A., Garnett, J., Lillington, J., Bulgin, R.R., Berger, C.N., Lea, S.M., *et al*. (2010) EspM2 is a RhoA guanine nucleotide exchange factor. *Cell Microbiol* **12:** 654–664.

Arbeloa, A., Oates, C.V., Marches, O., Hartland, E.L., and Frankel, G. (2011) Enteropathogenic *Escherichia coli* type III secretion effector EspV induces radical morphological changes in eukaryotic cells. *Infect Immun* **79:** 1067–1076.

Barthold, S.W., Coleman, G.L., Jacoby, R.O., Livestone, E.M., and Jonas, A.M. (1978) Transmissible murine colonic hyperplasia. *Vet Pathol* **15:** 223–236.

Baruch, K., Gur-Arie, L., Nadler, C., Koby, S., Yerushalmi, G., Ben-Neriah, Y., *et al*. (2011) Metalloprotease type III effectors that specifically cleave JNK and NF-kappaB. *EMBO J* **30:** 221–231.

Batchelor, M., Guignot, J., Patel, A., Cummings, N., Cleary, J., Knutton, S., *et al*. (2004) Involvement of the intermediate filament protein cytokeratin-18 in actin pedestal formation during EPEC infection. *EMBO Rep* **5:** 219.

Berdichevsky, T., Friedberg, D., Nadler, C., Rokney, A., Oppenheim, A., and Rosenshine, I. (2005) Ler is a negative autoregulator of the LEE1 operon in enteropathogenic *Escherichia coli*. *J Bacteriol* **187:** 349–357.

Berger, C.N., Crepin, V.F., Jepson, M.A., Arbeloa, A., and Frankel, G. (2009) The mechanisms used by enteropathogenic *Escherichia coli* to control filopodia dynamics. *Cell Microbiol* **11:** 309–322.

Bommarius, B., Maxwell, D., Swimm, A., Leung, S., Corbett, A., Bornmann, W., and Kalman, D. (2007) Enteropathogenic *Escherichia coli* Tir is an SH2/3 ligand that recruits and activates tyrosine kinases required for pedestal formation. *Mol Microbiol* **63:** 1748–1768.

Brady, M.J., Campellone, K.G., Ghildiyal, M., and Leong, J.M. (2007) Enterohaemorrhagic and enteropathogenic *Escherichia coli* Tir proteins trigger a common Nck-independent actin assembly pathway. *Cell Microbiol* **9:** 2242–2253.

Brown, M.D., Bry, L., Li, Z., and Sacks, D.B. (2008) Actin pedestal formation by enteropathogenic *Escherichia coli* is

regulated by IQGAP1, calcium, and calmodulin. *J Biol Chem* **283:** 35212–35222.

Brutinel, E.D., and Yahr, T.L. (2008) Control of gene expression by type III secretory activity. *Curr Opin Microbiol* **11:** 128–133.

Bulgin, R., Arbeloa, A., Goulding, D., Dougan, G., Crepin, V.F., Raymond, B., and Frankel, G. (2009) The T3SS effector EspT defines a new category of invasive enteropathogenic *E. coli* (EPEC) which form intracellular actin pedestals. *PLoS Pathog* **5:** e1000683.

Bulgin, R., Raymond, B., Garnett, J.A., Frankel, G., Crepin, V.F., Berger, C.N., and Arbeloa, A. (2010) Bacterial guanine nucleotide exchange factors SopE-like and WxxxE effectors. *Infect Immun* **78:** 1417–1425.

Buss, C., Muller, D., Ruter, C., Heusipp, G., and Schmidt, M.A. (2009) Identification and characterization of Ibe, a novel type III effector protein of A/E pathogens targeting human IQGAP1. *Cell Microbiol* **11:** 661–677.

Bustamante, V.H., Santana, F.J., Calva, E., and Puente, J.L. (2001) Transcriptional regulation of type III secretion genes in enteropathogenic *Escherichia coli*: Ler antagonizes H-NS-dependent repression. *Mol Microbiol* **39:** 664–678.

Buttner, D., and Bonas, U. (2002) Port of entry – the type III secretion translocon. *Trends Microbiol* **10:** 186–192.

Campellone, K.G., and Leong, J.M. (2005) Nck-independent actin assembly is mediated by two phosphorylated tyrosines within enteropathogenic *Escherichia coli* Tir. *Mol Microbiol* **56:** 416–432.

Campellone, K.G., Rankin, S., Pawson, T., Kirschner, M.W., Tipper, D.J., and Leong, J.M. (2004a) Clustering of Nck by a 12-residue Tir phosphopeptide is sufficient to trigger localized actin assembly. *J Cell Biol* **164:** 407–416.

Campellone, K.G., Robbins, D., and Leong, J.M. (2004b) EspFU is a translocated EHEC effector that interacts with Tir and N-WASP and promotes Nck-independent actin assembly. *Dev Cell* **7:** 217–228.

Campellone, K.G., Cheng, H.C., Robbins, D., Siripala, A.D., McGhie, E.J., Hayward, R.D., *et al*. (2008) Repetitive N-WASP-binding elements of the enterohemorrhagic *Escherichia coli* effector EspF(U) synergistically activate actin assembly. *PLoS Pathog* **4:** e1000191.

Cantarelli, V.V., Kodama, T., Nijstad, N., Abolghait, S.K., Nada, S., Okada, M., *et al*. (2007) Tyrosine phosphorylation controls cortactin binding to two enterohaemorrhagic *Escherichia coli* effectors: Tir and EspFu/TccP. *Cell Microbiol* **9:** 1782–1795.

Caron, E., and Hall, A. (1998) Identification of two distinct mechanisms of phagocytosis controlled by different Rho GTPases. *Science* **282:** 1717–1721.

Charpentier, X., and Oswald, E. (2004) Identification of the secretion and translocation domain of the enteropathogenic and enterohemorrhagic *Escherichia coli* effector Cif, using TEM-1 beta-lactamase as a new fluorescence-based reporter. *J Bacteriol* **186:** 5486–5495.

Cheng, H.C., Skehan, B.M., Campellone, K.G., Leong, J.M., and Rosen, M.K. (2008) Structural mechanism of WASP activation by the enterohaemorrhagic *E. coli* effector EspF(U). *Nature* **454:** 1009–1013.

Coppolino, M.G., Krause, M., Hagendorff, P., Monner, D.A., Trimble, W., Grinstein, S., *et al*. (2001) Evidence for a molecular complex consisting of Fyb/SLAP, SLP-76, Nck, VASP and WASP that links the actin cytoskeleton to Fcgamma receptor signalling during phagocytosis. *J Cell Sci* **114:** 4307–4318.

Cox, D., Berg, J.S., Cammer, M., Chinegwundoh, J.O., Dale, B.M., Cheney, R.E., and Greenberg, S. (2002) Myosin X is a downstream effector of PI(3)K during phagocytosis. *Nat Cell Biol* **4:** 469–477.

Crane, J.K., Majumdar, S., and Pickhardt, D.F., 3rd (1999) Host cell death due to enteropathogenic Escherichia coli has features of apoptosis. *Infect Immun* **67:** 2575–2584.

Crane, J.K., McNamara, B.P., and Donnenberg, M.S. (2001) Role of EspF in host cell death induced by enteropathogenic *Escherichia coli*. *Cell Microbiol* **3:** 197–211.

Creasey, E.A., Delahay, R.M., Bishop, A.A., Shaw, R.K., Kenny, B., Knutton, S., and Frankel, G. (2003) CesT is a bivalent enteropathogenic *Escherichia coli* chaperone required for translocation of both Tir and Map. *Mol Microbiol* **47:** 209–221.

Crepin, V.F., Girard, F., Schuller, S., Phillips, A.D., Mousnier, A., and Frankel, G. (2010) Dissecting the role of the Tir:Nck and Tir:IRTKS/IRSp53 signalling pathways in vivo. *Mol Microbiol* **75:** 308–323.

Cui, J., Yao, Q., Li, S., Ding, X., Lu, Q., Mao H., *et al*. (2010) Glutamine deamidation and dysfunction of ubiquitin/NEDD8 induced by a bacterial effector family. *Science* **329:** 1215–1218.

Daniell, S.J., Takahashi, N., Wilson, R., Friedberg, D., Rosenshine, I., Booy, F.P., *et al*. (2001) The filamentous type III secretion translocon of enteropathogenic *Escherichia coli*. *Cell Microbiol* **3:** 865–871.

Dean, P., and Kenny, B. (2004) Intestinal barrier dysfunction by enteropathogenic *Escherichia coli* is mediated by two effector molecules and a bacterial surface protein. *Mol Microbiol* **54:** 665–675.

Dean, P., Maresca, M., Schuller, S., Phillips, A.D., and Kenny, B. (2006) Potent diarrheagenic mechanism mediated by the cooperative action of three enteropathogenic *Escherichia coli*-injected effector proteins. *Proc Natl Acad Sci USA* **103:** 1876–1881.

Dean, P., Scott, J.A., Knox, A.A., Quitard, S., Watkins, N.J., and Kenny, B. (2010) The enteropathogenic *E. coli* effector EspF targets and disrupts the nucleolus by a process regulated by mitochondrial dysfunction. *PLoS Pathog* **6:** e1000961.

Deibel, C., Kramer, S., Chakraborty, T., and Ebel, F. (1998) EspE, a novel secreted protein of attaching and effacing bacteria, is directly translocated into infected host cells, where it appears as a tyrosine-phosphorylated 90 kDa protein. *Mol Microbiol* **28:** 463–474.

Deng, W., Puente, J.L., Gruenheid, S., Li, Y., Vallance, B.A., Vazquez, A., *et al*. (2004) Dissecting virulence: systematic and functional analyses of a pathogenicity island. *Proc Natl Acad Sci USA* **101:** 3597–3602.

Deng, W., Li, Y., Hardwidge, P.R., Frey, E.A., Pfuetzner, R.A., Lee, S., *et al*. (2005) Regulation of type III secretion hierarchy of translocators and effectors in attaching and effacing bacterial pathogens. *Infect Immun* **73:** 2135–2146.

Diakonova, M., Bokoch, G., and Swanson, J.A. (2002) Dynamics of cytoskeletal proteins during Fcgamma receptor-mediated phagocytosis in macrophages. *Mol Biol Cell* **13:** 402–411.

Dong, N., Liu, L., and Shao, F. (2010) A bacterial effector targets host DH-PH domain RhoGEFs and antagonizes macrophage phagocytosis. *EMBO J* **29:** 1363–1376.

Elliott, S.J., Wainwright, L.A., McDaniel, T.K., Jarvis, K.G., Deng, Y.K., Lai, L.C., *et al*. (1998) The complete sequence of the locus of enterocyte effacement (LEE) from enteropathogenic *Escherichia coli* E2348/69. *Mol Microbiol* **28:** 1–4.

Elliott, S.J., Hutcheson, S.W., Dubois, M.S., Mellies, J.L., Wainwright, L.A., Batchelor, M., *et al*. (1999) Identification of CesT, a chaperone for the type III secretion of Tir in enteropathogenic *Escherichia coli*. *Mol Microbiol* **33:** 1176–1189.

Elliott, S.J., Sperandio, V., Giron, J.A., Shin, S., Mellies, J.L., Wainwright, L., *et al*. (2000) The locus of enterocyte effacement (LEE)-encoded regulator controls expression of both LEE- and non-LEE-encoded virulence factors in enteropathogenic and enterohemorrhagic *Escherichia coli*. *Infect Immun* **68:** 6115–6126.

Frankel, G., and Phillips, A.D. (2008) Attaching effacing *Escherichia coli* and paradigms of Tir-triggered actin polymerization: getting off the pedestal. *Cell Microbiol* **10:** 549–556.

Frankel, G., Phillips, A.D., Rosenshine, I., Dougan, G., Kaper, J.B., and Knutton, S. (1998) Enteropathogenic and enterohaemorrhagic *Escherichia coli*: more subversive elements. *Mol Microbiol* **30:** 911–921.

Freeman, N.L., Zurawski, D.V., Chowrashi, P., Ayoob, J.C., Huang, L., Mittal, B., *et al*. (2000) Interaction of the enteropathogenic *Escherichia coli* protein, translocated intimin receptor (Tir), with focal adhesion proteins. *Cell Motil Cytoskeleton* **47:** 307–318.

Gao, X., Wan, F., Mateo, K., Callegari, E., Wang, D., Deng, W., *et al*. (2009) Bacterial effector binding to ribosomal protein s3 subverts NF-kappaB function. *PLoS Pathog* **5:** e1000708.

Garmendia, J., Phillips, A.D., Carlier, M.F., Chong, Y., Schuller, S., Marches, O., *et al*. (2004) TccP is an enterohaemorrhagic *Escherichia coli* O157:H7 type III effector protein that couples Tir to the actin-cytoskeleton. *Cell Microbiol* **6:** 1167–1183.

Garmendia, J., Carlier, M.F., Egile, C., Didry, D., and Frankel, G. (2006) Characterization of TccP-mediated N-WASP activation during enterohaemorrhagic *Escherichia coli* infection. *Cell Microbiol* **8:** 1444–1455.

Gauthier, A., and Finlay, B.B. (2003) Translocated intimin receptor and its chaperone interact with ATPase of the type III secretion apparatus of enteropathogenic *Escherichia coli*. *J Bacteriol* **185:** 6747–6755.

Germane, K.L., and Spiller, B.W. (2011) Structural and functional studies indicate that the EPEC effector, EspG, directly binds p21-activated kinase. *Biochemistry* **50:** 917–919.

Ghosh, P. (2004) Process of protein transport by the type III secretion system. *Microbiol Mol Biol Rev* **68:** 771–795.

Goosney, D.L., DeVinney, R., Pfuetzner, R.A., Frey, E.A., Strynadka, N.C., and Finlay, B.B. (2000) Enteropathogenic *E. coli* translocated intimin receptor, Tir, interacts directly with alpha-actinin. *Curr Biol* **10:** 735–738.

Gruenheid, S., DeVinney, R., Bladt, F., Goosney, D., Gelkop, S., Gish, G.D., *et al*. (2001) Enteropathogenic *E. coli* Tir binds Nck to initiate actin pedestal formation in host cells. *Nat Cell Biol* **3:** 856–859.

Gruenheid, S., Sekirov, I., Thomas, N.A., Deng, W., O'Donnell, P., Goode, D., *et al*. (2004) Identification and characterization of NleA, a non-LEE-encoded type III translocated virulence factor of enterohaemorrhagic *Escherichia coli* O157:H7. *Mol Microbiol* **51:** 1233–1249.

Gu, B.J., Saunders, B.M., Jursik, C., and Wiley, J.S. (2010) The P2X7-nonmuscle myosin membrane complex regulates phagocytosis of nonopsonized particles and bacteria by a pathway attenuated by extracellular ATP. *Blood* **115:** 1621–1631.

Guttman, J.A., Li, Y., Wickham, M.E., Deng, W., Vogl, A.W., and Finlay, B.B. (2006) Attaching and effacing pathogen-induced tight junction disruption in vivo. *Cell Microbiol* **8:** 634–645.

Hamaguchi, M., Hamada, D., Suzuki, K.N., Sakata, I., and Yanagihara, I. (2008) Molecular basis of actin reorganization promoted by binding of enterohaemorrhagic *Escherichia coli* EspB to alpha-catenin. *FEBS J* **275:** 6260–6267.

Hardwidge, P.R., Deng, W., Vallance, B.A., Rodriguez-Escudero, I., Cid, V.J., Molina, M., and Finlay, B.B. (2005) Modulation of host cytoskeleton function by the enteropathogenic *Escherichia coli* and *Citrobacter rodentium* effector protein EspG. *Infect Immun* **73:** 2586–2594.

Hartland, E.L., Batchelor, M., Delahay, R.M., Hale, C., Matthews, S., Dougan, G., *et al*. (1999) Binding of intimin from enteropathogenic *Escherichia coli* to Tir and to host cells. *Mol Microbiol* **32:** 151–158.

Hartland, E.L., Daniell, S.J., Delahay, R.M., Neves, B.C., Wallis, T., Shaw, R.K., *et al*. (2000) The type III protein translocation system of enteropathogenic *Escherichia coli* involves EspA-EspB protein interactions. *Mol Microbiol* **35:** 1483–1492.

Hemrajani, C., Marches, O., Wiles, S., Girard, F., Dennis, A., Dziva, F., *et al*. (2008) Role of NleH, a type III secreted effector from attaching and effacing pathogens, in colonization of the bovine, ovine, and murine gut. *Infect Immun* **76:** 4804–4813.

Hemrajani, C., Berger, C.N., Robinson, K.S., Marches, O., Mousnier, A., and Frankel, G. (2010) NleH effectors interact with Bax inhibitor-1 to block apoptosis during enteropathogenic *Escherichia coli* infection. *Proc Natl Acad Sci USA* **107:** 3129–3134.

Hodges, K., Alto, N.M., Ramaswamy, K., Dudeja, P.K., and Hecht, G. (2008) The enteropathogenic *Escherichia coli* effector protein EspF decreases sodium hydrogen exchanger 3 activity. *Cell Microbiol* **10:** 1735–1745.

Huang, Z., Sutton, S.E., Wallenfang, A.J., Orchard, R.C., Wu, X., Feng, Y., *et al*. (2009) Structural insights into host GTPase isoform selection by a family of bacterial GEF mimics. *Nat Struct Mol Biol* **16:** 853–860.

Hughes, D.T., and Sperandio, V. (2008) Inter-kingdom signalling: communication between bacteria and their hosts. *Nat Rev Microbiol* **6:** 111–120.

Ide, T., Laarmann, S., Greune, L., Schillers, H., Oberleithner, H., and Schmidt, M.A. (2001) Characterization of translocation pores inserted into plasma membranes by type III-secreted Esp proteins of enteropathogenic *Escherichia coli*. *Cell Microbiol* **3:** 669–679.

Iguchi, A., Thomson, N.R., Ogura, Y., Saunders, D., Ooka, T.,

Henderson, I.R., *et al*. (2009) Complete genome sequence and comparative genome analysis of enteropathogenic *Escherichia coli* O127:H6 strain E2348/69. *J Bacteriol* **191:** 347–354.

Iizumi, Y., Sagara, H., Kabe, Y., Azuma, M., Kume, K., Ogawa, M., *et al*. (2007) The enteropathogenic *E. coli* effector EspB facilitates microvillus effacing and antiphagocytosis by inhibiting myosin function. *Cell Host Microbe* **2:** 383–392.

Iyoda, S., Koizumi, N., Satou, H., Lu, Y., Saitoh, T., Ohnishi, M., and Watanabe, H. (2006) The GrlR-GrlA regulatory system coordinately controls the expression of flagellar and LEE-encoded type III protein secretion systems in enterohemorrhagic *Escherichia coli*. *J Bacteriol* **188:** 5682–5692.

Jarvis, K.G., Giron, J.A., Jerse, A.E., McDaniel, T.K., Donnenberg, M.S., and Kaper, J.B. (1995) Enteropathogenic *Escherichia coli* contains a putative type III secretion system necessary for the export of proteins involved in attaching and effacing lesion formation. *Proc Natl Acad Sci USA* **92:** 7996–8000.

Jerse, A.E., Yu, J., Tall, B.D., and Kaper, J.B. (1990) A genetic locus of enteropathogenic *Escherichia coli* necessary for the production of attaching and effacing lesions on tissue culture cells. *Proc Natl Acad Sci USA* **87:** 7839–7843.

Jubelin, G., Taieb, F., Duda, D.M., Hsu, Y., Samba-Louaka, A., Nobe, R., *et al*. (2010) Pathogenic bacteria target NEDD8-conjugated cullins to hijack host-cell signaling pathways. *PLoS Pathog* **6:** e1001128.

Kelly, M., Hart, E., Mundy, R., Marches, O., Wiles, S., Badea, L., *et al*. (2006) Essential role of the type III secretion system effector NleB in colonization of mice by *Citrobacter rodentium*. *Infect Immun* **74:** 2328–2337.

Kenny, B. (1999) Phosphorylation of tyrosine 474 of the enteropathogenic *Escherichia coli* (EPEC) Tir receptor molecule is essential for actin nucleating activity and is preceded by additional host modifications. *Mol Microbiol* **31:** 1229–1241.

Kenny, B., and Jepson, M. (2000) Targeting of an enteropathogenic *Escherichia coli* (EPEC) effector protein to host mitochondria. *Cell Microbiol* **2:** 579–590.

Kenny, B., DeVinney, R., Stein, M., Reinscheid, D.J., Frey, E.A., and Finlay, B.B. (1997) Enteropathogenic *E. coli* (EPEC) transfers its receptor for intimate adherence into mammalian cells. *Cell* **91:** 511–520.

Kenny, B., Ellis, S., Leard, A.D., Warawa, J., Mellor, H., and Jepson, M.A. (2002) Co-ordinate regulation of distinct host cell signalling pathways by multifunctional enteropathogenic *Escherichia coli* effector molecules. *Mol Microbiol* **44:** 1095–1107.

Khan, M.A., Bouzari, S., Ma, C., Rosenberger, C.M., Bergstrom, K.S., Gibson, D.L., *et al*. (2008) Flagellin-dependent and -independent inflammatory responses following infection by enteropathogenic *Escherichia coli* and *Citrobacter rodentium*. *Infect Immun* **76:** 1410–1422.

Kim, D.W., Lenzen, G., Page, A.L., Legrain, P., Sansonetti, P.J., and Parsot, C. (2005) The *Shigella flexneri* effector OspG interferes with innate immune responses by targeting ubiquitin-conjugating enzymes. *Proc Natl Acad Sci USA* **102:** 14046–14051.

Kim, J., Thanabalasuriar, A., Chaworth-Musters, T., Fromme, J.C., Frey, E.A., Lario, P.I., *et al*. (2007) The bacterial virulence factor NleA inhibits cellular protein secretion by disrupting mammalian COPII function. *Cell Host Microbe* **2:** 160–171.

Kim, M., Ogawa, M., Fujita, Y., Yoshikawa, Y., Nagai, T., Koyama, T., *et al*. (2009) Bacteria hijack integrin-linked kinase to stabilize focal adhesions and block cell detachment. *Nature* **459:** 578–582.

Knappstein, S., Ide, T., Schmidt, M.A., and Heusipp, G. (2004) Alpha 1-antitrypsin binds to and interferes with functionality of EspB from atypical and typical enteropathogenic *Escherichia coli* strains. *Infect Immun* **72:** 4344–4350.

Knutton, S., Rosenshine, I., Pallen, M.J., Nisan, I., Neves, B.C., Bain, C., *et al*. (1998) A novel EspA-associated surface organelle of enteropathogenic *Escherichia coli* involved in protein translocation into epithelial cells. *EMBO J* **17:** 2166–2176.

Kodama, T., Akeda, Y., Kono, G., Takahashi, A., Imura, K., Iida, T., and Honda, T. (2002) The EspB protein of enterohaemorrhagic *Escherichia coli* interacts directly with alpha-catenin. *Cell Microbiol* **4:** 213–222.

Kubori, T., and Galan, J.E. (2003) Temporal regulation of *Salmonella* virulence effector function by proteasome-dependent protein degradation. *Cell* **115:** 333–342.

Kurushima, J., Nagai, T., Nagamatsu, K., and Abe, A. (2010) EspJ effector in enterohemorrhagic *E. coli* translocates into host mitochondria via an atypical mitochondrial targeting signal. *Microbiol Immunol* **54:** 371–379.

Lee, S.F., Kelly, M., McAlister, A., Luck, S.N., Garcia, E.L., Hall, R.A., *et al*. (2008) A C-terminal class I PDZ binding motif of EspI/NleA modulates the virulence of attaching and effacing *Escherichia coli* and *Citrobacter rodentium*. *Cell Microbiol* **10:** 499–513.

Li, Q., and Verma, I.M. (2002) NF-kappaB regulation in the immune system. *Nat Rev Immunol* **2:** 725–734.

Lommel, S., Benesch, S., Rottner, K., Franz, T., Wehland, J., and Kuhn, R. (2001) Actin pedestal formation by enteropathogenic *Escherichia coli* and intracellular motility of *Shigella flexneri* are abolished in N-WASP-defective cells. *EMBO Rep* **2:** 850–857.

Ma, C., Wickham, M.E., Guttman, J.A., Deng, W., Walker, J., Madsen, K.L., *et al*. (2006) *Citrobacter rodentium* infection causes both mitochondrial dysfunction and intestinal epithelial barrier disruption in vivo: role of mitochondrial associated protein (Map). *Cell Microbiol* **8:** 1669–1686.

McNamara, B.P., Koutsouris, A., O'Connell, C.B., Nougayrede, J.P., Donnenberg, M.S., and Hecht, G. (2001) Translocated EspF protein from enteropathogenic *Escherichia coli* disrupts host intestinal barrier function. *J Clin Invest* **107:** 621–629.

Marches, O., Ledger, T.N., Boury, M., Ohara, M., Tu, X., Goffaux, F., *et al*. (2003) Enteropathogenic and enterohaemorrhagic *Escherichia coli* deliver a novel effector called Cif, which blocks cell cycle G2/M transition. *Mol Microbiol* **50:** 1553–1567.

Marches, O., Wiles, S., Dziva, F., Ragione, R.M.L., Schuller, S., Best, A., *et al*. (2005) Characterization of two non-locus of enterocyte effacement-encoded type III-translocated effectors, NleC and NleD, in attaching and effacing pathogens. *Infect Immun* **73:** 8411–8417.

Marches, O., Batchelor, M., Shaw, R.K., Patel, A., Cummings, N., Nagai, T., *et al.* (2006) EspF of enteropathogenic *Escherichia coli* binds sorting nexin 9. *J Bacteriol* **188:** 3110–3115.

Marches, O., Covarelli, V., Dahan, S., Cougoule, C., Bhatta, P., Frankel, G., and Caron, E. (2008) EspJ of enteropathogenic and enterohaemorrhagic *Escherichia coli* inhibits opsono-phagocytosis. *Cell Microbiol* **10:** 1104–1115.

Martinez, E., Schroeder, G.N., Berger, C.N., Lee, S.F., Robinson, K.S., Badea, L., *et al.* (2010) Binding to Na(+) /H(+) exchanger regulatory factor 2 (NHERF2) affects trafficking and function of the enteropathogenic *Escherichia coli* type III secretion system effectors Map, EspI and NleH. *Cell Microbiol* **12:** 1718–1731.

Matsuzawa, T., Kuwae, A., Yoshida, S., Sasakawa, C., and Abe, A. (2004) Enteropathogenic *Escherichia coli* activates the RhoA signaling pathway via the stimulation of GEF-H1. *EMBO J* **23:** 3570–3582.

Mills, E., Baruch, K., Charpentier, X., Kobi, S., and Rosenshine, I. (2008) Real-time analysis of effector translocation by the type III secretion system of enteropathogenic *Escherichia coli*. *Cell Host Microbe* **3:** 104–113.

Miyahara, A., Nakanishi, N., Ooka, T., Hayashi, T., Sugimoto, N., and Tobe, T. (2009) Enterohemorrhagic *Escherichia coli* effector EspL2 induces actin microfilament aggregation through annexin 2 activation. *Cell Microbiol* **11:** 337–350.

Moreau, V., Frischknecht, F., Reckmann, I., Vincentelli, R., Rabut, G., Stewart, D., and Way, M. (2000) A complex of N-WASP and WIP integrates signalling cascades that lead to actin polymerization. *Nat Cell Biol* **2:** 441–448.

Morikawa, H., Kim, M., Mimuro, H., Punginelli, C., Koyama, T., Nagai, S., *et al.* (2010) The bacterial effector Cif interferes with SCF ubiquitin ligase function by inhibiting deneddylation of Cullin1. *Biochem Biophys Res Commun* **401:** 268–274.

Morita-Ishihara, T., Terajima, J., Watanabe, H., and Izumiya, H. (2009) Interaction between enterohemorrhagic *Escherichia coli* O157:H7 EspFu and IRSp53 induces dynamic membrane remodeling in epithelial cells. *Jpn J Infect Dis* **62:** 351–355.

Muehlen, S., Ruchaud-Sparagano, M.H., and Kenny, B. (2011) Proteasome-independent degradation of canonical NF{kappa}B complex components by the NleC protein of pathogenic *E.coli*. *J Biol Chem* **286:** 5100–5107.

Munera, D., Crepin, V.F., Marches, O., and Frankel, G. (2010) N-terminal type III secretion signal of enteropathogenic *Escherichia coli* translocator proteins. *J Bacteriol* **192:** 3534–3539.

Muza-Moons, M.M., Schneeberger, E.E., and Hecht, G.A. (2004) Enteropathogenic *Escherichia coli* infection leads to appearance of aberrant tight junctions strands in the lateral membrane of intestinal epithelial cells. *Cell Microbiol* **6:** 783–793.

Nadler, C., Baruch, K., Kobi, S., Mills, E., Haviv, G., Farago, M., *et al.* (2010) The Type III Secretion Effector NleE Inhibits NF-kappaB Activation. *PLoS Pathog* **6:** e1000743.

Nataro, J.P., and Kaper, J.B. (1998) Diarrheagenic *Escherichia coli*. *Clin Microbiol Rev* **11:** 142–201.

Newton, H.J., Pearson, J.S., Badea, L., Kelly, M., Lucas, M., Holloway, G., *et al.* (2010) The type III effectors NleE and NleB from enteropathogenic *E. coli* and OspZ from *Shigella* block nuclear translocation of NF-kappaB p65. *PLoS Pathog* **6:** e1000898.

Nieto-Pelegrin, E., and Martinez-Quiles, N. (2009) Distinct phosphorylation requirements regulate cortactin activation by TirEPEC and its binding to N-WASP. *Cell Commun Signal* **7:** 11.

Nobe, R., Nougayrede, J.P., Taieb, F., Bardiau, M., Cassart, D., Navarro-Garcia, F., *et al.* (2009) Enterohaemorrhagic *Escherichia coli* serogroup O111 inhibits NF-{kappa}B-dependent innate responses in a manner independent of a type III secreted OspG orthologue. *Microbiology* **155:** 3214–3225.

Nougayrede, J.P., and Donnenberg, M.S. (2004) Enteropathogenic *Escherichia coli* EspF is targeted to mitochondria and is required to initiate the mitochondrial death pathway. *Cell Microbiol* **6:** 1097–1111.

Nougayrede, J.P., Foster, G.H., and Donnenberg, M.S. (2007) Enteropathogenic *Escherichia coli* effector EspF interacts with host protein Abcf2. *Cell Microbiol* **9:** 680–693.

O'Connell, C.B., Creasey, E.A., Knutton, S., Elliott, S., Crowther, L.J., Luo, W., *et al.* (2004) SepL, a protein required for enteropathogenic *Escherichia coli* type III translocation, interacts with secretion component SepD. *Mol Microbiol* **52:** 1613–1625.

Ogura, Y., Ooka, T., Whale, A., Garmendia, J., Beutin, L., Tennant, S., *et al.* (2007) TccP2 of O157:H7 and non-O157 enterohemorrhagic *Escherichia coli* (EHEC): challenging the dogma of EHEC-induced actin polymerization. *Infect Immun* **75:** 604–612.

Papatheodorou, P., Domanska, G., Oxle, M., Mathieu, J., Selchow, O., Kenny, B., and Rassow, J. (2006) The enteropathogenic *Escherichia coli* (EPEC) Map effector is imported into the mitochondrial matrix by the TOM/Hsp70 system and alters organelle morphology. *Cell Microbiol* **8:** 677–689.

Patel, A., Cummings, N., Batchelor, M., Hill, P.J., Dubois, T., Mellits, K.H., *et al.* (2006) Host protein interactions with enteropathogenic *Escherichia coli* (EPEC): 14-3-3tau binds Tir and has a role in EPEC-induced actin polymerization. *Cell Microbiol* **8:** 55–71.

Pearson, J.S., Riedmaier, P., Marches, O., Frankel, G., and Hartland, E.L. (2011) A type III effector protease NleC from enteropathogenic *Escherichia coli* targets NF-κB for degradation. *Mol Microbiol* **80:** 219–230.

Peralta-Ramirez, J., Hernandez, J.M., Manning-Cela, R., Luna-Munoz, J., Garcia-Tovar, C., Nougayrede, J.P., *et al.* (2008) EspF Interacts with nucleation-promoting factors to recruit junctional proteins into pedestals for pedestal maturation and disruption of paracellular permeability. *Infect Immun* **76:** 3854–3868.

Perkins, N.D. (2007) Integrating cell-signalling pathways with NF-kappaB and IKK function. *Nat Rev Mol Cell Biol* **8:** 49–62.

Perna, N.T., Plunkett, G., Burland, V., Mau, B., Glasner, J.D., Rose, D.J., *et al.* (2001) Genome sequence of enterohaemorrhagic *Escherichia coli* O157:H7. *Nature* **409:** 529–533.

Petty, N.K., Bulgin, R., Crepin, V.F., Cerdeno-Tarraga, A.M., Schroeder, G.N., Quail, M.A., *et al.* (2010) The *Citrobacter rodentium* genome sequence reveals convergent evolution

with human pathogenic *Escherichia coli*. *J Bacteriol* **192:** 525–538.
Phillips, N., Hayward, R.D., and Koronakis, V. (2004) Phosphorylation of the enteropathogenic *E. coli* receptor by the Src-family kinase c-Fyn triggers actin pedestal formation. *Nat Cell Biol* **6:** 618–625.
Quitard, S., Dean, P., Maresca, M., and Kenny, B. (2006) The enteropathogenic *Escherichia coli* EspF effector molecule inhibits PI-3 kinase-mediated uptake independently of mitochondrial targeting. *Cell Microbiol* **8:** 972–981.
Ramesh, N., Anton, I.M., Hartwig, J.H., and Geha, R.S. (1997) WIP, a protein associated with wiskott-aldrich syndrome protein, induces actin polymerization and redistribution in lymphoid cells. *Proc Natl Acad Sci USA* **94:** 14671–14676.
Ritchie, J.M., Brady, M.J., Riley, K.N., Ho, T.D., Campellone, K.G., Herman, I.M., *et al*. (2008) EspFU, a type III-translocated effector of actin assembly, fosters epithelial association and late-stage intestinal colonization by *E. coli* O157:H7. *Cell Microbiol* **10:** 836–847.
Robins-Browne, R.M., and Hartland, E.L. (2002) *Escherichia coli* as a cause of diarrhea. *J Gastroenterol Hepatol* **17:** 467–475.
Robins-Browne, R.M., Tokhi, A.M., Adams, L.M., Bennett-Wood, V., Moisidis, A.V., Krejany, E.O., and O'Gorman, L.E. (1994) Adherence characteristics of attaching and effacing strains of *Escherichia coli* from rabbits. *Infect Immun* **62:** 1584–1592.
Robinson, K.S., Mousnier, A., Hemrajani, C., Fairweather, N., Berger, C.N., and Frankel, G. (2010) The enteropathogenic *Escherichia coli* effector NleH inhibits apoptosis induced by Clostridium difficile toxin B. *Microbiology* **156:** 1815–1823.
Robinson, K.S., Clements, A., Williams, A.C., Berger, C.N., and Frankel, G. (2011) Bax inhibitor 1 in apoptosis and disease. *Oncogene* (in press).
Roe, A.J., Naylor, S.W., Spears, K.J., Yull, H.M., Dransfield, T.A., Oxford, M., *et al*. (2004) Co-ordinate single-cell expression of LEE4- and LEE5-encoded proteins of *Escherichia coli* O157:H7. *Mol Microbiol* **54:** 337–352.
Rohatgi, R., Nollau, P., Ho, H.Y., Kirschner, M.W., and Mayer, B.J. (2001) Nck and phosphatidylinositol 4,5-bisphosphate synergistically activate actin polymerization through the N-WASP-Arp2/3 pathway. *J Biol Chem* **276:** 26448–26452.
Royan, S.V., Jones, R.M., Koutsouris, A., Roxas, J.L., Falzari, K., Weflen, A.W., *et al*. (2010) Enteropathogenic *E. coli* non-LEE encoded effectors NleH1 and NleH2 attenuate NF-kappaB activation. *Mol Microbiol* **78:** 1232–1245.
Ruchaud-Sparagano, M.H., Maresca, M., and Kenny, B. (2007) Enteropathogenic *Escherichia coli* (EPEC) inactivate innate immune responses prior to compromising epithelial barrier function. *Cell Microbiol* **9:** 1909–1921.
Russell, R.M., Sharp, F.C., Rasko, D.A., and Sperandio, V. (2007) QseA and GrlR/GrlA regulation of the locus of enterocyte effacement genes in enterohemorrhagic *Escherichia coli*. *J Bacteriol* **189:** 5387–5392.
Sallee, N.A., Rivera, G.M., Dueber, J.E., Vasilescu, D., Mullins, R.D., Mayer, B.J., and Lim, W.A. (2008) The pathogen protein EspF(U) hijacks actin polymerization using mimicry and multivalency. *Nature* **454:** 1005–1008.
Samba-Louaka, A., Nougayrede, J.P., Watrin, C., Jubelin, G., Oswald, E., and Taieb, F. (2008) Bacterial cyclomodulin Cif blocks the host cell cycle by stabilizing the cyclin-dependent kinase inhibitors p21 and p27. *Cell Microbiol* **10:** 2496–2508.
Samba-Louaka, A., Nougayrede, J.P., Watrin, C., Oswald, E., and Taieb, F. (2009) The enteropathogenic *Escherichia coli* effector Cif induces delayed apoptosis in epithelial cells. *Infect Immun* **77:** 5471–5477.
Sason, H., Milgrom, M., Weiss, A.M., Melamed-Book, N., Balla, T., Grinstein, S., *et al*. (2009) Enteropathogenic *Escherichia coli* subverts phosphatidylinositol 4,5-bisphosphate and phosphatidylinositol 3,4,5-trisphosphate upon epithelial cell infection. *Mol Biol Cell* **20:** 544–555.
Schauer, D.B., and Falkow, S. (1993) Attaching and effacing locus of a *Citrobacter freundii* biotype that causes transmissible murine colonic hyperplasia. *Infect Immun* **61:** 2486–2492.
Schuller, S., Chong, Y., Lewin, J., Kenny, B., Frankel, G., and Phillips, A.D. (2007) Tir phosphorylation and Nck/N-WASP recruitment by enteropathogenic and enterohaemorrhagic *Escherichia coli* during ex vivo colonization of human intestinal mucosa is different to cell culture models. *Cell Microbiol* **9:** 1352–1364.
Schuller, S., Lucas, M., Kaper, J.B., Giron, J.A., and Phillips, A.D. (2009) The ex vivo response of human intestinal mucosa to enteropathogenic *Escherichia coli* infection. *Cell Microbiol* **11:** 521–530.
Selbach, M., Paul, F.E., Brandt, S., Guye, P., Daumke, O., Backert, S., *et al*. (2009) Host cell interactome of tyrosine-phosphorylated bacterial proteins. *Cell Host Microbe* **5:** 397–403.
Selyunin, A.S., Sutton, S.E., Weigele, B.A., Reddick, L.E., Orchard, R.C., Bresson, S.M., *et al*. (2011) The assembly of a GTPase-kinase signalling complex by a bacterial catalytic scaffold. *Nature* **469:** 107–111.
Shakhnovich, E.A., Davis, B.M., and Waldor, M.K. (2009) Hfq negatively regulates type III secretion in EHEC and several other pathogens. *Mol Microbiol* **74:** 347–363.
Shames, S.R., Deng, W., Guttman, J.A., de Hoog, C.L., Li, Y., Hardwidge, P.R., *et al*. (2010) The pathogenic *E. coli* type III effector EspZ interacts with host CD98 and facilitates host cell prosurvival signalling. *Cell Microbiol* **2:** 1322–1339.
Sharma, R., Tesfay, S., Tomson, F.L., Kanteti, R.P., Viswanathan, V.K., and Hecht, G. (2006) Balance of bacterial pro- and anti-inflammatory mediators dictates net effect of enteropathogenic *Escherichia coli* on intestinal epithelial cells. *Am J Physiol Gastrointest Liver Physiol* **290:** G685–G694.
Shaw, R.K., Smollett, K., Cleary, J., Garmendia, J., Straatman-Iwanowska, A., Frankel, G., and Knutton, S. (2005) Enteropathogenic *Escherichia coli* type III effectors EspG and EspG2 disrupt the microtubule network of intestinal epithelial cells. *Infect Immun* **73:** 4385–4390.
Shen, Y., Kawamura, I., Nomura, T., Tsuchiya, K., Hara, H., Dewamitta, S.R., *et al*. (2010) Toll-like receptor 2- and MyD88-dependent phosphatidylinositol 3-kinase and Rac1 activation facilitates the phagocytosis of *Listeria monocytogenes* by murine macrophages. *Infect Immun* **78:** 2857–2867.
Simovitch, M., Sason, H., Cohen, S., Zahavi, E.E., Melamed-Book, N., Weiss, A., *et al*. (2010) EspM inhibits pedestal

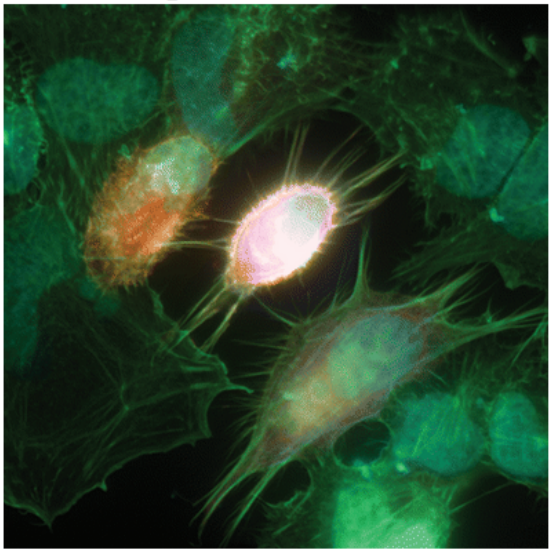
formation by enterohaemorrhagic *Escherichia coli* and enteropathogenic *E. coli* and disrupts the architecture of a polarized epithelial monolayer. *Cell Microbiol* **12:** 489–505.
Simpson, N., Shaw, R., Crepin, V.F., Mundy, R., FitzGerald, A.J., Cummings, N., *et al*. (2006) The enteropathogenic *Escherichia coli* type III secretion system effector Map binds EBP50/NHERF1: implication for cell signalling and diarrhoea. *Mol Microbiol* **60:** 349–363.
Smith, K., Humphreys, D., Hume, P.J., and Koronakis, V. (2010) Enteropathogenic *Escherichia coli* recruits the cellular inositol phosphatase SHIP2 to regulate actin-pedestal formation. *Cell Host Microbe* **7:** 13–24.
Swimm, A., Bommarius, B., Li, Y., Cheng, D., Reeves, P., Sherman, M., *et al*. (2004) Enteropathogenic *Escherichia coli* use redundant tyrosine kinases to form actin pedestals. *Mol Biol Cell* **15:** 3520–3529.
Taieb, F., Nougayrede, J.P., Watrin, C., Samba-Louaka, A., and Oswald, E. (2006) *Escherichia coli* cyclomodulin Cif induces G2 arrest of the host cell cycle without activation of the DNA-damage checkpoint-signalling pathway. *Cell Microbiol* **8:** 1910–1921.
Taylor, K.A., O'Connell, C.B., Luther, P.W., and Donnenberg, M.S. (1998) The EspB protein of enteropathogenic *Escherichia coli* is targeted to the cytoplasm of infected HeLa cells. *Infect Immun* **66:** 5501–5507.
Thanabalasuriar, A., Koutsouris, A., Weflen, A., Mimee, M., Hecht, G., and Gruenheid, S. (2010a) The bacterial virulence factor NleA is required for the disruption of intestinal tight junctions by enteropathogenic *Escherichia coli*. *Cell Microbiol* **12:** 31–41.
Thanabalasuriar, A., Koutsouris, A., Hecht, G., and Gruenheid, S. (2010b) The bacterial virulence factor NleA's involvement in intestinal tight junction disruption during enteropathogenic *E. coli* infection is independent of its putative PDZ binding domain. *Gut Microbes* **1:** 114–118.
Tomson, F.L., Viswanathan, V.K., Kanack, K.J., Kanteti, R.P., Straub, K.V., Menet, M., *et al*. (2005) Enteropathogenic *Escherichia coli* EspG disrupts microtubules and in conjunction with Orf3 enhances perturbation of the tight junction barrier. *Mol Microbiol* **56:** 447–464.
Tu, X., Nisan, I., Yona, C., Hanski, E., and Rosenshine, I. (2003) EspH, a new cytoskeleton-modulating effector of enterohaemorrhagic and enteropathogenic *Escherichia coli*. *Mol Microbiol* **47:** 595–606.
Vingadassalom, D., Kazlauskas, A., Skehan, B., Cheng, H.C., Magoun, L., Robbins, D., *et al*. (2009) Insulin receptor tyrosine kinase substrate links the *E. coli* O157:H7 actin assembly effectors Tir and EspF(U) during pedestal formation. *Proc Natl Acad Sci USA* **106:** 6754–6759.
Vingadassalom, D., Campellone, K.G., Brady, M.J., Skehan, B., Battle, S.E., Robbins, D., *et al*. (2010) Enterohemorrhagic *E. coli* requires N-WASP for efficient type III translocation but not for EspFU-mediated actin pedestal formation. *PLoS Pathog* **6:** e1001056.
Viswanathan, V.K., Lukic, S., Koutsouris, A., Miao, R., Muza, M.M., and Hecht, G. (2004) Cytokeratin 18 interacts with the enteropathogenic *Escherichia coli* secreted protein F (EspF) and is redistributed after infection. *Cell Microbiol* **6:** 987–997.
Viswanathan, V.K., Hodges, K., and Hecht, G. (2009) Enteric infection meets intestinal function: how bacterial pathogens cause diarrhoea. *Nat Rev Microbiol* **7:** 110–119.
Vossenkamper, A., Marches, O., Fairclough, P.D., Warnes, G., Stagg, A.J., Lindsay, J.O., *et al*. (2010) Inhibition of NF-kappaB signaling in human dendritic cells by the enteropathogenic *Escherichia coli* effector protein NleE. *J Immunol* **185:** 4118–4127.
Wachter, C., Beinke, C., Mattes, M., and Schmidt, M.A. (1999) Insertion of EspD into epithelial target cell membranes by infecting enteropathogenic *Escherichia coli*. *Mol Microbiol* **31:** 1695–1707.
Wan, F., Anderson, D.E., Barnitz, R.A., Snow, A., Bidere, N., Zheng, L., *et al*. (2007) Ribosomal protein S3: a KH domain subunit in NF-kappaB complexes that mediates selective gene regulation. *Cell* **131:** 927–939.
Wan, F., Weaver, A., Gao, X., Bern, M., Hardwidge, P.R., and Lenardo, M.J. (2011) IKKbeta phosphorylation regulates RPS3 nuclear translocation and NF-kappaB function during infection with *Escherichia coli* strain O157:H7. *Nat Immunol* **12:** 335–343.
Weflen, A.W., Alto, N.M., Viswanathan, V.K., and Hecht, G. (2010) *E. coli* secreted protein F promotes EPEC invasion of intestinal epithelial cells via an SNX9-dependent mechanism. *Cell Microbiol* **12:** 919–929.
Weiss, S.M., Ladwein, M., Schmidt, D., Ehinger, J., Lommel, S., Stading, K., *et al*. (2009) IRSp53 links the enterohemorrhagic *E. coli* effectors Tir and EspFU for actin pedestal formation. *Cell Host Microbe* **5:** 244–258.
Weisswange, I., Newsome, T.P., Schleich, S., and Way, M. (2009) The rate of N-WASP exchange limits the extent of ARP2/3-complex-dependent actin-based motility. *Nature* **458:** 87–91.
Whale, A.D., Hernandes, R.T., Ooka, T., Beutin, L., Schuller, S., Garmendia, J., *et al*. (2007) TccP2-mediated subversion of actin dynamics by EPEC 2 – a distinct evolutionary lineage of enteropathogenic *Escherichia coli*. *Microbiology* **153:** 1743–1755.
Wickham, M.E., Lupp, C., Vazquez, A., Mascarenhas, M., Coburn, B., Coombes, B.K., *et al*. (2007) *Citrobacter rodentium* virulence in mice associates with bacterial load and the type III effector NleE. *Microbes Infect* **9:** 400–407.
Wu, B., Skarina, T., Yee, A., Jobin, M.C., Dileo, R., Semesi, A., *et al*. (2010) NleG Type 3 effectors from enterohaemorrhagic *Escherichia coli* are U-Box E3 ubiquitin ligases. *PLoS Pathog* **6:** e1000960.
Yen, H., Ooka, T., Iguchi, A., Hayashi, T., Sugimoto, N., and Tobe, T. (2010) NleC, a type III secretion protease, compromises NF-kappaB activation by targeting p65/RelA. *PLoS Pathog* **6:** e1001231.
Yoshida, S., Katayama, E., Kuwae, A., Mimuro, H., Suzuki, T., and Sasakawa, C. (2002) *Shigella* deliver an effector protein to trigger host microtubule destabilization, which promotes Rac1 activity and efficient bacterial internalization. *EMBO J* **21:** 2923–2935.
Younis, R., Bingle, L.E., Rollauer, S., Munera, D., Busby, S.J., Johnson, S., *et al*. (2010) SepL resembles an aberrant effector in binding to a class 1 type III secretion chaperone and carrying an N-terminal secretion signal. *J Bacteriol* **192:** 6093–6098.
Zettl, M., and Way, M. (2002) The WH1 and EVH1 domains

of WASP and Ena/VASP family members bind distinct sequence motifs. *Curr Biol* **12:** 1617–1622.

Zhang, J., Zhu, J., Bu, X., Cushion, M., Kinane, T.B., Avraham, H., and Koziel, H. (2005) Cdc42 and RhoB activation are required for mannose receptor-mediated phagocytosis by human alveolar macrophages. *Mol Biol Cell* **16:** 824–834.

Zurawski, D.V., Mumy, K.L., Badea, L., Prentice, J.A., Hartland, E.L., McCormick, B.A., and Maurelli, A.T. (2008) The NleE/OspZ family of effector proteins is required for polymorphonuclear transepithelial migration, a characteristic shared by enteropathogenic *Escherichia coli* and *Shigella flexneri* infections. *Infect Immun* **76:** 369–379.

Featured Image

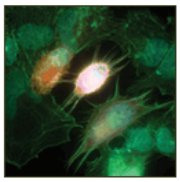


Featured Image: Bacterial RhoGEFs are active in the presence of the mammalian RhoGEF inhibitor EspH. Immunofluorescence microscopy of HeLa cells cotransfected with Myc-tagged Map (magenta) or RFP-EspH (red), and stained for F actin (green) and nuclei (cyan). Map is a bacterial Cdc42 GEF that induces filopodia formation, while EspH promiscuously binds and inhibits mammalian RhoGEFs, leading to cell rounding. When coexpressed, filopodia are still evident, showing that Map is insensitive to the inhibitory effects of EspH. [See related article: A. R. C. Wong et al., mBio 3(1):**e00250-11**, 2012.] (Copyright (c) 2012, Wong et al. All Rights Reserved.)

january/february 2012, volume 3, issue 1

» Table of Contents
» Table of Contents (pdf)
» Board of Editors (pdf)
» Index by Author

Current Issue
january/february 2012, volume 3 issue 1



- editors' picks

New genome sequence data to aid the advance detection of pathogenic enterococci

Unique gut bacteria found in autistic kids with GI disturbances

Dead deep-sea vents host new communities of life

alert me to new issues of mBio

about mBio
for authors
for reviewers
for librarians
for fellows
for advertisers
inquiries from the press
permissions for commercial reuse & commercial reprints
mBio rss feeds
content delivery options

submit to mBio

Journals.ASM.org

HighWire

Most Read

Staphylococcus aureus CC398: Host Adaptation and Emergence of Methicillin Resistance in Livestock

The H5N1 Manuscript Redaction Controversy

Mammalian-Transmissible H5N1 Influenza: Facts and Perspective

Mammalian-Transmissible H5N1 Influenza: the Dilemma of Dual-Use Research

Role of Complement in Dengue Virus Infection: Protection or Pathogenesis?

» View all Most Read articles

Downloaded from mbio.asm.org on March 15, 2012 - Published by mbio.asm.org



The Interplay between the *Escherichia coli* Rho Guanine Nucleotide Exchange Factor Effectors and the Mammalian RhoGEF Inhibitor EspH

Alexander R. C. Wong, Abigail Clements, Benoit Raymond, et al.

2012. The Interplay between the *Escherichia coli* Rho Guanine Nucleotide Exchange Factor Effectors and the Mammalian RhoGEF Inhibitor EspH. mBio 3(1): . doi:10.1128/mBio.00250-11.

Updated information and services can be found at:
http://mbio.asm.org/content/3/1/e00250-11.full.html

SUPPLEMENTAL MATERIAL **http://mbio.asm.org/content/3/1/e00250-11.full.html#SUPPLEMENTAL**

REFERENCES This article cites 36 articles, 8 of which can be accessed free at:
http://mbio.asm.org/content/3/1/e00250-11.full.html#ref-list-1

CONTENT ALERTS Receive: RSS Feeds, eTOCs, free email alerts (when new articles cite this article), **more>>**

Information about commercial reprint orders: **http://mbio.asm.org/misc/reprints.xhtml**
Information about Print on Demand and other content delivery options:
http://mbio.asm.org/misc/contentdelivery.xhtml
To subscribe to another ASM Journal go to: **http://journals.asm.org/subscriptions/**

Journals.ASM.org

Downloaded from mbio.asm.org on March 15, 2012 - Published by mbio.asm.org

RESEARCH ARTICLE

The Interplay between the *Escherichia coli* Rho Guanine Nucleotide Exchange Factor Effectors and the Mammalian RhoGEF Inhibitor EspH

Alexander R. C. Wong, Abigail Clements, Benoit Raymond, Valerie F. Crepin, and Gad Frankel

Centre for Molecular Microbiology and Infection, Division of Cell and Molecular Biology, Imperial College London, London, United Kingdom

ABSTRACT **Rho GTPases are important regulators of many cellular processes. Subversion of Rho GTPases is a common infection strategy employed by many important human pathogens. Enteropathogenic *Escherichia coli* and enterohemorrhagic *Escherichia coli* (EPEC and EHEC) translocate the effector EspH, which inactivates mammalian Rho guanine exchange factors (GEFs), as well as Map, EspT, and EspM2, which, by mimicking mammalian RhoGEFs, activate Rho GTPases. In this study we found that EspH induces focal adhesion disassembly, triggers cell detachment, activates caspase-3, and induces cytotoxicity. EspH-induced cell detachment and caspase-3 activation can be offset by EspT, EspM2, and the *Salmonella* Cdc42/Rac1 GEF effector SopE, which remain active in the presence of EspH. EPEC and EHEC therefore use a novel strategy of controlling Rho GTPase activity by translocating one effector to inactivate mammalian RhoGEFs, replacing them with bacterial RhoGEFs. This study also expands the functional range of bacterial RhoGEFs to include cell adhesion and survival.**

IMPORTANCE **Many human pathogens use a type III secretion system to translocate effectors that can functionally be divided into signaling, disabling, and countervirulence effectors. Among the signaling effectors are those that activate Rho GTPases, which play a central role in coordinating actin dynamics. However, many pathogens also translocate effectors with antagonistic or counteractive functions. For example, *Salmonella* translocates SopE and SptP, which sequentially turn Rac1 and Cdc42 on and off. In this paper, we show that enteropathogenic *E. coli* translocates EspH, which inactivates mammalian RhoGEFs and triggers cytotoxicity and at the same time translocates the bacterial RhoGEFs EspM2 and EspT, which are insensitive to EspH, and so neutralizes EspH-induced focal adhesion disassembly, cell detachment, and caspase-3 activation. Our data point to an intriguing infection strategy in which EPEC and EHEC override cellular Rho GTPase signaling by disabling mammalian RhoGEFs and replacing them with with bacterial RhoGEFs that promote cell adhesion and survival.**

Received 19 October 2011 **Accepted** 19 December 2011 **Published** 17 January 2012

Citation Wong ARC, Clements A, Raymond B, Crepin VF, Frankel G. 2012. The interplay between the *Escherichia coli* Rho guanine nucleotide exchange factor effectors and the mammalian RhoGEF inhibitor EspH. mBio 3(1):e00250-11. doi:10.1128/mBio.00250-11.

Invited Editor Fabio Bagnoli, Novartis **Editor** Rino Rappuoli, Novartis

Copyright © 2012 Wong et al. This is an open-access article distributed under the terms of the Creative Commons Attribution-Noncommercial-Share Alike 3.0 Unported License, which permits unrestricted noncommercial use, distribution, and reproduction in any medium, provided the original author and source are credited.

Address correspondence to Gad Frankel, g.frankel@imperial.ac.uk.

The Rho family of small GTPases, including RhoA, Rac1, and Cdc42, are important regulators of actin organization (1), as well as many other cellular processes, including cell adhesion and migration, vesicle trafficking, cytokinesis, and apoptosis (2). Rho GTPases switch between active GTP-bound and inactive GDP-bound forms. The cycling of these two states is regulated by guanine nucleotide exchange factors (GEFs), which promote dissociation of GDP and subsequent binding of GTP and GTPase-activating proteins (GAPs), which enhance the rate of GTP hydrolysis to GDP, while guanine nucleotide dissociation inhibitors (GDIs) maintain Rho GTPases in an inactive state in the cytosol (1, 2).

An important mediator of focal adhesion (FA) signaling is focal adhesion kinase (FAK) (3). FAK is a protein-tyrosine kinase that is implicated in formation of nascent focal complexes at lamellipodial protrusions, as well as disassembly of mature focal adhesions in a dynamic process known as "FA turnover" (3). FAK-null fibroblasts exhibit high Rho activity, reduced migration, and severe FA turnover defects (4). The major phosphorylation site of FAK is Y397, which recruits c-Src to form a FAK-Src signaling complex that then activates multiple signaling pathways (3). Recent studies have shown that FAK regulates the localized activity of Rho GTPases by recruiting RhoGEFs and RhoGAPs at focal adhesion sites to facilitate FA turnover and cell migration (5).

Several important bacterial pathogens subvert Rho GTPase signaling by utilizing a type III secretion system (T3SS) to translocate effector proteins into eukaryotic host cells (6). Enteropathogenic *Escherichia coli* (EPEC) and enterohemorrhagic *Escherichia coli* (EHEC) translocate the effector EspH, which by binding to tandem Dbl homology-pleckstrin homology (DH-PH) domains of Dbl-family RhoGEFs blocks the activation of Rho GTPases (7). EPEC and EHEC also translocate the effectors Map, EspM, and EspT, which, based on an invariant Trp-XXX-Glu motif, are grouped with IpgB1 and IpgB2 (*Shigella*) and SifA and SifB (*Salmonella*) into the WxxxE family of effectors (8–11).

Structural analysis of Map and EspM2 revealed that the WxxxE effectors share a three-dimensional fold with the *Salmonella* GEF

Downloaded from mbio.asm.org on March 15, 2012 - Published by mbio.asm.org

SopE, which catalyzes the exchange of GDP to GTP by binding to the switch I and II regions of Rho GTPases (12–14). Map exhibits a GEF activity for Cdc42 (13) and induces transient filopodium formation at bacterial attachment sites during the early stages of EPEC infection (15, 16). EspM2 is a bacterial RhoA GEF that induces stress fiber formation (10, 14), while EspT activates both Cdc42 and Rac1, leading to formation of membrane ruffles and lamellipodia (11).

Importantly, EspH was implicated in modulating Map-induced filopodium kinetics, as deletion of *espH* results in filopodium persistence and overexpression of EspH inhibits filopodium formation (17). However, the overall functional relationships between these effectors during infection are poorly understood. Moreover, it is not known if EspH can inhibit the activity of the SopE-like WxxxE effectors; while structurally distinct from DH-PH eukaryotic RhoGEFs (12), they activate Rho GTPases by a similar mechanism. The aim of this study was to characterize the interplay between EspH and bacterial RhoGEFs in the context of actin remodeling, cell adhesion, and cell death.

RESULTS

EspH induces cell detachment, cytotoxicity, and focal adhesion disassembly. EspH binds to DH-PH mammalian RhoGEFs and induces actin cytoskeletal disruption and cell rounding (7, 17). We further characterized EspH-induced cytotoxicity by assessing the levels of cell rounding, cell detachment, and lactate dehydrogenase (LDH) release. Myc-tagged EspH (Myc-EspH), or Myc-tagged green fluorescent protein (Myc-GFP) as a control, was ectopically expressed for 24 h, and the levels of cell rounding were quantified by immunofluorescence microscopy. Cells transfected with Myc-EspH showed a marked increase in cell rounding compared to those transfected with Myc-GFP (Fig. 1A).

The level of cell detachment following Myc-EspH or Myc-GFP expression was measured and quantified as the percentage of total cells. Myc-EspH was found to induce 45.8 ± 5.5% cell detachment, compared to 8.2 ± 5.0% cell detachment in the Myc-GFP control (Fig. 1B). A cell detachment assay was also performed to assess the role of EspH during EPEC infection. HeLa cells were infected with wild-type (WT) EPEC, Δ*espH* EPEC, or Δ*espH* EPEC complemented with EspH (Δ*espH*/pEspH) for 1 h and then incubated for a further 3 h with gentamicin to stop bacterial replication. Treatment of cells with the apoptotic inducer staurosporine (STS) for 5 h was used as a positive control. Quantification of cells postinfection showed that 11.0 ± 9.5% of cells infected with wild-type EPEC were detached (Fig. 1C). In contrast, only 2.9 ± 8.7% of cells were detached following infection with Δ*espH* EPEC. Complementation of the mutant with a plasmid-encoded EspH dramatically increased the level of cell detachment relative to that of the STS control, as 51.1 ± 1.8% of cells infected with Δ*espH*/pEspH EPEC were detached.

The contribution of EspH to cytotoxicity during EPEC infection was also measured by LDH release, which results from plasma membrane damage. Treatment of cells with STS for 5 h was used as a positive control. Infection with wild-type EPEC resulted in a slightly higher LDH release than did infection with the Δ*espH* mutant (Fig. 1D). Complementation of the Δ*espH* mutant significantly increased LDH release to levels comparable to those observed with the STS control. EspH is thus a potent inducer of cytotoxicity and cell detachment.

The phenotype of cell rounding and cell detachment led us to examine whether EspH had an effect on focal adhesions. To investigate this, we performed a time course study of HeLa cells infected with Δ*espH*/pEspH EPEC, as this strain gave the most distinct phenotype compared to wild-type EPEC or Δ*espH* EPEC. When coverslips were fixed hourly for 3 h and vinculin was used as a marker for focal adhesions, immunofluorescence microscopy revealed that EspH progressively induces disassembly of focal adhesions concomitantly with actin disruption; no focal adhesions were observed when cells were rounded at the end of infection (Fig. 1E).

EspH mediates focal adhesion disassembly in a caspase-independent manner. Inhibition of Rho GTPase signaling is also a trigger for caspase activation and apoptosis (18), and the EspH-mediated focal adhesion disassembly observed could therefore be a result of caspase-mediated cleavage of focal adhesion proteins (19). The ability of EspH to induce caspase-3 activation was tested by infecting HeLa cells with WT, Δ*espH*, or Δ*espH*/pEspH EPEC for 1 h and incubating them for a further 3 h in the presence of gentamicin. Treatment of cells with STS for 5 h was used as a positive control, and cleaved caspase-3 was detected by immunofluorescence microscopy. In this assay, 61.1 ± 0.8% of STS-treated cells stained positive for active caspase-3, whereas only 2.9 ± 0.5% of untreated cells stained positive (Fig. 2A and B); 16.9 ± 3.7% of WT EPEC-infected cells stained positive for caspase-3 activation, compared to 9.7 ± 2.1% of cells infected with the Δ*espH* mutant (Fig. 2A and B). Complementation of the Δ*espH* mutant with plasmid-encoded EspH significantly increased caspase-3 activation, as 29.0 ± 1.6% of cells infected with Δ*espH*/pEspH EPEC stained positive for active caspase-3 (Fig. 2A and B).

To determine if EspH alone was sufficient to induce caspase-3 activation, cleaved caspase-3 was detected in cells ectopically expressing EspH (Myc-EspH) or Myc-tagged GFP (Myc-GFP) for 24 h. We observed that while 35.9 ± 8.7% of cells expressing EspH stained positive for active caspase-3, only 1.9 ± 0.8% of GFP-expressing cells exhibited the presence of cleaved caspase-3 (Fig. 2C and D).

We then used the pan-caspase inhibitor zVAD-fmk to assess the levels of cell detachment following infection with Δ*espH*/pEspH EPEC (Fig. 2E). STS was again used as a control, and as expected, STS-induced cell detachment was inhibited by zVAD-fmk, as it is caspase mediated (cell detachment was reduced from 53.9 ± 3.1% to 11.6 ± 2.6% in the presence of zVAD-fmk). However, treatment with zVAD-fmk did not diminish cell detachment induced by infection with Δ*espH*/pEspH EPEC (62.3 ± 3.1% cell detachment without and 53.0 ± 2.2% cell detachment with zVAD-fmk). Immunofluorescence microscopy of Δ*espH*/pEspH EPEC-infected cells treated with zVAD-fmk further showed that cells were still rounded, and no focal adhesions (vinculin) were observed after a 3-h infection (Fig. 2F). These results suggest that EspH-induced cell detachment was a result of FA disassembly rather than caspase activation.

FAK is involved in EspH-induced cell rounding, detachment, and caspase-3 activation. As FAK regulates localized Rho GTPase activity and focal adhesion dynamics (3), we investigated if FAK is involved in EspH-induced cell rounding and caspase-3 activation. FAK-null ($FAK^{-/-}$) and FAK-reconstituted ($FAK^{+/+}$) fibroblasts were transfected with Myc-tagged EspH or Myc-tagged GFP as a control and stained for F actin and cleaved caspase-3. Immunofluorescence microscopy revealed that EspH induced cell rounding and caspase-3 activation in $FAK^{+/+}$ fibroblasts (Fig. 3A to C).

Downloaded from mbio.asm.org on March 15, 2012 - Published by mbio.asm.org

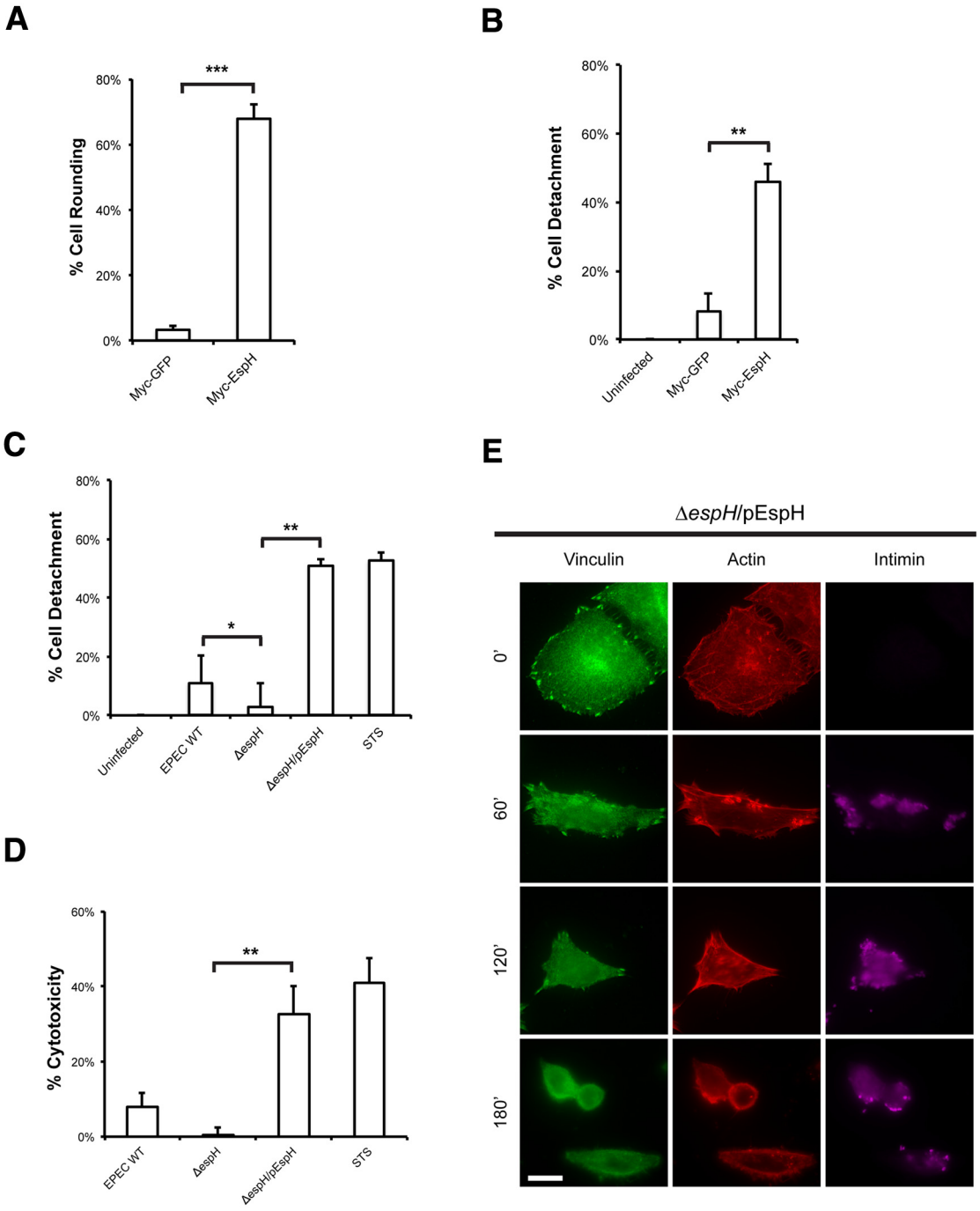


FIG 1 EspH induces cell detachment, cytotoxicity, and focal adhesion disassembly. (A) Quantification of cell rounding of HeLa cells transfected with Myc-GFP or Myc-EspH for 24 h. One hundred transfected cells were counted in triplicate. Ectopic expression of EspH induced a significant increase in cell rounding compared to GFP expression. Results are means plus standard deviations (SD) of three independent experiments. (B) Quantification of detachment levels of HeLa cells transfected with Myc-GFP or Myc-EspH for 24 h. Ectopic expression of EspH induced a significant increase in cell detachment compared to GFP. Results are means plus SDs of three independent experiments. **, $P < 0.01$. (C) Quantification of detachment levels of HeLa cells infected with WT EPEC, Δ*espH* EPEC, or Δ*espH* EPEC complemented with EspH (Δ*espH*/pEspH) for 1 h and then incubated with gentamicin for 3 h. STS treatment of HeLa cells for 5 h was used as a positive control. Cell detachment was expressed as a percentage of the value for uninfected cells. Cell detachment was reduced in the Δ*espH* mutant compared to WT EPEC. Complementation with EspH increased cell detachment to STS levels. Results are means ± SD of three independent experiments. *, $P < 0.05$; **, $P < 0.01$. (D) Quantification of cytotoxicity to HeLa cells infected with WT EPEC, Δ*espH* EPEC, or Δ*espH* EPEC complemented with EspH (Δ*espH*/pEspH) for 30 min and then incubated with gentamicin for 4 h. STS treatment of HeLa cells for 5 h was used as a positive control. Cytotoxicity was assayed by quantifying the levels of LDH release into the culture supernatant from cells 4 h postinfection. Results are means ± SD of three independent experiments. (E) Immunofluorescence microscopy of HeLa cells infected with Δ*espH* EPEC complemented with EspH (Δ*espH*/pEspH) for 0, 60, 120, and 180 min. Bacteria were visualized with anti-intimin antibody (magenta), vinculin was detected with anti-vinculin antibody (green), and actin was stained with TRITC-phalloidin (red). Infection with Δ*espH*/pEspH EPEC progressively induced focal adhesion disassembly, as cells were rounded after 180 min of infection. Bar = 10 μm.

Downloaded from mbio.asm.org on March 15, 2012 - Published by mbio.asm.org

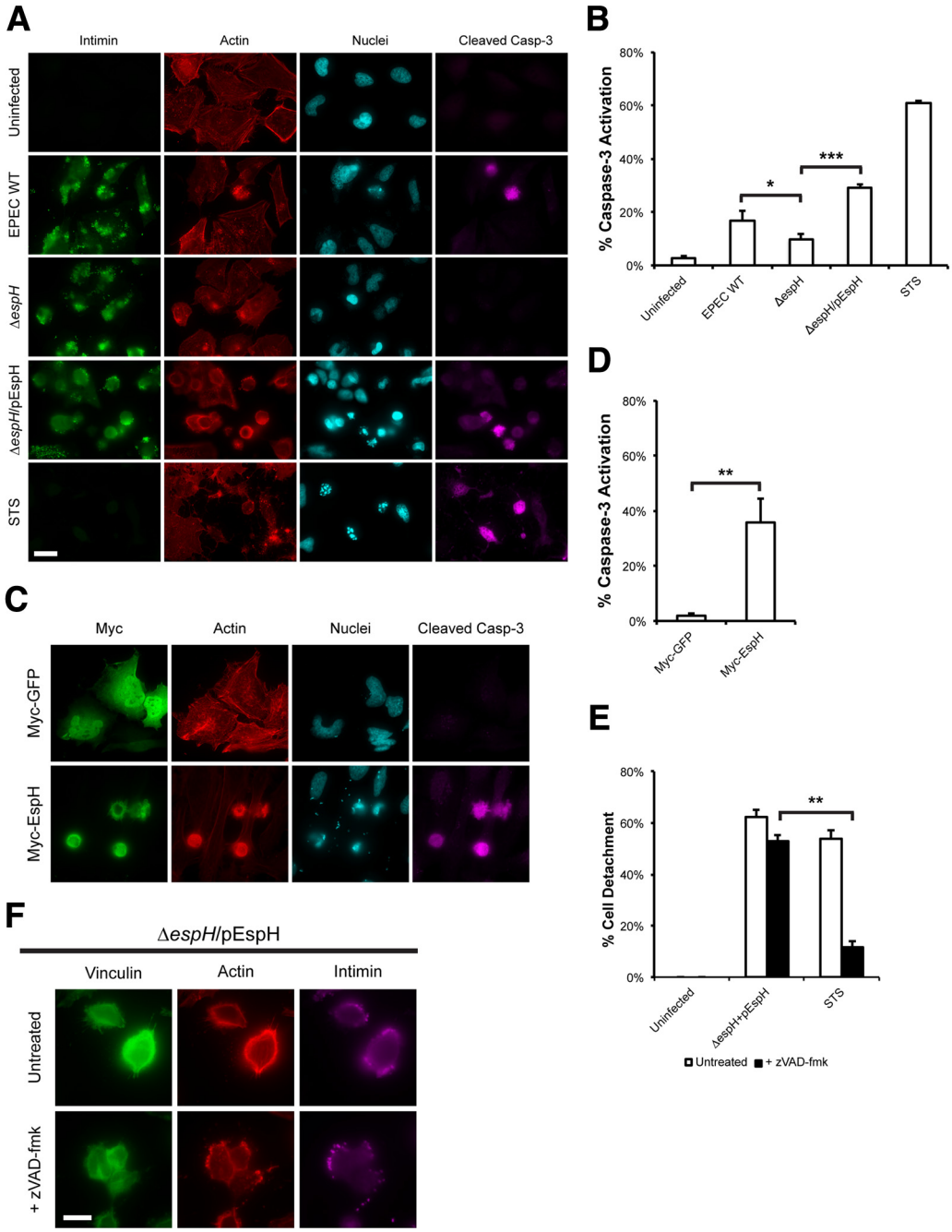


FIG 2 EspH induces focal adhesion disassembly in a caspase-independent manner. (A) Immunofluorescence microscopy of uninfected HeLa cells or cells infected with WT EPEC, Δ*espH* EPEC, or Δ*espH* EPEC complemented with EspH (Δ*espH*/pEspH) for 1 h, then incubated with gentamicin for 3 h. Bacteria were visualized with anti-intimin antibody (green), active caspase-3 was detected with anti-caspase-3 (cleaved) antibody (magenta), actin was stained with TRITC-phalloidin (red) and cell nuclei were stained with DAPI (cyan). The Δ*espH* mutant induced reduced levels of caspase-3 activation compared to WT EPEC. Complementation with EspH resulted in a marked increase in caspase-3 activation when compared to Δ*espH* alone. Bar = 20 μm. (B) Quantification of caspase-3 activation of infected cells from (A). STS treatment of HeLa cells for 5 h was used as a positive control. 100 infected cells were counted in triplicates. Results are means ± SD of three independent experiments. *, $P < 0.05$), ***, $P < 0.001$). (C) Immunofluorescence microscopy of HeLa cells transfected with Myc-GFP or Myc-EspH. Myc-tagged proteins were visualized with anti-Myc antibody (green), active caspase-3 was detected with anti-caspase-3 (cleaved) antibody (magenta), actin was stained with TRITC-phalloidin (red) and nuclei were stained with DAPI (cyan). Ectopic expression of EspH, but not GFP, induced caspase-3 activation. Bar = 20 μm. (D) Quantification of caspase-3 activation of transfected cells from (C). STS treatment of HeLa cells for 5 h was used as a positive control. 100 transfected cells were counted in triplicates. Results are means ± SD of three independent experiments. **, $P < 0.01$). (E) Quantification of detachment levels of HeLa cells, with or without zVAD-fmk treatment, infected with Δ*espH* EPEC complemented with EspH (Δ*espH*/pEspH) for 1 h, then incubated with gentamicin for 3 h. STS treatment of HeLa cells for 5 h was used as a positive control. Cell detachment was expressed as a percentage of uninfected cells. Treatment with zVAD-fmk inhibited STS-induced cell detachment, but not cell detachment following infection with Δ*espH*/pEspH EPEC. Results are means ± SD of three independent experiments. (F) Immunofluorescence microscopy of HeLa cells infected with Δ*espH* EPEC complemented with EspH (Δ*espH*/pEspH) for 180 min, with or without zVAD-fmk treatment. Bacteria were visualized with anti-intimin antibody (magenta), vinculin was detected with anti-vinculin antibody (green), and actin was stained with TRITC-phalloidin (red). Treatment with zVAD-fmk did not prevent focal adhesion disassembly. Bar = 10 μm.

Downloaded from mbio.asm.org on March 15, 2012 - Published by mbio.asm.org

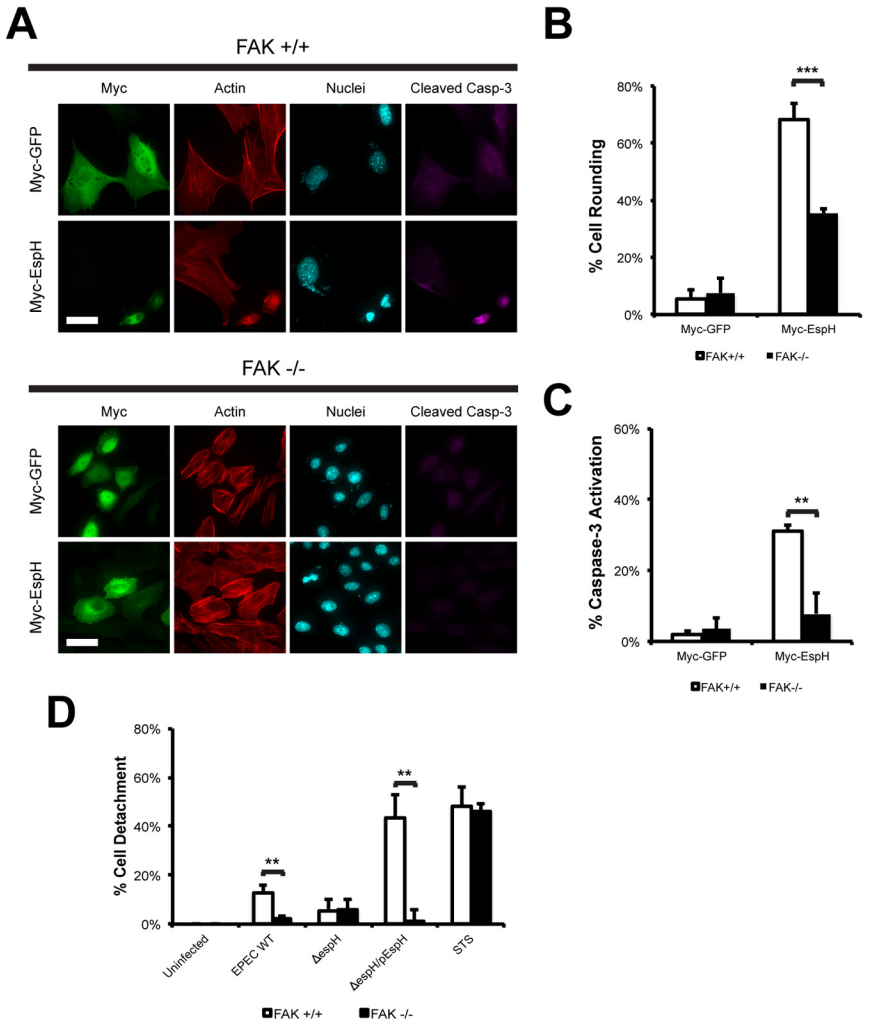


FIG 3 FAK is involved in EspH-induced cell rounding, detachment, and caspase-3 activation. (A) Immunofluorescence microscopy of FAK$^{+/+}$ or FAK$^{-/-}$ fibroblasts transfected with Myc-GFP or Myc-EspH. Myc-tagged proteins were visualized with anti-Myc antibody (green), active caspase-3 was detected with anti-caspase-3 (cleaved) antibody (magenta), actin was stained with TRITC-phalloidin (red), and cell nuclei were stained with DAPI (cyan). Ectopic expression of EspH induced cell rounding, nuclear condensation, and caspase-3 activation in FAK$^{+/+}$ cells but not FAK$^{-/-}$ fibroblasts. Bar = 20 μm. (B) Quantification of cell rounding of FAK$^{+/+}$ or FAK$^{-/-}$ fibroblasts transfected with Myc-GFP or Myc-EspH. 100 transfected cells were counted in triplicates. Results are means plus SD of three independent experiments. ***, $P < 0.001$. (C) Quantification of caspase-3 activation of FAK$^{+/+}$ or FAK$^{-/-}$ fibroblasts transfected with Myc-GFP or Myc-EspH. One hundred transfected cells were counted in triplicate. Results are means plus SD of three independent experiments. **, $P < 0.01$. (D) Quantification of detachment levels of FAK$^{+/+}$ or FAK$^{-/-}$ fibroblasts infected with WT EPEC, Δ*espH* EPEC, or Δ*espH* EPEC complemented with EspH (Δ*espH*/pEspH) for 1 h and then incubated with 200 μg ml^{-1} gentamicin for 3 h. Treatment of FAK$^{+/+}$ or FAK$^{-/-}$ fibroblasts with 1 μM staurosporine (STS) for 5 h was used as a positive control. Cell detachment was expressed as a percentage of the value for uninfected cells. Cell detachment was drastically reduced in FAK$^{-/-}$ fibroblasts infected with WT EPEC or Δ*espH*/pEspH EPEC compared to that in FAK$^{+/+}$ fibroblasts. Results are means plus SD of three independent experiments. **, $P < 0.01$.

In contrast, FAK$^{-/-}$ fibroblasts exhibited reduced levels of cell rounding and little caspase-3 activation (Fig. 3A to C). As FAK$^{-/-}$ fibroblasts were resistant to EspH-induced cell rounding, the role of FAK on cell adhesion during EPEC infection was examined. FAK$^{-/-}$ and FAK$^{+/+}$ fibroblasts were assessed for levels of cell detachment following infection with wild-type, Δ*espH*, or Δ*espH*/pEspH EPEC. STS treatment was used as a control and showed similar levels of cell detachment in FAK$^{-/-}$ and FAK$^{+/+}$ fibroblasts (Fig. 3D). Consistent with the results described above, FAK$^{-/-}$ fibroblasts did not show any significant levels of cell detachment after infection with any of the strains (Fig. 3D). In contrast, 43.2 ± 9.5% of cells were detached following infection of FAK$^{+/+}$ fibroblasts with Δ*espH*/pEspH EPEC (Fig. 3D). Taken together, our results show that FAK is an important mediator of EspH-induced cell rounding and cell detachment and suggest that defects in focal adhesion disassembly diminish the ability of EspH to induce cell rounding and caspase-3 activation.

Bacterial RhoGEFs are active in the presence of EspH. We next investigated whether, in addition to blocking mammalian DH-PH RhoGEFs, EspH inhibits the activity of bacterial RhoGEFs. HeLa cells transfected with Myc-tagged EspH or Myc-tagged GFP were infected with Δ*map*/pMap EPEC for 30 min or with EPEC/pEspT or EPEC/pEspM2 for 90 min and assessed for filopodium, lamellipodium, and stress fiber formation, respectively. For consistency, we deleted endogenous *map* so that all three effectors were expressed exclusively from inducible genes. Staining with F actin revealed that cells infected with EPEC expressing the WxxxE effectors were able to induce formation of their respective actin structures in cells transfected with either GFP or EspH (Fig. 4A). This suggests that EspH does not inhibit the activity of the WxxxE-family RhoGEFs during EPEC infection.

To affirm this observation, cells were cotransfected with red fluorescent protein (RFP) or RFP-EspH and Myc-tagged Map, EspT, EspM2, or the catalytic region of SopE (SopE$_{78\text{-}240}$); cotransfection with Myc-tagged p115-RhoGEF, a mammalian RhoA GEF which has been shown to bind EspH (7), was used as a control. After staining for F actin, we observed that EspH was able to inhibit stress fiber formation by p115-RhoGEF, and the cotransfected cells were rounded (Fig. 4B). In contrast, cotransfection of RFP-EspH with Map, EspT, EspM2, or SopE$_{78\text{-}240}$ did not inhibit formation of filopodia (Map), lamellipodia (EspT/SopE), or stress fibers (EspM2) (Fig. 4B; also, see Fig. S1 in the supplemental material). When cotransfected with RFP, the RhoA GEFs p115-RhoGEF and EspM2 induced stress fiber formation in 79.7 ± 3.3% and 90.6 ± 1.1% of cells, respectively (Fig. 4C). When cotransfected with RFP-EspH, p115-RhoGEF showed markedly reduced stress fiber formation, with only 14.5 ± 2.8% of

Downloaded from mbio.asm.org on March 15, 2012 - Published by mbio.asm.org

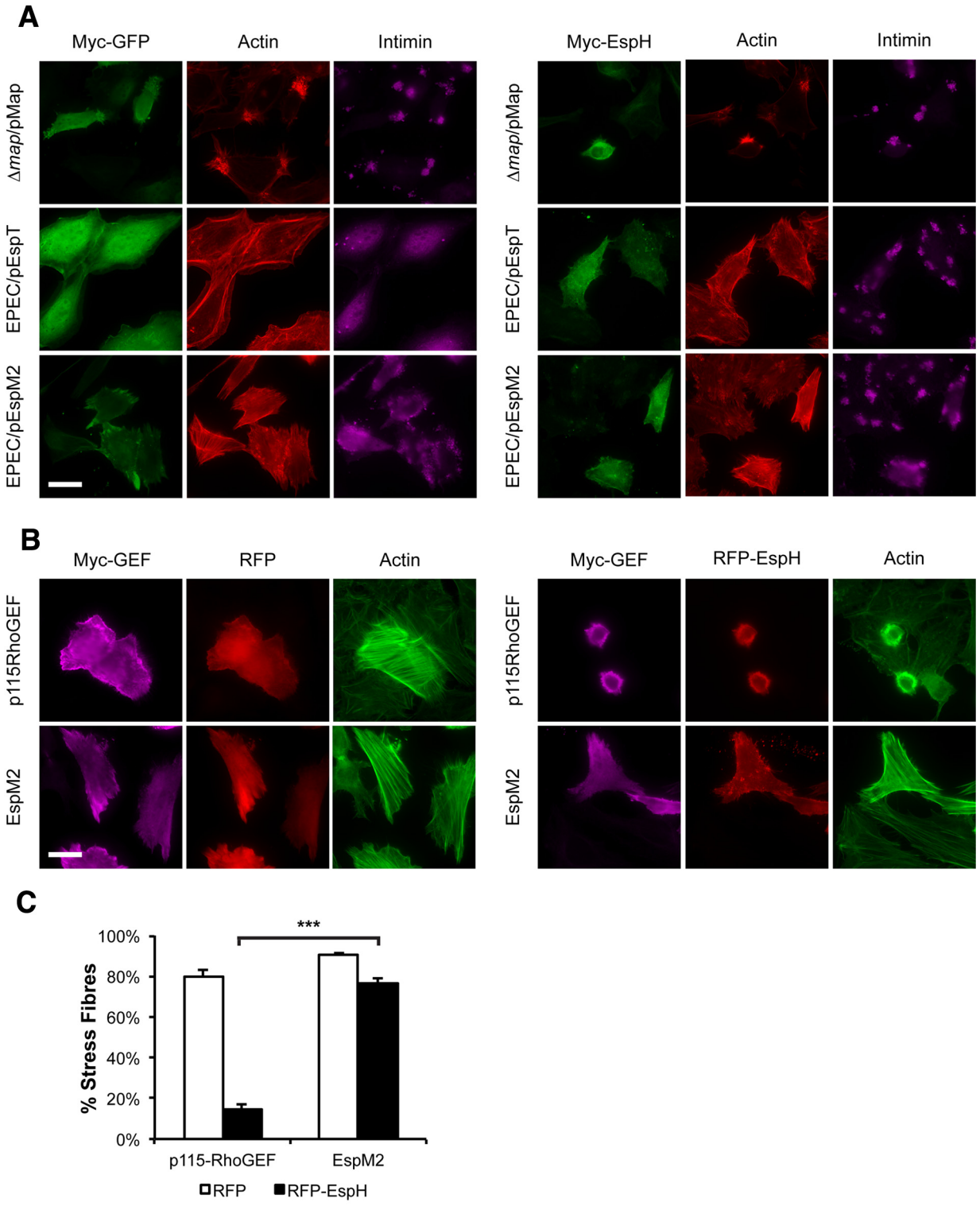


FIG 4 Bacterial RhoGEFs are active in the presence of EspH. (A) Immunofluorescence microscopy of HeLa cells transfected with Myc-GFP or Myc-EspH and then infected with Δ*map*/pMap EPEC for 30 min or EPEC expressing EspT (EPEC/pEspT) or EspM2 (EPEC/pEspM2) for 90 min. Myc-tagged proteins were visualized with anti-Myc antibody (green), bacteria were visualized with anti-intimin antibody (magenta), and actin was stained with TRITC-phalloidin (red). Ectopic expression of EspH did not inhibit the formation of filopodia (Map), lamellipodia (EspT), or stress fibers (EspM2). Bar = 20 μm. (B) Immunofluorescence microscopy of HeLa cells cotransfected with Myc-p115RhoGEF or Myc-EspM2 and with RFP or RFP-EspH (red). Myc-tagged proteins were visualized with anti-Myc antibody (magenta), and actin was stained with Oregon green phalloidin (green). Cotransfection of Myc-p115RhoGEF and RFP-EspH but not Myc-EspM2 and RFP-EspH drastically reduced stress fiber formation. Bar = 20 μm. (C) Quantification of stress fiber formation in HeLa cells cotransfected with Myc-p115RhoGEF or Myc-EspM2 and with RFP or RFP-EspH. One hundred cotransfected cells were counted in triplicate. Results are means plus SD of three independent experiments. ***, $P < 0.001$.

Downloaded from mbio.asm.org on March 15, 2012 - Published by mbio.asm.org

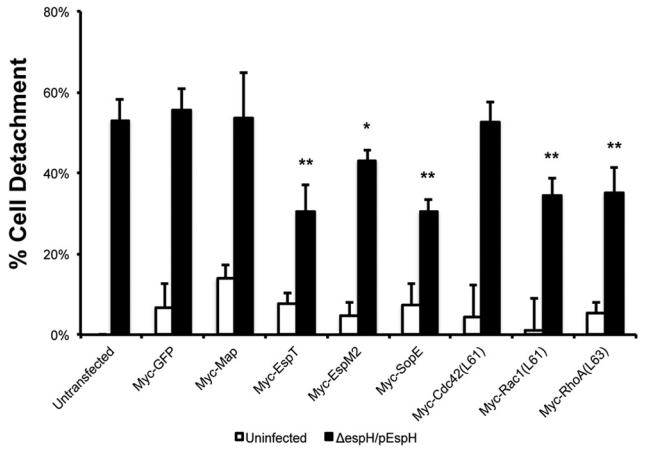


FIG 5 EspT, EspM2, and SopE block EspH-induced cell detachment. Detachment levels in HeLa cells transfected with Myc-GFP or Myc-tagged bacterial RhoGEFs, uninfected or infected with EPEC with Δ*espH* complemented with EspH (Δ*espH*/pEspH) for 1 h, followed by incubation with 200 μg ml^{-1} gentamicin for 3 h, were quantified. Transfection with dominant-positive Cdc42 (Cdc42L61), Rac1 (Rac1L61), and RhoA (RhoAL63) was used as positive controls. Cell detachment was expressed as a percentage of that in nontransfected, noninfected cells. Ectopic expression of Myc-tagged EspT, EspM2, or SopE$_{78\text{-}240}$ resulted in reduced cell detachment following infection with Δ*espH*/pEspH EPEC but not Myc-tagged GFP or Map. Results are means plus SD of three independent experiments. Statistical significance is based on a Student's *t* test compared to the Myc-GFP control. *, $P < 0.05$; **, $P < 0.01$.

cells displaying stress fibers. In contrast, only a modest decrease in stress fiber formation was observed in cells cotransfected with EspM2 and RFP-EspH, as 76.5 ± 2.1% of cells were positive for stress fibers (Fig. 4C). Taken together, these results demonstrate that bacterial RhoGEFs are insensitive to EspH.

EspT, EspM2, and SopE block EspH-induced cell detachment and focal adhesion disassembly. Next, we determined if the bacterial RhoGEFs could mitigate the detrimental effects of EspH. To investigate if bacterial RhoGEFs could block EspH-induced cell detachment, we transfected HeLa cells with Myc-tagged bacterial RhoGEFs or their respective Rho GTPase dominant positives as controls and then infected them with Δ*espH*/pEspH EPEC for 1 h, followed by gentamicin treatment for a further 3 h. No construct induced significant levels of cell detachment by transfection alone compared to the Myc-GFP control (Fig. 5). Infection of Myc-GFP-transfected cells with Δ*espH*/pEspH EPEC resulted in 55.6 ± 5.1% detachment (Fig. 5). Interestingly, cells transfected with the Rac1-activating effectors EspT and SopE$_{78\text{-}240}$ and dominant-positive Rac1 (Rac1L61) showed a significant reduction in cell detachment following infection with Δ*espH*/pEspH EPEC, as only 30.3 ± 6.7%, 30.6 ± 2.8%, and 34.4 ± 4.2% of cells were detached, respectively (Fig. 5). We also observed an intermediate reduction in cell detachment of cells transfected with dominant-positive RhoA (RhoAL63) and its corresponding GEF EspM2, as 43.1 ± 2.7% and 35.0 ± 6.4% of cells were detached, respectively (Fig. 5). Neither the Cdc42 GEF Map nor dominant positive Cdc42 (Cdc42L61) could inhibit cell detachment following infection with Δ*espH*/pEspH EPEC, as 53.7 ± 11.2% and 52.7% ± 4.9% of cells were detached, respectively (Fig. 5). These results imply that Cdc42 activation alone is unable to block EspH-induced cell detachment.

We next examined if EspT, EspM2, and SopE also inhibited EspH-induced focal adhesion disassembly. In contrast to GFP- and Map-transfected cells, EspT- and SopE$_{78\text{-}240}$-transfected cells blocked EspH-induced cell rounding, and vinculin staining revealed that large focal adhesions were still present in a radial pattern following infection with Δ*espH*/pEspH EPEC (see Fig. S2 in the supplemental material). EspM2-transfected cells also retained stress fiber-associated focal adhesions following infection with Δ*espH*/pEspH EPEC (see Fig. S2). These results suggest that Rac1 and RhoA activation is critical for inhibition of EspH-induced cell detachment and focal adhesion disassembly.

EspT, EspM2, and SopE inhibit caspase-3 activation. We next investigated if the bacterial RhoGEFs could also block EspH-induced caspase-3 activation. When the transfection-infection delivery strategy described above was used, Δ*espH*/pEspH EPEC induced caspase activation in 33.0 ± 8.5% of cells transfected with the GFP control (Fig. 6; also, see Fig. S3 in the supplemental material). Map was unable to inhibit EspH-induced caspase-3 activation, as 32.1 ± 6.7% of transfected cells were positive for caspase-3 activation. In contrast, EspT, EspM2, and SopE$_{78\text{-}240}$ inhibited EspH-induced caspase-3 activation, as only 8.3 ± 2.8%, 13.9 ± 3.3%, and 9.2 ± 2.2% of transfected cells, respectively, were positive for caspase-3 activation (Fig. 6; also, see Fig. S3).

As Rho GTPases play a role in cell survival (1), we investigated if the bacterial RhoGEFs could play an additional role in inhibiting apoptosis. To investigate this, we transfected HeLa cells with Myc-tagged Map, EspT, EspM2, and SopE$_{78\text{-}240}$ and treated them with STS for 5 h. Transfection of anti-apoptotic Myc-tagged NleH1, which inhibits caspase-3 activation induced by STS (20), was used as a control. Quantification of cleaved caspase-3 by immunofluorescence revealed that cells transfected with the Myc-GFP control or Map displayed high levels of cleaved caspase-3 (Fig. 7; also, see Fig. S4 in the supplemental material). In contrast, cells transfected with Myc-tagged EspT, EspM2, or SopE$_{78\text{-}240}$ all showed a marked

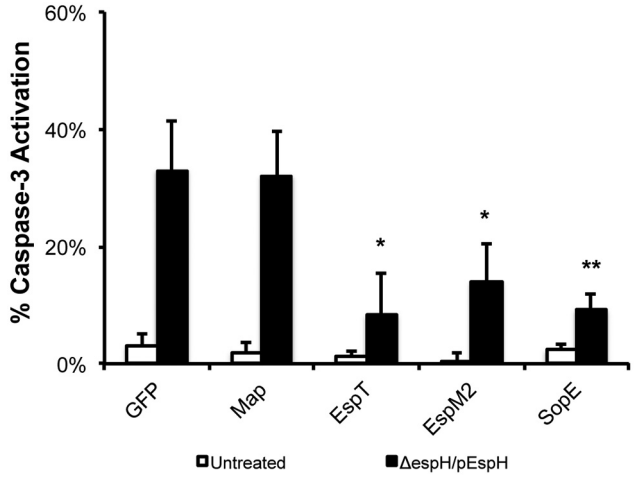


FIG 6 EspT, EspM2, and SopE inhibit EspH-induced caspase-3 activation. Caspase-3 activation of HeLa cells transfected with Myc-GFP or Myc-tagged bacterial RhoGEFs, uninfected or infected with EPEC with Δ*espH* complemented with EspH (Δ*espH*/pEspH) for 1 h, followed by incubation with 200 μg/ml gentamicin for 3 h, was quantified. One hundred transfected cells were counted in triplicate. Ectopic expression of Myc-tagged EspT, EspM2, or SopE$_{78\text{-}240}$ markedly reduced caspase-3 activation in cells infected with Δ*espH*/pEspH EPEC but not Myc-tagged GFP or Map. Results are means plus SD of three independent experiments. Statistical significance is based on a Student's *t* test compared to the Myc-GFP control. *, $P < 0.05$; **, $P < 0.01$.

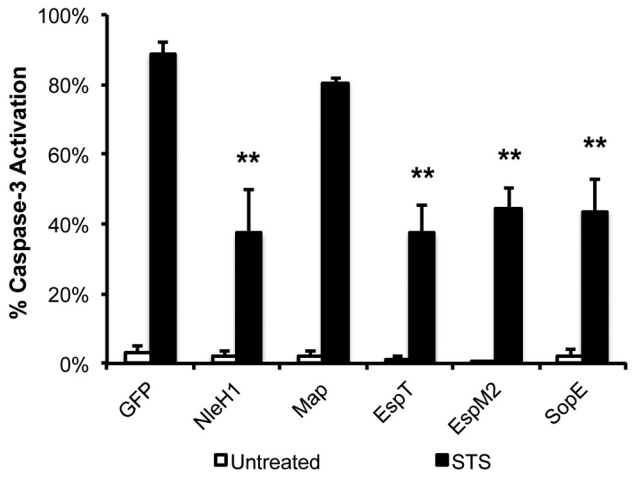


FIG 7 EspT, EspM2, and SopE inhibit staurosporine-induced caspase-3 activation. Caspase-3 activation of HeLa cells transfected with Myc-GFP or Myc-tagged bacterial RhoGEFs and then treated with 1 μM staurosporine (STS) for 5 h was quantified. Transfection of Myc-NleH1 and Myc-NleH2 was used as positive controls. One hundred transfected cells were counted in triplicate. Ectopic expression of Myc-tagged EspT, EspM2, or $SopE_{78-240}$ markedly reduced caspase-3 activation in cells treated with STS compared to expression of NleH effectors but not Myc-tagged GFP or Map. Results are means plus SD of three independent experiments. Statistical significance is based on a Student's *t* test compared to the Myc-GFP control. **, $P < 0.01$.

reduction in levels of cleaved caspase-3 similar to that seen in cells transfected with anti-apoptotic effector NleH (Fig. 7; also, see Fig. S4).

To demonstrate the role of EspT and EspM2 in promoting cell survival during EPEC infection, we utilized a Δ*nleH1* Δ*nleH2* EPEC mutant that induces high levels of apoptosis upon infection (20). We infected HeLa cells with wild-type EPEC, Δ*nleH1*Δ*nleH2* EPEC, or Δ*nleH1* Δ*nleH2* EPEC expressing plasmid-encoded NleH1 (positive control), EspT, EspT(W63A) (defective in Rac1 activation), EspM2, or EspM2(W70A) (defective in RhoA activation) and assessed the levels of caspase-3 activation, cell detachment, and cytotoxicity (see Fig. S5 in the supplemental material). Intriguingly, EspT and EspM2, but not EspT(W63A) or EspM2(W70A), partially restored the wild-type phenotype in terms of caspase-3 activation, cell detachment, and cytotoxicity (see Fig. S5). Taken together, these results show that EspT and EspM2 are able to inhibit EspH- and STS-induced caspase-3 activation and promote cell survival dependent on Rac1 or RhoA activation during EPEC infection.

DISCUSSION

Several roles have been described for SopE and the WxxxE bacterial RhoGEFs, including actin remodeling, bacterial invasion, innate host cell response, and tight junction disruption (reviewed in reference 6). In this study, we expanded the repertoire of bacterial RhoGEF functions to include promotion of cell adhesion and survival. We also found that bacterial RhoGEFs are resistant to the DH-PH mammalian RhoGEF inhibitor EspH. EPEC and EHEC are thus able to neutralize mammalian RhoGEFs while translocating their own bacterial RhoGEFs to hijack Rho GTPase signaling for the proprietary benefit of the pathogen.

Bacterial pathogens manipulate Rho GTPase signaling in a coordinated, spatiotemporal manner. *Yersinia* translocates several T3SS effectors that inactivate Rho GTPases: YopE is a RhoGAP (21), YopT is a cysteine protease that cleaves Rho GTPases to prevent membrane localization (22), and YpkA/YopO has a RhoGDI activity (23). *Vibrio parahaemolyticus* delivers VopS, which contains a Fic domain that inactivates Rho GTPases through AMPylation (24). *Salmonella enterica* serovar Typhimurium temporally regulates Cdc42 and Rac1 by delivering SopE and SptP. SopE activates Cdc42/Rac1 to induce the "trigger mechanism" of bacterial invasion but is quickly degraded (25). SptP exhibits GAP activity but slower degradation kinetics, thus allowing recovery from SopE-induced membrane ruffling (25).

While EPEC and EHEC translocate several WxxxE RhoGEFs, thus far no effector with RhoGAP activity has been identified (26). Instead, EPEC uses a novel strategy by which EspH globally inhibits its mammalian DH-PH RhoGEFs (7). The WxxxE effector Map triggers transient Cdc42-dependent filopodium formation at the site of bacterial attachment (15) before re-localizing to the mitochondria via its N-terminal mitochondrial targeting sequence (27). Filopodium dynamics is spatially regulated by Map interaction, through its carboxy-terminal PSD-95/Disk-large/ZO-1 (PDZ)-binding motif (DTRL), with the scaffold proteins sodium-hydrogen exchanger regulatory factors 1 and 2 (NHERF1/2) at the cell surface (8, 9, 28). In addition, the RhoA/ROCK pathway has been implicated in control of Map-induced filopodium dynamics (16). As Map was still able to induce filopodia in the presence of EspH, it is unlikely that EspH directly affects Map GEF activity for Cdc42. Rather, we speculate that EspH inhibits Map-induced filopodia by inhibiting the RhoA/ROCK pathway.

Indeed, the ability of EspH to induce cell rounding, focal adhesion disassembly, and caspase-3 activation is reminiscent of clostridial toxin B (TcdB) intoxication (18). This is not surprising given the fact that EspH, like TcdB, inactivates Rho GTPases, although TcdB directly targets Rho GTPases and inactivates them by glucosylation of Thr-37 (reviewed in reference 29). Significantly, we show that the ability of EPEC to antagonize EspH is mediated by the WxxxE effectors EspT and EspM2 and that neither Map nor Cdc42 activation was able to block EspH-induced cell detachment or caspase-3 activation. While it was previously reported that Map induces mitochondrial dysfunction (27), we did not observe any significant Map-induced cell detachment or caspase-3 activation by transfection. Consistent with our findings that Rac1 and RhoA activation are sufficient to inhibit EspH-induced cell detachment and caspase-3 activation, we also found that FAK, which coordinates the activities of Rac1 and RhoA to regulate focal adhesion dynamics, is an important mediator of EspH-induced cell rounding, cell detachment, and caspase-3 activation. As EspT and SopE are unable to trigger lamellipodium formation in $FAK^{-/-}$ fibroblasts (data not shown), our results support a model in which EPEC and EHEC utilize EspH and bacterial RhoGEFs to mediate focal adhesion dynamics through subversion of FAK signaling pathways.

Intriguingly, EspT, EspM2, and SopE (but not Map) can also inhibit STS-induced caspase-3 activation to the same extent as the anti-apoptotic effector NleH. In addition, EspT and EspM2 promote host cell survival during EPEC infection. Indeed, several reports have demonstrated that Rac1- and RhoA-activating RhoGEFs are able to activate mitogen-activated protein kinase (MAPK) and NF-κB pathways (30–32), which have pivotal roles in the regulation of cell survival (33, 34). As FAK-mediated signaling cascades are also involved in the regulation of cell survival by

Downloaded from mbio.asm.org on March 15, 2012 - Published by mbio.asm.org

Downloaded from mbio.asm.org on March 15, 2012 - Published by mbio.asm.org

bacterial RhoGEFs, more work is required to dissect the mechanisms by which WxxxE-family effectors are able to modulate the cell death response. Thus, in characterizing the interplay between EspH and bacterial RhoGEFs we found that EPEC and EHEC have evolved sophisticated mechanisms to subvert Rho GTPase signaling pathways in a functionally coordinated manner.

MATERIALS AND METHODS

Bacterial strains and plasmids. Strains, plasmids, and primers are listed in Tables S1, S2, and S3, respectively, in the supplemental material. Bacteria were grown from single colonies in Luria-Bertani (LB) broth in a shaking incubator at 37°C. Culture medium or agar was supplemented with ampicillin (100 μg ml^{-1}), chloramphenicol (34 μg ml^{-1}), or kanamycin (50 μg ml^{-1}) as appropriate. Bacterial cultures were primed for infection by dilution of 1:50 of overnight bacterial culture with prewarmed Dulbecco's minimal Eagle medium (DMEM) with low glucose (1,000 mg liter^{-1}) (Sigma) and incubated as static cultures at 37°C in 5% CO_2 for 3 h. Static cultures were induced with 1 mM isopropyl thiogalactopyranoside (IPTG) for pSA10 effector expression 30 min prior to infection.

Molecular cloning. The *espH* gene of E2348/69 was amplified by PCR using the primer pair EcoRI-EspH-E69-Fw–PstI-EspH-E69-Rv, BamHI-EspH-E69-Fw–PstI-EspH-E69-Rv, or HindIII-EspH-E69-Fw–EcoRI-EspH-E69-Rv and cloned into the pSA10, pRK5myc, or pCMV-RFP vector to generate pICC1098, pICC529, and pICC1099, respectively. All constructs were verified by DNA sequencing.

Tissue culture, transfection, and infection with EPEC E2348/69. HeLa (ATCC), FAK$^{-/-}$ (ATCC), and FAK$^{+/+}$ (ATCC) cells were grown at 37°C in a humidified atmosphere containing 5% CO_2 in DMEM with low glucose (1,000 mg liter^{-1}) (Sigma) supplemented with 10% (vol/vol) heat-inactivated fetal bovine serum (Gibco) and 2 mM GlutaMAX (Sigma). Cells were grown in 24-well cell culture plates to 80% confluence. HeLa cells were transfected with mammalian expression vectors using Fugene 6 (Roche) according to the manufacturer's instructions. FAK$^{-/-}$ or FAK$^{+/+}$ cells were transfected with mammalian expression vectors using Lipofectamine 2000 (Invitrogen) according to the manufacturer's instructions. Transfected cells were incubated at 37°C in a humidified incubator with 5% CO_2 for 24 h prior to infection. For EPEC infection, HeLa cells were washed twice with phosphate-buffered saline (PBS) and then infected with primed bacterial culture (multiplicity of infection [MOI], 1:100) at 37°C in a humidified atmosphere containing 5% CO_2 for the appropriate time or treatment. Coverslips were washed three times in PBS and fixed with 3% paraformaldehyde for 15 min before being processed for immunofluorescence microscopy.

Pharmacology. Staurosporine (STS) (Calbiochem) was used at a final concentration of 1 μM for 5 h to induce apoptosis. The pan-caspase inhibitor zVAD-fmk (Promega) was used at a final concentration of 66 μM (together with bacteria or with STS).

Immunofluorescence microscopy. Cells were quenched for 15 min with 50 mM NH_4Cl and then permeabilized for 5 min in PBS–0.2% Triton X-100. Coverslips were washed three times in PBS and blocked in PBS–1% BSA for 10 min before addition of primary antibodies. Coverslips were incubated with primary antibodies diluted in PBS–1% BSA for 1 h. For caspase-3 staining, primary antibodies were incubated overnight at 4°C. After three washes with PBS, coverslips were incubated with secondary antibodies diluted in PBS–1% BSA for a further 1 h. Coverslips were washed three times with PBS and once in water before being mounted in gold Pro-Long antifade medium (Invitrogen) and examined by conventional epifluorescence microscopy using a Zeiss Axio LSM-510 microscope. Images were deconvoluted and processed using AxioVision 4.8 LE software (Zeiss) and Adobe Photoshop CS4.

Antibodies. Actin was detected with Oregon green-conjugated phalloidin antibody (1:100 dilution) (Invitrogen) or tetramethyl rhodamine isothiocyanate (TRITC)-conjugated phalloidin (1:500 dilution) (Sigma). Intimin was labeled with polyclonal chicken anti-intimin antibody serum (1:200 dilution) (kindly provided by Roberto La Ragione). DNA was stained with 4′,6-diamidino-2-phenylindole (DAPI) (1:1,000 dilution). Cleaved caspase-3 (active) was detected using rabbit anti-cleaved caspase-3 antibody (1:50 dilution) (Cell Signaling). Vinculin was visualized using mouse antivinculin antibody (1:200 dilution) (Abcam). Myc-tagged proteins were labeled with mouse anti-Myc antibody (1:500 dilution) (Millipore). Cy2-, RRX-, or Cy5-conjugated donkey anti-mouse, anti-chicken, or anti-rabbit antibodies (1:200 dilution) (Jackson ImmunoResearch) were used as secondary antibodies.

Cell detachment assay. HeLa cells grown in 24-well plates were infected for 1 h (MOI, 1:100) and then treated with 200 μg ml^{-1} gentamicin (Sigma) for a further 3 h. Cells were washed five times with PBS and then trypsinized; trypsin was inactivated with culture medium. Cells were counted using a Neubauer hemocytometer. Counts were expressed as a percentage of uninfected cells and plotted as a graph of percent detached cells.

Cytotoxicity assay. HeLa cells grown in 96-well plates were infected with primed bacterial culture (MOI, 1:200) in phenol red-free DMEM and centrifuged for 4 min at 200 × *g* to synchronize infection. Cells were incubated for 30 min, washed once with PBS, and then incubated with 200 μg ml^{-1} gentamicin (Sigma) in phenol red-free DMEM for a further 4 h. LDH release during EPEC infection was assayed using a CytoTox96 cytotoxicity assay kit (Promega) according to the manufacturer's instructions. Cytotoxicity was calculated as follows: [(experimental LDH activity − basal LDH activity)/(total LDH activity − basal LDH activity)] × 100.

Statistical analysis. Results were expressed as means and standard deviations. Statistical significance was determined by a two-tailed Student *t* test. A *P* value of <0.05, <0.01, or <0.001 was considered significant.

ACKNOWLEDGMENTS

We thank Rey Carabeo (Imperial College London, London, United Kingdom) for the FAK-null and FAK-reconstituted cell lines, Alan Hall (Sloan-Kettering Institute, New York, New York) for the Myc-p115RhoGEF and Myc-Rac(L61) expression vectors, Miguel Seabra (Imperial College London, London, United Kingdom) for the pCMV-RFP expressions vector, and the late Emmanuelle Caron for the Myc-Cdc42(L61) and RhoA(L63) expression vectors. We also thank Abderrahman Hachani, Ana Arbeloa, Leah Ensell, and Tristan Thwaites for technical assistance. This work was supported by grants from the Wellcome Trust.

SUPPLEMENTAL MATERIAL

Supplemental material for this article may be found at http://mbio.asm.org/lookup/suppl/doi:10.1128/mBio.00250-11/-/DCSupplemental.

Figure S1, TIF file, 2.8 MB.
Figure S2, TIF file, 1.4 MB.
Figure S3, TIF file, 0.7 MB.
Figure S4, TIF file, 1 MB.
Figure S5, TIF file, 0.9 MB.
Table S1, PDF file, 0.1 MB.
Table S2, PDF file, 0.1 MB.
Table S3, PDF file, 0.1 MB.

REFERENCES

1. **Hall A.** 1998. Rho GTPases and the actin cytoskeleton. Science **279**:509–514.
2. **Etienne-Manneville S, Hall A.** 2002. Rho GTPases in cell biology. Nature **420**:629–635.
3. **Mitra SK, Hanson DA, Schlaepfer DD.** 2005. Focal adhesion kinase: in command and control of cell motility. Nat. Rev. Mol. Cell Biol. **6**:56–68.
4. **Ilić D, et al.** 1995. Reduced cell motility and enhanced focal adhesion contact formation in cells from FAK-deficient mice. Nature **377**:539–544.
5. **Tomar A, Schlaepfer DD.** 2009. Focal adhesion kinase: switching between GAPs and GEFs in the regulation of cell motility. Curr. Opin. Cell Biol. **21**:676–683.
6. **Bulgin RR, et al.** 2010. Bacterial guanine nucleotide exchange factors SopE-like and WxxxE effectors. Infect. Immun. **78**:1417–1425.
7. **Dong N, Liu L, Shao F.** 2010. A bacterial effector targets host DH-PH

domain RhoGEFs and antagonizes macrophage phagocytosis. EMBO J. **29**:1363–1376.
8. **Alto NM, et al.** 2006. Identification of a bacterial type III effector family with G protein mimicry functions. Cell **124**:133–145.
9. **Simpson N, et al.** 2006. The enteropathogenic *Escherichia coli* type III secretion system effector Map binds EBP50/NHERF1: implication for cell signalling and diarrhoea. Mol. Microbiol. **60**:349–363.
10. **Arbeloa A, et al.** 2008. Subversion of actin dynamics by EspM effectors of attaching and effacing bacterial pathogens. Cell. Microbiol. **10**: 1429–1441.
11. **Bulgin RR, Arbeloa A, Chung JC, Frankel G.** 2009. EspT triggers formation of lamellipodia and membrane ruffles through activation of Rac-1 and Cdc42. Cell. Microbiol. **11**:217–229.
12. **Buchwald G, et al.** 2002. Structural basis for the reversible activation of a Rho protein by the bacterial toxin SopE. EMBO J. **21**:3286–3295.
13. **Huang Z, et al.** 2009. Structural insights into host GTPase isoform selection by a family of bacterial GEF mimics. Nat. Struct. Mol. Biol. **16**: 853–860.
14. **Arbeloa A, et al.** 2010. EspM2 is a RhoA guanine nucleotide exchange factor. Cell. Microbiol. **12**:654–664.
15. **Kenny B, et al.** 2002. Co-ordinate regulation of distinct host cell signalling pathways by multifunctional enteropathogenic *Escherichia coli* effector molecules. Mol. Microbiol. **44**:1095–1107.
16. **Berger CN, Crepin VF, Jepson MA, Arbeloa A, Frankel G.** 2009. The mechanisms used by enteropathogenic *Escherichia coli* to control filopodia dynamics. Cell. Microbiol. **11**:309–322.
17. **Tu X, Nisan I, Yona C, Hanski E, Rosenshine I.** 2003. EspH, a new cytoskeleton-modulating effector of enterohaemorrhagic and enteropathogenic *Escherichia coli*. Mol. Microbiol. **47**:595–606.
18. **Fiorentini C, et al.** 1998. *Clostridium difficile* toxin B induces apoptosis in intestinal cultured cells. Infect. Immun. **66**:2660–2665.
19. **Gervais FG, Thornberry NA, Ruffolo SC, Nicholson DW, Roy S.** 1998. Caspases cleave focal adhesion kinase during apoptosis to generate a FRNK-like polypeptide. J. Biol. Chem. **273**:17102–17108.
20. **Hemrajani C, et al.** 2010. NleH effectors interact with Bax inhibitor-1 to block apoptosis during enteropathogenic *Escherichia coli* infection. Proc. Natl. Acad. Sci. U. S. A. **107**:3129–3134.
21. **Andor A, et al.** 2001. YopE of *Yersinia*, a GAP for Rho GTPases, selectively modulates Rac-dependent actin structures in endothelial cells. Cell. Microbiol. **3**:301–310.
22. **Shao F, et al.** 2003. Biochemical characterization of the *Yersinia* YopT protease: cleavage site and recognition elements in Rho GTPases. Proc. Natl. Acad. Sci. U. S. A. **100**:904–909.
23. **Prehna G, Ivanov MI, Bliska JB, Stebbins CE.** 2006. *Yersinia* virulence depends on mimicry of host Rho-family nucleotide dissociation inhibitors. Cell **126**:869–880.
24. **Yarbrough ML, et al.** 2009. AMPylation of Rho GTPases by *Vibrio* VopS disrupts effector binding and downstream signaling. Science **323**: 269–272.
25. **Kubori T, Galán JE.** 2003. Temporal regulation of *Salmonella* virulence effector function by proteasome-dependent protein degradation. Cell **115**:333–342.
26. **Wong AR, et al.** 2011. Enteropathogenic and enterohaemorrhagic *Escherichia coli*: even more subversive elements. Mol. Microbiol. **80**: 1420–1438.
27. **Ma C, et al.** 2006. *Citrobacter rodentium* infection causes both mitochondrial dysfunction and intestinal epithelial barrier disruption *in vivo*: role of mitochondrial associated protein (Map). Cell. Microbiol. **8**:1669–1686.
28. **Martinez E, et al.** 2010. Binding to Na^+/H^+ exchanger regulatory factor 2 (NHERF2) affects trafficking and function of the enteropathogenic *Escherichia coli* type III secretion system effectors Map, EspI and NleH. Cell. Microbiol. **12**:1718–1731.
29. **Voth DE, Ballard JD.** 2005. *Clostridium difficile* toxins: mechanism of action and role in disease. Clin. Microbiol. Rev. **18**:247–263.
30. **Fukazawa A, et al.** 2008. GEF-H1 mediated control of NOD1 dependent NF-κB activation by *Shigella* effectors. PLoS Pathog. **4**:e1000228.
31. **Bruno V, et al.** 2009. *Salmonella typhimurium* type III secretion effectors stimulate innate immune responses in cultured epithelial cells. PLoS Pathog. **5**:e1000538.
32. **Raymond B, Crepin VF, Collins JW, Frankel G.** 2011. The WxxxE effector EspT triggers expression of immune mediators in an Erk/JNK and NF-κB-dependent manner. Cell. Microbiol. **13**:1881–1893.
33. **Karin M, Lin A.** 2002. NF-κB at the crossroads of life and death. Nat. Immunol. **3**:221–227.
34. **Wada T, Penninger JM.** 2004. Mitogen-activated protein kinases in apoptosis regulation. Oncogene **23**:2838–2849.
35. **Levine MM, et al.** 1978. *Escherichia coli* that cause diarrhoea but do not produce heat-labile or heat-stable enterotoxins and are non-invasive. Lancet **1**:119–122.
36. **Marchès O, et al.** 2008. EspJ of enteropathogenic and enterohaemorrhagic *Escherichia coli* inhibits opsono-phagocytosis. Cell. Microbiol. **10**: 1104–1115.

Downloaded from mbio.asm.org on March 15, 2012 - Published by mbio.asm.org

Cellular Microbiology (2012) doi:10.1111/j.1462-5822.2012.01778.x

The enteropathogenic *E. coli* effector EspH promotes actin pedestal formation and elongation via WASP-interacting protein (WIP)

Alexander R. C. Wong, Benoit Raymond, James W. Collins, Valerie F. Crepin and Gad Frankel*

Centre for Molecular Microbiology and Infection, Division of Cell and Molecular Biology, Imperial College London, London SW7 2AZ, UK.

Summary

Enteropathogenic and enterohaemorrhagic *Escherichia coli* (EPEC and EHEC) are diarrheagenic pathogens that colonize the gut mucosa via attaching-and-effacing lesion formation. EPEC and EHEC utilize a type III secretion system (T3SS) to translocate effector proteins that subvert host cell signalling to sustain colonization and multiplication. EspH, a T3SS effector that modulates actin dynamics, was implicated in the elongation of the EHEC actin pedestals. In this study we found that EspH is necessary for both efficient pedestal formation and pedestal elongation during EPEC infection. We report that EspH induces actin polymerization at the bacterial attachment sites independently of the Tir tyrosine residues Y474 and Y454, which are implicated in binding Nck and IRSp53/ITRKS respectively. Moreover, EspH promotes recruitment of neural Wiskott–Aldrich syndrome protein (N-WASP) and the Arp2/3 complex to the bacterial attachment site, in a mechanism involving the C-terminus of Tir and the WH1 domain of N-WASP. Dominant negative of WASP-interacting protein (WIP), which binds the N-WASP WH1 domain, diminished EspH-mediated actin polymerization. This study implicates WIP in EPEC-mediated actin polymerization and pedestal elongation and represents the first instance whereby N-WASP is efficiently recruited to the EPEC attachment sites independently of the Tir:Nck and Tir:IRTKS/IRSp53 pathways. Our study reveals the intricacies of Tir and EspH-mediated actin signalling pathways that comprise of distinct, convergent and synergistic signalling cascades.

Received 18 October, 2011; revised 8 December, 2011; accepted 12 December, 2011. *For correspondence. E-mail g.frankel@imperial.ac.uk; Tel. (+44) 20 75945253; Fax (+44) 20 75943069.

© 2012 Blackwell Publishing Ltd

Introduction

The actin cytoskeleton plays a critical role in many cellular processes, including cell morphology, migration, cytokinesis and apoptosis. As a result, many bacterial pathogens hijack the host actin machinery to enhance colonization and dissemination. Enteropathogenic *Escherichia coli* (EPEC), enterohaemorrhagic *E. coli* (EHEC) (Nataro and Kaper, 1998; Wong *et al*., 2011) and the closely related mouse pathogen *Citrobacter rodentium* (Mundy *et al*., 2005) belong to a group of mainly extracellular diarrheagenic pathogens that colonize the gut epithelium by attaching-and-effacing (A/E) lesions (Frankel and Phillips, 2008). The A/E histopathology is characterized by effacement of the brush border microvilli, intimate bacterial adherence to the enterocyte apical plasma membrane, and the accumulation of polymerized actin beneath the attached bacteria (Knutton *et al*., 1987). In cultured cells, EPEC-induced actin polymerization leads to formation of actin-rich pedestals.

Formation of A/E legions *in vivo* and actin pedestals *in vitro* is dependent on the outer membrane bacterial adhesin intimin (Jerse and Kaper, 1991) and the translocated intimin receptor (Tir) (Kenny *et al*., 1997). Upon translocation, Tir is inserted into the plasma membrane in a hairpin loop topology, with cytoplasmic N- and C-termini and an extracellular middle loop which binds intimin (Kenny *et al*., 1997; Hartland *et al*., 1999). Intimin : Tir interaction results in Tir clustering and the initiation of downstream signalling events that lead to the formation of the actin-rich pedestals (Frankel and Phillips, 2008).

EPEC-induced actin polymerization is attributed to the C-terminus of Tir. In the prototypical EPEC strain E2348/69, phosphorylation of the Tir tyrosine residue 474 (Y474) by host cell tyrosine kinases (Phillips *et al*., 2004; Swimm *et al*., 2004; Bommarius *et al*., 2007) generates a binding site for the mammalian cell adaptor protein Nck, which then recruits and activates the neural Wiskott–Aldrich syndrome protein (N-WASP) leading to stimulation of strong Arp2/3-mediated actin polymerization (Kenny, 1999; Gruenheid *et al*., 2001). In addition, Tir can also promote weak Nck-independent actin polymerization through tyrosine residue Y454 that forms part of a conserved Asn-Pro-Tyr (NPY) motif (Campellone and Leong, 2005; Brady *et al*., 2007). The NPY motif recruits the insulin receptor tyrosine kinase substrate p53 (IRSp53)

Fig. 1. EspH localizes to plasma membrane surrounding actin pedestals and promotes localized actin polymerization independently of Tir tyrosine residues Y454 and Y474.
A. Schematic representation of tir_{EPEC} chromosomal mutagenesis strategy. Amplified fragments of recombinant pGEMT plasmids containing *tir* Y454 and/or Y474 mutations were used to introduce the mutations in tandem with an *aphT* kanamycin-resistance cassette into the endogenous tir_{EPEC} locus to generate E2348/69 Tir_{Y454A}, Tir_{Y474A} and $Tir_{Y454A/Y474A}$ mutants. As a control recombination of *tir*, an *aphT* kanamycin-resistance cassette with no mutations was inserted (E2348/69 Tir_{WT}).
B. Quantification of EPEC microcolonies associated with actin on cells infected with E2348/69 expressing Tir_{WT}, Tir_{Y454A}, Tir_{Y474A} or $Tir_{Y454A/Y474A}$, with or without EspH-HA (pEspH-HA). A total of 100 microcolonies were counted in triplicates. Results are presented as a mean ± SD of three independent experiments. Asterisks indicate statistical significance ($P < 0.01$).
C. Infection of Swiss 3T3 fibroblasts with E2348/69 expressing Tir_{WT}, $Tir_{Y454A/Y474A}$ or E2348/69Δ*tir*, with or without plasmid-expressed haemagglutinin-tagged EspH (pEspH-HA). Actin was stained with Oregon green phalloidin (green), HA-tagged EspH was detected with anti-HA antibody (red), Tir was detected with anti-Tir antibody (magenta) and bacteria were visualized with DAPI staining (cyan). EspH localized to the pedestal membrane (arrows). Ectopic expression of EspH induced localized F-actin accumulation under E2348/69 expressing $Tir_{Y454A/Y474A}$ (arrows), but not E2348/69 $Tir_{Y454A/Y474A}$ alone. No detection of actin was observed in E2348/69Δ*tir* + pEspH. Bar = 5 μm.

family of proteins IRTKS (Vingadassalom *et al*., 2009) and IRSp53 (Weiss *et al*., 2009) in EPEC, leading to activation of yet unknown downstream actin polymerization signalling pathways. Importantly, we have recently reported that although not affecting *C. rodentium* bacterial load and A/E lesion formation *in vivo*, Tir residues Y451 and Y471, and by extension Tir:Nck and Tir:IRTKS/IRSp53 signalling pathways, provide the bacterium with competitive edge and higher fitness *in vivo* (Crepin *et al*., 2009).

N-WASP consists of several domains. The C-terminal verprolin-central-acidic (VCA) domain binds and activates the Arp2/3 complex (Rohatgi *et al*., 1999), while the WASP-homology 1 (WH1), Basic (B), GTPase-binding domain (GBD) and proline-rich domain (PRD) integrate multiple upstream signals to regulate the localization and activation of the protein (Takenawa and Suetsugu, 2007; Padrick and Rosen, 2010). Although Nck binds directly to N-WASP via the PRD domain (Anton *et al*., 1998; Rohatgi *et al*., 2001), the PRD domain is dispensable for pedestal formation. Instead, the WH1 domain of N-WASP is required for EPEC pedestal formation (Lommel *et al*., 2001). The WASP-interacting protein (WIP) family, which comprise WIP (Ramesh *et al*., 1997), CR16 (Weiler *et al*., 1996; Ho *et al*., 2001) and WICH/WIRE (Aspenstrom, 2002; Kato *et al*., 2002), are known interacting partners of the WH1 domain of WASP/N-WASP. WIP binds WH1 domain via its C-terminus region, termed the WASP-binding domain (WBD) (Volkman *et al*., 2002; Peterson *et al*., 2007).

EspH is a T3SS effector that was implicated in modulating actin dynamics. Deletion of *espH* in EHEC resulted in short pedestals, while overexpression of EspH led to pedestal elongation (Tu *et al*., 2003). Although EspH is not required for A/E lesion formation, several studies have indicated its importance in bacterial adherence and colonization (Ritchie and Waldor, 2005; Shaw *et al*., 2005). Recently, Dong *et al*. (2010) reported that EspH is a RhoGEF inhibitor that acts by competitively binding to the tandem Dbl-homology and pleckstrin-homology (DH-PH) domains of Dbl-family mammalian RhoGEFs (Dong *et al*., 2010). The aim of this study is to further characterize the role EspH plays in modulating actin dynamics during EPEC infection.

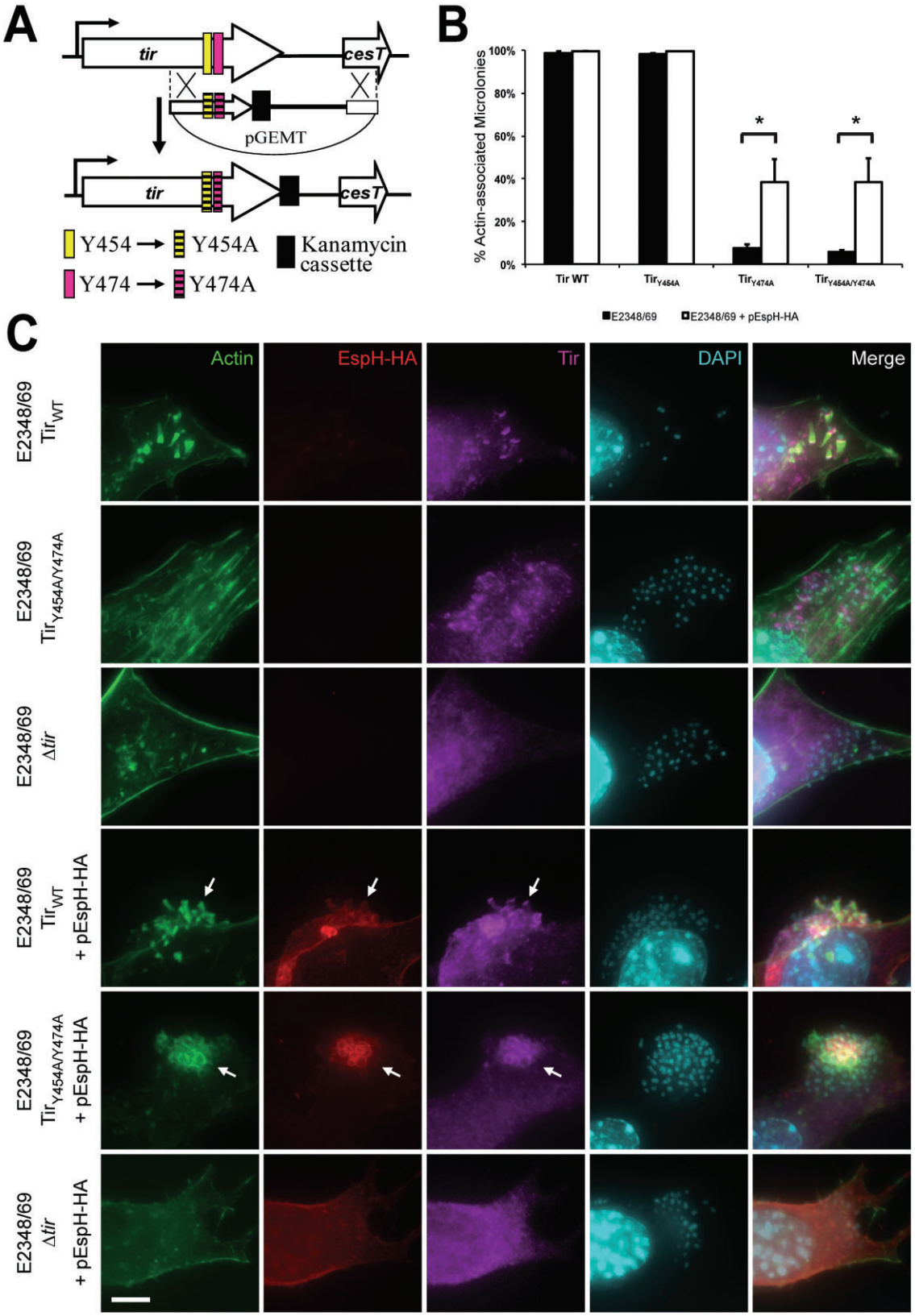
Results

EspH promotes both pedestal formation and pedestal elongation during EPEC infection

To assess the role of EspH in the kinetics of EPEC-induced pedestal formation, Swiss 3T3 fibroblasts were infected with wild-type E2348/69, E2348/69Δ*espH* or E2348/69Δ*espH* complemented with EspH. Microcolonies (5 or more bacteria) associated with pedestals were then enumerated by immunofluorescence microscopy at time intervals of 10, 20, 30, 45 or 90 min post infection. Actin pedestals were observed in 88.8 ± 5.8% of E2348/69 microcolonies at 30 min post infection (Fig. S1A). In contrast, only 41.7 ± 5.5% of microcolonies were associated with pedestals in the *espH* mutant. In addition, at 90 min, pedestals formed by the E2348/69Δ*espH* mutant were markedly shorter than those observed in the other strains (Fig. S1B). Pedestals formed by the E2348/69Δ*espH* mutant did not appear elongated even after 2 h of infection (data not shown). These results confirm that EspH is involved in promoting the formation and elongation of EPEC actin pedestals (Tu *et al*., 2003).

EspH triggers actin signalling pathways independently of Tir tyrosine residues Y454 and Y474

As EspH modulates the length of the EPEC actin pedestals, we hypothesized that it could amplify one of the Tir actin signalling pathways. We constructed E2348/69 chromosomally expressing Tir_{Y454A} (mutated at the IRSp53/IRTKS binding site), Tir_{Y474A} (mutated at the Nck-binding site) and $Tir_{Y454A/Y474A}$ (double mutant), using the lambda red mutagenesis strategy (Datsenko and Wanner, 2000; Crepin *et al*., 2009) involving insertion of a kanamycin cassette in the *tir-cesT* intergenic region (Fig. 1A). A



© 2012 Blackwell Publishing Ltd, *Cellular Microbiology*

control mock mutant was also generated with the insertion of the kanamycin cassette, but without modification to the *tir* coding sequence (Tir_{WT}). We first assessed the ability of these Tir mutants to translocate Tir and induce actin polymerization in infected Swiss 3T3 fibroblasts. Tir_{WT} and Tir_{Y454A} localized under adherent bacteria and formed actin pedestals (Figs 1B and S2), while Tir_{Y474A} and $Tir_{Y454A/Y474A}$ were detected underneath E2348/69 but did not trigger actin polymerization (Figs 1B and S2). Neither Tir nor actin polymerization was observed under the attached E2348/69Δ*tir* control strain.

We then expressed HA-tagged EspH in the same strains and assessed its impact on actin polymerization. Unexpectedly, EspH triggered localized actin polymerization in 38.5 ± 10.6% and 38.5 ± 10.9% of adherent E2348/69 expressing HA-EspH and Tir_{Y474A} or $Tir_{Y454A/Y474A}$ (Fig. 1B and C; Fig. S2). However, EspH-mediated actin polymerization was different from that formed by E2349/69 expressing Tir_{WT}, as the microcolonies were surrounded by an actin 'coat', rather than associated with distinctive pedestals (Fig. 1B and C; Fig. S2). EspH was mainly localized to the membrane surrounding F-actin, and the plasma membrane of infected cells (Fig. 2C). In contrast, neither actin polymerization nor EspH was detected beneath adherent E2348/69Δ*tir* expressing HA-tagged EspH (Fig. 1C), indicating that recruitment of EspH and F-actin at the bacterial attachment site is Tir-dependent.

EspH promotes recruitment of N-WASP to the bacterial attachment site

To investigate the mechanism of actin polymerization triggered by E2348/69 coexpressing $Tir_{Y454A/Y474A}$ and EspH, we determined which actin promoting factors are recruited to the bacterial attachment site. Infection of Swiss 3T3 with E2348/69 expressing Tir_{WT} and $Tir_{Y454A/Y474A}$ was used as controls. Staining for N-WASP (Fig. 2A) and the Arp2 subunit of the Arp2/3 complex (Fig. 2B) 2 h post infection revealed that both proteins were accumulated underneath E2348/69 expressing Tir_{WT} and E2348/69 coexpressing $Tir_{Y454A/Y474A}$ and EspH. In contrast, only a few microcolonies of E2348/69 expressing $Tir_{Y454A/Y474A}$ were associated with N-WASP and the Arp2 subunit. We also investigated recruitment of IRSp53 and WAVE2 by transfection of their respective Myc-tagged constructs, but did not observe their recruitment to the bacterial attachment site, indicating that they are not required for EspH-mediated actin polymerization (Fig. S3). These results show that EspH promotes efficient recruitment of N-WASP and the Arp2/3 complex beneath EPEC microcolonies independently of the Tir tyrosine residues Y454 and Y474.

EspH promotes actin polymerization independently of Nck or Rho GTPases

In order to determine if Nck plays a role in EspH-mediated actin polymerization, we infected Nck-deficient ($Nck^{-/-}$) fibroblasts with E2348/69 expressing Tir_{WT} or $Tir_{Y454A/Y474A}$, with or without coexpression of EspH-HA. While E2348/69 coexpressing Tir_{WT} or $Tir_{Y454A/Y474A}$ and EspH triggered localized actin polymerization, E2348/69 expressing Tir_{WT} or $Tir_{Y454A/Y474A}$ alone did not (Fig. 3A). This result suggests that EspH mediates actin polymerization dependently of Nck.

To assess if the repression of Rho GTPases is involved in EspH-mediated actin polymerization, we performed siRNA knockdown of Cdc42, Rac1 and RhoA, and infected Swiss 3T3 fiboblasts with E2348/69 expressing $Tir_{Y454A/Y474A}$ with or without EspH. Specificity of RNAi-mediated silencing was assessed by Western blot (Fig. 3B). Quantification of EPEC microcolonies revealed no difference in actin-associated microcolonies compared with the scrambled siRNA control (Fig. 3B). This suggests that EspH-mediated actin polymerization is not a result of Rho GTPase inactivation.

EspH-mediated actin polymerization requires the C-terminus of Tir

We next determine which of the cytoplasmic Tir domains is involved in EspH-mediated N-WASP recruitment. Towards this end, we utilized a Tir complementation assay previously described (Campellone *et al*., 2004a). We obtained an HA-tagged Tir derivative that has its N-terminus replaced with the transmembrane domain of the Newcastle Disease Virus HN protein, followed by the intimin-binding extracellular loop and C-terminus of Tir (HA-TirMC), and a similar construct but with a point Y474F mutation (HA-$TirMC_{Y474F}$) (kindly provided by J. Leong). Using HA-TirMC as a template, we deleted the C-terminus tail and inserted the N-terminus of Tir before the HN transmembrane domain to generate HA-TirNM (Fig. 4A). Using GFP as negative control, we transfected the Tir derivatives into Swiss 3T3 fibroblasts; 30 h later the cells were infected for 2 h with E2348/69Δ*tir* expressing EspH. Triple staining of HA-tagged Tir, N-WASP, and intimin revealed that both HA-TirMC and HA-$TirMC_{Y474F}$, but not HA-TirNM, recruited N-WASP at the site of intimin-clustered Tir (Fig. 4B). These results suggest that EspH-mediated recruitment of N-WASP is dependent on the C-terminus of Tir independently of Y474.

The WH1 domain of N-WASP is required for EspH-mediated actin polymerization

To investigate the role of N-WASP in EspH-mediated actin polymerization we constructed several deletion variants of

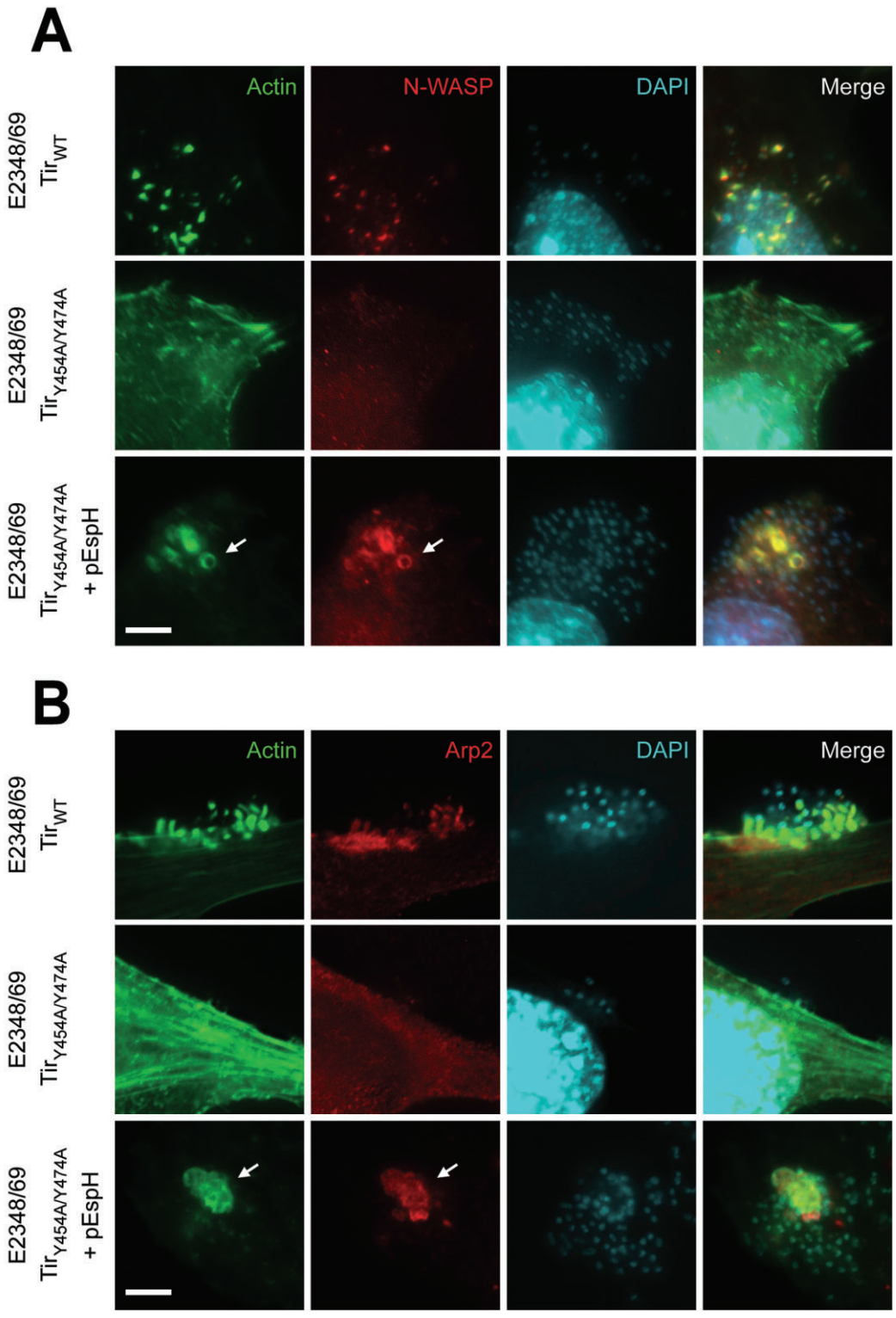


Fig. 2. EspH promotes recruitment of N-WASP and the Arp2 subunit of the Arp2/3 complex independently of Tir tyrosine residues Y454 and Y474.
Infection of Swiss 3T3 fibroblasts with E2348/69 expressing Tir_{WT}, $Tir_{Y454A/Y474A}$, or coexpressing $Tir_{Y454A/Y474A}$ and EspH (E2348/69 $Tir_{Y454A/Y474A}$ + pEspH). N-WASP (A) or the Arp2/3 complex (B) was detected with anti-N-WASP antibody or anti-Arp2 antibody respectively (red). Actin was stained with Oregon green phalloidin (green), and bacteria were visualized with DAPI staining (cyan). N-WASP (A) and the Arp2 subunit (B) were both detected under adherent E2348/69 expressing Tir_{WT} and E2348/69 $Tir_{Y454A/Y474A}$ + pEspH (arrows), but not $Tir_{Y454A/Y474A}$ alone. Bar = 5 μm.

© 2012 Blackwell Publishing Ltd, *Cellular Microbiology*

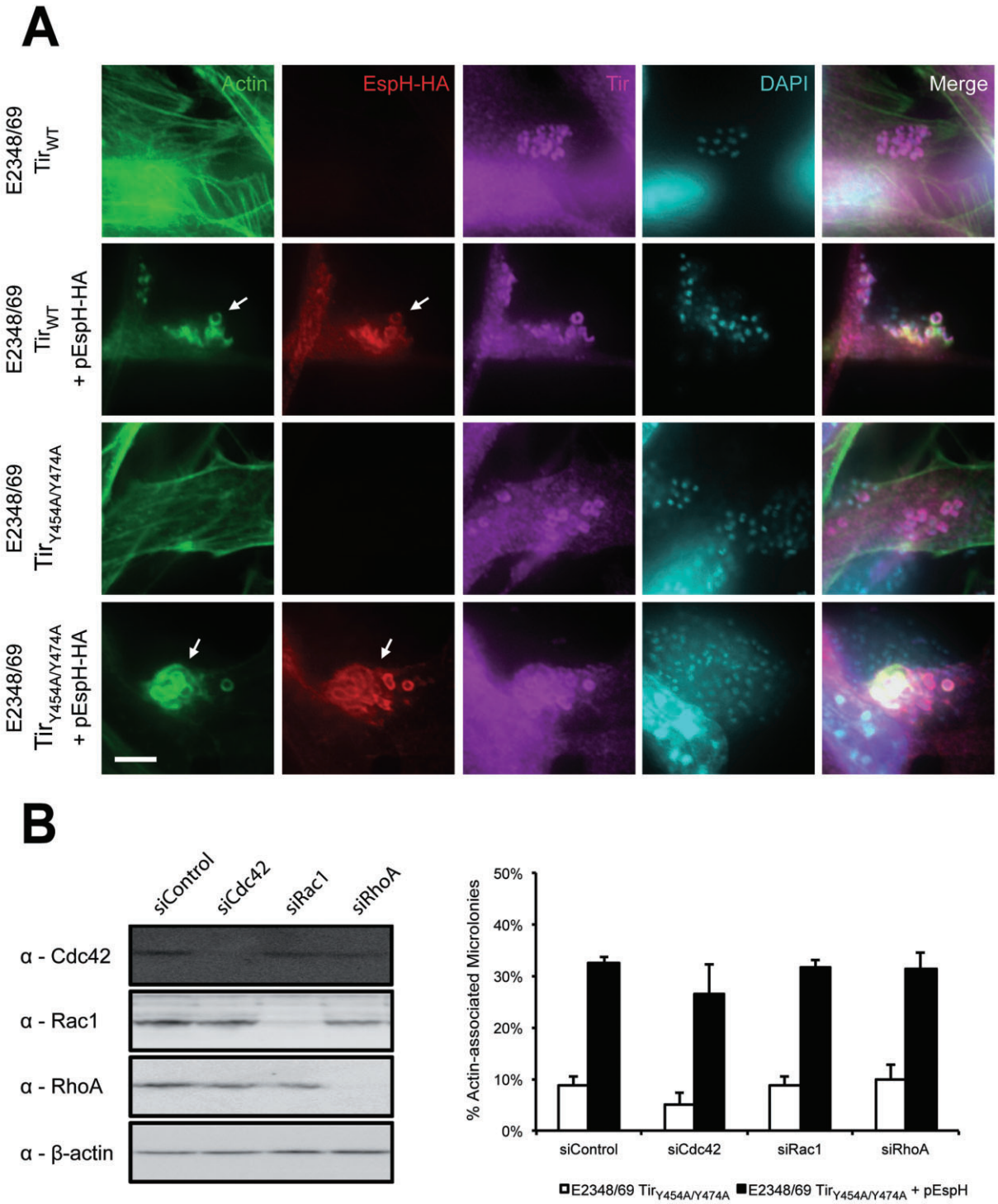


Fig. 3. Nck and Rho GTPases are not involved in EspH-mediated actin polymerization.
A. Infection of Nck-deficient (Nck$^{-/-}$) fibroblasts with E2348/69 Tir$_{WT}$ or E2348/69 Tir$_{Y454A/Y474A}$, with or without pEspH-HA. Actin was stained with Oregon green phalloidin (green), HA-tagged EspH was detected with anti-HA antibody (red), Tir was detected with anti-Tir antibody (magenta) and bacteria were visualized with DAPI staining (cyan). Expression of EspH induced localized actin polymerization in both E2348/69 Tir$_{WT}$ and E2348/69 Tir$_{Y454A/Y474A}$ (arrows). Bar = 5 μm.
B. Immunoblotting of Swiss 3T3 fibroblasts treated with siRNA against Cdc42, Rac1 or RhoA. Scramble siRNA was used as a control (siControl). Specific RNAi-mediated silencing was detected with anti-Cdc42, anti-Rac1 or anti-RhoA antibodies, with β-actin used as loading control. Quantification of EPEC microcolonies associated with actin on siRNA-treated cells infected with E2348/69 expressing Tir$_{Y454A/Y474A}$, with or without EspH (pEspH) revealed that the Rho GTPases play no role in formation of EspH-induced actin coats. A total of 100 microcolonies were counted in triplicates. Results are presented as a mean ± SD of three independent experiments.

© 2012 Blackwell Publishing Ltd, *Cellular Microbiology*

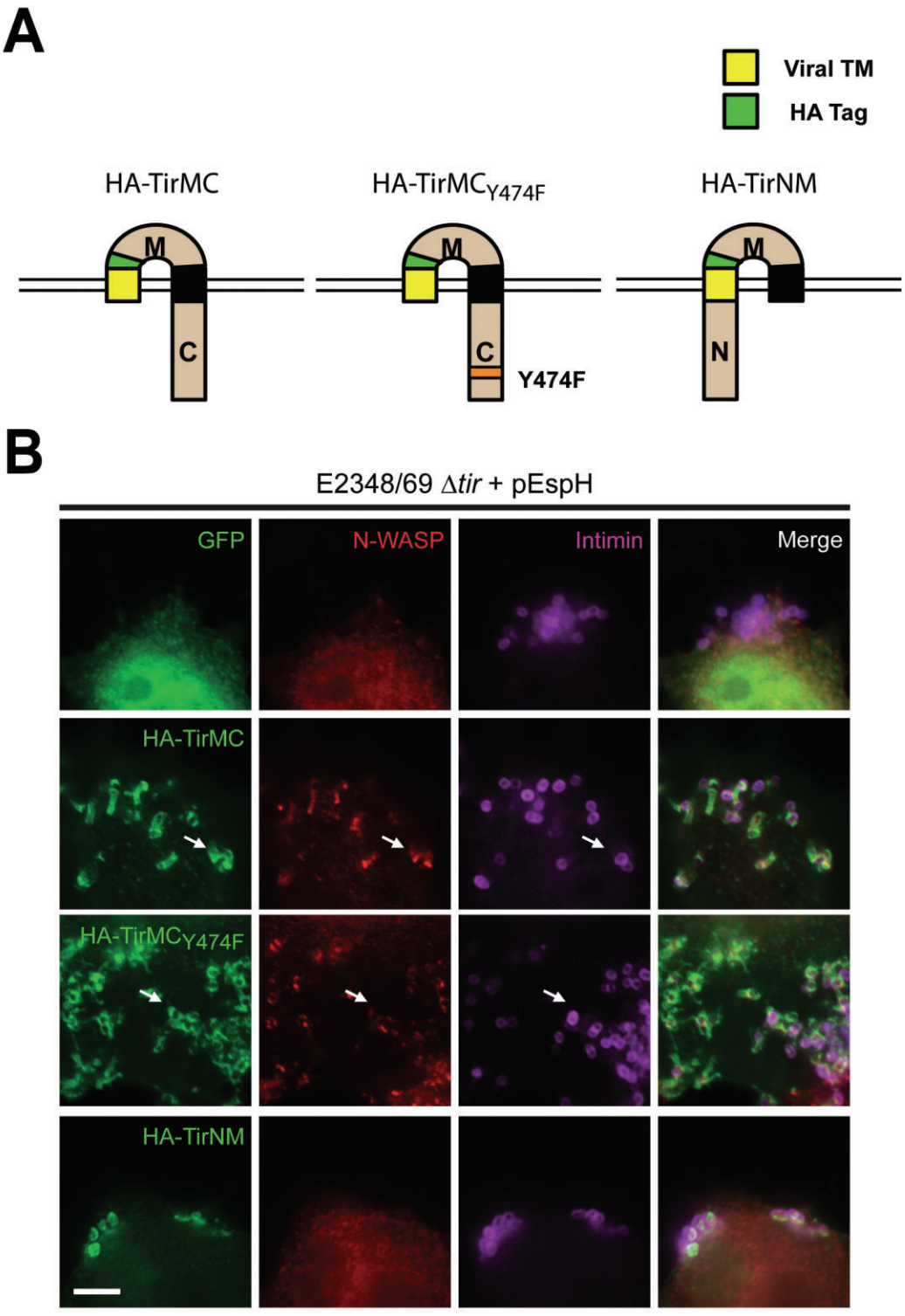


Fig. 4. EspH-mediated N-WASP recruitment is dependent on the C-terminus of Tir.
A. Schematic representation of Tir transfection derivatives comprising HA-TirMC, HA-TirMC$_{Y474F}$ and HA-TirNM.
B. Swiss 3T3 fibroblasts were transfected with the Tir derivatives, or GFP as negative control and infected with E2348/69Δ*tir* expressing EspH (E2348/69Δ*tir* + pEspH). HA-tagged Tir was detected with anti-HA antibody (green), N-WASP was detected with an anti-N-WASP antibody (red) and bacteria were visualized with an anti-intimin antibody (magenta) to indicate positive Tir clustering. N-WASP was not detected beneath adherent microcolonies in cells transfected with GFP or HA-TirNM. Transfection of HA-TirMC or HA-TirMC$_{Y474F}$ complemented recruitment of N-WASP by E2348/69Δ*tir* + pEspH (arrows). Bar = 5 μm.

© 2012 Blackwell Publishing Ltd, *Cellular Microbiology*

Fig. 5. EspH-mediated actin polymerization is dependent on the WH1 domain of N-WASP.
A. Schematic representation of N-WASP deletion variants GFP-ΔWH1, GFP-ΔB, GFP-ΔCRIB, GFP-ΔGBD, GFP-ΔPRD and GFP-WH1-VCA.
B. Lysates of N-WASP$^{-/-}$ mouse embryonic fibroblasts (MEFs) transfected with GFP or GFP-N-WASP deletion variants were immunoblotted and probed with anti-N-WASP antibodies. GFP-N-WASP was detected as a ~ 90 kDa protein; no N-WASP was detected on N-WASP$^{-/-}$ MEFs transfected with GFP alone. Ectopic expression of GFP-ΔWH1, GFP-ΔB, GFP-ΔCRIB, GFP-ΔGBD, GFP-ΔPRD and GFP-WH1-VCA resulted in accumulation of intact fusion proteins.
C. Quantification of EPEC microcolonies associated with actin in N-WASP$^{-/-}$ MEFs expressing GFP-N-WASP deletion variants and infected with E2348/69 expressing Tir_{WT}, $Tir_{Y454A/Y474A}$, or coexpressing $Tir_{Y454A/Y474A}$ and EspH-HA (E2348/69 $Tir_{Y454A/Y474A}$ + pEspH-HA). A total of 100 microcolonies were counted in triplicates. Results are presented as a mean ± SD of three independent experiments. Asterisks indicate statistical significance ($P < 0.001$).
D. N-WASP$^{-/-}$ MEFs transfected with different GFP-N-WASP deletion variants were infected with E2348/69 Tir_{WT} or E2348/69 $Tir_{Y454A/Y474A}$ + pEspH-HA. HA-tagged EspH was detected with anti-HA antibody (green), actin was stained with TRITC phalloidin (red) and bacteria were visualized with DAPI staining (cyan). No actin was detected beneath adherent microcolonies in GFP-transfected cells. Actin polymerization was significantly impaired in GFP-ΔWH1-transfected cells infected with either E2348/69 Tir_{WT} or $Tir_{Y454A/Y474A}$ + pEspH-HA. Transfection with GFP-WH1-VCA was sufficient to restore actin polymerization in E2348/69 Tir_{WT} and $Tir_{Y454A/Y474A}$ + pEspH-HA (arrow). Bar = 5 μm.

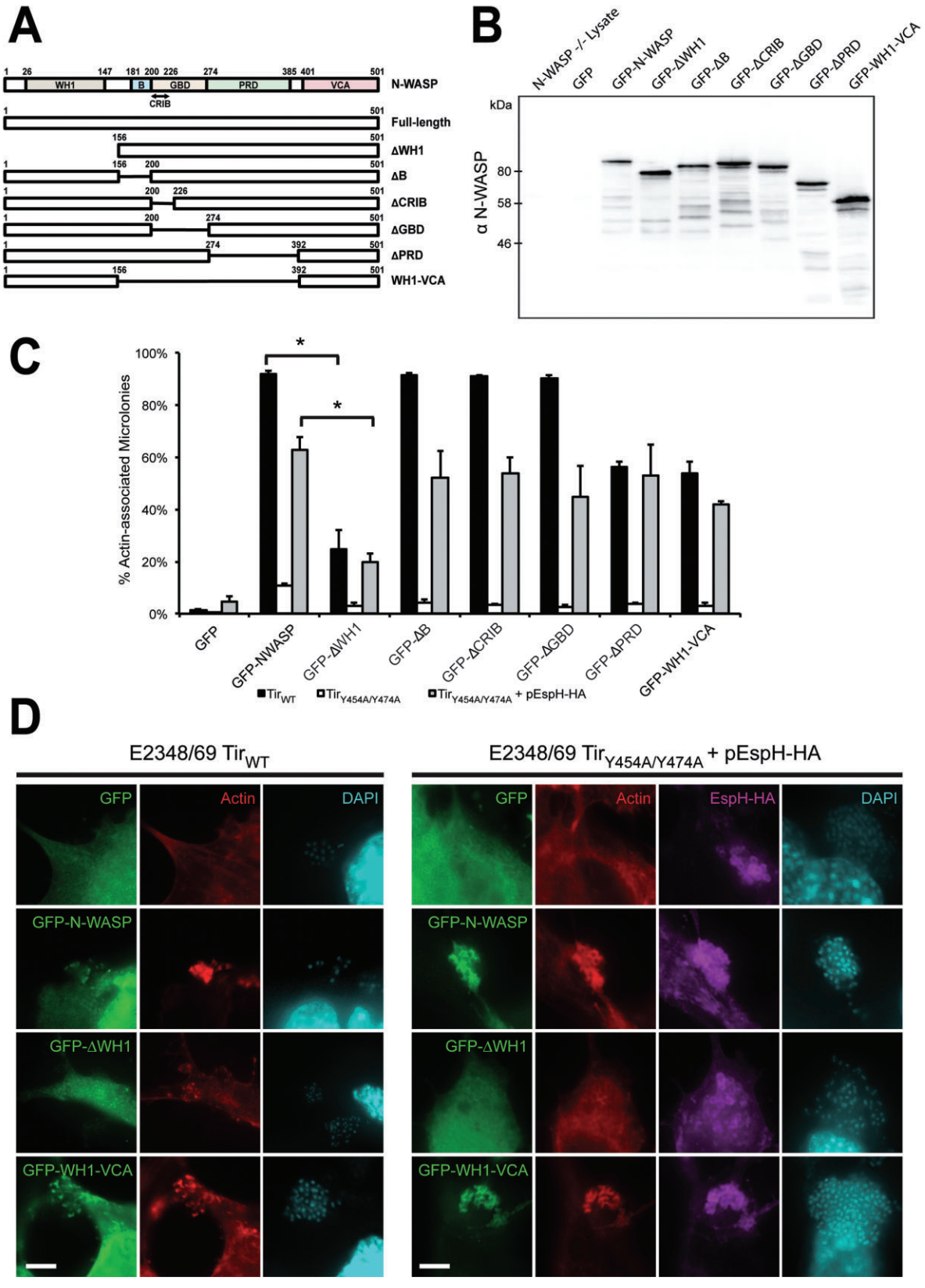
murine N-WASP fused to GFP (Fig. 5A), and transfected them into N-WASP-deficient (N-WASP$^{-/-}$) mouse embryonic fibroblasts (MEFs). GFP alone was used as a control. Immunoblotting of N-WASP$^{-/-}$ MEF cell lysates with anti-GFP (Fig. S4A) or anti-N-WASP (Fig. 5B) antibodies showed that the fusion proteins were expressed and stable. We next infected the transfected N-WASP$^{-/-}$ MEFs with E2348/69 expressing Tir_{WT}, $Tir_{Y454A/Y474A}$ or coexpressing $Tir_{Y454A/Y474A}$ and EspH-HA. No polymerized actin was detected in GFP transfected MEFs infected with any of the EPEC strains (Fig. 5C and D). Transfection of GFP-N-WASP restored pedestal formation by E2348/69 expressing Tir_{WT}, with 91.9 ± 1.3% of microcolonies associated with polymerized actin (Fig. 5C and D). Only 10.8 ± 0.9% of microcolonies were associated with polymerized actin in the GFP-N-WASP transfected cells infected with E2348/69 expressing $Tir_{Y454A/Y474A}$ (Fig. 5C). However, infection of the GFP-N-WASP transfected cells with E2348/69 coexpressing $Tir_{Y454A/Y474A}$ and EspH-HA resulted in 62.7 ± 5.0% of microcolonies associated with polymerized actin and N-WASP recruitment to the site of bacterial adherence (Fig. 5C and D).

We then assessed the importance of the individual domains of N-WASP for EspH-mediated actin polymerization. Deletion of the WASP-homology 1 (GFP-ΔWH1) or proline-rich (GFP-ΔPRD) domains of N-WASP resulted in a marked decrease in pedestal formation by E2348/69 expressing Tir_{WT}, as 24.7 ± 7.3% and 56.1 ± 2.1% respectively of EPEC microcolonies were associated with polymerized actin (Fig. 5C). When the transfected MEFs were infected with E2348/69 coexpressing $Tir_{Y454A/Y474A}$ and EspH, only the deletion of the WH1 domain of N-WASP (GFP-ΔWH1) resulted a significant reduction, with 19.8 ± 3.2% of EPEC microcolonies associated with polymerized actin (Fig. 5C and D). Compared with full-length N-WASP, we did not observe a significant difference in actin polymerization triggered by E2348/69 expressing Tir_{WT} or E2348/69 coexpressing $Tir_{Y454A/Y474A}$ and EspH-HA in N-WASP$^{-/-}$ MEFs expressing GFP-N-WASP deletions in Basic (GFP-ΔB), Cdc42/Rac-interactive binding (GFP-ΔCRIB) or GTPase-binding (GFP-ΔGBD) domains (Figs 5C and S4B).

To establish the role of the WH1 domain in EPEC-mediated actin polymerization, we constructed an expression variant with the WH1 domain fused directly to the VCA domain of N-WASP (GFP-WH1-VCA), and ectopically expressed this construct in N-WASP$^{-/-}$ MEFs. Infection with E2348/69 expressing Tir_{WT} resulted in 53.7 ± 4.7% of microcolonies associated with polymerization actin, compared with 91.9 ± 1.3% of microcolonies associated with polymerization actin in N-WASP$^{-/-}$ MEFs complemented with the full length N-WASP (Fig. 5C and D). However, the GFP-WH1-VCA construct was as functional as the full-length N-WASP in the context of infection with E2348/69 coexpressing $Tir_{Y454A/Y474A}$ and EspH-HA (Fig. 5C and D). Taken together, these results show that both the WH1 and PRD domains are required for efficient Tir-mediated pedestal formation and elongation. Moreover, the WH1 domain of N-WASP is necessary for EspH-mediated actin polymerization.

Disruption of WIP/N-WASP binding abolishes EspH-mediated actin polymerization

The WH1 domain of N-WASP binds the WASP/N-WASP-binding domain (WBD) of WASP interacting protein (WIP) (Volkman *et al.*, 2002). To investigate the role of WIP in triggering EspH-mediated actin polymerization, we transfected Swiss 3T3 fibroblasts with GFP or a GFP-WBD to determine if the latter exhibited a dominant-negative effect. Fluorescence microscopy of GFP-WBD transfected cells infected with E2348/69 expressing Tir_{WT} exhibited a marked reduction in actin polymerization (Fig. 6A), as only 40.1 ± 5.2% of microcolonies formed pedestals (Fig. 6B), which were shorter than those produced in infected control cells (Fig. 6A). Transfection of GFP-WBD severely attenuated EspH-mediated actin polymerization (Fig. 6A), as only 3.4 ± 0.1% of the microcolonies of E2348/69 coexpressing $Tir_{Y454A/Y474A}$ and



© 2012 Blackwell Publishing Ltd, *Cellular Microbiology*

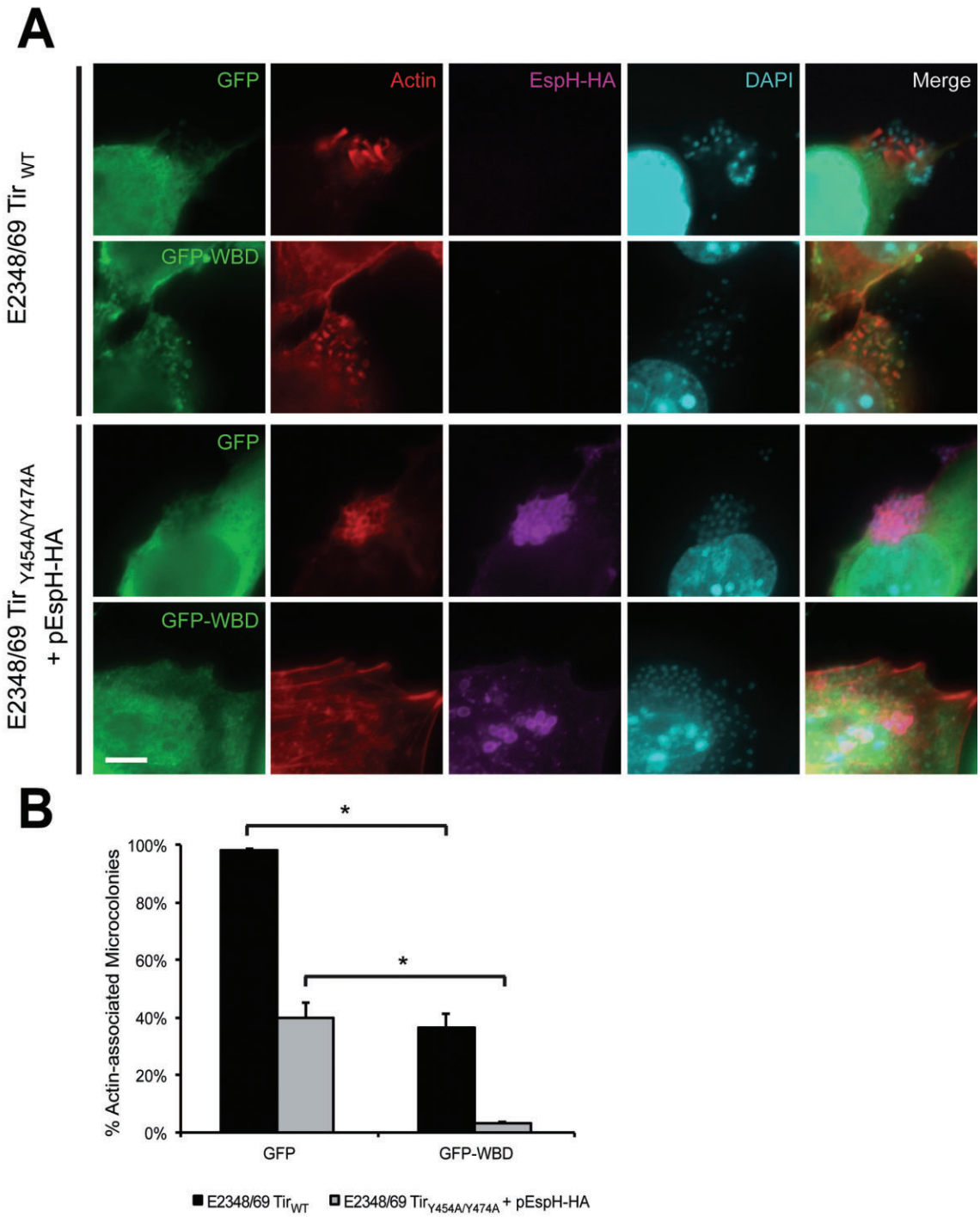


Fig. 6. Disruption of WIP/N-WASP binding abolishes EspH-mediated actin polymerization.
A. Swiss 3T3 fibroblasts transfected with GFP or GFP fused to the WASP binding domain of WIP (GFP-WBD), with infected with E2348/69 expressing Tir_{WT} or $Tir_{Y454A/Y474A}$ + pEspH-HA. Actin was stained with TRITC phalloidin (red), HA-tagged EspH was detected with anti-HA antibody (magenta), and bacteria were visualized with DAPI staining (cyan). Transfection with GFP-WBD diminished actin pedestal formation and elongation in E2348/69 Tir_{WT}, but completely abolishes EspH-mediated actin polymerization in $Tir_{Y454A/Y474A}$ + pEspH-HA (arrows). Bar = 5 μm.
B. Quantification of EPEC microcolonies associated with actin in transfected cells infected with E2348/69 Tir_{WT} or $Tir_{Y454A/Y474A}$ + pEspH-HA. A total of 100 microcolonies were counted in triplicates. Results are presented as a mean ± SD of three independent experiments. Asterisks indicate statistical significance ($P < 0.001$).

© 2012 Blackwell Publishing Ltd, *Cellular Microbiology*

EspH-HA were associated with polymerized actin (Fig. 6B). These results suggest that WIP is involved in pedestal elongation and that N-WASP recruitment by the EspH pathway is primarily mediated by WIP/N-WASP binding.

EspH and Tir recruit WIP to EPEC attachment sites

The observation that both efficient pedestal formation and EspH-mediated actin polymerization requires WIP/N-WASP suggests that EPEC may utilize two distinct, yet synergistic, actin signalling pathways that converge on WIP recruitment. To test this hypothesis, we constructed an E2348/69Δ*espH* expressing $Tir_{Y454A/Y474A}$ mutant that is deficient in Nck-dependent, NPY-dependent and EspH-mediated actin signalling pathways. We ectopically expressed GFP-WIP in Swiss 3T3 fibroblasts, and infected them with E2348/69 expressing Tir_{WT}, E2348/69Δ*espH* expressing $Tir_{Y454A/Y474A}$, or E2348/69Δ*espH* expressing $Tir_{Y454A/Y474A}$ complemented with either Tir or EspH. GFP-WIP localized to the tip of the pedestal following infection with E2348/69 expressing Tir_{WT} (Fig. 7A). Cells infected with E2348/69Δ*espH* expressing $Tir_{Y454A/Y474A}$ recruited neither WIP nor F-actin. Complementation of the E2348/69Δ*espH* expressing $Tir_{Y454A/Y474A}$ with Tir restored the recruitment of WIP and formation of short actin pedestals (Fig. 7A). Intriguingly, complementation of E2348/69Δ*espH* expressing $Tir_{Y454A/Y474A}$ with EspH induced intense actin rearrangement and formation of a protrusive structure with an actin core surrounded by GFP-WIP. Scanning electron microscopy revealed that these structures are associated with EPEC microcolonies (Fig. 7A). We also transfected N-WASP$^{-/-}$ MEFs with GFP-WIP and infected them with E2348/69 expressing Tir_{WT}, E2348/69Δ*espH* expressing $Tir_{Y454A/Y474A}$ or coexpressing $Tir_{Y454A/Y474A}$ and EspH. None of the strains recruited WIP in the absence of N-WASP (Fig. 7B), suggesting that Tir and EspH recruit WIP in an N-WASP dependent manner. Moreover, these results affirm our hypothesis that the actin signalling pathways mediated by Tir Y474 and EspH converge on WIP and N-WASP.

EspH induces colocalization of WIP, Tir and N-WASP, but not Nck

WIP has been shown to bind to Nck and N-WASP (Anton *et al*., 1998; Rohatgi *et al*., 2001; Volkman *et al*., 2002). To determine if Nck and N-WASP are present at the site of EspH-mediated actin polymerization, Swiss 3T3 fibroblasts transfected with GFP-WIP and infected with E2348/69Δ*espH* expressing $Tir_{Y454A/Y474A}$ complemented with EspH-HA were fixed and stained for Tir, EspH, N-WASP and Nck. Immunofluoresence microscopy revealed that Tir, EspH and N-WASP colocalized with WIP (Fig. 8A). Interestingly, although WIP can bind Nck *in vitro* (Anton *et al*., 1998), Nck did not colocalize at the site of bacterial attachment. As a control, we infected the GFP-WIP transfected cells with E348/69 expressing Tir_{WT} and E2348/69Δ*espH* expressing $Tir_{Y454A/Y474A}$. Tir, Nck and N-WASP were all recruited beneath E348/69 expressing Tir_{WT}, but only Tir was recruited beneath E2348/69Δ*espH* expressing $Tir_{Y454A/Y474A}$ (Fig. 8B). These results reaffirm that Nck is not required for EspH-mediated actin polymerization. Taken together, our results show that EspH recruits WIP and N-WASP independently of Nck to trigger localized actin polymerization and promote elongation of Nck-mediated actin pedestals (Fig. 9).

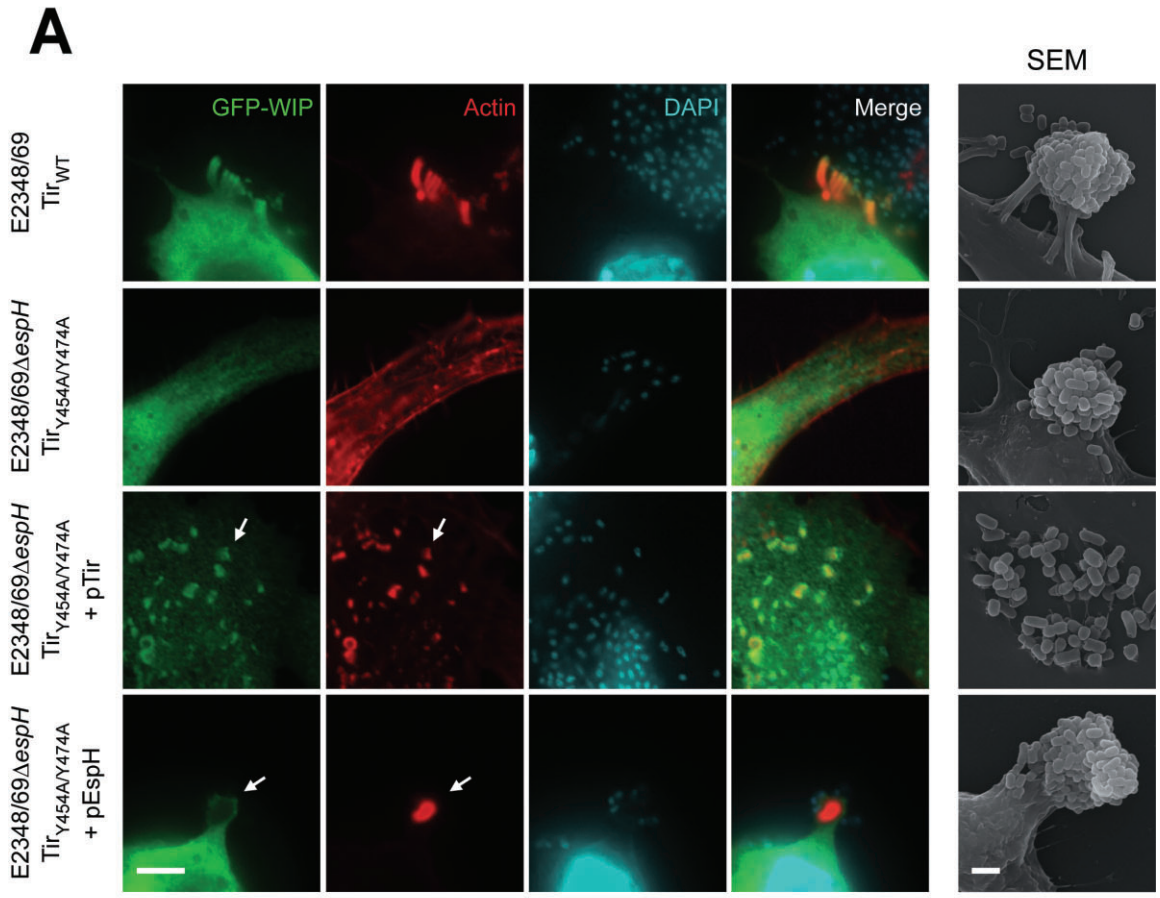
Discussion

In this paper we report that EspH promotes N-WASP recruitment and Arp2/3-mediated actin polymerization independently of Tir residues Y454 and Y474 and by extension the Tir:Nck and Tir:IRTKS/IRSp53 actin signalling pathways. Accordingly, EPEC triggers localized actin polymerization by parallel mechanisms that eventually converge on WIP and N-WASP, and that WIP is required for efficient formation and elongation of EPEC actin pedestals.

Using deletion variants of N-WASP, we identified WH1 and PRD domains as important regions for Tir-mediated actin pedestal formation. Consistent with this observation, the expression of a WBD construct exerted a dominant-negative effect that markedly reduced pedestal formation and elongation. This observation differs from a previous report that the PRD domain of N-WASP is dispensable for actin pedestal formation, and that the WBD construct did not exert a dominant-negative effect on actin pedestal formation (Lommel *et al*., 2001). Furthermore, it was previously reported that WIP is found throughout the pedestal length (Lommel *et al*., 2001), while we observed that WIP mainly localizes to the tip of pedestals together with Tir, Nck and N-WASP, suggesting that WIP might have an active role at the site of actin nucleation. As N-WASP is required for WIP recruitment to the bacterial attachment site, both proteins appear to be recruited in complex. Since WIP can also binds Nck (Anton *et al*., 1998; Rohatgi *et al*., 2001), our results give further evidence for a model whereby the Tir:Nck pathway recruits a WIP/N-WASP complex via both Nck/WIP and Nck/N-WASP interactions that synergistically trigger actin polymerization in a process similar to *Vaccinia* virus actin-based motility (Moreau *et al*., 2000).

Intriguingly, EspH is also able to promote the recruitment of WIP and N-WASP independently of Nck or repression of Rho GTPases. Moreover, while the CRIB domain of N-WASP, which binds activated Rho GTPases,

© 2012 Blackwell Publishing Ltd, *Cellular Microbiology*



© 2012 Blackwell Publishing Ltd, *Cellular Microbiology*

Fig. 7. Tir and EspH recruit WIP to EPEC attachment sites.
A. Swiss 3T3 fibroblasts transfected with GFP-WIP were infected with E2348/69 expressing Tir_{WT}, E2348/69Δ*espH* expressing $Tir_{Y454A/Y474A}$ or E2348/69Δ*espH* $Tir_{Y454A/Y474A}$ complemented with either plasmid-expressed Tir (pTir) or EspH (pEspH). Actin was stained with TRITC phalloidin (red), and bacteria were visualized with DAPI staining (cyan). WIP is recruited to the tip of the pedestal in cells infected with E2348/69 expressing Tir_{WT}, but not E2348/69Δ*espH* expressing $Tir_{Y454A/Y474A}$. Complementation of E2348/69Δ*espH* $Tir_{Y454A/Y474A}$ with either EPEC Tir or EspH restored the recruitment of WIP (arrows). Bar = 5 μm. Scanning electron microscopy of the same experiment is displayed on the far right column (original magnification: ×6000). Bar = 2 μm.
B. Infection of N-WASP$^{-/-}$ MEFs transfected with GFP-WIP, with E2348/69 expressing Tir_{WT}, E2348/69Δ*espH* expressing $Tir_{Y454A/Y474A}$, or E2348/69Δ*espH* $Tir_{Y454A/Y474A}$ + pEspH. Tir was detected with anti-TirEPEC antibody (magenta), actin was stained with TRITC phalloidin (red), and bacteria were visualized with DAPI staining (cyan). Both E2348/69 Tir_{WT} and E2348/69Δ*espH* $Tir_{Y454A/Y474A}$ + pEspH were unable to recruit WIP or trigger actin polymerization. Bar = 5 μm.

was dispensable, dominant-negative WIP abolished EspH-mediated actin polymerization. Expression of GFP-WIP during infection with E2348/69 coexpressing $Tir_{Y454A/Y474A}$ and EspH induced extensive actin cytoskeletal rearrangements at the site of bacterial attachment. This unique actin structure is characterized by the recruitment of Tir, EspH, WIP and N-WASP, but not Nck, around an actin core. Our results suggest that EspH promotes Nck-independent WIP and N-WASP recruitment via an unknown pathway and enhances Nck-mediated actin pedestal formation and elongation. Indeed, WIP overexpression has previously been reported to increase F-actin content and induce formation of subcortical actin clusters in human B cell lines (Ramesh *et al*., 1997).

A question that remains unanswered is why endogenous levels of EspH are insufficient to trigger localized actin polymerization during EPEC infection. This question is not limited to EspH as phenotypes of other cytoskeletal-modulating T3SS effectors, e.g. EspV (Arbeloa *et al*., 2011), EspT (Bulgin *et al*., 2009) and EspM (Arbeloa *et al*., 2008), could only be seen using *in vitro* cell models following overexpression. This might reflect the existence of a complex regulatory mechanism of effectors expression and translocation *in vivo*, which we do not yet understand, that the cell culture conditions do not mimic. Alternatively, overexpression of EspH may simply shorten the length of time needed by EPEC to initiate EspH-mediated actin polymerization, which endogenous levels could only achieve beyond the viability of the infected monolayer. Nevertheless, EspH has previously been shown to be important for bacterial adherence and colonization *in vivo* (Ritchie and Waldor, 2005; Shaw *et al*., 2005). Coupled with the observation that Tir:Nck and Tir:IRTKS/IRSp53 pathways play a role in the *in vivo* competitiveness of *C. rodentium* in mice and EHEC in rabbits (Ritchie and Waldor, 2005; Crepin *et al*., 2009), our data suggest that just as TccP/$EspF_U$ in EHEC (Garmendia *et al*., 2004; 2006; Campellone *et al*., 2004b; Cheng *et al*., 2008; Sallee *et al*., 2008) and EPEC lineage 2 (Whale *et al*., 2006) strains is able to amplify the inefficient Tir:IRTKS/IRSp53 actin polymerization pathway, EspH might contribute to competitiveness and *in vivo* fitness of A/E pathogens by intensifying actin polymerization pathways through WIP, in a mechanism dependent on the C-terminus of Tir.

The mechanism by which EspH recruits WIP to the bacterial attachment site remains elusive. As we were unable to co-immunoprecipitate EspH with WIP or N-WASP (data not shown), it is unlikely that EspH directly binds WIP/N-WASP to drive actin polymerization. Since Nck is not recruited during EspH-mediated actin polymerization, other adaptor protein/s are likely to be involved in the EspH-mediated actin signalling upstream of WIP. Indeed, EspH localizes to the plasma membrane and promiscuously binds DH-PH containing RhoGEFs (Dong *et al*., 2010), which contain other domains such as regulator of G-protein signalling (RGS) and Src-homology 3 (SH3) domains (Rossman *et al*., 2005). It is thus possible that EspH could recruit WIP/N-WASP complex via interactions with specific RhoGEFs. For example, intersectin is a Cdc42-specific GEF that is able to bind directly to N-WASP via its SH3 domain to promote actin polymerization in a positive feedback loop (Hussain *et al*., 2001). Interestingly, previous studies also demonstrate that the WIP/N-WASP complex can localize and trigger actin polymerization dependent on the curvature of the membrane (Takano *et al*., 2008). EspH could thus trigger actin polymerization at the plasma membrane as an indirect result of its ability to induce dramatic changes to cell shape (Tu *et al*., 2003; Dong *et al*., 2010). Further work is required to determine if membrane dynamics play a role in modulating EspH-mediated actin remodelling.

In assessing the role of EspH during EPEC infection, we found that like many EPEC T3SS effectors, e.g. NleH effectors that can subvert NF-κB function (Gao *et al*., 2009) and block apoptosis (Hemrajani *et al*., 2010), EspH is multi-functional. EspH blocks the activation of Rho GTPases by inactivating endogenous mammalian RhoGEFs to inhibit phagocytosis (Dong *et al*., 2010), but also plays an additional role in recruiting WIP to the site of bacterial adherence to promote actin polymerization and pedestal elongation. Our results also demonstrate the intricate complexities of Tir and EspH-mediated actin polymerization that involves distinct, convergent and synergistic signalling cascades.

© 2012 Blackwell Publishing Ltd, *Cellular Microbiology*

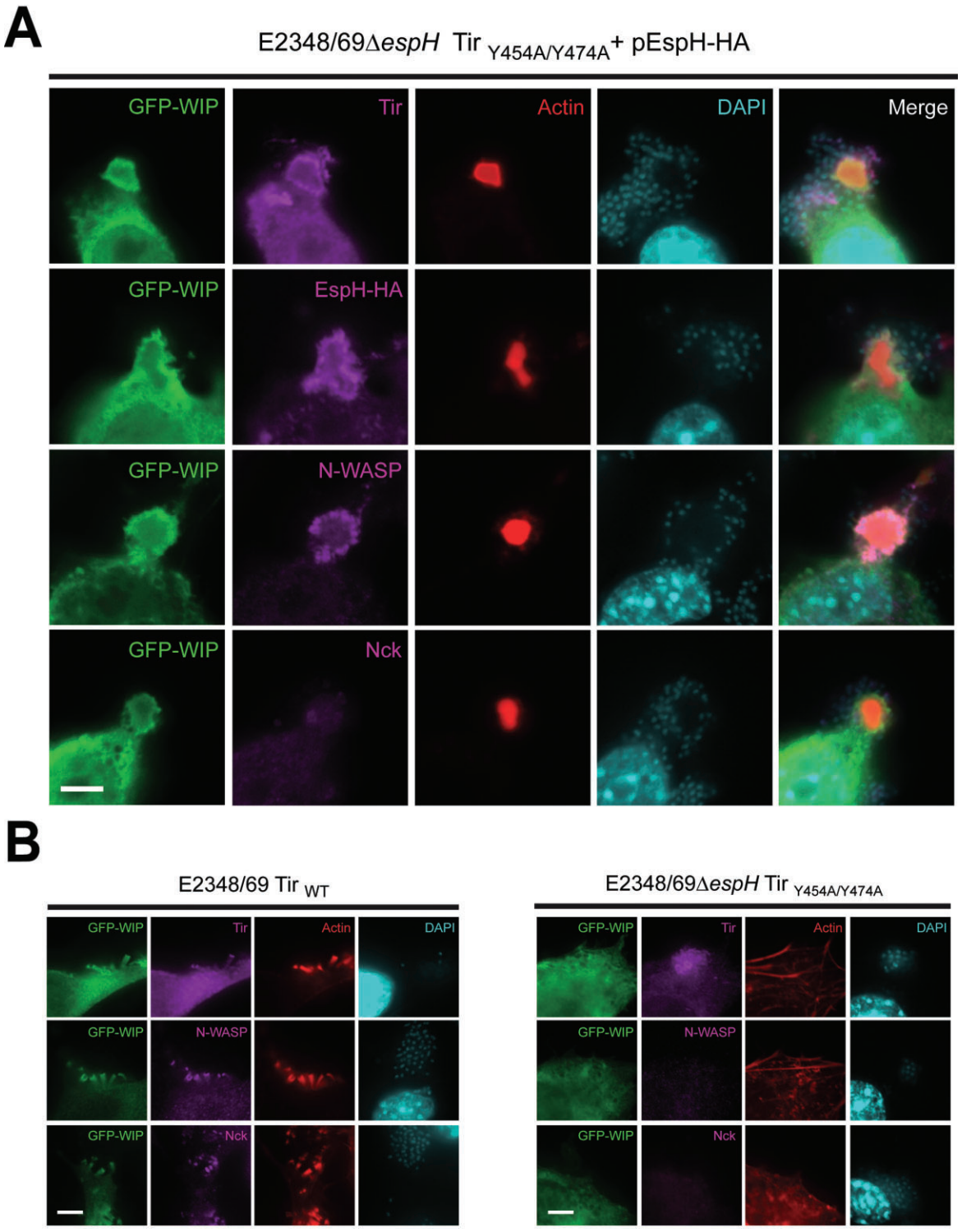


Fig. 8. EspH induces colocalization of Tir, WIP and N-WASP, but not Nck.
A. Swiss 3T3 fibroblasts transfected with GFP-WIP were infected with E2348/69Δ*espH* coexpressing $Tir_{Y454A/Y474A}$ and HA-tagged EspH (E2348/69Δ*espH* $Tir_{Y454A/Y474A}$ + pEspH-HA). Tir, EspH-HA, N-WASP and Nck were labelled with respective antibodies (magenta), actin was stained with TRITC phalloidin (red), and bacteria were visualized with DAPI staining (cyan). Tir, EspH and N-WASP colocalized with WIP, but not Nck. Bar = 5 μm.
B. Swiss 3T3 fibroblasts transfected with GFP-WIP were infected with E2348/69 expressing Tir_{WT}, or E2348/69Δ*espH* expressing $Tir_{Y454A/Y474A}$. Tir, N-WASP, and Nck were labelled with respective antibodies (magenta), actin was stained with TRITC phalloidin (red), and bacteria were visualized with DAPI staining (cyan). Tir, Nck and N-WASP colocalizes with WIP at the tip of actin pedestals in E2348/69 Tir_{WT}. Bar = 5 μm.

© 2012 Blackwell Publishing Ltd, *Cellular Microbiology*

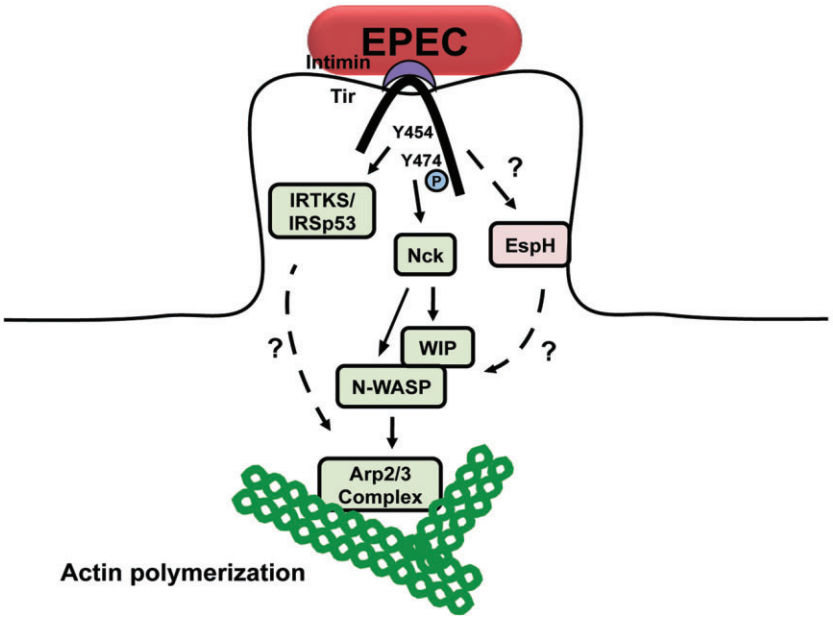


Fig. 9. EPEC induces distinctive, convergent and synergistic Tir actin signalling cascades. A model for Tir-mediated actin signalling cascades. Upon translocation, Tir inserts into the plasma membrane, where clustering with the bacterial adhesion intimin initiates several actin signalling pathways. Phosphorylation at Y474 leads to Nck binding. Nck, which binds both WIP and N-WASP, then induces actin pedestal formation. Y454 forms part of an NPY motif that binds IRTKS/IRSp53 to induce weak actin polymerization, although the mechanism remains unknown. In addition, EspH is recruited via the C-terminus of Tir to the bacterial attachment site where the effector, directly or indirectly, promotes WIP and N-WASP recruitment independently of Nck or Y454/Y474 to promote formation and elongation of EPEC actin pedestals.

Experimental procedures

Bacterial strains and plasmids

Bacterial strains and plasmids used in this study are listed in Tables 1 and 2. Bacteria were grown from single colonies in Luria–Bertani (LB) broth in a shaking incubator at 37°C, except those transformed with the temperature-sensitive pKD46 plasmid (30°C). Culture media or agar was supplemented with ampicillin (100 μg ml^{-1}), chloramphenicol (34 μg ml^{-1}) or kanamycin (50 μg ml^{-1}) as appropriate. Bacterial cultures were primed for infection by dilution of 1:100 of overnight bacterial culture with pre-warmed in Dulbecco's minimal Eagle media (DMEM) high glucose (4500 mg l^{-1}) (Sigma), and incubated as static cultures at 37°C in 5% CO_2 for 3 h. Static cultures were induced with 1 mM Isopropyl thio-galactopyranoside for pSA10-effector expression 30 min prior to infection.

EPEC tir *mutagenesis*

E2348/69 strains expressing mutated Tir were generated using a lambda red-based mutagenesis system (Datsenko and Wanner, 2000; Crepin *et al*., 2009), via the introduction of site-directed *tir* mutagenesis into the endogenous chromosomal *tir* gene together with a kanamycin cassette in the *tir-cesT* intergenic region as previously described. Primers are listed in Table 3. To mutate the C-terminus tyrosine residues of *tir*, the 3′ end of *tir*, followed by a non-polar *aphT* cassette, and then the *tir-cesT* intergenic region and 5′ end of *cesT* were first cloned into pGEMT vector. The 3′ end of *tir* was amplified using primer pair TirC-E69-Fw/EcoRI-TirC-E69-Rv, while the intergenic region and 5′ end of *cesT* was amplified using primer pair EcoRI-NcesT-E69-Fw/NcesT-E69-Rv. Both fragments were then digested with EcoRI, ligated together, and then cloned into pGEMT. The non-polar *aphT* cassette was then inserted into the EcoRI site between the two fragments and the orientation of the *aphT* cassette ascertained by PCR. This plasmid, pICC530, was used to generate the control mutant Tir_{WT}.

EPEC *tir* mutagenesis was carried out by inverse-PCR using pICC530. The primer pairs TirC-E69-Y454A-Fw/TirC-E69-Y454A-Rv and TirC-E69-Y474A-Fw/TirC-E69-Y474A-Rv were used to mutate the tyrosine residues Y454 and Y474 into alanines (Tir_{Y454A} and Tir_{Y474A}) generating pICC531 and pICC532 respectively. The double tyrosine mutant ($Tir_{Y454A/Y474A}$) was generated by superimposing Y474A on the Y454A mutant, generating pICC533. All pGEMT derivatives were checked by DNA sequencing. To introduce tir_{WT}, tir_{Y454A}, tir_{Y474A} and $tir_{Y454A/Y474A}$ site-directed mutants into bacterial chromosome, the inserts in all pGEMT derivatives were amplified using the primer pair TirC-E69-Fw/NcesT-E69-Rv. The PCR products were electroporated into E2348/69 containing pKD46 encoding lambda red recombi-

Table 1. List of strains.

ICC No.	Name	Description	Source/reference
	E2348/69	Wild-type EPEC 1 O127:H6 strain	Levine *et al*. (1978)
ICC225	E2348/69Δ*tir*	E2348/69 *tir* deletion mutant	Berger *et al*. (2009)
ICC308	E2348/69 Tir_{WT}	Control for Tir chromosomal mutants (with kanamycin cassette)	This study
ICC309	E2348/69 Tir_{Y454A}	E2348/69 chromosomal mutant expressing Tir_{Y454A}	This study
ICC310	E2348/69 Tir_{Y474A}	E2348/69 chromosomal mutant expressing Tir_{Y474A}	This study
ICC311	E2348/69 $Tir_{Y454A/Y474A}$	E2348/69 chromosomal mutant expressing $Tir_{Y454A/Y474A}$	This study
ICC312	E2348/69Δ*espH* $Tir_{Y454A/Y474A}$	E2348/69 chromosomal mutant expressing $Tir_{Y454A/Y474A}$, with *espH* deletion	This study

© 2012 Blackwell Publishing Ltd, *Cellular Microbiology*

Table 2. List of plasmids.

pICC No.	Plasmids	Description	Source/reference
	pSA10	pKK177-3 containing *lacI* gene	Levine *et al*. (1978)
	pGEMT	Cloning vector	Promega
	pKD46	Coding the lambda-red recombinase	Datsenko and Wanner (2000)
	pSB315	Coding the kanamycin resistance *aphT* cassette	Galan *et al*. (1992)
pICC618	PSB315-CM	pSB315 with chloramphenicol resistance *cat* cassette replacing the *aphT* cassette	This study
pICC619	pSA10-EspH	pSA10 derivative encoding EPEC EspH	This study
pICC394	pSA10-Tir	pSA10 derivative encoding EPEC Tir	Berger *et al*. (2009)
pICC528	pSA10-EspH-HA	pSA10 derivative encoding haemagglutinin (HA)-tagged EspH	This study
pICC530		pGEMT vector containing 3′ end of tir_{EPEC} (bp 1072–1653), *aphT, tir-cesT* intergenic region and 5′ end of *cesT* (bp 1–369)	This study
pICC531		pICC530 containing the tir_{EPEC} Y454A mutation	This study
pICC532		pICC530 containing the tir_{EPEC} Y474A mutation	This study
pICC533		pICC530 containing the tir_{EPEC} Y454A/Y474A mutation	This study
	pEGFP-C1	Coding a GFPmut1 variant for expression in mammalian cells	Invitrogen
	pEGFP-N-WASP	pEGFP-C1 derivative encoding N-WASP	E. Caron
pICC620	pEGFP-ΔWH1	pEGFP-N-WASP with aa 1–156 deletion	This study
pICC621	pEGFP-ΔB	pEGFP-N-WASP with aa 156–200 deletion	This study
pICC622	pEGFP-ΔCRIB	pEGFP-N-WASP with aa 200–226 deletion	This study
pICC623	pEGFP-ΔGBD	pEGFP-N-WASP with aa 200–274 deletion	This study
pICC624	pEGFP-ΔPRD	pEGFP-N-WASP with aa 274–385 deletion	This study
pICC625	pEGFP-WH1-VCA	pEGFP-N-WASP with aa 156–385 deletion	This study
	pCB6-WIP	GFP fused to WIP transfection vector	Moreau *et al*. (2000)
	pCB6-WBD	GFP fused to WASP-binding domain of WIP transfection vector	Moreau *et al*. (2000)
	pRK5myc-IRSp53	Myc-tagged IRSp53 construct	Millard *et al*. (2007)
	pRK5myc-WAVE2	Myc-tagged WAVE2 construct	L. Machesky
	pCDNA3-TirMC	HA-tagged Tir derivative	Campellone *et al*. (2004a)
	pCDNA3-$TirMC_{Y474}$	HA-tagged Tir derivative	Campellone *et al*. (2004a)
pICC626	pCDNA3-TirNMC	pCDNA3-TirMC with Tir N-terminus (aa 1–233) insertion at the HindIII restriction site	This study
pICC627	pCDNA3-TirNM	pCDNA-TirNMC with aa 388–547 deletion	This study
pICC628		pGEMT vector containing 325 bp upstream region of $espH_{EPEC}$, *cat*, and 499 bp downstream region of $espH_{EPEC}$	This study

nase. Transformants were selected on kanamycin agar plates and the insertion of site-directed *tir* mutants confirmed by PCR and DNA sequencing.

*E2348/69Δ*espH *$Tir_{Y454A/Y474A}$ mutagenesis*

A 325 bp upstream region of *espH* was amplified using primer pair Up-EspH-E69-Fw/BamHI-Up-EspH-E69-Rv, and a 499 bp downstream region of *espH* was amplified using primer pair BamHI-Dn-EspH-E69-Fw/Dn-EspH-E69-Rv. Both fragments were then digested with BamHI, ligated together, and then cloned into pGEMT. The non-polar *cat* cassette was then inserted into the BamHI site between the two fragments and the orientation of the *cat* cassette ascertained by PCR. This plasmid, pICC628, was then amplified using the primer pair Up-EspH-E69-Fw/Dn-EspH-E69-Rv. The PCR products were electroporated into E23478/69 $Tir_{Y454A/Y474A}$ containing pKD46 encoding lambda red recombinase. Transformants were selected on chloramphenicol agar plates and *espH* deletion confirmed by PCR and DNA sequencing.

Construction of GFP-N-WASP and HA-TirNM expression variants

Construction of the different GFP-NWASP expression variants was carried out by inverse PCR, using pEGFP-N-WASP expression vector (kindly provided by Dr. Emmanuelle Caron) as template. The primer pairs NWASP-WH1del-Rv/NWASP-WH1del-Fw, NWASP-Bdel-Rv/NWASP-Bdel-Fw, NWASP-CRIBdel-Rv/NWASP-CRIBdel-Fw, NWASP-CRIBdel-Rv/NWASP-GBDdel-Fw, NWASP-PRDdel-Rv/NWASP-PRDdel-Fw and NWASP-WH1del-Rv/NWASP-PRDdel-Fw were used to delete the WH1 (1–156), B (156–200), CRIB (200–226), GBD (226–274), PRD (274–392) and all domains except WH1 (156–392), generating GFP-ΔWH1, GFP-ΔB, GFP-ΔCRIB, GFP-ΔGBD, GFP-ΔPRD and GFP-WH1-VCA respectively. All pEGFP-N-WASP expression variants were sequenced and assessed with Western blot analysis to ensure stable expression.

Construction of HA-TirNM was carried out first by re-inserting the N-terminus of Tir (aa 1–233) into the HindIII restriction site of pCDNA3-TirMC to generate pICC626. Using pICC626 as template, the primer pairs pCDNA3-TirNM(EPEC)-Rv/pCDNA3-TirNM(EPEC)-Fw was used to delete the C-terminus of Tir (aa 388–547), generating pCDN3-TirNM. All pCDNA3-Tir expression variants were sequenced and assessed for membrane localization by transfection.

siRNA knockdown of Rho GTPases

For siRNA knockdown of Cdc42, Rac1 and RhoA, siRNA pool sequences were selected from a proprietary Rho GTPase siRNA library (Dharmacon). siRNA knockdown was performed on Swiss 3T3 fibroblasts using HiPerfect (Qiagen) according to manufac-

Table 3. List of primers.

Name	Nulceotide sequence (5′–3′) (restriction sites in bold)
EcoRI-EspH-E69-Fw	CGG**GAATTC**ATGTCGTCATCATTATCAGGTATAAC
PstI-EspH-E69-Rv	AAAA**CTGCAG**TTAAACTGTCACACCTGATAAAG
PstI-EspH-E69-HA-Rv	AAAA**CTGCAG**TTATGCGTAATCTGGTACATCGTATGGGTATGCTCCAA CTGTCACACCTGATAAAGAGTTTAATG
EPEC *tir* mutagenesis	
TirC-E69-Fw	TACAGCTTTCATCGGGTATTGG
EcoRI-TirC-E69-Rv	CGG**GAATTC**TTAAACGAAACGTACTGGTCCC
EcoRI-NcesT-E69-Fw	CGG**GAATTC**ATATATCTGTGAGTATTTAGTTGAG
NcesT-E69-Rv	CGTTAAGTCGATGGAAAATCTG
TirC-E69-Y454A-Rv	GGCAGGATTAACCACTTCGCTAGA
TirC-E69-Y454A-Fw	GCTGAAGTTGGGGGGGCTC
TirC-E69-Y474A-Rv	GGCTATATGCTCTTCTGGCTGATG
TirC-E69-Y474A-Fw	GATGAGGTCGCTGCAGATCCT
EPEC *espH* mutagenesis	
Up-EspH-E69-Fw	GGCAACCGTAAAGCTGAGC
BamHI-Up-EspH-E69-Rv	CGC**GGATCC**CATACACCTCCCTATATAACG
BamHI-Dn-EspH-E69-Fw	CGC**GGATCC**CTCTTTATCAGGTGTGACAG
Dn-EspH-E69-Rv	GTCATGAGTGGATACTTGAG
GFP-N-WASP variants	
NWASP-WH1del-Rv	CATGGTGTCGCCGGACTTG
NWASP-WH1del-Fw	GCTACAGTTGACATAAAAAATCC
NWASP-Bdel-Rv	CATGGGTAGATTGGGACCATT
NWASP-Bdel-Fw	GGAACACCAAGTAATTTCCAGC
NWASP-CRIBdel-Rv	AATATCTGCCTTGGTTAATCTCTTC
NWASP-CRIBdel-Fw	CCAGAATTAAAGAATCTTTTTGATATG
NWASP-GBDdel-Fw	CCACCACCTCCACCCTCGAG
NWASP-PRDdel-Rv	TGGTGCTTGTCTTCGGAGTTC
NWASP-PRDdel-Fw	CATCAAGTTCCAGCTCCTTCAG
HA-TirNM	
HindIII-TirN(1–233)-E69-Fw	CCC**AAGCTT**CAATGCCTATTGGTAACCTTGGTAAT
HindIII-TirN(1–233)-E69-Rv	CCC**AAGCTT**GTTTAGGATCTGAGCGAACGCTG
pCDNA3-TirNM(EPEC)-Rv	TCTATGGAGCGCAGTCGTTAC
pCDNA3-TirNM(EPEC)-Fw	CGTTTCGTTTAAATATATCCGCG

turer's instructions. siRNA knockdown was allowed to proceed at 37°C in a humidified incubator with 5% CO_2 for 48 h before EPEC infection. Effectiveness of RNAi-mediated gene silencing of Rho GTPases was assessed by Western blot using the appropriate antibodies.

Transfection and Infection of cells with EPEC E2348/69

Swiss 3T3 fibroblasts (ATCC CCL-92), $Nck^{-/-}$ fibroblasts (Bladt *et al.*, 2003) and N-$WASP^{-/-}$ mouse embryonic fibroblasts (MEFs) were grown at 37°C in a humidified atmosphere containing 5% CO_2 in DMEM high glucose (4500 mg l^{-1}) (Sigma) supplemented with 10% (v/v) heat-inactivated fetal bovine serum (Gibco) and 2 mM glutamax (Sigma). Cells were grown in 24-well cell culture plates to 80% confluence. Cells were transfected in serum-free DMEM with mammalian expression vectors using lipofectamine2000 (Invitrogen) according to the manufacturer's instructions. Transfected cells were incubated at 37°C in a humidified incubator with 5% CO_2 for 4 h before having their media replaced with pre-warmed serum-containing DMEM, and incubated for a further 20 h unless otherwise stated. Monolayers were washed twice with PBS and then infected with 0.5 ml of primed bacterial culture at 37°C in a humidified atmosphere containing 5% CO_2 for 2 h unless otherwise stated. Coverslips were washed three times in PBS and fixed with 3% paraformaldehyde for 15 min before being processed for immunofluorescence microscopy.

Immunofluorescence microscopy

Cells were quenched for 15 min with 50 mM NH_4Cl, and then permeabilized for 5 min in PBS/0.2% Triton X-100. Coverslips were washed thrice in PBS and blocked in PBS/1% BSA for 10 min before addition of primary antibodies. Coverslips were incubated with primary antibodies diluted in PBS/1% BSA for 1 h. After washing thrice with PBS, coverslips were then incubated with secondary antibodies diluted in PBS/1% BSA for a further 1 h. Coverslips were washed thrice again PBS and once in water before being mounted in Gold Pro-Long Anti-fade medium (Invitrogen), and examined by conventional epifluoresecence microscopy using a Zeiss Axio LSM-510 microscope. Images were deconvoluted and processed using Zeiss Axiovision 4.8 software and Adobe Photoshop CS4.

Antibodies

Actin was detected with Oregon Green conjugated Phalloidin antibody (1:100 dilution) (Invitrogen) or TRITC-conjugated Phalloidin (1:500 dilution) (Sigma). Intimin or Tir were labelled with polyclonal chicken anti-intimin (1:200 dilution) or anti-Tir (1:500 dilution) antibody serum respectively (kindly provided by Dr Roberto La Ragione, Veterinary Laboratory Agency, UK). Arp2/3 complex was visualized using mouse anti-Arp2 subunit antibody (1:200 dilution) (kindly provided by Laura Machesky). N-WASP was visualized using a polyclonal rabbit anti-N-WASP antibody

© 2012 Blackwell Publishing Ltd, *Cellular Microbiology*

(1:100 dilution) (Sigma). Nck was visualized using a polyclonal rabbit anti-Nck antibody (1:100 dilution) (Millipore/Upstate). HA-tagged proteins were labelled with monoclonal anti-HA.11 (1:500 dilution) (Covance), while transfected cells expressing myc-tagged proteins were labelled with monoclonal anti-myc antibody (1:500 dilution) (Millipore). Cy2, RRX or Cy5 conjugated donkey anti-mouse, anti-chicken or anti-rabbit antibodies (1:200 dilution) (Jackson ImmunoResearch) were used as secondary antibodies.

Scanning electron microscopy

Cells were infected as previously described, and fixed in 2.5% glutaraldehyde PBS overnight at 4°C. Coverslips were then washed thrice in PBS for 1.5 h with regular changes. Cells were further post-fixed in aqueous 1% osmium tetroxide (OsO_4), rinsed in water, then dehydrated in a graded series of 50%, 75%, 85%, 95% and 100% ethanol. Samples were processed for scanning electron microscopy using an Emitech K850 critical-point drier, coated with gold–palladium for 90 s using a Polaron SC7620 mini sputter-coater, and examined using a JEOL JSM-6390 scanning electron microscope.

Western blot

Proteins were extracted from cells using RIPA buffer. Samples were separated on a 12% polyacrylamide gel, and transferred to nitrocellulose membrane (Bio-Rad). Blots were then blocked in TBS/0.1% Tween-20 containing 5% BSA and probed with polyclonal rabbit anti-Cdc42 (BD Biosciences), monoclonal mouse anti-Rac1 (Cell Signalling), polyclonal rabbit anti-RhoA (Santa Cruz), polyclonal rabbit anti-N-WASP (Sigma) (1:1000 dilution) or anti-GFP (Abcam) (1:1000 dilution) overnight at 4°C. After washing, immunoreactive bands were visualized using horseradish peroxidase-linked secondary antibodies (1:10 000 dilution) (Jackson ImmunoResearch) and ECL reagent (GE Healthcare). Chemiluminescence was detected using a LAS-3000 Fuji Imager.

Statistical analysis

Results were expressed as mean ± standard deviation. Statistical significance was determined by an unpaired two-tailed *t*-test. A *P*-value of < 0.01 was considered to be significant.

Acknowledgements

We thank Dr Roberto La Ragione (Veterinary Laboratory Agency, UK) for the anti-O127 antibodies, Dr Laura Machesky (Beatson Institute, Glasgow) for the anti-Arp2 antibody and pRK5myc-IRSp53 and pRK5myc-WAVE2 expression vectors, Dr Scott Snapper (Harvard Medical School, Boston) for the N-WASP knockout cell line, Dr Michael Way (Cancer Research, UK) for the GFP-WIP and GFP-WBD expression vectors, and the late Dr Emmanuelle Caron for the pEGFP-N-WASP expression vector. This work was supported by grants from the Wellcome Trust.

References

Anton, I.M., Lu, W., Mayer, B.J., Ramesh, N., and Geha, R.S. (1998) The Wiskott–Aldrich syndrome protein-interacting protein (WIP) binds to the adaptor protein Nck. *J Biol Chem* **273:** 20992–20995.

Arbeloa, A., Bulgin, R.R., MacKenzie, G., Shaw, R.K., Pallen, M.J., Crepin, V.F., *et al*. (2008) Subversion of actin dynamics by EspM effectors of attaching and effacing bacterial pathogens. *Cell Microbiol* **10:** 1429–1441.

Arbeloa, A., Oates, C.V., Marches, O., Hartland, E.L., and Frankel, G. (2011) Enteropathogenic and enterohemorrhagic *Escherichia coli* type III secretion effector EspV induces radical morphological changes in eukaryotic cells. *Infect Immun* **79:** 1067–1076.

Aspenstrom, P. (2002) The WASP-binding protein WIRE has a role in the regulation of the actin filament system downstream of the platelet-derived growth factor receptor. *Exp Cell Res* **279:** 21–33.

Berger, C.N., Crepin, V.F., Jepson, M.A., Arbeloa, A., and Frankel, G. (2009) The mechanisms used by enteropathogenic *Escherichia coli* to control filopodia dynamics. *Cell Microbiol* **11:** 309–322.

Bladt, F., Aippersbach, E., Gelkop, S., Strasser, G.A., Nash, P., Tafuri, A., *et al*. (2003) The murine Nck SH2/SH3 adaptors are important for the development of mesoderm-derived embryonic structures and for regulating the cellular actin network. *Mol Cell Biol* **23:** 4586–4597.

Bommarius, B., Maxwell, D., Swimm, A., Leung, S., Corbett, A., Bornmann, W., and Kalman, D. (2007) Enteropathogenic *Escherichia coli* Tir is an SH2/3 ligand that recruits and activates tyrosine kinases required for pedestal formation. *Mol Microbiol* **63:** 1748–1768.

Brady, M.J., Campellone, K.G., Ghildiyal, M., and Leong, J.M. (2007) Enterohaemorrhagic and enteropathogenic *Escherichia coli* Tir proteins trigger a common Nck-independent actin assembly pathway. *Cell Microbiol* **9:** 2242–2253.

Bulgin, R.R., Arbeloa, A., Chung, J.C., and Frankel, G. (2009) EspT triggers formation of lamellipodia and membrane ruffles through activation of Rac-1 and Cdc42. *Cell Microbiol* **11:** 217–229.

Campellone, K.G., and Leong, J.M. (2005) Nck-independent actin assembly is mediated by two phosphorylated tyrosines within enteropathogenic *Escherichia coli* Tir. *Mol Microbiol* **56:** 416–432.

Campellone, K.G., Rankin, S., Pawson, T., Kirschner, M.W., Tipper, D.J., and Leong, J.M. (2004a) Clustering of Nck by a 12-residue Tir phosphopeptide is sufficient to trigger localized actin assembly. *J Cell Biol* **164:** 407–416.

Campellone, K.G., Robbins, D., and Leong, J.M. (2004b) EspFU is a translocated EHEC effector that interacts with Tir and N-WASP and promotes Nck-independent actin assembly. *Dev Cell* **7:** 217–228.

Cheng, H.C., Skehan, B.M., Campellone, K.G., Leong, J.M., and Rosen, M.K. (2008) Structural mechanism of WASP activation by the enterohaemorrhagic *E. coli* effector EspF(U). *Nature* **454:** 1009–1013.

Crepin, V.F., Girard, F., Schuller, S., Phillips, A.D., Mousnier, A., and Frankel, G. (2009) Dissecting the role of the Tir:Nck and Tir:IRTKS/IRSp53 signalling pathways *in vivo*. *Mol Microbiol* **75:** 308–323.

Datsenko, K.A., and Wanner, B.L. (2000) One-step inactivation of chromosomal genes in *Escherichia coli* K-12 using PCR products. *Proc Natl Acad Sci USA* **97:** 6640–6645.

Dong, N., Liu, L., and Shao, F. (2010) A bacterial effector targets host DH-PH domain RhoGEFs and antagonizes macrophage phagocytosis. *EMBO J* **29:** 1363–1376.

Frankel, G., and Phillips, A.D. (2008) Attaching effacing *Escherichia coli* and paradigms of Tir-triggered actin polymerization: getting off the pedestal. *Cell Microbiol* **10:** 549–556.

Galan, J.E., Ginocchio, C., and Costeas, P. (1992) Molecular and functional characterization of the *Salmonella* invasion gene invA: homology of InvA to members of a new protein family. *J Bacteriol* **174:** 4338–4349.

Gao, X., Wan, F., Mateo, K., Callegari, E., Wang, D., Deng, W., *et al*. (2009) Bacterial effector binding to ribosomal protein s3 subverts NF-kappaB function. *PLoS Pathog* **5:** e1000708.

Garmendia, J., Phillips, A.D., Carlier, M.F., Chong, Y., Schuller, S., Marches, O., *et al*. (2004) TccP is an enterohaemorrhagic *Escherichia coli* O157:H7 type III effector protein that couples Tir to the actin-cytoskeleton. *Cell Microbiol* **6:** 1167–1183.

Garmendia, J., Carlier, M.F., Egile, C., Didry, D., and Frankel, G. (2006) Characterization of TccP-mediated N-WASP activation during enterohaemorrhagic *Escherichia coli* infection. *Cell Microbiol* **8:** 1444–1455.

Gruenheid, S., DeVinney, R., Bladt, F., Goosney, D., Gelkop, S., Gish, G.D., *et al*. (2001) Enteropathogenic *E. coli* Tir binds Nck to initiate actin pedestal formation in host cells. *Nat Cell Biol* **3:** 856–859.

Hartland, E.L., Batchelor, M., Delahay, R.M., Hale, C., Matthews, S., Dougan, G., *et al*. (1999) Binding of intimin from enteropathogenic *Escherichia coli* to Tir and to host cells. *Mol Microbiol* **32:** 151–158.

Hemrajani, C., Berger, C.N., Robinson, K.S., Marches, O., Mousnier, A., and Frankel, G. (2010) NleH effectors interact with Bax inhibitor-1 to block apoptosis during enteropathogenic *Escherichia coli* infection. *Proc Natl Acad Sci USA* **107:** 3129–3134.

Ho, H.Y., Rohatgi, R., Ma, L., and Kirschner, M.W. (2001) CR16 forms a complex with N-WASP in brain and is a novel member of a conserved proline-rich actin-binding protein family. *Proc Natl Acad Sci USA* **98:** 11306–11311.

Hussain, N.K., Jenna, S., Glogauer, M., Quinn, C.C., Wasiak, S., Guipponi, M., *et al*. (2001) Endocytic protein intersectin-l regulates actin assembly via Cdc42 and N-WASP. *Nat Cell Biol* **3:** 927–932.

Jerse, A.E., and Kaper, J.B. (1991) The *eae* gene of enteropathogenic *Escherichia coli* encodes a 94-kilodalton membrane protein, the expression of which is influenced by EAF plasmid. *Infect Immun* **59:** 4302–4309.

Kato, M., Miki, H., Kurita, S., Endo, T., Nakagawa, H., Miyamoto, S., and Takenawa, T. (2002) WICH, a novel verprolin homology domain-containing protein that functions cooperatively with N-WASP in actin-microspike formation. *Biochem Biophys Res Commun* **291:** 41–47.

Kenny, B. (1999) Phosphorylation of tyrosine 474 of the enteropathogenic *Escherichia coli* (EPEC) Tir receptor molecule is essential for actin nucleating activity and is preceded by additional host modifications. *Mol Microbiol* **31:** 1229–1241.

Kenny, B., DeVinney, R., Stein, M., Reinscheid, D.J., Frey, E.A., and Finlay, B.B. (1997) Enteropathogenic *E. coli* (EPEC) transfers its receptor for intimate adherence into mammalian cells. *Cell* **91:** 511–520.

Knutton, S., Lloyd, D.R., and McNeish, A.S. (1987) Adhesion of enteropathogenic *Escherichia coli* to human intestinal enterocytes and cultured human intestinal mucosa. *Infect Immun* **55:** 69–77.

Levine, M.M., Berquist, E.J., Nalin, D.R., Waterman, D.H., Hornick, R.B., Young, C.R., and Sotman, S. (1978) *Escherichia coli* strains that cause diarrhoea but do not produce heat-labile or heat-stable enterotoxins and are non-invasive. *Lancet* **1:** 1119–1122.

Lommel, S., Benesch, S., Rottner, K., Franz, T., Wehland, J., and Kuhn, R. (2001) Actin pedestal formation by enteropathogenic *Escherichia coli* and intracellular motility of *Shigella flexneri* are abolished in N-WASP-defective cells. *EMBO Rep* **2:** 850–857.

Millard, T.H., Dawson, J., and Machesky, L.M. (2007) Characterisation of IRTKS, a novel IRSp53/MIM family actin regulator with distinct filament bundling properties. *J Cell Sci* **120:** 1663–1672.

Moreau, V., Frischknecht, F., Reckmann, I., Vincentelli, R., Rabut, G., Stewart, D., and Way, M. (2000) A complex of N-WASP and WIP integrates signalling cascades that lead to actin polymerization. *Nat Cell Biol* **2:** 441–448.

Mundy, R., MacDonald, T.T., Dougan, G., Frankel, G., and Wiles, S. (2005) *Citrobacter rodentium* of mice and man. *Cell Microbiol* **7:** 1697–1706.

Nataro, J.P., and Kaper, J.B. (1998) Diarrheagenic *Escherichia coli*. *Clin Microbiol Rev* **11:** 142–201.

Padrick, S.B., and Rosen, M.K. (2010) Physical mechanisms of signal integration by WASP family proteins. *Ann Rev Biochem* **79:** 707–735.

Peterson, F.C., Deng, Q., Zettl, M., Prehoda, K.E., Lim, W.A., Way, M., and Volkman, B.F. (2007) Multiple WASP-interacting protein recognition motifs are required for a functional interaction with N-WASP. *J Biol Chem* **282:** 8446–8453.

Phillips, N., Hayward, R.D., and Koronakis, V. (2004) Phosphorylation of the enteropathogenic *E. coli* receptor by the Src-family kinase c-Fyn triggers actin pedestal formation. *Nat Cell Biol* **6:** 618–625.

Ramesh, N., Anton, I.M., Hartwig, J.H., and Geha, R.S. (1997) WIP, a protein associated with Wiskott–Aldrich syndrome protein, induces actin polymerization and redistribution in lymphoid cells. *Proc Natl Acad Sci USA* **94:** 14671–14676.

Ritchie, J.M., and Waldor, M.K. (2005) The locus of enterocyte effacement-encoded effector proteins all promote enterohemorrhagic *Escherichia coli* pathogenicity in infant rabbits. *Infect Immun* **73:** 1466–1474.

Rohatgi, R., Ma, L., Miki, H., Lopez, M., Kirchhausen, T., Takenawa, T., and Kirschner, M.W. (1999) The interaction between N-WASP and the Arp2/3 complex links Cdc42-dependent signals to actin assembly. *Cell* **97:** 221–231.

Rohatgi, R., Nollau, P., Ho, H.Y., Kirschner, M.W., and Mayer, B.J. (2001) Nck and phosphatidylinositol 4,5-bisphosphate synergistically activate actin polymerization through the N-WASP-Arp2/3 pathway. *J Biol Chem* **276:** 26448–26452.

Rossman, K.L., Der, C.J., and Sondek, J. (2005) GEF means go: turning on RHO GTPases with guanine nucleotide-exchange factors. *Nat Rev Mol Cell Biol* **6:** 167–180.

© 2012 Blackwell Publishing Ltd, *Cellular Microbiology*

Sallee, N.A., Rivera, G.M., Dueber, J.E., Vasilescu, D., Mullins, R.D., Mayer, B.J., and Lim, W.A. (2008) The pathogen protein EspF(U) hijacks actin polymerization using mimicry and multivalency. *Nature* **454:** 1005–1008.

Shaw, R.K., Cleary, J., Murphy, M.S., Frankel, G., and Knutton, S. (2005) Interaction of enteropathogenic *Escherichia coli* with human intestinal mucosa: role of effector proteins in brush border remodeling and formation of attaching and effacing lesions. *Infect Immun* **73:** 1243–1251.

Swimm, A., Bommarius, B., Li, Y., Cheng, D., Reeves, P., Sherman, M., *et al*. (2004) Enteropathogenic *Escherichia coli* use redundant tyrosine kinases to form actin pedestals. *Mol Biol Cell* **15:** 3520–3529.

Takano, K., Toyooka, K., and Suetsugu, S. (2008) EFC/F-BAR proteins and the N-WASP-WIP complex induce membrane curvature-dependent actin polymerization. *EMBO J* **27:** 2817–2828.

Takenawa, T., and Suetsugu, S. (2007) The WASP-WAVE protein network: connecting the membrane to the cytoskeleton. *Nat Rev Mol Cell Biol* **8:** 37–48.

Tu, X., Nisan, I., Yona, C., Hanski, E., and Rosenshine, I. (2003) EspH, a new cytoskeleton-modulating effector of enterohaemorrhagic and enteropathogenic *Escherichia coli*. *Mol Microbiol* **47:** 595–606.

Vingadassalom, D., Kazlauskas, A., Skehan, B., Cheng, H.C., Magoun, L., Robbins, D., *et al*. (2009) Insulin receptor tyrosine kinase substrate links the *E. coli* O157:H7 actin assembly effectors Tir and EspF(U) during pedestal formation. *Proc Natl Acad Sci USA* **106:** 6754–6759.

Volkman, B.F., Prehoda, K.E., Scott, J.A., Peterson, F.C., and Lim, W.A. (2002) Structure of the N-WASP EVH1 domain-WIP complex: insight into the molecular basis of Wiskott–Aldrich syndrome. *Cell* **111:** 565–576.

Weiler, M.C., Smith, J.L., and Masters, J.N. (1996) CR16, a novel proline-rich protein expressed in rat brain neurons, binds to SH3 domains and is a MAP kinase substrate. *J Mol Neurosci* **7:** 203–215.

Weiss, S.M., Ladwein, M., Schmidt, D., Ehinger, J., Lommel, S., Stading, K., *et al*. (2009) IRSp53 links the enterohemorrhagic *E. coli* effectors Tir and EspFU for actin pedestal formation. *Cell Host Microbe* **5:** 244–258.

Whale, A.D., Garmendia, J., Gomes, T.A., and Frankel, G. (2006) A novel category of enteropathogenic *Escherichia coli* simultaneously utilizes the Nck and TccP pathways to induce actin remodelling. *Cell Microbiol* **8:** 999–1008.

Wong, A.R., Pearson, J.S., Bright, M.D., Munera, D., Robinson, K.S., Lee, S.F., *et al*. (2011) Enteropathogenic and enterohaemorrhagic *Escherichia coli*: even more subversive elements. *Mol Microbiol* **80:** 1420–1438.

Supporting information

Additional Supporting Information may be found in the online version of this article:

Fig. S1. EspH promotes formation and elongation of EPEC actin pedestals.

Kinetic (A) and fluorescence microscopy (B) of microcolony-associated actin pedestals in Swiss 3T3 fibroblasts infected with wild-type E2348/69, E2348/69Δ*espH* or E2348/69Δ*espH* complemented with EspH (E2348/69Δ*espH* + pEspH). A total of 100 microcolonies were counted in triplicates for pedestals at 10, 20, 30, 45 and 90 min post infection. Actin was stained with Oregon green phalloidin (green) and EPEC were detected with anti-O127 antibody (red). Only 41.7 ± 5.5% of E2348/69Δ*espH* microcolonies formed actin pedestals at 30 min post infection, compared with over 85% in the wild type and the complemented mutant strains. Deletion of *espH* resulted in formation of short pedestals at 90 min. Results are presented as a mean ± SD of three independent experiments. Bar = 5 μm.

Fig. S2. EspH localizes to the plasma membrane surrounding actin pedestals and promotes localized actin polymerization independently of Tir tyrosine residues Y454 and Y474. Infection of Swiss 3T3 fibroblasts with E2348/69 Tir_{Y454A} or E2348/69 Tir_{Y474A}, with or without pEspH-HA. Actin was stained with Oregon green phalloidin (green), HA-tagged EspH was detected with anti-HA antibody (red), Tir was detected with anti-Tir antibody (magenta) and bacteria were visualized with DAPI staining (cyan). Bar = 5μm.

Fig. S3. EspH does not recruit IRSp53 or WAVE2 to the site of bacterial attachment Swiss 3T3 fibroblasts were transfected with Myc-tagged IRSp53 or WAVE2, and infected with E2348/69 Tir_{WT}, E2348/69 $Tir_{Y454A/Y474A}$, or E2348/69 $Tir_{Y454A/Y474A}$ + pEspH. IRSp53 (A) or WAVE2 (B) were detected with anti-Myc antibody (red). Actin was stained with Oregon green phalloidin (green), and bacteria were visualized with DAPI staining (cyan). IRSp53 (A) and WAVE2 (B) were not detected under adherent $Tir_{Y454A/Y474A}$ + pEspH. Bar = 5μm.

Fig. S4. EspH-mediated actin polymerization is independent of B, CRIB, GBD and PRD domains of N-WASP.

A. Lysates of N-WASP$^{-/-}$ MEFs transfected with GFP or GFP-N-WASP deletion variants were immunoblotted and probed with anti-GFP antibody. GFP-N-WASP was detected as a 90kDa protein; no GFP was detected on N-WASP$^{-/-}$ MEF lysate alone. Ectopic expression of GFP, GFP-ΔWH1, GFP-ΔB, GFP-ΔCRIB, GFP-ΔGBD, GFP-ΔPRD and GFP-WH1-VCA resulted in accumulation of intact fusion proteins.

B. N-WASP$^{-/-}$ MEFs transfected with different GFP-N-WASP deletion variants were infected with E2348/69 Tir_{WT} or E2348/69 $Tir_{Y454A/Y474A}$ + pEspH-HA. HA-tagged EspH was detected with anti-HA antibody (green), actin was stained with TRITC phalloidin (red) and bacteria were visualized with DAPI staining (cyan). Actin was detected beneath adherent microcolonies of E2348/69 Tir_{WT} and E2348/69 $Tir_{Y454A/Y474A}$ + pEspH-HA on infected MEFs transfected with GFP-ΔB, GFP-ΔCRIB, GFP-ΔGBD or GFP-ΔPRD. Bar = 5 μm.

Please note: Wiley-Blackwell are not responsible for the content or functionality of any supporting materials supplied by the authors. Any queries (other than missing material) should be directed to the corresponding author for the article.